

Chemical aspects of dissolution of fast reactor nuclear fuel

By

N. DESIGAN

(CHEM02201004016)

**Indira Gandhi Centre for Atomic Research,
Kalpakkam, India**

*A thesis submitted to the
Board of Studies in Chemical Sciences
In partial fulfillment of requirements
for the Degree of*

Doctor of Philosophy

of

Homi Bhabha National Institute (HBNI)



October, 2017

Homi Bhabha National Institute¹

Recommendations of the Viva Voce Committee

As members of the Viva Voce Committee, we certify that we have read the dissertation prepared by **N. DESIGAN** entitled “*CHEMICAL ASPECTS OF DISSOLUTION OF FAST REACTOR NUCLEAR FUEL*” and recommend that it may be accepted as fulfilling the thesis requirement for the award of Degree of Doctor of Philosophy.

Chairman – Prof. N. Sivaraman

N. Sivaraman

Date: 22.12.17

Guide / Convener – Dr. U. Kamachi Mudali

U. Kamachi Mudali

Date: 22/12/17

Co-guide - Prof. J. B. Joshi

J. B. Joshi

Date: 22/12/17

Examiner - Prof. Ashwin W Patwardhan

Ashwin W Patwardhan

Date: 22/12/2017

Member 1- Prof. S. Anthonysamy

S. Anthonysamy

Date: 22/12/17

Member 2- Shri N. K. Pandey

N. K. Pandey

Date: 22/12/17

Final approval and acceptance of this thesis is contingent upon the candidate's submission of the final copies of the thesis to HBNI.

I/We hereby certify that I/we have read this thesis prepared under my/our direction and recommend that it may be accepted as fulfilling the thesis requirement.

Date: 22.12.17

Place: Kalpakkom

U. Kamachi Mudali

Guide

¹ This page is to be included only for final submission after successful completion of viva voce.

STATEMENT BY AUTHOR

This dissertation has been submitted in partial fulfillment of requirements for an advanced degree at Homi Bhabha National Institute (HBNI) and is deposited in the Library to be made available to borrowers under rules of the HBNI.

Brief quotations from this dissertation are allowable without special permission, provided that accurate acknowledgement of source is made. Requests for permission for extended quotation from or reproduction of this manuscript in whole or in part may be granted by the Competent Authority of HBNI when in his or her judgment the proposed use of the material is in the interests of scholarship. In all other instances, however, permission must be obtained from the author.



N. DESIGAN

DECLARATION

I, hereby declare that the investigation presented in the thesis has been carried out by me. The work is original and has not been submitted earlier as a whole or in part for a degree / diploma at this or any other Institution / University.



N. DESIGAN

List of Publications arising from the thesis

Journal

1. Published

- a. **N. Desigan**, Elizabeth Augustine, Remya Murali, N.K. Pandey, U. Kamachi Mudali, R. Natarajan, J.B. Joshi, “Dissolution kinetics of Indian PHWR natural UO₂ fuel pellets in nitric acid - Effect of initial acidity and temperature”, Prog. Nucl. Ener. 83 (2015) 52-58
- b. **N. Desigan**, Nirav P Bhatt, N. K. Pandey, U. Kamachi Mudali, R. Natarajan and J. B. Joshi, “Mechanism of dissolution of nuclear fuel in nitric acid relevant to nuclear fuel reprocessing”, J. Radioanal. Nucl. Chem. (2017), April 2017, Volume 312, Issue 1, pp 141–149

2. Communicated:

- a. **Desigan N**, Nirav P Bhatt, Madhuri A. Shetty, G. Sreekumar, N. K. Pandey, U. Kamachi Mudali, R. Natarajan, Jyeshtharaj B. Joshi, “Dissolution of Nuclear Materials in Aqueous Acid Solutions: A Review”, Under review in Rev. Chem. Engg.

Conferences

1. **N. Desigan**, N. K. Pandey, C. Mallika, U. Kamachi Mudali, R. Natarajan and J. B. Joshi, “Mechanism of dissolution of UO₂ pellets in nitric acid – New insights”, Poster presentation in Pu-75 theme meeting to be organized in IGCAR from 23-25 May, 2016
2. **N. Desigan**, N.K. Pandey, U. Kamachi Mudali, J.B. Joshi, “Role of nitrous acid during the dissolution of UO₂ in nitric acid”, SESTEC 2016 Proceedings, page 198, SESTEC 2016 held at IIT Guwahati from May 17-20, 2016
3. **N. Desigan**, Nirav P Bhatt, N. K. Pandey, U. Kamachi Mudali, R. Natarajan and J. B. Joshi, “Reducing effect of mixing on the dissolution kinetics of UO₂ pellets in nitric acid”, Poster presentation in International Conference on Sustainable Chemistry and Engineering (SusChemE 2015), Hotel Lalit, Mumbai Organized by ICT, Mumbai from 8-9 Oct, 2015
4. **N. Desigan**, N. K. Pandey, U. Kamachi Mudali, “Effect of nitrous acid on the dissolution kinetics of UO₂ pellets in nitric acid”, Poster presentation at CHEMNUT

- 2015 organized in IGCAR on 30th and 31st July 2015
5. **N. Desigan**, P. Velavendan, Remya Murali, Elizabeth Augustine, N. K. Pandey, U. Kamachi Mudali and R. Natarajan, “Development of an analytical method for estimating the composition of NO_x gas using ion chromatography”, Poster presentation in NUCAR 2015 held at Mumbai from Feb 09-13 2015
 6. **N. Desigan**, Nirav P Bhatt, N. K. Pandey, U. Kamachi Mudali, R. Natarajan, J. B. Joshi, “Dissolution kinetics of UO₂ in nitric acid – Effect of mixing”, Poster presentation in NUCAR 2015 held at Mumbai from Feb 09-13 2015
 7. **N. Desigan**, P. Velavendan, Remya Murali, Elizabeth Augustine, N. K. Pandey, U. Kamachi Mudali, R. Natarajan and J.B. Joshi, “Determination of the composition of NO_x gases during the reprocessing of spent nuclear fuel”, Poster presentation in CHEMENT– 2014, 06 – 07 MARCH – 2014, Kalpakkam
 8. **N.Desigan**, Elizabeth Augustine, Remya Murali, N.K.Pandey, U.Kamachi Mudali, R.Natarajan, “Determination of activation energy for the Dissolution of sintered UO₂ Pellet in Nitric Acid”, Poster presentation in SESTEC 2014 conference, BARC from Feb 25-28, 2014
 9. **N. Desigan**, Elizabeth Augustine, Remya Murali, N. K. Pandey, U. Kamachi Mudali, R. Natarajan, Nirav Bhatt and J. B. Joshi, “Kinetic study on the dissolution of sintered UO₂ pellet in HNO₃”, Poster presentation in CHEMCON 2013 held at ICT Mumbai from December 27-30, 2013



N. DESIGAN

**DEDICATED TO
MY BELOVED MOM,
WIFE AND KIDS**

ACKNOWLEDGEMENTS

I am extremely thankful to **The Almighty** for this cheerful life. I express my sincere gratitude to **Prof. U. Kamachi Mudali** for guiding me through this research work. I am greatly indebted to him for his efforts in getting all the fuel pellets required for the current research work. His vision was instrumental in choosing an appropriate simulated MOX fuel system which helped me to a great extent in working out the strategy to study the urania plutonia MOX fuel dissolution behaviour systematically.

I also extend my gratitude to **Prof J. B. Joshi**, my co-guide, for his technical guidance all through my research work. More than a co-guide he has been my mentor. in spite of being physically away from me at Mumbai and at times even in abroad, he was more than efficient in guiding me through this research work.

I sincerely express my heart felt gratitude to **Dr. R. Natarajan**, former Director, RPG, IGCAR, for his motivational presence. My interactions with him helped me to fine tune my work as and when required. I am also greatly indebted to him for introducing me to experts like **Prof U. Kamachi Mudali** and **Prof J. B. Joshi**.

I am also greatly indebted to **Dr. A. Ravisankar**, Director, Reprocessing Group, IGCAR who was kind enough to provide me with the required facilities to complete my PhD.

I also thank the members of my DC, **Prof. S. Anthonysamy** and **Dr. C. Mallika** for their technical supports all through the tenure of my Ph.D. I am particularly grateful to **Shri N K Pandey**, Head, RR&DD, who provided me with sufficient opportunities to work in other R&D areas relevant to reprocessing along with my Ph.D. This helped me in deriving inspirations and ideas from those work which were very relevant and useful to my own research works.

Shri N. K. Pandey and **Dr. Nirav P Bhatt** of IIT, Madras has offered great support in fine tuning the data analysis. All the technical discussions that I had with them were very informative.

The assistance rendered by **Dr. S. Ganesh** in carrying out MOX dissolution experiments, by **Smt. Elizabeth Augustine** and **Ms. Remya Murali** in UO₂ dissolution experiments were timely and appropriate. They provided me with reliable hands for carrying out experiments promptly and precisely. The assistance of **Smt. Elizabeth Augustine** in carrying out the data analysis extensively needs a special mention here.

Shri P Velavendan helped in carrying out the NO_x composition analysis by IC which was very important from the context of this thesis. The motherly presence of **Smt. Ramakannan** all through my work was very motivating and her assistance was beyond words. The innumerable discussions that I had with **Dr. R. Srinivasan** and **Dr. Felix Lawrence** were thought provoking and enlightening. The presence of **Shri Chinnusamy** during the sintering of simulated MOX pellets helped me to overcome the physical and mental fatigue at odd hours.

I am also thankful to **Dr. R. V. Subba Rao** and **Shri K. Dhamodaran** for providing me with sufficient quantities of MOX pellets required for the current research work.

The technical and experimental assistance provided by the staff members of the then Advanced Fuel Studies Section (AFSS), MC&MFCG headed by **Dr. K. Ananthasivan** in preparing the simulated MOX pellets were timely and thankless. I was particularly indebted to **Shri Dasarath Maji** and **Shri Yuvaraj** for their help. **Dr. R. Venkatakrishnan** and **Dr. Chandramouli** provided me with suitable equipments and gadgets at appropriate time.

The sample analysis during the simulated MOX pellet studies was possible thanks to the **Prof. N. Sivaraman** who humbly taught and helped me to analyze them by HPLC in his lab. During several occasions I had thought provoking and informative discussions with him and **Dr. C. V. S. Brammananda Rao** that helped me in fine tuning the experiments. I am also grateful to **Dr. T. S. Lakshmi Narasimhan** in particular for his assistance in improving the readability of the thesis in putting forward my findings in a logical and meaningful way.

No official work is complete without the presence of one's family members who play a very intimate role in their success. I am no way exceptional to this fact. My better half **Smt Jayashree** was very understanding and stood by me all the time. She was my power backup with her soothing and nourishing influence. My mother **Smt Padmasini** is the sole stake holder of all my motivation. Ever since I lost my dad early in my life, she was my world. But for her sincere effort in bringing me up, I would be nowhere near to where I am socially now.

Sometimes we derive ideas, motivation, inspiration etc from unknown and unexpected corners. My kids, master **Ashwath** and Ms **Anjana**, played that role perfectly for me. All the discussions that I had with them improved my understanding of basic science. It is

their constant above par performance in all their activities that kindled me to strive for achieving more. It was all their probing questions that made me to redefine the way I documented all my work so that they are vivid enough to be understood by any reader.

As with anyone, my acknowledgement is also endless as I have many more left out to be thanked in inspiring me in many ways however miniscule they are. All those friends with whom I shared the best of my successes and failures during my school and college days, all my teachers who inspired me to take up science as my career, all my NCC (national cadet corps) instructors and friends who played their part to instill some good character in me and so on.

Finally I would like to thank the former and present Directors of IGCAR and HBNI for providing me with facilities and opportunities to carry out my research work.

At this juncture I also would take this opportunity to thank all the staff members of RPG and RRDD in particular who had contributed towards the betterment of my research work.



N. DESIGAN

CONTENTS

	Page No.
SYNOPSIS	xxv
LIST OF FIGURES	xxxv
LIST OF TABLES	xl
LIST OF ABBREVIATIONS	xli
LIST OF SYMBOLS	xliii

CHAPTER 1

Introduction

CHAPTER 1.	Introduction	1
1.1.	The need for energy sources	1
1.2.	Disadvantages of fossil fuels.....	2
1.3.	Why Nuclear Energy?	3
1.4.	Nuclear Fuel Cycle.....	4
1.5.	Spent nuclear fuel.....	5
1.6.	Management of spent nuclear fuel	6
1.7.	Three stage Indian Nuclear Power Program	7
1.8.	UO ₂ as nuclear fuel	8
1.9.	MOX as nuclear fuel	12
1.10.	Aim and scope of the thesis	13
1.11.	References	14

CHAPTER 2

Spent Nuclear Fuel Reprocessing

CHAPTER 2.	Spent nuclear fuel reprocessing.....	16
2.1.	Why reprocessing?.....	16
2.2.	Nature of spent nuclear fuel	16
2.3.	Choice of reprocessing process.....	17
2.4.	Chemistry of the reprocessing of spent nuclear fuel by PUREX process.....	18

2.4.1.	Chemistry in the head-end steps in the PUREX process	19
2.4.1.1.	Chemistry involved in the decladding of nuclear fuel	19
2.4.1.2.	Chemistry involved in the dissolution of nuclear fuel	20
2.4.1.2.1.	Dissolution reactions	23
2.4.1.2.1.1.	Dissolution of uranium metal.....	23
2.4.1.2.1.2.	Dissolution of plutonium metal (in the presence of HF).....	23
2.4.1.2.1.3.	Dissolution of UO ₂ with emission of NO _x gases.....	23
2.4.1.2.1.4.	Dissolution of PuO ₂ with emission of NO _x gases	24
2.4.1.2.1.5.	Dissolution of UC, PuC and their mixture	24
2.4.1.2.2.	Kinetics, mechanism and modeling of dissolution.....	25
2.4.1.3.	Chemistry of the dissolver off-gas treatment	25
2.4.1.3.1.	Gas phase reactions	25
2.4.1.3.2.	Liquid phase reactions.....	25
2.4.1.4.	Decladding chemistry.....	26
2.4.1.5.	Chemistry of feed clarification.....	27
2.4.2.	Chemistry involved in feed conditioning.....	27
2.4.2.1.	Conditioning by chemical methods.....	27
2.4.2.2.	Conditioning by electrochemical methods.....	28
2.4.3.	Chemistry of solvent extraction process	30
2.4.4.	Chemistry of U/Pu partitioning in the PUREX process.....	31
2.4.5.	Chemistry of the uranium purification cycle.....	32
2.4.6.	Chemistry of the plutonium purification cycle	32
2.4.7.	Chemistry of the tail-end processes during reprocessing.....	33
2.5.	Options for the dissolution of spent nuclear fuel in aqueous media	34
2.6.	Importance of studying UO ₂ and MOX dissolution kinetics	35
2.7.	References.....	36

CHAPTER 3

Literature review on the dissolution of nuclear fuel

3.1	Introduction.....	42
3.2	Aqueous dissolution of urania, plutonia and their powders and pellets	42
3.3	Effect of various parameters on UO ₂ dissolution in nitric acid.....	49

3.3.1	Effect of initial concentration of the acid	49
3.3.2	Effect of mixing/agitation rate.....	50
3.3.3	Effect of temperature	50
3.3.4	Effect of specific surface area of the pellets	51
3.3.5	Effect of the presence of other ions/species	51
3.4	Dissolution of PuO ₂ in nitric acid.....	51
3.5	PuO ₂ dissolution in aqueous acids with fluoride promoters.....	52
3.6	PuO ₂ dissolution in HNO ₃ -Ce(IV) solution.....	54
3.7	PuO ₂ dissolution in HNO ₃ with other additives	56
3.8	Dissolution of PuO ₂ in medium other than nitric acid.....	57
3.9	Dissolution of MOX fuel in nitric acid.....	57
3.9.1	Dissolution of urania, plutonia MOX fuel in nitric acid.....	57
3.9.2	Dissolution of urania, thoria MOX fuel in nitric acid	58
3.10	Other means of dissolving nuclear materials.....	59
3.10.1	Chemical dissolution using reagents other than nitric acid	59
3.10.2	Sonochemical or Ultrasound aided dissolution of nuclear fuel materials	60
3.10.3	Photochemical dissolution of nuclear fuel materials	62
3.10.4	Microwave assisted dissolution of nuclear materials	63
3.10.5	Electrochemical dissolution of nuclear fuel materials.....	64
3.10.6	Electrolytic dissolution of nuclear fuel materials	66
3.10.7	Other modes of dissolving nuclear fuel materials	67
3.11	Consolidation of literature information on nuclear fuel dissolution.....	68
3.11.1	Dissolution of UO ₂	68
3.11.2	Role of nitrous acid and NO _x gas composition on UO ₂ dissolution kinetics.....	68
3.11.3	Nitric acid as the medium for nuclear fuel dissolution.....	69
3.11.4	MOX fuel dissolution	69
3.11.5	Dissolution behaviour of simulated MOX fuel	70
3.12	References.....	71

CHAPTER 4

Experimental

4.1. Procurement of UO ₂ pellets	79
4.2. Physical characterization of UO ₂ pellets	79
4.3. Physical characterization of MOX pellets	80
4.4. Reagents used in the experiments.....	81
4.5. Free acidity measurement.....	82
4.6. Analysis of nitrous acid	82
4.7. Analysis of the composition of NO _x gas evolved during dissolution	83
4.8. Analysis of uranium in UO ₂ and UO ₂ -PuO ₂ MOX fuel dissolution studies	83
4.9. Analysis of U and Ce in UO ₂ -CeO ₂ simulated MOX fuel dissolution studies.....	84
4.10. Analysis of plutonium.....	84
4.11. Analytical techniques and instruments used.....	84
4.12. References	85

CHAPTER 5

Dissolution kinetics of UO₂ pellets in nitric acid medium

5.1	Design of reactor for UO ₂ dissolution.....	89
5.2	Choice of the concentration of nitric acid.....	90
5.3	Choice of temperature for the dissolution experiments	92
5.4	Effect of initial concentration of nitric acid and temperature on UO ₂ dissolution	93
5.4.1	Experimental Procedure.....	93
5.4.2	Modeling of the dissolution of UO ₂ in nitric acid by SCM.....	94
5.4.3	Results and Discussion	97
5.4.3.1.	Effect of concentration of nitric acid	97
5.4.3.2.	Effect of temperature	98
5.4.4	Conclusion based on the initial experiments on UO ₂ dissolution in HNO ₃	103
5.5	Effect of mixing on the dissolution kinetics of UO ₂ pellets in nitric acid	103
5.5.1	Introduction.....	104

5.5.2	Experimental procedure	104
5.5.3	Results and discussion	105
5.5.3.1	Role of nitrous acid	106
5.5.4	Conclusions of experiments on the mixing effect on UO ₂ dissolution rate	110
5.6	Effect of temperature on the intrinsic kinetics of UO ₂ dissolution	110
5.6.1	Introduction	110
5.6.2	Experimental details and procedure	111
5.6.3	Results and discussion	111
5.7	Determination of the composition of NO _x gas evolved during dissolution	113
5.7.1	Importance of measurement of NO _x gas composition during dissolution.....	113
5.7.2	Principle of analysis	114
5.7.3	Reactions involved.....	114
5.7.4	Experimental setup and procedure	115
5.7.5	Analytical instruments	116
5.7.6	Analytical procedure	116
5.7.7	Results and conclusion on NO _x gas compositions measurements.....	118
5.8	Mechanism of UO ₂ dissolution relevant to PUREX process	118
5.8.1	Introduction.....	118
5.8.2	Consolidation of experimental observations.....	119
5.8.3	Proposed mechanism for UO ₂ dissolution under PUREX conditions	121
5.8.3.1.	Time zone 1: (0 to 300 min).....	121
5.8.3.2.	Time zone 2: (300-600 min)	123
5.8.3.3.	Time zone 3: (above 600 mins).....	123
5.8.4	Conclusion on the proposal of UO ₂ dissolution mechanism.....	125
5.9	Effect of surface area	125
5.9.1.	Basis for studying the surface area effect on dissolution kinetics	125
5.9.2.	Experimental procedure	126
5.9.3.	Surface area measurements during the dissolution of UO ₂ in HNO ₃	126
5.9.4.	Principle of surface area measurements.....	127
5.9.5.	Results and discussion for the surface area measurements.....	128
5.10	Modeling of UO ₂ dissolution reaction	131

5.10.1.	Introduction about solid-liquid reactions.....	131
5.10.2.	Basis of modeling	131
5.10.3.	Methodologies of modeling.....	132
5.10.3.1	Method 1 – Based on surface penetration phenomenon.....	133
5.10.3.1.1	Case-I: Considering the effect of nitrous acid	134
5.10.3.1.2	Case II: Neglecting the effect of HNO ₂	140
5.10.3.2	Method 2 – Based on surface area measurements	143
5.10.3.2.1	Method – 2A: Correlation of the surface area to the conversion.....	144
5.10.3.2.2	Method – 2B: Based on surface area estimations.....	144
5.10.3.2.2.1	Case 1	146
5.10.3.2.2.2	Case 2	148
5.10.3.2.2.3	Case 3	150
5.10.3.2.2.4	Case 4	152
5.10.3.3	Method 3 - Considering non-ideal nature of particle during reaction	154
5.10.3.3.1	Introduction	154
5.10.3.3.2	Generalized characteristics of the shrinking particle model.....	154
5.10.3.3.3	Interaction of chemical reaction and diffusion	155
5.10.3.3.4	Fluid–solid mass transfer coefficients	156
5.10.3.3.4.1	Reaction area and reaction order with respect to solid phase component	158
5.10.3.3.4.1.1.	Case 1	163
5.10.3.3.4.1.2.	Case 2	164
5.10.4.	Conclusion on modeling of UO ₂ dissolution reaction	166
5.11	References	167

CHAPTER 6

Fabrication and dissolution studies of UO₂-CeO₂ simulated MOX pellets

6.1	Introduction.....	173
6.2	Justification for using Ce as the surrogate for Pu	173
6.3	Fabrication of UO ₂ -CeO ₂ simulated MOX pellets	174
6.3.1.	Introduction.....	174

6.3.2.	Chemicals used	174
6.3.3.	Preparation of simulated MOX powder by gel combustion synthesis	174
6.3.4.	Calcination and sintering	175
6.4	Characterisation of powders and compacts	175
6.5	Effect of initial acidity on the dissolution kinetics of simulated MOX pellets	177
6.5.1.	Introduction.....	177
6.5.2.	Results and discussion	177
6.6	Effect of cerium composition	180
6.6.1.	Preamble	180
6.6.2.	Experiments, results and discussion	180
6.7	Effect of mixing on the dissolution kinetics of simulated MOX pellets	182
6.7.1.	Introduction.....	182
6.7.2.	Experiments, results and discussion	182
6.8	Effect of temperature on the dissolution kinetics of simulated MOX pellets.....	184
6.8.1.	Introduction.....	184
6.8.2.	Experiments, results and discussion	184
6.8.3.	Role of nitrous acid on the dissolution of simulated MOX pellets.....	185
6.9	Modeling of simulated MOX dissolution behavior	187
6.9.1.	Introduction.....	187
6.9.2.	Methodologies	187
6.9.2.1.	Method 1 – Based on surface penetration of nitric acid into pellets	188
6.9.2.1.1.	Case-I: Considering the effect of nitrous acid to be negligible.....	188
6.9.2.1.2.	Case II: Neglecting the autocatalytic effect of uranyl ion in solution	191
6.9.2.2.	Method 2: Considering non-ideal nature of particle during the reaction.....	195
6.9.2.2.1.	Introduction	195
6.9.2.2.2.	Model equations	195
6.9.2.2.2.1.	Case 1: Order w.r.t. nitric acid is 1	196
6.9.2.2.2.2.	Case 2: Order w.r.t. nitric acid is 2	198
6.10	Conclusion on the modeling of simulated U, Ce MOX pellet dissolution	199
6.11	References.....	201

CHAPTER 7

Dissolution studies of $\text{UO}_2\text{-PuO}_2$ MOX pellets in nitric acid medium

7.1	Introduction.....	203
7.2	Nature of fuel pellets	203
7.3	Erection of the experimental set-up.....	204
7.4	Effect of initial concentration of nitric acid on the dissolution kinetics.....	204
7.5	Effect of temperature on the dissolution kinetics of MOX.....	209
7.6	Effect of mixing on the dissolution kinetics of MOX pellets in nitric acid.....	212
7.7	Evaluation of dissolution kinetics of $\text{UO}_2\text{-PuO}_2$ fuel pellets.....	216
7.7.1	Introduction.....	216
7.7.2	Methodologies	216
7.7.2.1.	Method 1 – Based on surface penetration of nitric acid into solid pellets.....	216
7.7.2.1.1.	Case-I: Considering the effect of nitrous acid to be negligible.....	217
7.7.2.1.2.	Case II: Neglecting the autocatalytic effect of uranyl ion in solution	220
7.7.2.2.	Method 2: Considering non-ideal nature of particle during the reaction.....	224
7.7.2.2.1.	Introduction.....	224
7.7.2.2.2.	Model equations.....	224
7.7.2.2.2.1.	Case 1: Order w.r.t. nitric acid is 1	225
7.7.2.2.2.2.	Case 2: Order w.r.t. nitric acid is 2	227
7.7.3	Conclusion on the modeling of simulated U, Pu MOX pellet dissolution	228
7.8	Post justification of using cerium as a surrogate of plutonium	230
7.9	Overall rate equation for the nuclear fuel dissolution process	230
7.10	References.....	231

CHAPTER 8

Conclusion and Scope for future work

8.1.	Summary of the findings of the current work	232
8.1.1	Major findings of UO_2 fuel pellet dissolution studies.....	232
8.1.2	Major findings of simulated MOX fuel pellet dissolution studies.....	233

8.1.3	Major findings of U, Pu MOX fuel pellet dissolution studies	233
8.2.	Scope for future work.....	234
8.2.1	Surface area measurement for radioactive samples	234
8.2.2	Dissolution experiments on radioactive spent fuel samples	235
8.2.3	Dissolution of MOX fuel with varying plutonium composition.....	235

CHAPTER 9

Appendix

9.1.	Derivation of rate equations for the modelling of UO ₂ dissolution.....	236
9.2	Derivation of rate equations for the modelling of simulated MOX fuel dissolution.....	239
9.3.	Derivation of rate equations for the modelling of (U, Pu) MOX fuel dissolution	240

SYNOPSIS

Preamble

The ever increasing demand for energy world over and particularly in developing countries like India has resulted in exploring and harnessing various sources of energy [1]. Nuclear energy is an attractive option, among all the sources, as it is environmentally benign and practically inexhaustible [2]. While considering the nuclear fuel cycle, reprocessing of spent nuclear fuel is an important step as it retrieves the unused as well as freshly generated fissile material for recycling. India has judiciously adopted a three stage nuclear power program following closed fuel cycle to generate huge electricity. This could be possible by deploying the abundant Thorium reserve of our country at the third stage of its nuclear power program in securing our long term energy security. The first stage involves setting up of Pressurised Heavy Water Reactors (PHWRs) driven by natural UO_2 fuel and the second stage involves the setting up of Fast Breeder Reactors (FBRs) employing Pu obtained by reprocessing the spent fuel from the PHWRs. Reprocessing of spent nuclear fuel adopts the PUREX (Plutonium Uranium EXtraction) process which involves chopping of fuel rods/pins into small pieces, dissolution in nitric acid, solvent extraction using TBP (Tri-n-butyl phosphate)-diluent medium and separation of U and Pu by further extraction and striping. It is during dissolution that the spent fuel is brought into a suitable physical and chemical form amenable for further unit operations. The kinetics of dissolution of the spent fuel is a necessary input data for the design of dissolvers and route for batch and continuous dissolution. Hence the present work intended to study and establish the dissolution kinetics of typical nuclear fuel materials including UO_2 , simulated UO_2 based mixed oxide (MOX) and UO_2 - PuO_2 MOX fuel in nitric acid medium relevant to PUREX process.

To study the dissolution behaviour of a simulated MOX fuel, CeO_2 was used as the non-radioactive surrogate for PuO_2 [3]. The experimental, analytical and mathematical modeling procedures employed initially in understanding the dissolution of UO_2 fuel system in nitric acid was subsequently extended for evaluating the dissolution kinetics of UO_2 - CeO_2 and UO_2 - PuO_2 MOX fuel systems

in nitric acid under typical PUREX (Plutonium Uranium EXtraction) process conditions.

Objectives and scope of the thesis

The main goal of this thesis is to develop a chemical model (combination of mass transfer and chemical reaction) for the dissolution of UO_2 , $\text{UO}_2\text{-CeO}_2$ and $\text{UO}_2\text{-PuO}_2$ nuclear fuels in nitric acid medium. This model will allow to compute the overall rate of the reaction in terms of concentrations of participating species etc., temperature and particle characteristics (size and shape distribution, contact area, etc.) of fuels based on model-based analysis of experimental data. Thus main objectives are (i) investigation of dissolution kinetics of UO_2 , simulated $\text{UO}_2\text{-CeO}_2$ and $\text{UO}_2\text{-PuO}_2$ MOX fuels in nitric acid, and (ii) development of a detailed dissolution model equation to understand the kinetics of dissolution.

Methodology of the study

Initial experiments were carried out to study the effect of mixing intensity on the dissolution kinetics of various fuel systems. Under saturated conditions of mixing, the effect of diffusion on the overall reaction kinetics is at its barest minimum and the kinetics to be determined under these conditions will be intrinsic in nature. The mass transfer coefficient was estimated under such conditions. This coupled with mechanism of the reaction was made use in evaluating the overall reaction kinetics. This methodology was systematically followed for UO_2 fuel followed $\text{UO}_2\text{-CeO}_2$ and then $\text{UO}_2\text{-PuO}_2$ dissolution studies.

Organization of the thesis

The thesis is organized into seven technical chapters followed by the conclusion and the references at the end. The first three chapters provide the background of this thesis with general & specific introduction and the detailed literature survey. Chapter 4 comprises the experimental part of the thesis. The results of the dissolution studies and the evaluation of the dissolution kinetics of UO_2 fuel, $\text{UO}_2\text{-CeO}_2$ simulated MOX fuel and $\text{UO}_2\text{-PuO}_2$ fuel in nitric acid respectively forms the fifth and sixth chapters. The overall rate expression for the dissolution of MOX fuel in nitric acid is given in the seventh chapter.

Chapter 1 - Introduction

The growing population all over the world has led to an increasing demand for the available natural resources in meeting the world's growing energy requirements [4]. This coupled with the advantages and the uniqueness of nuclear power over other modes of power generation [5], and the huge Th reserve in the country are the strong reasons behind the choice of nuclear route as one of the option for securing the long-term energy requirement of the country. Initially UO_2 was used extensively as the driver nuclear fuel for the thermal reactors. Subsequently with the generation of Pu^{239} in these reactors, MOX fuel became the prominent driver fuel for FBRs due to its favorable neutronic properties in the fast neutron spectrum [6]. Hence the study of U and Pu based nuclear fuel materials and their behaviour in the nuclear fuel cycle operations are important and have evolved over the years.

Chapter 2 – Spent nuclear fuel reprocessing

Primarily there are two ways of managing the spent nuclear fuel namely **open fuel cycle** and **closed fuel cycle** options. Reprocessing offers many advantages like extraction of more energy from the given fuel, conservation of natural resources, better management of nuclear wastes, minimization of environmental impact, strengthening the fuel cycle economics and its sustainability, better proliferation resistance and so on. Chemically the spent nuclear fuel practically comprises of almost all the elements in the periodic table barring the lower atomic number elements below Iron. Though the typical chemical composition of the spent fuel varies depending on the type of reactor from which it is discharged and its burnup, the overall composition remains more or less the same. The choice of method for reprocessing the spent fuel depends on its chemical nature [7]. This thesis, as it deals with dissolution of oxide fuel in nitric acid medium, considers only the PUREX process. This chapter also explains the basic chemistry involved in the reprocessing of spent MOX fuel by PUREX process stepwise [8].

Chapter 3 – Literature survey

This chapter consolidates the information prevailing in the open literature on dissolution behaviour of urania and its mixtures with other actinide oxides in various acid media. As the current topic is more relevant to MOX dissolution in nitric acid, more emphasis is given for urania and (U, Pu) MOX fuel dissolution.

Many previous works have reported the effect of various parameters like acidity, temperature, mixing intensity, presence of U(VI) etc on the dissolution kinetics of UO_2 in nitric acid [9, 10]. Some of the work also attempted to understand the reaction mechanism and dissolution kinetics [11-14]. But none could address the dissolution behaviour of UO_2 under typical PUREX plant conditions till date. For the dissolution of Pu rich MOX fuel which is relatively difficult there are only limited information available in the literature [9, 15]. It was with this background that the current research work was initiated with an aim to evaluate the dissolution kinetics of Pu rich MOX fuel which is the typical driver fuel for FBRs whose results would pave way for designing a continuous dissolution process system. To achieve this, it was decided to first study the dissolution behaviour of UO_2 in nitric acid systematically followed by similar studies with a simulated MOX fuel using CeO_2 as the non-radioactive surrogate for PuO_2 . Minimum and necessary experiments will be carried out with the UO_2 - PuO_2 fuel pellets to evaluate its intrinsic kinetics.

Chapter 4 - Experimental

Sintered UO_2 pellets were obtained from NFC, Hyderabad and its dissolution studies were carried out to evaluate its kinetics. Typical PUREX process conditions were chosen for the studies like 80°C , 8M starting nitric acid etc. The dissolution experiments were carried out in a cylindrical glass vessel with all necessary provisions to measure and control temperature and mixing rate. The off-gas was passed through a reflux condenser and scrubbed in sodium hydroxide and DM water bubblers to completely trap and analyze the composition of the NO_x gases evolved during the dissolution. The parameters estimated during the course of dissolution like free acidity, uranium, plutonium, nitrous acid, cerium, composition of NO_x in the off-gas etc were analyzed by standard procedures like titrimetry, spectrophotometry, radiometry and ion chromatography. The surface area of the pellets during the course of dissolution was measured by adsorption method.

Chapter 5 - Dissolution kinetics of UO_2 pellets in nitric acid

The dissolution rate of sintered UO_2 pellets in nitric acid was found to be proportional to the initial nitric acid concentration and temperature [16]. Shrinking core model was invoked to evaluate the rate parameters of the dissolution reaction.

The apparent activation energy for the reaction was estimated to be 85kJ/mol and 97.5kJ/mol respectively with 8.05M and 10.28M starting nitric acid concentrations and the pseudo first order rate constant was estimated in the temperature range of 60-90°C with different starting nitric acid concentrations. It was found that the reaction rate was inversely related to the mixing intensity [17]. Under the experimental conditions, the reaction rate gradually decreased from unstirred to about 600 rpm of stirring rate. Further increase in mixing doesn't change the reaction rate practically. Hence it was concluded that the diffusion control of the reaction was at its barest minimum from 600 rpm and upwards of mixing intensity under the conditions of the experiments. Also the plot of [U] / percentage dissolved against time gave a sigmoidal distribution indicating an autocatalytic behaviour. It was found that nitrous acid produced insitu during the course of dissolution at the pellet-solution interface, plays an autocatalytic role in the oxidative dissolution of UO₂ in nitric acid. The role of nitrous acid on the dissolution was further established in the presence of hydrazine in which case the dissolution rate was very low [18]. The change in surface area of the pellet during the course of dissolution was determined as it would be required for evaluating the reaction rate. The composition of the NO_x (NO & NO₂) gas evolved during the course of dissolution was measured by ion chromatography. Based on the concentration profiles of uranium, nitric acid, nitrous acid and the NO_x gases, the mechanism of the dissolution process was determined under typical PUREX process conditions.

For UO₂ dissolution in nitric acid, as the mass transfer effect was found to be at minimum starting from the mixing intensity of 600 rpm and upwards, it was decided to carry out the data analysis of the results to evaluate the kinetics only at 600 rpm. The same was also followed during the data analysis of the dissolution behaviour of simulated and the actual MOX fuel in nitric acid.

Primarily three different methods were used and compared for the modelling and determination of kinetic parameters of UO₂ dissolution reaction in nitric acid. The first method was based on penetration theory [19]. In this method the entire reaction was split into two processes, namely penetration and the chemical reaction. Model equations based on the weight of the pellet dissolved, exposed to acid and unexposed were developed to predict the concentration profiles of the experiment.

The model was found to predict the experimental data reasonably well. The values of rate constant for the penetration and chemical reaction process were estimated for different conditions of temperature and stirring speed. The apparent activation energy estimated in the experimental temperature range was found to be 72kJ/mol and 44.3kJ/mol for the penetration and chemical reaction processes at 600 rpm. These values indicate that the reaction is chemical reaction controlled under these conditions.

The second method for modelling dissolution reaction was based on the correlation of the surface area to the conversion rate. But since the method of surface area measurement has a sizeable amount of uncertainty in it, this method wasn't found to be very accurate and hence it wasn't perused further. The method was then modified to use the surface area measured for the dissolving pellet under static condition, in this case using nitrogen physisorption. The total surface area of the pellet, including the open pores, is assumed to react with the nitric acid as a whole in this method. The model equation was developed using the measured surface area, concentration of nitric acid and that of uranium in the solid. A rate equation was derived which seemed to predict the concentration profiles of uranium in solid and nitric acid reasonably well. Rate was measured at various temperatures.

The surface nature of a dissolving solid in liquid will exhibit a non-ideal behaviour in reality. Hence a third method was developed for modelling the dissolution reaction which introduces a new parameter called the shape factor [20, 21]. The method invokes the shrinking core theory and uses a generalized Thiele modulus to predict the concentration profiles. It calculates and uses Sherwood, Reynolds and Schmidt numbers for the prediction. The concentration profiles of nitric acid and uranium predicted by the model was found to be fitting satisfactorily. The activation energy estimated for the overall reaction in the temperate range of 343-363K was 41.6kJ/mol which again confirms that the dissolution of UO_2 in nitric acid is chemical reaction controlled.

Chapter 6 - Dissolution studies of UO_2 - CeO_2 MOX pellets in nitric acid

This chapter deals with the fabrication and the results of the dissolution experiments on the simulated (U, Ce) MOX pellets in nitric acid. The pellets were fabricated using standard established procedures. The results indicate the increase

in dissolution rates under similar conditions when the pellets are more homogeneous with respect to its chemical composition. The results also indicate the reduction in dissolution rate as more CeO_2 is added to the pellet. Mixing intensity was found to have an inverse effect on the dissolution rate of $\text{UO}_2\text{-CeO}_2$ pellets and only minor positive effect on plain Ceria pellets under similar experimental conditions. This proves that both urania and ceria doesn't follow the same mechanism during their dissolution in nitric acid. Similar results were observed during the dissolution of $\text{UO}_2\text{-PuO}_2$ pellets in nitric acid.

Chapter 7 – Dissolution kinetics of $\text{UO}_2\text{-PuO}_2$ MOX pellets in nitric acid

The results of the dissolution experiments were analyzed for the determination of the kinetic parameters like rate constant and apparent activation energy for all the type of fuel employed in this work. The effect of various parameters like acidity, temperature, mixing intensity and presence of other species on the dissolution rate of all the fuel used in this research studies have been established. The results clearly indicate that the dissolution is chemical reaction controlled and there is a lot of scope in the design of the continuous dissolution system for increasing the throughput of the dissolution process in a nuclear fuel reprocessing facility.

Conclusion and scope for future work

The chemical aspects of the dissolution of a typical fast reactor nuclear fuel was studied systematically starting with UO_2 fuel pellets. The gradual understanding of the dissolution behaviour of PuO_2 based fuels was gained by first studying $\text{UO}_2\text{-CeO}_2$ fuel where Ce is employed as a non-radioactive surrogate of Pu. Finally few experiments were carried out with $\text{UO}_2\text{-PuO}_2$ fuel system under typical PUREX process conditions which paved way for understanding the dissolution chemistry of this fuel. The data generated through this research studies would be useful for designing a continuous dissolution system for FBR spent fuel reprocessing.

The methods employed in the present research will be further extended in studying the dissolution behaviour of various other nuclear fuel systems in a similar way. In the future, dissolution studies of spent nuclear fuel in appropriately shielded systems could also be taken up to provide a real assessment of the rate equations proposed in the present thesis work.

References

1. Frank Niele, "Energy – Engine of Evolution", First edition, Shell Global Solutions, 2005 Elsevier Publications,
2. Raymond L Murray, Keith E Holber, "Nuclear Energy – An introduction to the concepts, systems and applications of nuclear processes", 7th Edition, Elsevier 2015
3. Han Soo Kim et al., "Applicability of CeO₂ as a surrogate for PuO₂ in a MOX fuel development", J Nucl. Mat., 378 (2008) 98-104
4. BP statistical review of world energy 2015
5. Balasubramanian Viswanathan, "Energy Sources. Fundamentals of Chemical Conversion Processes and Applications", 2016 Elsevier Publications
6. V. S. Yemel'yanov and A.L Yevstyukhin, "The Metallurgy of Nuclear Fuel - Properties and Principles of the Technology of Uranium, Thorium and Plutonium", Translated by Anne Foster, 1969 Pergamon Press Ltd.
7. IAEA Tecdoc 1587, "Spent fuel reprocessing options", IAEA, Vienna, 2008;
8. A. P. Paiva, P. Malik, "Recent advances on the chemistry of solvent extraction applied to the reprocessing of spent nuclear fuels and radioactive wastes", J Radioanal. Nucl. Chem., Vol. 261, No. 2 (2004) 485-496
9. Uriarte, A. L.; Rainey, R. H. Dissolution of high-density UO₂, PuO₂ and UO₂-PuO₂ pellets in inorganic acids; Technical Report ORNL-3695. Oak Ridge National Laboratory, Union Carbide Corporation 1965.
10. Taylor, R. F.; Sharratt, E. W.; Chazal, L. E.; Logsdail, D. H. Dissolution rate of uranium dioxide sintered pellets in nitric acid systems. J. Appl. Chem. 1963, 13, 32–40
11. Akihiko Inoue, "Mechanism of the oxidative dissolution of UO₂ in HNO₃ solution", J. Nucl. Mat., 138, 1986, 152-154
12. M. Shabbir, R. G. Robins, "Kinetics of the dissolution of uranium dioxide in nitric acid – I", J. Appl. Chem., 18, 129 (1968)
13. M. Shabbir, R. G. Robins, "Kinetics of the dissolution of uranium dioxide in nitric acid – II", *ibid.*, 19, 52 (1969)
14. Inoue, A.; Tsujino, T. "Dissolution rates of U₃O₈ powders in nitric acid", *Ind.*

- Eng. Chem. Process Des. Dev. 1984, 23, 122–125.
15. Ryan, J. L. and L. A. Bray, 1980. "Dissolution of Plutonium Dioxide - A Critical Review," Actinide Separations, J.D. Navratil and W.W. Schultz eds., ACS Symposium Series, 17th ACS National Meeting, Honolulu, HI, 1980,117, Chapter 35, pp 499–514.
 16. N. Desigan, Elizabeth Augustine, Remya Murali, N.K. Pandey, U. Kamachi Mudali, R. Natarajan, J.B. Joshi, "Dissolution kinetics of Indian PHWR natural UO₂ fuel pellets in nitric acid - Effect of initial acidity and temperature", Prog. Nucl. Ener. 83 (2015) 52-58
 17. N. Desigan, Nirav P Bhatt, N. K. Pandey, U. Kamachi Mudali, R. Natarajan, J. B. Joshi, "Dissolution kinetics of UO₂ in nitric acid – Effect of mixing", Poster presentation in NUCAR 2015 held at Mumbai from Feb 09-13 2015
 18. N. Desigan, N.K. Pandey, U. Kamachi Mudali, J.B. Joshi, "Role of nitrous acid during the dissolution of UO₂ in nitric acid", SESTEC 2016 Proceedings, page 198, SESTEC 2016 held at IIT Guwahati from May 17-20, 2016
 19. Shunji Homma, Jiro Koga, Shiro Matsumoto, Tomio Kawata., Dissolution rate equation of UO₂ pellet, J. Nucl. Sci. Technol., 30(9), 1993, pp. 959-961
 20. Tapio Salmi, Henrik Grénman, Johan Wärn, Dmitry Yu. Murzin., New modelling approach to liquid–solid reaction kinetics: From ideal particles to real particles., Chemical engineering research and design 91, 2013
 21. Tapio Salmi, Henrik Grénman, Johan Wärn, Dmitry Yu. Murzin, Revisiting shrinking particle and product layer models for fluid–solid reactions – From ideal surfaces to real surfaces, Chemical Engineering and Processing 50, 2011.

LIST OF FIGURES

Fig. 1.1.	Latest typical shares and demand for global primary energy by sources	2
Fig. 1.2.	Schematic of Nuclear Fuel Cycle	5
Fig. 1.3.	Three Stage Indian Nuclear Power Program	8
Fig. 1.4.	Various types of interactions between a neutron and nucleus	10
Fig. 1.5.	η values for various fissile nuclides as a function of neutron energy	12
Fig. 2.1.	Schematic diagram of PUREX process flowsheet	19
Fig. 2.2.	Effect of acidity on the K_D of various species in 30% TBP	29
Fig. 4.1.	Typical PHWR natural UO_2 pellets	79
Fig. 4.2.	Typical dimensions of sintered UO_2 pellets	80
Fig. 4.3.	Typical FBR MOX pellet	81
Fig. 5.1.	Schematic sketch of the experimental dissolver with mechanical mixing	90
Fig. 5.2.	Schematic sketch of air sparging dissolution set-up	90
Fig. 5.3.	Cylindrical glass dissolver with mechanical mixing	91
Fig. 5.4.	Glass bubble dissolver with air sparging	91
Fig. 5.5.	General schematic representation of a solid-fluid reaction	94
Fig. 5.6.	Dissolution of UO_2 pellets in 8.05, 10.3 and 11.5 M HNO_3 at 353 K	98
Fig. 5.7.	Effect of temperature on the dissolution of UO_2 pellets in 8.05 M HNO_3	99
Fig. 5.8.	Effect of temperature on the dissolution of UO_2 pellets in 10.3 M HNO_3	100
Fig. 5.9.	Experimental and modelled UO_2 dissolution curves in 8.05 M HNO_3	100
Fig. 5.10.	Experimental and calculated UO_2 dissolution curves in 10.3 M	101
Fig. 5.11.	Arrhenius plot of $\ln(k)$ vs $1/T$ for UO_2 dissolution in 8.05 M HNO_3	102
Fig. 5.12.	Arrhenius plot of $\ln(k)$ vs $1/T$ for UO_2 dissolution in 10.3 M HNO_3	102
Fig. 5.13.	Percentage UO_2 dissolution in nitric acid at various mixing rate	105
Fig. 5.14.	Schematic representation of the effect of mixing intensity	107
Fig. 5.15.	$[HNO_2]$ profile in the reaction mixture during the dissolution of UO_2	108
Fig. 5.16.	Effect of hydrazine on the $[U]$ profile during UO_2 dissolution in nitric acid	109
Fig. 5.17.	Effect of hydrazine on $[HNO_2]$ profile during UO_2 dissolution in nitric acid	109
Fig. 5.18.	Effect of temperature on the dissolution kinetics of UO_2 pellets in HNO_3	112
Fig. 5.19.	HNO_2 concentration profile during UO_2 dissolution at various temperatures	113

Fig. 5.20.	Calibration graph for the nitrate concentration varies from 10-100 ppm	116
Fig. 5.21.	Calibration graph for the nitrite concentration varies from 10-100 ppm	117
Fig. 5.22.	Typical Ion –Chromatogram of nitrite and nitrate ions (10 ppm)	117
Fig. 5.23.	Overlay view of the chromatogram peaks against the base line	118
Fig. 5.24.	Ratio of HNO ₃ consumed to uranium dissolved	120
Fig. 5.25.	Concentration profiles during UO ₂ dissolution	120
Fig. 5.26.	Profiles of [NO], [NO ₂] and [U(VI)/2] during dissolution	121
Fig. 5.27.	Various time zones during the dissolution of UO ₂ in nitric acid	122
Fig. 5.28.	Concentration profiles of NO, NO ₂ , HNO ₂ and uranium in time zone 1	122
Fig. 5.29.	Concentration profiles of NO, NO ₂ , HNO ₂ and uranium in time zone 2	124
Fig. 5.30.	Concentration profiles of NO, NO ₂ , HNO ₂ and uranium in time zone 3	124
Fig. 5.31.	Dissolution of UO ₂ in nitric acid as a function of initial surface area	129
Fig. 5.32.	Surface area profile for UO ₂ dissolution in nitric acid	129
Fig. 5.33.	Variation of specific surface area for UO ₂ dissolution in nitric acid	130
Fig. 5.34.	Experimental and calculated concentration profiles of U and HNO ₃ at 343K	135
Fig. 5.35.	Experimental and calculated concentration profiles of U and HNO ₃ at 348K	136
Fig. 5.36.	Experimental and calculated concentration profiles of U and HNO ₃ at 353 K	136
Fig. 5.37.	Experimental and calculated concentration profiles of U and HNO ₃ at 358 K	136
Fig. 5.38.	Experimental and calculated concentration profiles of U and HNO ₃ at 363 K	137
Fig. 5.39.	Experimental and calculated concentration profiles of U and HNO ₃ at 368 K	137
Fig. 5.40.	Experimental and calculated concentration profiles of U and HNO ₃ at 373 K	137
Fig. 5.41.	Arrhenius plot for determining the E _a of penetration process	138
Fig. 5.42.	Arrhenius plot for nitric acid aided dissolution process	139
Fig. 5.43.	Arrhenius plot for chemical reaction controlled dissolution process	141
Fig. 5.44.	Experimental and calculated concentration profiles of U and HNO ₃ at 353 K	142
Fig. 5.45.	Arrhenius plot for penetration process without the effect of nitrous acid	142
Fig. 5.46.	Arrhenius plot for nitric acid aided dissolution process without HNO ₂	142
Fig. 5.47.	Arrhenius plot for chemical reaction controlled dissolution without HNO ₂	143
Fig. 5.48.	Comparison of experimental and calculated [HNO ₃] profile at 353 K	147
Fig. 5.49.	Comparison of experimental and calculated [U] profile at 353 K	147
Fig. 5.50.	Comparison of experimental and calculated surface area profile	147
Fig. 5.51.	Comparison of experimental and calculated [HNO ₃] profile at 353 K	149

Fig. 5.52.	Comparison of experimental and calculated [U] profile at 353 K	149
Fig. 5.53.	Comparison of experimental and calculated pellet surface area profile	149
Fig. 5.54.	Comparison of experimental and calculated [HNO ₃] profile at 353 K	151
Fig. 5.55.	Comparison of experimental and calculated [U] profile at 353 K	151
Fig. 5.56.	Comparison of experimental and calculated pellet surface area profile	151
Fig. 5.57.	Comparison of experimental and calculated [HNO ₃] profile at 353 K	152
Fig. 5.58.	Comparison of experimental and calculated [U] profile at 353 K	153
Fig. 5.59.	Comparison of experimental and calculated pellet surface area profile	153
Fig. 5.60.	Comparison between experimental and calculated [U(VI)] profiles at 353 K	163
Fig. 5.61.	Comparison between experimental and calculated [HNO ₃] profiles at 353 K	164
Fig. 5.62.	Comparison between experimental and calculated [U(VI)] profiles at 353 K	165
Fig. 5.63.	Comparison between experimental and calculated [HNO ₃] profiles at 353 K	165
Fig. 6.1.	Schematic flow diagram for the fabrication of simulated (U, Ce) MOX pellets	175
Fig. 6.2.	XRD pattern of the sintered simulated MOX pellets of all compositions	176
Fig. 6.3.	Effect of initial [HNO ₃] on the dissolution of (U _{0.78} Ce _{0.22})O ₂ MOX pellets	178
Fig. 6.4.	Acidity profile for the dissolution of (U _{0.78} Ce _{0.22})O ₂ MOX pellets	178
Fig. 6.5.	Concentration profiles during the dissolution of (U _{0.78} Ce _{0.22})O ₂ MOX pellets	179
Fig. 6.6.	U and Ce percentage during the dissolution of (U _{0.78} Ce _{0.22})O ₂ MOX pellets	180
Fig. 6.7.	Effect of Ce on the dissolution kinetics of simulated MOX pellets	181
Fig. 6.8.	Concentration profiles during the dissolution of (U _{0.78} Ce _{0.22})O ₂ MOX pellet in 8M HNO ₃ at 100 and 600 RPM	183
Fig. 6.9.	Concentration profiles during the dissolution of (U _{0.72} Ce _{0.28})O ₂ MOX pellet in 8 M HNO ₃ at 100 and 600 RPM	183
Fig. 6.10.	Effect of temperature on the dissolution rate of simulated MOX pellets	185
Fig. 6.11.	Effect of cerium on the dissolution of (U, Ce)MOX pellets in nitric acid	186
Fig. 6.12.	Effect of mixing on CeO ₂ dissolution rate in nitric acid	187
Fig. 6.13.	Modelled [U] profile for the dissolution of (U _{0.78} Ce _{0.22})O ₂ MOX pellets	190
Fig. 6.14.	Modelled [HNO ₃] profile for the dissolution of (U _{0.78} Ce _{0.22})O ₂ MOX pellets	191
Fig. 6.15.	Modelled [Ce] profile for the dissolution of (U _{0.78} Ce _{0.22})O ₂ MOX pellets	191
Fig. 6.16.	Modelled [U] profile for the dissolution of (U _{0.78} Ce _{0.22})O ₂ MOX pellets	193
Fig. 6.17.	Modelled [HNO ₃] profile for the dissolution of (U _{0.78} Ce _{0.22})O ₂ MOX pellets	194
Fig. 6.18.	Modelled [Ce] profile for the dissolution of (U _{0.78} Ce _{0.22})O ₂ MOX pellets	194

Fig. 6.19. Comparison of experimental and calculated profiles of [U(VI)] at 353 K for $U_{0.78}Ce_{0.22}O_2$ MOX pellet dissolution assuming 1 st order w.r.t. HNO_3	197
Fig. 6.20. Comparison of experimental and calculated 1 st order $[HNO_3]$ profiles at 353 K for $U_{0.78}Ce_{0.22}O_2$ MOX pellet dissolution	197
Fig. 6.21. Comparison of experimental and calculated profiles of [Ce(IV)] at 353 K for $U_{0.78}Ce_{0.22}O_2$ MOX pellet dissolution assuming 1 st order w.r.t. HNO_3	198
Fig. 6.22. Comparison between experimental and calculated profiles of [U(VI)] at 353 K for $U_{0.78}Ce_{0.22}O_2$ MOX pellet dissolution assuming 2 nd order w.r.t. HNO_3	198
Fig. 6.23. Comparison of experimental and calculated 2 nd order $[HNO_3]$ profiles at 353 K for $U_{0.78}Ce_{0.22}O_2$ MOX pellet dissolution	199
Fig. 6.24. Comparison of experimental and calculated profiles of [Ce(IV)] at 353 K for $U_{0.78}Ce_{0.22}O_2$ MOX pellet dissolution assuming 2 nd order w.r.t. HNO_3	199
Fig. 7.1. Schematic sketch of the dissolution set-up for dissolving MOX pellets	204
Fig. 7.2. Effect of initial acidity on the dissolution kinetics of $(U_{0.782}Pu_{0.218})O_2$ MOX pellet at 353 K and 600 RPM	205
Fig. 7.3. Typical dissolution curve for $(U_{0.782}Pu_{0.218})O_2$ MOX pellet in 8 M nitric acid	206
Fig. 7.4. Effect of acidity on the dissolution of $(U_{0.782}Pu_{0.218})O_2$ MOX pellets	207
Fig. 7.5. Effect of acidity on the relative dissolution of UO_2 and PuO_2	207
Fig. 7.6. Consolidated effect of acidity on the dissolution of $(U_{0.782}Pu_{0.218})O_2$ MOX pellet at 80°C and 600 RPM with expanded view in the inset	209
Fig. 7.7. Effect of temperature on the dissolution kinetics of $(U_{0.782}Pu_{0.218})O_2$ MOX pellet in 8 M HNO_3 and 600 RPM	210
Fig. 7.8. Effect of temperature on the composition of the dissolved solution during the dissolution of $(U_{0.782}Pu_{0.218})O_2$ MOX pellet in 8 M HNO_3 at 600 RPM	211
Fig. 7.9. Effect of temperature on the relative dissolution of uranium and plutonium from $(U_{0.782}Pu_{0.218})O_2$ MOX pellet at 8 M nitric acid and 600 RPM	211
Fig. 7.10. Consolidated effect of temperature on the dissolution of $(U_{0.782}Pu_{0.218})O_2$ MOX pellet at 8 M nitric acid and 600 RPM with expanded view in the inset	212
Fig. 7.11. Effect of mixing on the dissolution kinetics of $(U_{0.782}Pu_{0.218})O_2$ MOX pellet in 8 M nitric acid at 353 K	213
Fig. 7.12. Effect of mixing rate on the rate of dissolution of UO_2 and PuO_2 in $(U_{0.782}Pu_{0.218})O_2$ MOX pellet in 8 M HNO_3 at 353 K	214

Fig. 7.13. Effect of mixing rate on the relative dissolution of uranium and plutonium from $(U_{0.782}Pu_{0.218})O_2$ MOX pellet in 8 M nitric acid at 353 K	215
Fig. 7.14. Consolidated effect of mixing rate on the dissolution of $(U_{0.782}Pu_{0.218})O_2$ MOX pellet in 8 M nitric acid at 353 K	215
Fig. 7.15. Modelled uranium concentration profile for the dissolution of $(U_{0.78}Pu_{0.22})O_2$ MOX pellet in 8 M HNO_3 at 348 K and 600 RPM	219
Fig. 7.16. Modeled nitric acid concentration profile for the dissolution of $(U_{0.78}Pu_{0.22})O_2$ MOX pellet in 8 M HNO_3 at 348 K and 600 RPM	219
Fig. 7.17. Modelled plutonium concentration profile for the dissolution of $(U_{0.78}Pu_{0.22})O_2$ MOX pellet in 8 M HNO_3 at 348 K and 600 RPM	220
Fig. 7.18. Modelled uranium concentration profile for the dissolution of $(U_{0.78}Pu_{0.22})O_2$ MOX pellet in 8 M HNO_3 at 353 K and 600 RPM	222
Fig. 7.19. Modelled nitric acid concentration profile for the dissolution of $(U_{0.78}Pu_{0.22})O_2$ MOX pellet in 8 M HNO_3 at 353 K and 600 RPM	222
Fig. 7.20. Modelled plutonium concentration profile for the dissolution of $(U_{0.78}Pu_{0.22})O_2$ MOX pellet in 8 M HNO_3 at 353 K and 600 RPM	223
Fig. 7.21. Comparison of experimental and calculated profiles of [U(VI)] at 353 K for $U_{0.78}Pu_{0.22}O_2$ MOX pellet dissolution assuming 1 st order w.r.t. HNO_3	226
Fig. 7.22. Comparison of experimental and calculated 1 st order $[HNO_3]$ profiles at 353 K for $U_{0.78}Pu_{0.22}O_2$ MOX pellet dissolution	226
Fig. 7.23. Comparison of experimental and calculated profiles of [Ce(IV)] at 353 K for $U_{0.78}Ce_{0.22}O_2$ MOX pellet dissolution assuming 1 st order w.r.t. HNO_3	227
Fig. 7.24. Comparison between experimental and calculated profiles of [U(VI)] at 353 K for $U_{0.78}Ce_{0.22}O_2$ MOX pellet dissolution assuming 2 nd order w.r.t. HNO_3	227
Fig. 7.25. Comparison of experimental and calculated 2 nd order $[HNO_3]$ profiles at 353 K for $U_{0.78}Ce_{0.22}O_2$ MOX pellet dissolution	228
Fig. 7.26. Comparison of experimental and calculated profiles of [Ce(IV)] at 353 K for $U_{0.78}Ce_{0.22}O_2$ MOX pellet dissolution assuming 2 nd order w.r.t. HNO_3	228

LIST OF TABLES

Table 1.1.	Neutron cross-sections of Fissile nuclides	11
Table 1.2.	Comparison of nuclear properties of ^{235}U and ^{239}Pu	12
Table 2.1.	Typical composition of the spent fuel from a commercial LWR	17
Table 3.1.	Chronological list of important literature information relevant to nuclear fuel dissolution as on date	43
Table 4.1.	Typical physical properties of the UO_2 pellets	80
Table 4.2.	Typical physical properties of PFBR inner core MOX pellets	81
Table 4.3.	Analytical techniques and instruments used	85
Table 5.1.	Pseudo 1 st order rate constant for UO_2 dissolution in HNO_3	101
Table 5.2.	The values of the rate constants k_p , k_h and k_c as a function of temperature	138
Table 5.3.	The values of the rate constants k_p , k_h and k_c as a function of temperature	141
Table 5.4.	Estimated values of rate constant at different temperature	148
Table 5.5.	Estimated values of rate constant at different temperature	150
Table 5.6.	Estimated values of rate constant at different temperature	152
Table 5.7.	Estimated values of rate constant at different temperature	153
Table 5.8.	Estimated rate constants at various temperatures	164
Table 5.9.	Estimated rate constants at various temperatures	166
Table 6.1.	Rate constants for the dissolution of simulated MOX fuel	189
Table 6.2.	Rate constants for the dissolution of simulated MOX fuel at different acidity	190
Table 6.3.	Rate constants for the dissolution of simulated MOX fuel at different Temp.	192
Table 6.4.	Rate constants for simulated MOX fuel dissolution at different acidity	193
Table 7.1.	Details of the inner core PFBR MOX pellets	203
Table 7.2.	Rate constants for the dissolution of MOX fuel at different temperatures	218
Table 7.3.	Rate constants for the dissolution of MOX fuel at different acidity	218
Table 7.4.	Rate constants for the dissolution of MOX fuel at different temperatures	221
Table 7.5.	Rate constants for MOX fuel dissolution at different acidity	221

LIST OF ABBREVIATIONS

Abbreviation	Expansion
ADU	Ammonium Diuranate
AFFF	Advanced Fuel Fabrication Facility
AHWR	Advanced Heavy Water Reactor
BARC	Bhabha Atomic Research Centre, Mumbai
BET	Brunauer–Emmett–Teller method of surface area measurement
CANDU	Canada Deuterium Uranium, a Canadian PHWR
CEPOD	Catalyzed Electrolytic Plutonium Oxide Dissolution
CORAL	COmpact Reprocessing of Advanced fuels in Lead shielded facility
CSTR	Continuous Stirred Tank Reactor
DAE	Department of Atomic Energy
FBR	Fast Breeder Reactor
HEPA	High Efficiency Particulate Air
HPLC	High Performance Liquid Chromatography
HTGR	High Temperature Gas-Cooled Reactor
IC	Ion Chromatography
ICPMS	Inductively Coupled Plasma Mass Spectrometer
IDR	Instantaneous Dissolution Rate
IGCAR	Indira Gandhi Centre for Atomic Research
INPP	Indian Nuclear Power Program
LMC	Lead Mini Cell
LMFBR	Liquid Metal Cooled Fast Breeder Reactor
MC	Mixed Carbide Fuel
MDU	Magnesium Diuranate
MOC	Material of Construction
MOX	Mixed Oxide Fuel
NFC	Nuclear Fuel Complex, Hyderabad
OLW	Organic Liquid Waste
PAR	4-(2-Pyridylazo)resorcinol
PCM	Progressive Conversion Model
PEEK	Polyetheretherketone

PFBR	Prototype Fast Breeder Reactor
PHWR	Pressurised Heavy Water Reactor
PNS	Purified plutonyl nitrate solution
PPM	Parts Per Million
PuRC	Plutonium Reconversion
PUREX	Plutonium Uranium Redox Extraction
RPM	Rotations Per Minute
SA	Subassembly
SC-CO ₂	Super Critical Carbon-Dioxide
SPM	Shrinking Particle Model
SEM	Scanning Electron Microscope
TBP	Tri-n-butyl phosphate
THM	Total Heavy Metal
UNS	Purified uranyl nitrate solution

LIST OF SYMBOLS

Symbols	Expansion
σ	Specific Surface Area
D	Distribution co-efficient
D_A	Diffusivity
k_{LA}	Mass Transfer Coefficient
N_p	Power Number
Re	Reynolds Number
Sc	Schmidt Number
Sh	Sherwood Number

CHAPTER 1. Introduction

The invention of electricity has made a significant impact in the quality of human life and the growth of a country is often judged by its per capita consumption of electricity. With increasing concern of environmental degradation due to release of greenhouse gases, namely, NO_x , SO_x and CO_x from indiscriminate burning of fossil fuels, nuclear fuels take the centre stage as a viable alternative source for electricity production. As this form of energy is also sustainable and contributes to the reduction in global warming, it is considered as an essential element in any nation's energy policy.

In 1942, when the team led by Enrico Fermi, achieved the world's first controlled nuclear chain reaction in the University of Chicago, United States Of America¹, it was envisioned that nuclear electricity will be economical. Though, this dream has not been realized, the fact that, the nuclear fission generates tremendous amount of energy with relatively small amounts of fuel material, makes it attractive for exploitation.

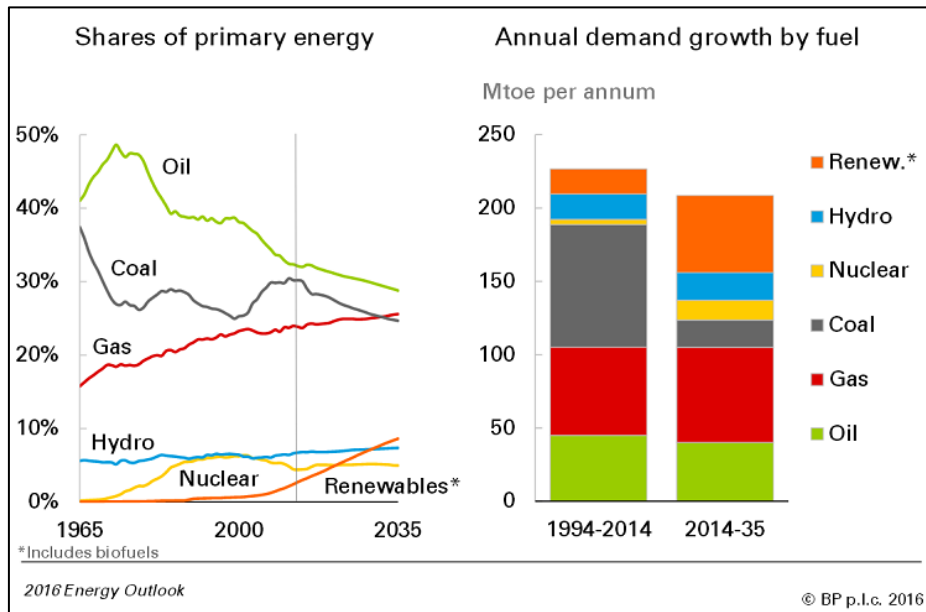
While the energy that could be obtained from coal, oil and gas is of the order of 22.3×10^6 J/kg², nuclear fuel typically could provide energy of about 7.28×10^{13} J/kg. Hence the amount of fuel needed to extract the same amount of energy is roughly of the order of 3×10^6 times more in the case of coal, oil and gas when compared to that of nuclear route.

The nuclear fuel cannot be completely burnt at a single stretch in the reactor, either due to the fission products which inhibit the nuclear chain reaction or due to the degradation of the structural materials which contain the fuel. By recovering the unburnt uranium and the fissile materials produced in the reactor, more power could be tapped from this fuel. To realize this objective, reprocessing the spent fuel from the reactor is necessary.

1.1. The need for energy sources

Right from the early struggle for biological survival to the present technological world, the human life continues to exist due to the discovery and exploitation of various new sources of energy. Starting from learning to generate and make use of fire for their existence, humans have harnessed various forms of energies like wind using ships and windmills, hydropower using rivers and waterfalls, exploitation of chemical energy using coal, oil and natural gas. Only in the middle of 20th century nuclear energy was discovered and used on a large scale.³ Fig. 1.1 shows the shares of the global primary energy sources as on 2014.

Fig. 1.1. Latest typical shares and demand for global primary energy by sources[#]



- BP statistical review of world energy 2016

1.2. Disadvantages of fossil fuels

The long-standing impetus for the development of nuclear power has been the eventual need to replace the fossil fuels - oil (or petroleum), coal, and natural gas. Their supply is finite and eventually, at different rates for the different fuels, will be consumed. Natural gas resources may exceed those of oil, measured in terms of total energy content. Nonetheless, gas is also a limited resource. Coal resources are much more abundant than those of either oil or natural gas, but are the least desirable from the environmental safety point of view. The production of carbon dioxide in the combustion of fossil fuels presents a more difficult problem. Unless much of this carbon dioxide could be captured and sequestered, the resulting increase in the concentration of carbon dioxide in the atmosphere carries with it the possibility of significant global climate change.

Among the fossil fuels, natural gas has significant advantages. It is environmentally least damaging, in terms of both chemical pollutants and carbon dioxide production. If the projected supplies of “unconventional” natural gas live up to some of the estimates⁴, then supply difficulties may be postponed for many decades. Further, natural gas could be used in highly efficient combustion turbines operating in a combined cycle mode, in which much of the (otherwise) waste heat from the combustion turbine is used to drive a steam turbine. Nonetheless, reliance on natural gas as more than a short-term stop gap involves two significant issues. First, the gas supplies may be limited to the standard conventional

resources, advancing the time at which the availability of gas will become a problem and prices will rise substantially. Second, although preferable to coal in this regard, natural gas is still a source of greenhouse gases, primarily carbon dioxide from combustion and secondarily methane from leaks.

*1.3. Why Nuclear Energy?*⁵

The predominant reason that the nuclear energy managers put forward for switching over to nuclear energy from the fossil fuels is the fact that, unlike the fossil fuels, the by-products of nuclear power are more benign to the environment. Also with appropriate choice of nuclear reactors, the nuclear fuel could be used inexhaustibly. This translates into the fact that with the same amount of fuel that was used to start a nuclear reactor, infinite amount of energy could be generated. Nuclear fission, the basic process for power production using nuclear reactors, emits huge amount of energy (~1 MWd per g of U²³⁵ atoms). Hence with a small amount of fuel, large amount of energy could be generated⁶.

In addition, some of the fission products generated in nuclear reactors possess many societal benefits like in medicine, industry, agriculture, food preservation, water resource management, environmental studies etc⁷. In the health care sector, the applications of radioisotopes for diagnostic and therapeutic purposes are innumerable. Today, nuclear medicine offers nearly one hundred procedures that are immensely helpful to a broad span of medical specialties ranging from oncology and cardiology to psychiatry due to which several millions of patients benefit annually, all over the world. Radiopharmaceuticals are preparations containing radioactivity used in medicine for either diagnostic or therapeutic purpose. The industrial applications of nuclear energy can be broadly categorized into four types, namely, (i) Non-destructive evaluation and testing, (ii) Nucleonic measurement and control systems (nucleonic gauges) which are essentially non-contact/non-intrusive mechanisms for measurement and control of process parameters such as thickness, density, level and composition, (iii) Radiotracer applications for industrial process troubleshooting and optimization and (iv) Radiation processing like development of commercial processes such as polymer modifications and sterilizations etc.

The nuclear energy route for power production though offers various advantages over the conventional fossil fuels as stated above, it is certain that great caution needs to be exercised in deploying it. The biggest concern of all is the environmental impact of the nuclear materials and the radioactive wastes generated in the process of nuclear fission

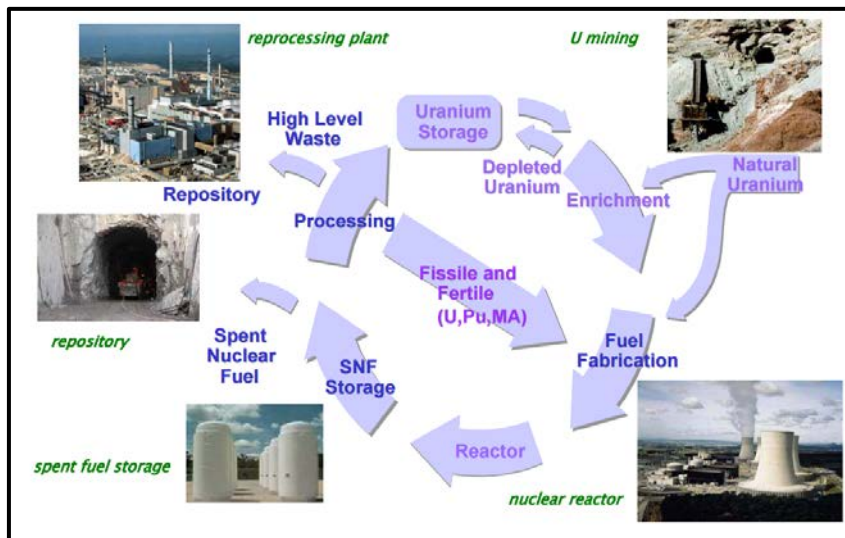
which demands for a better way of disposition of the spent nuclear fuel and its associated radioactive wastes. The next big challenge is the probability of any nuclear accidents during any of the nuclear fuel cycle operations. These challenges could be overcome by engineering the process design in the most practically safest manner. The International Atomic Energy Agency (IAEA), Vienna and the Atomic Energy Regulatory Board (AERB), India have laid out various pre requisites for the safety of the operating personnel and the general public while carrying out any operation, be it industrial or R&D, which when followed meticulously ensures the management of the above challenges. Additionally, continuous use of nuclear energy also reduces the finite availability of the nuclear materials from the earth's crust. But the concepts like breeder reactor wherein one can breed more fuel and end with excess fuel materials over and above the initial inventory, the issue of finite availability of nuclear material is already overcome by the world's nuclear energy fraternity. Finally the most horrifying issue with nuclear energy is the deployment of nuclear energy in harmful ways by anti-social elements. To overcome this, the world nuclear bodies are setting up various treaties and unions which ensure the non-proliferation resistance of nuclear materials.

1.4. Nuclear Fuel Cycle⁸

The nuclear fuel cycle refers to the series of operations which the nuclear fuel undergoes since its fabrication⁹. The cycle starts with the mining of the nuclear fuel materials from the earth's crust followed by its purification and fabrication to a suitable physical and chemical form as nuclear fuel. The various chemical forms include metals and alloys and also some ceramic forms like oxide, carbide and nitride. The usual physical forms include sheets of metal like in APSARA reactor at the Bhabha Atomic Research Centre (BARC) in Mumbai or rods for the rest of the chemical forms. Once the fuel is fabricated in the desired physical and chemical form, it is irradiated in the nuclear reactor for power production. When the burn up (amount of energy extracted from the given quantity of fuel) of the fuel reaches a certain set limit, the irradiated fuel is then unloaded from the reactor and is allowed to cool for certain period of time so that the radioactivity and the decay heat reduces to acceptable levels. Subsequently the cooled fuel is reprocessed wherein the unburnt and the newly bred fissile material are separated and recycled back to the fabrication plant for fresh fuel fabrication. The radioactive waste generated during the reprocessing operations is then sent to a waste management plant wherein the waste are

segregated and treated accordingly. The most important of that waste are the high level liquid waste (HLLW) which is finally fixed in glass matrix and then enclosed in SS canisters for short term storage in special shallow underground storage locations called **tile holes**. After surveillance during the short term storage period when the decay heat and radioactivity reduces considerably, they will be transferred into deep geological repositories for long term storage. Fig. 1.2 shows a typical nuclear fuel cycle.

Fig. 1.2. Schematic of Nuclear Fuel Cycle



1.5. Spent nuclear fuel

The nuclear fuel once loaded into a nuclear reactor in an appropriate physical and chemical form, will be subjected to neutron induced fission for power production. For various reasons, this fuel could not be consumed completely or otherwise the burnup (the amount of energy extracted/extractable from the fuel) of the fuel is limited. In case of thermal nuclear reactors, the burnup is limited due to the accumulation of certain neutron absorbing fission products, like ^{83}Kr , ^{95}Mo , ^{143}Nd , ^{147}Pm , ^{149}Sm , ^{157}Gd etc., which also start competing with the fuel material in consuming the neutrons. These are called **neutron poisons** as the neutron absorbed in them does not lead to any fission. In the case of FBRs also these neutron absorbing fission products does get formed. But as their neutron absorption cross section is very low for the fast neutrons, neutron poisoning is never an issue in reaching higher burnup. But as the burnup increases, the physical integrity of the fuel clad and the reactor structural materials becomes an issue which limits further increasing the burnup. Hence the fuel has to be discharged. This discharged fuel from the

reactor after irradiation is termed as the **spent nuclear fuel**. In any given type of reactor, in addition to these factors, nature of the fissioning nuclide also plays a major role in determining the maximum amount of energy that could be extracted from the given fuel. Thus in a FBR, ^{239}Pu and ^{241}Pu are the better fuel materials than other fissile materials as their fission cross section with fast neutrons are much better. This is explained more in detail in section 1.8 and 1.9. Also they tend to emit higher number of neutrons per fission in the fast region than the other fissile nuclides which would ensure sustained criticality with comparatively lesser fissile content than other fissile nuclides when all other parameters are maintained the same.

1.6. Management of spent nuclear fuel

The spent nuclear fuel, though could be managed in various different ways¹⁰, they all fall into basically three different types¹¹. It could either be stored as such as a nuclear waste in an appropriate location and manner or it could be reprocessed for the recovery of unburnt and the newly bred fissile material present in it. The former case is called the **open or once through fuel cycle** and is normally practiced in countries where there is no dearth of nuclear fuel availability or any other alternate source of energy to meet their power requirements. Countries like USA, Canada, Czech Republic, Germany, Sweden, Finland, Spain, South Africa etc. follow this policy¹². These countries, have judged it to be more advantageous to implement the open fuel cycle, in which the spent fuel elements discharged from the reactor are stored and after a period of interim storage, the fuel will be conditioned and disposed of directly in a deep geological repository.

The latter case is referred as the **closed nuclear fuel cycle** where the spent nuclear fuel is reprocessed to recover the uranium and plutonium from the waste products for their recycle as new fuel elements for use in thermal and fast reactors for power production. In addition to uranium and plutonium, other nuclides such as ^{137}Cs , ^{90}Sr , ^{99}Tc etc., will also be recovered separately for their use in the radiopharmaceutical and other societal beneficiary applications⁷. The third way of managing the spent fuel is called the “**storage and postponed decision**” or “**wait and see option**”. This is essentially a strategy devised by many countries to postpone the decision for a certain period and to take a delayed decision based on the then current scenario.

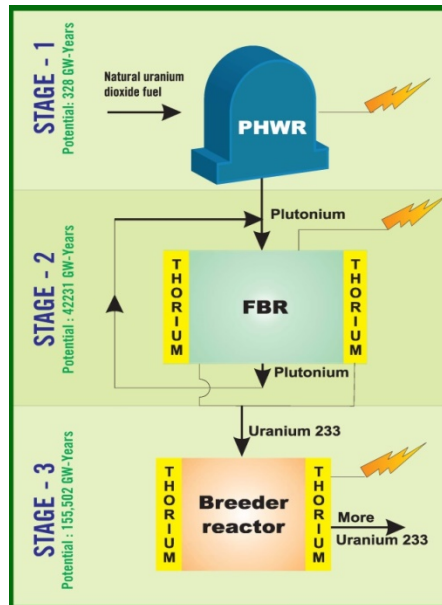
1.7. Three stage Indian Nuclear Power Program

India's three-stage nuclear power programme (INPP) was judiciously formulated by Late Homi Bhabha, the founding father of the department of atomic energy (DAE), India, in the 1950s to secure the country's long term energy independence, through the use of uranium and thorium reserves found in the monazite sands of coastal regions of South India¹³. The ultimate focus of the programme is on enabling the thorium reserves of India, which is the largest in the world, to be utilized in meeting the country's long-term energy requirements. In the 1st stage, nuclear power would be generated using pressurized heavy water reactors (PHWRs) driven by the available natural uranium fuel in the country. The spent fuel from these reactors would be reprocessed in-house for the recovery of newly bred Pu²³⁹ from U²³⁸. At a strategic point in time, Fast Breeder Reactors (FBRs) would be set-up which forms the 2nd stage of the program. The plutonium recovered by reprocessing the spent nuclear fuel from the 1st stage would be used for fabricating U, plutonium mixed oxide fuel which will drive the FBRs in the second stage. FBRs due to their inherent design and the neutronics are potential producers of huge amount of energy from the given fuel.¹⁴ The breeding ability of FBRs will be carefully manipulated in multiplying the fuel and thereby making them self-reliant as well as fuel breeders to set-up more such FBRs subsequently. At an appropriate juncture of time, the blankets of the FBRs will be loaded with the fertile element thorium which is available in abundance in our country to breed more U²³³ out of it. The U²³³ so obtained, will be separated, purified by reprocessing and would be refabricated as fresh fuel to drive the U-Th based Advanced Heavy Water Reactors (AHWR) in the 3rd stage of INPP. A simplified schematic sketch of the three stage INPP is presented in Fig. 1.3.

Thorium is particularly attractive for India, since the country has only around 1–2% of the global uranium reserves, but one of the largest shares of global thorium reserves, at about 25% of the world's known thorium reserves. Closing the nuclear fuel cycle by reprocessing the spent fuel and to recycle the recovered fissile materials back to the reactor for power production is one of the key steps to the success of the entire INPP. Presently the INPP is in the transition between the 1st and 2nd stage wherein the plutonium produced in the first stage by breeding U²³⁸ using thermal neutrons in the natural UO₂ driven Pressurised Heavy Water Reactors (PHWRs) is reprocessed, recovered and used as driver fuel for the second stage. Thus reprocessing forms the necessary link between the first two stages and hence fast reactor fuel reprocessing plants are required to be set-up for the

successful implementation of the INPP¹⁵.

Fig. 1.3. Three Stage Indian Nuclear Power Program



1.8. UO_2 as nuclear fuel

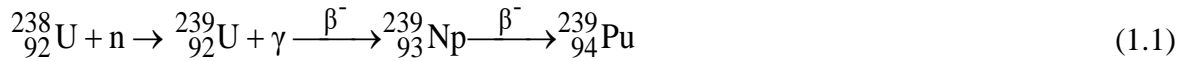
Uranium was discovered in 1789 by the German chemist Klaproth and named in honor of the planet Uranus, discovered five years earlier. It was not until 1841, half a century after the discovery of uranium that the French chemist Peligot succeeded in obtaining this element in a pure state¹⁶. Historically, 1941 marked the beginning of the Uranium era when investigation for deploying the atomic energy of uranium for military purposes began¹⁷.

Natural uranium refers to uranium with the isotopic ratio of 0.72% U^{235} , 99.27% U^{238} and a trace of U^{234} by weight (0.0055%). In terms of the amount of radioactivity, approximately 2.2% comes from U^{235} , 48.6% U^{238} and 49.2% U^{234} . Among all these isotopes only U^{235} is fissile that could be used as fuel in the nuclear reactors. The 0.72% U^{235} is not sufficient to produce a self-sustaining critical chain reaction in light water reactors or nuclear weapons; these applications must use enriched uranium. Nuclear weapons require a concentration of 90% U^{235} and light water reactors requires roughly 3% ^{235}U ¹⁸. Natural uranium is an appropriate fuel for a heavy-water reactor, like the CANDU reactor.

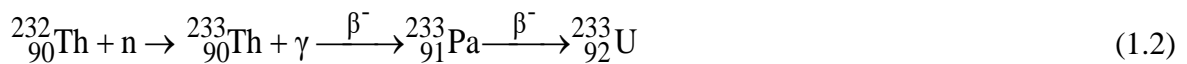
In rare occasions, earlier in geologic history when U^{235} was more abundant, uranium ore was found to have naturally engaged in fission, forming natural nuclear fission reactors¹⁹. U^{235} decays at a faster rate (half-life of 700 million years) compared to U^{238} , which decays

extremely slowly (half-life of 4.5 billion years). Therefore a billion years ago, there was more than double the U^{235} compared to now.

Uranium though has major applications in military sector as penetrators owing to the high density of the metal. However its most common application is in the civilian sector as nuclear fuel. One g of U^{235} on nuclear fission produces about 1 MWd of energy. This is equivalent to the energy produced from about 3.2 tonnes of coal²⁰. Commercial nuclear power plants use fuel that is typically enriched to around 3% U^{235} . The CANDU and Magnox designs are the only commercial reactors capable of using natural uranium as the driver fuel. In a breeder reactor, U^{238} could also be converted into plutonium (referred to as breeding) through the following nuclear reaction²¹:



Uranium is also an extremely effective fuel or explosive substance. Some isotopes of uranium and plutonium are capable of undergoing nuclear fission or disintegration by the action of neutrons and are referred as fissile isotopes: U^{235} , U^{233} , Pu^{239} and Pu^{241} . Of these 4 isotopes, only U^{235} occurs in nature while the other three are obtained in nuclear reactors by neutron bombardment of thorium or natural uranium or Pu^{240} respectively. U^{233} is formed from Th^{232} according to the following reaction.



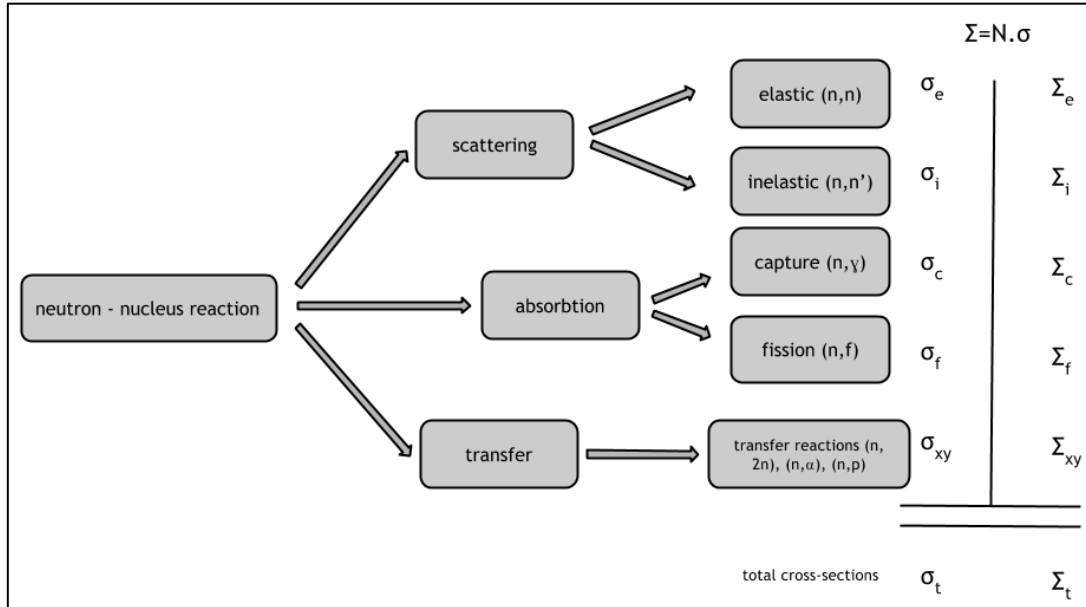
The probability of nuclear fission reactions is usually expressed in terms of the effective cross-section (σ), in area dimensions, since the probability of reaction between the fuel and a bombarding particle is proportional to the area of the transverse cross-section of the target nucleus. The unit of cross-section is 10^{-24} cm^2 , which is called a **barn**. This value is approximately the same as the geometric cross-section of an atomic nucleus, the radius of which is equal to 10^{-12} - 10^{-13} cm . The value of σ basically depends upon the nature of the bombarding particles and their energy.

In nuclear and particle physics, the concept of a neutron cross section²² is used to express the likelihood of interaction between an incident neutron and a target nucleus. In conjunction with the neutron flux, it enables the calculation of the reaction rate, for

example to derive the thermal power of a nuclear power plant. Larger the neutrons cross section, the more likely a neutron would react with the nucleus.

An isotope (or nuclide) could be classified according to its neutron cross section and how it reacts with an incident neutron. The various types of interaction between a neutron and a nucleus are pictorially depicted in Fig. 1.4.

Fig. 1.4. Various types of interactions between a neutron and nucleus



Radionuclides that tend to absorb a neutron and either decay or keep the neutron in its nucleus are neutron absorbers. Corresponding to this reaction, the nuclide will possess a cross section designated as neutron capture cross section (σ_c). Isotopes that undergo fission are fissile and have a corresponding fission cross section (σ_f). When a fissile nuclide absorbs a neutron, there could be only two possible outcomes namely capture or fission. Hence for all fissile nuclides, the sum of σ_c and σ_f is called **the absorption cross section** designated by σ_a . Thus $\sigma_a = \sigma_c + \sigma_f$. The remaining isotopes will simply scatter the neutron, and have a scatter cross section (σ_s).

Some isotopes, like U^{238} , have finite values for all three types of cross sections mentioned above. Isotopes with a large scatter cross section and a low mass are good neutron moderators (H^1 , H^2/D etc.). Nuclides which have a large absorption cross section are neutron poisons if they are neither fissile nor undergo decay (example Gd^{157} , B^{10} etc.). A poison that is purposely inserted into a nuclear reactor for controlling its reactivity in the

long term and improves its shutdown margin is called a **burnable poison**.

The consolidated values of various cross sections for the fissile nuclides are provided in Table 1.1²³.

Table 1.1. Neutron cross-sections of Fissile nuclides*

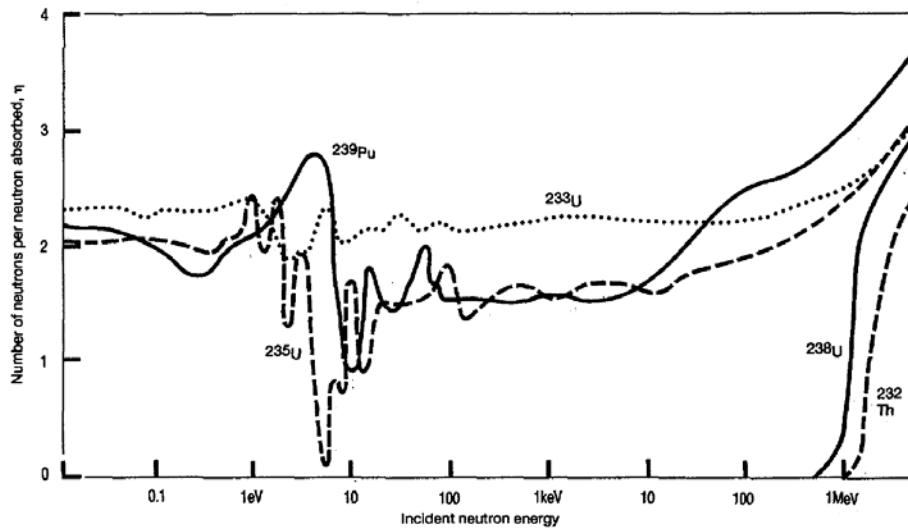
Nuclide	Neutron cross section (b)											
	Average over thermal spectrum				Slowing-down region resonance integrals				Average over fast spectrum [†]			
	σ_s	σ_c	σ_f	η	σ_s	σ_c	σ_f	η	σ_c	σ_f	σ_a	η
²³³ U	12.19	42.20	468.20	2.495	141.90	134.16	751.71	2.498				
²³⁵ U	15.98	86.70	504.81	2.433	152.82	131.97	271.53	2.438	0.25	1.40	1.65	2.2
²³⁹ Pu	7.90	274.32	699.34	2.882	155.87	184.06	289.36	2.876	0.26	1.85	2.11	2.52
²⁴¹ Pu	12.19	334.11	936.65	2.946	148.68	169.13	570.66	2.933				

Here η is the regeneration factor and refers to the average number of neutrons emitted per fission. When η is high, the number of neutrons available to sustain the chain reaction is higher and thus the probability of fission reaction is accordingly higher. Fig. 5 depicts pictorially the changes in the value of η as a function of incident neutron energy for various fissile and fertile nuclides²⁴. These values provide a clear understanding of which is the best fuel for the given type of nuclear reactor in order to have maximum breeding. Thus as both ²³⁹Pu and ²⁴¹Pu have relatively very high value of η in the fast neutron region, they are the best fuel with respect to their breeding potential. Hence in principle they could be deployed in FBRs to extract infinite amount of energy from them, provided, they are sufficiently available initially and a closed fuel cycle is adopted. Similarly ²³³U and ²³⁵U are the best available fuel to be employed in the thermal neutron region. In this region the η value of ²³⁹Pu is pretty low and hence is not considered a good fuel. It is also interesting to note from Fig. 1.5 that ²³³U could be considered as a universal nuclear fuel as its η value is relatively pretty high and consistent under all neutron energy region barring the sharp dips in the resonance regions.

* <http://www.kayelaby.npl.co.uk/> (Kaye and Laby Online, National Physical Laboratory)

† These values are intended as a rough guide as they are strongly influenced by the construction details and the physical characteristics of the FR (size, geometry, coolant, structural material etc.)

Fig. 1.5. η values for various fissile nuclides as a function of neutron energy



1.9. MOX as nuclear fuel

Mixed oxide fuel, commonly referred to as the MOX fuel, is a nuclear fuel that contains oxide of more than one fissile material. It generally consists of plutonium oxide blended with the oxide of natural, reprocessed or depleted uranium. MOX usually consists of two phases, UO_2 and PuO_2 , and/or a single phase solid solution of $(\text{U, Pu})\text{O}_2$. The content of PuO_2 may vary from 1.5 wt.% to about 28–30 wt.% depending on the type of nuclear reactor where the fuel is intended to be used. Although MOX fuel could be used in thermal reactors to provide energy, efficient fission of plutonium in MOX could only be achieved in fast reactors as explained using the η curve in the previous section²⁵.

The MOX fuel differs from UO_2 fuel as the fissile material is primarily ^{239}Pu , and to a lesser extent ^{241}Pu , rather than ^{235}U . Plutonium and uranium have fundamentally different nuclear cross sections that result in the different performance of the materials in a nuclear reactor. Table 1.2 shows the comparison of various important nuclear properties of the fissile nuclides ^{235}U and ^{239}Pu .

Table 1.2. Comparison of nuclear properties of ^{235}U and ^{239}Pu ²⁶

Parameter	^{235}U	^{239}Pu
Thermal neutron fission cross section (σ_f , barns)	577	741
Thermal neutron capture cross section (σ_c , barns)	98	266
Thermal neutron absorption cross section ($\sigma_a = \sigma_c + \sigma_f$, barns)	676	1007

Parameter	²³⁵U	²³⁹Pu
Average number of neutrons per fission	2.43	2.87
Delayed neutron fraction	0.0065	0.0020
Energy per fission (MeV)	192.9	198.5

Plutonium in comparison with uranium, as tabulated above, has a higher thermal absorption cross section and fission cross section, more number of neutron emissions per fission, a larger energy per fission and a smaller delayed neutron fraction. These different nuclear properties have an impact on the neutron spectrum, reactivity coefficients and absorber effectiveness. The smaller delayed neutron fraction results in changes in the kinetic response of the reactor with the reactor responding more rapidly to reactivity changes. One of the major advantages of MOX fuel is that it facilitates utilizing surplus weapons-grade plutonium peacefully (proliferation resistance).

1.10. Aim and scope of the thesis

The primary mandate for the current research work is to determine the intrinsic dissolution kinetics of the plutonium rich FBR MOX fuels in nitric acid medium under typical PUREX process condition. In the course of fulfilling this mandate, the quantitative effect of various parameters like initial concentration of nitric acid, presence of nitrous acid, temperate, mixing intensity etc., on the dissolution kinetics of various fuel materials employed in this research work would also be studied. But as MOX fuel is precious, one couldn't afford to carry out many experiments using them for various safety and economic reasons. Thus it was decided to carry out the initial studies with UO₂ fuel system for identifying the experimental conditions and methodology to determine the effect of various parameters influencing the rate of its dissolution in nitric acid and also to evaluate the quantitative effect of all these influencing parameters on the reaction rate. As the chemistry of UO₂ and MOX fuel systems does not vary much during the dissolution step, this will help in designing the proper dissolution system and also to identify the gross methods of carrying out the experiments. Subsequently based on the results obtained from UO₂ dissolution studies, more experiments would be performed using urania ceria simulated MOX fuel systems of various compositions with cerium used as the non-radioactive surrogate for plutonium. The results obtained in these studies will be extended for the (U, Pu) MOX fuel system. Followed by that, required number of limited

experiments will be carried out for the dissolution of (U, Pu) MOX fuel systems in nitric acid under typical PUREX process conditions to evaluate its dissolution kinetics. Finally, using the results of all the experimental studies, model equations will be developed to explain the dissolution behaviour of all the fuel materials in nitric acid medium. The model so developed for the UO₂ fuel system first, will be then gradually upgraded with the necessary changes to explain the dissolution behaviour of the MOX fuel material.

1.11. References

-
- ¹ Hans G. Graetzer and David L. Anderson, *The Discovery of Nuclear Fission*, Editor, I. Cohen, Ayer Co., (1981).
 - ² David M. Mason and Kiran N. Gandhi, “Formulas for calculating the calorific value of coal and coal chars: Development, tests and uses”, *Fuel Processing Technology*, 7 (1983) 11-22
 - ³ *Nuclear Energy – Principles, practices and prospects*, David Bodansky, 2nd Edition, 2004 Springer-Verlag, New York
 - ⁴ 2014 key world energy statistics, International Energy Agency
 - ⁵ Alan M. Herbst, George W. Hopley, “Nuclear Energy Now: Why the Time Has Come for the World's Most Misunderstood Energy Source”, 2007 Wiley publications
 - ⁶ Balasubramanian Viswanathan, “Energy Sources. Fundamentals of Chemical Conversion Processes and Applications”, 2016 Elsevier Publications
 - ⁷ V. Venugopal, “Societal applications of Nuclear Technology in Health Care, Industry and Water Resource Management in India”, *Energy Procedia*, Vol.7, 2011, 553-559
 - ⁸ Jordi Bruno, Rodney C. Ewing, “Spent Nuclear Fuel”, *Elements*, v. 2, i. 6, p. 343-349, December 2006
 - ⁹ *Nuclear Energy Encyclopedia: Science, Technology, and Applications*, First Edition, Edited by Steven B. Krivit, Jay H. Lehr, and Thomas B. Kingery, 2011 John Wiley & Sons, Inc. Published 2011 by John Wiley & Sons, Inc.
 - ¹⁰ OECD/Nuclear Energy Agency, “Advanced nuclear fuel cycles and radioactive waste management”, NEA No.5990, OECD/NEA, Paris 2006
 - ¹¹ Robin Taylor (Ed), “Reprocessing and Recycling of Spent Nuclear Fuel”, 2015 Elsevier, Woodhead Publishing Series in Energy: Number 79
 - ¹² *Country nuclear fuel cycle profiles*, 2nd edition., Technical report series No. 425, Vienna, IAEA 2005, ISBN 9201148038

-
- ¹³ Department of Atomic Energy annual report 2011-2012
- ¹⁴ Introduction of FBRs book
- ¹⁵ P.K. Dey, N.K. Bansal, “Spent fuel reprocessing: A vital link in Indian nuclear power program”, Nuclear Engineering and Design 236 (2006) 723–729
- ¹⁶ Gmelin handbook of inorganic chemistry – Behaviour of uranium fuels, Helmut Aßmann et.al., 8th edition, Supplement volume A4, Springer-Verlag 1981
- ¹⁷ SMITH, G. P. Atomic Energy for Peaceful Purposes
- ¹⁸ Loveland, W.; Morrissey, D.J.; Seaborg, G.T. (2006). "Chapter 16 Nuclear Reactor Chemistry". Modern Nuclear Chemistry, John Wiley & Sons
- ¹⁹ Gauthier-Lafaye, F.; Holliger, P.; Blanc, P.-L. (1996). "Natural fission reactors in the Franceville Basin, Gabon: a review of the conditions and results of a "critical event" in a geologic system". *Geochimica et Cosmochimica Acta* 60 (25): 4831–4852; doi:[10.1016/S0016-7037\(96\)00245-1](https://doi.org/10.1016/S0016-7037(96)00245-1)
- ²⁰ Lester R. Morss, Norman M. Edelstein and Jean Fuger, “The Chemistry of the Actinides and Transactinide Elements”, fourth edition, Volume 1, 2010 Springer
- ²¹ V. S. Yemelyanov and A.L Yevstyukhin, “The Metallurgy of Nuclear Fuel - Properties and Principles of the Technology of Uranium, Thorium and Plutonium”, Translated by Anne Foster, 1969 Pergamon Press Ltd.
- ²² DOE Fundamentals Handbook, Nuclear Physics and Reactor Theory, DOE-HDBK-1019/1-93 <http://energy.gov/sites/prod/files/2013/06/f2/h1019v1.pdf>
- ²³ S. F. Mughabghab (1984), “Neutron Cross-sections”, Volume 1, Neutron Resonance Parameters and Thermal Cross-sections, Part B: Z = 61–100, Academic Press, New York
- ²⁴ “Plutonium fuel an assessment: Report by an expert group”, OECD Publications and Information Centre 1989, p-29,
- ²⁵ Mieczyslaw Taube, “Chapter 2 – The fission of plutonium isotopes” in Plutonium – A General Survey, Vol 4, page 36-38
- ²⁶ J. C. Gehin, J. J. Carbajo, R. J. Ellis, “Issues in the use of MOX fuel in VVER-1000 nuclear reactors: Comparison of UO₂ and MOX fuels”, ORNL-2004/223, October 2004

CHAPTER 2. Spent nuclear fuel reprocessing

2.1. Why reprocessing?

For any fuel to make a significant impact in the energy scenario, its sustainability should be ensured. The sustainability of the nuclear fuel depends not only on the effectiveness of operating the reactor with the desired fuel but also on how far the fuel could be burnt completely. For this, unburnt material from the spent fuel has to be recovered for recycling back. Hence the aim of any nuclear fuel reprocessing plant should be to remove the fission products (and its associated radioactivities) quantitatively from the spent fuel and recover the plutonium and uranium in them to the purest extent possible. This would enable tapping of more energy from the given amount of fuel. From the Indian standpoint, the closed nuclear fuel cycle is the most preferred and advisable option for nurturing nuclear power in meeting the long term energy security of the country¹. This is because of the limited uranium reserve in the country. Additionally, if we have to devise a strategy to deploy our huge thorium reserve, this could be the best option. Hence reprocessing is a mandatory option for us. Reprocessing the spent fuel offers various other advantages as listed below².

1. By reprocessing and reusing the recovered fissile materials in breeder reactors, we are multiplying the amount of energy that could be extracted from the given quantity of fuel. Hence this leads to the **conservation of natural resources**
2. Nuclear fuel reprocessing is the precursor to the recovery of actinides from the spent fuel. Hence reprocessing paves way for **better management of nuclear waste**. Also the removal of long lived actinides (like ²⁴¹Am, ²³⁷Np etc.) from the spent fuel leads to **minimization of environmental impact** of the radioactive waste
3. When the recovered fissile materials are reused, it **strengthens fuel cycle economics**
4. As reprocessing recovers all the fissile materials from it, especially plutonium, they could be directed for peaceful applications, thereby taking care of **proliferation resistance**

2.2. Nature of spent nuclear fuel

Nuclear fuels are generally of three types, namely, metallic, ceramic and dispersion³. The latter includes two-phase metallic fuels such as Al-UAl₃ as well as dispersions of ceramics in metal or ceramic matrices. Irrespective of the chemical form of the nuclear fuel, the

irradiated/spent nuclear fuel will always be comprised of the unburnt initial fuel which is the bulk, fission products whose mass number ranges from about 70 to 160 and the minor actinides (mostly comprising of Am, Np and Cm). Depending on the burn up of the fuel, the composition of all these vary vastly. Depending on the type of fuel, the chemical form of the fission products and minor actinides also differ^{4, 5, 6}. The composition of the spent fuel depends on how long the fuel was in the reactor (burnup) and to a greater extent on how long the irradiated fuel has been out of the reactor. This amount of time for which the irradiated fuel is kept outside the reactor, with all the appropriate safety measures, from the time of its discharge till its further management in the nuclear fuel cycle is called the ex-vessel **cooling period**. For a light water reactor (like a PWR or BWR) the ²³⁵U levels get reduced from the initial amount by about 2-4%. The change is even lower for CANDU type reactors (less than 1%). About 95% of the spent fuel is still U²³⁸, which could be used again. The other radionuclides that now exist in the irradiated fuel are heavy elements and their isotopes (plutonium, americium, neptunium and curium) and fission products. Although there are thousands of tons of spent fuel, it is compact and uniform. This makes it relatively easy to manage this waste⁷. The typical composition of the spent fuel discharged from a commercial light water reactor is given in Table 2.1.

Table 2.1. Typical composition of the spent fuel from a commercial LWR⁸

Element or group	Percent, by weight
Uranium	95.6%
Plutonium	0.9%
Fission products	3%
Heat emitters like ¹³⁷ Cs and ⁹⁰ Sr	0.3%
Minor actinides	0.1%
Transmutable ¹³¹ I and ⁹⁹ Tc	0.1%

2.3. Choice of reprocessing process

Depending on the chemical form of the nuclear fuel, the method of reprocessing the spent nuclear fuel is chosen². Basically there are two primary means of reprocessing the spent nuclear fuel. They are the aqueous and non-aqueous methods. In the former, nitric acid medium is used for dissolving the spent fuel either with or without their cladding material. Once all the fuel material is brought into a suitable medium, they are separated from the

host of fission products and their associated radioactivity by solvent extraction process. In the latter method, a variety of non-aqueous methods like pyrometallurgical process, halide volatility process, carbo-chlorination process, direct electrochemical dissolution process etc. are available⁹. Since the current thesis focusses only on the dissolution of spent nuclear fuel in aqueous medium, methods associated to aqueous processes are only discussed here. For oxides, nitrides and carbides, the aqueous based methods could be adopted. The well-known PUREX process comes under this category^{10, 11}. For metallic fuels, as they are seldom soluble in aqueous based solvents, hence non-aqueous methods like pyrometallurgical and pyrochemical processes are employed.

2.4. Chemistry of the reprocessing of spent nuclear fuel by PUREX process

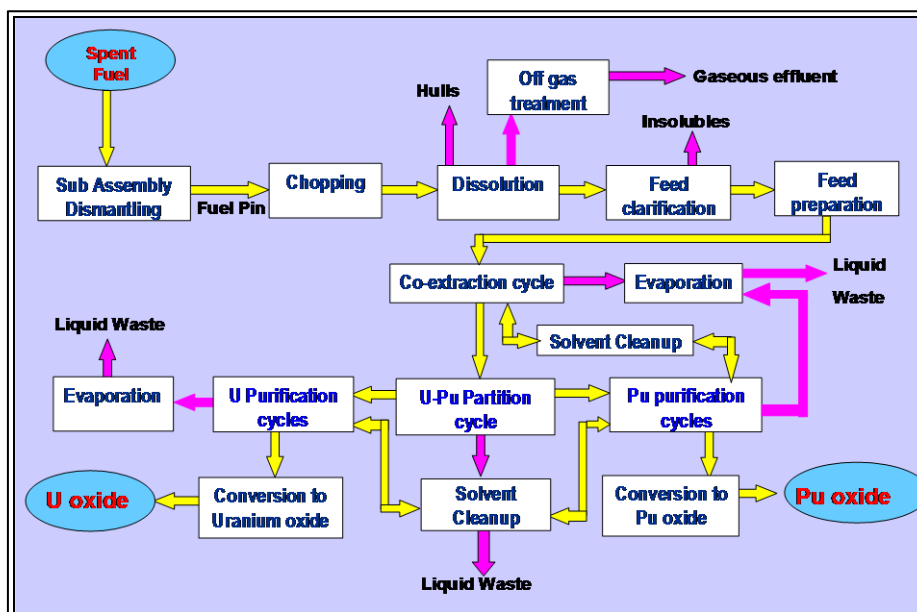
The subject of the present thesis is the dissolution kinetics of nuclear fuel in nitric acid medium. Hence information/discussion presented in the thesis would pertain to this aspect alone. However, a brief mention about the other processes also would be made in the thesis. The following is a brief account of the chemistry involved in the various process steps while processing a spent nuclear fuel by aqueous methods^{12,13}.

The process flowsheet for reprocessing of spent fuel by aqueous process (PUREX process in particular¹⁴) could be divided into three sections namely the head-end, solvent extraction and tail-end process sections¹⁵. The head-end processes comprises of dismantling the subassemblies (SAs) into individual pins in case of FBR fuel reprocessing or individual SAs in the case of thermal reactor fuel reprocessing, chopping them into small pieces of suitable size and dissolving them in nitric acid. The process chemistry comes into the picture only from the dissolution step as the spent fuel is converted to a suitable physical and chemical form for efficient downstream processes only in this step. The tail-end process refers to the conversion of the purified plutonium and uranium nitrates to their respective solid oxides which are the final products of a nuclear fuel reprocessing plant. Fig. 2.1 depicts the typical processes carried out in the reprocessing of spent nuclear fuel by PUREX process.

2.4.1. Chemistry in the head-end steps in the PUREX process

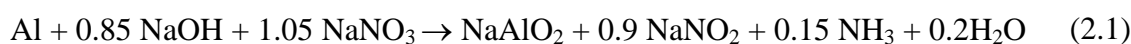
The head-end processes involve decladding, dissolution and feed filtration and conditioning. The chemistry involved in these processes is described in the following sections.

Fig. 2.1. Schematic diagram of PUREX process flowsheet



2.4.1.1. Chemistry involved in the decladding of nuclear fuel

Decladding refers to the pretreatment given to the spent fuel to ensure direct access for the aqueous solvent to the fuel material for further processing. Decladding could be carried out either by chemical methods or by mechanical means. In chemical decladding, preferential dissolution of cladding material is carried out with a suitable reagent, leaving the fuel undissolved. Subsequently, the fuel is dissolved in nitric acid. For example, aluminium clad uranium oxide spent fuel is decladded with caustic solution which dissolves aluminium as per the following reaction¹⁶.



The fuel does not dissolve in sodium hydroxide. There are processes to dissolve Zr and stainless steel clads as well. But they are not generally practiced in plant scale. While chemical decladding eliminates the use of mechanical system in radioactive areas, it increases the waste volume by introducing new chemical species in the process streams. Even though the chemical decladding procedure is followed in some plants for reprocessing the spent fuel from research reactors, chop-leach process is the widely followed process to expose the fuel to nitric acid in dissolution leaving the clad “undissolved” so that it could be handled separately. This enables cladding hulls to be compacted and disposed-off as high level solid waste separately.

Chopping is carried out in mechanical chopping equipment. Generally bundle chopping

procedure is followed for the thermal reactor fuel reprocessing plants while for FBR fuel reprocessing plants, single pin chopping is adopted. This avoids crimping of the chopped bits due to the slenderness of the fuel pins, which reduces the fuel dissolution rates.

2.4.1.2. Chemistry involved in the dissolution of nuclear fuel

The dissolution step in the PUREX process primarily aims at the following tasks¹⁷.

- i. Complete transfer of the fissile materials (U and Pu) into the aqueous solution
- ii. Complete separation of the fuel from the cladding material
- iii. Render feasibility for the accurate measurement of the amounts of fissile material taken for reprocessing for the purpose of nuclear material accounting and
- iv. Convert the entire spent fuel into an appropriate chemical form amenable for their subsequent separation and quantitative recovery.

In the PUREX process, the fuel is dissolved in boiling nitric acid. Generally 6-8 M nitric acid would be adequate for most of the spent fuels of PHWRs, but plutonium rich fuels require still higher acidities¹⁸.

Dissolution of FBR fuels with plutonium greater than 35% by weight in an oxide matrix is difficult with concentrated nitric acid alone.¹⁹ Higher plutonium concentration invariably demands advanced dissolution methods like addition of strong oxidizing/reducing agents or by electrolysis. When the reprocessing of a mixed carbide fast reactor spent fuel (FRSF) was taken up for the first time in the world at CORAL[‡], Kalpakkam, it was believed that a 70% plutonium rich FRSF cannot be dissolved in pure nitric acid. But the CORAL operating experience has revealed that reflux heating in boiling concentrated nitric acid could dissolve it completely.²⁰

Though, most of results in the published literature^{21, 22, 23, 24, 25, 26, 27} were inconclusive in recommending a specific condition for dissolving spent fuel on a commercial scale, they still provided certain important inferences, which helped in providing direction for the subsequent research, some of which are as follows.

- i. Initial dissolution rates depends on concentration of nitric acid and temperature²⁸
- ii. Similar to UO₂, plutonium lean spent fuels could be dissolved in nitric acid²⁹
- iii. Spent fuel with plutonium content above 35% by weight of the total heavy metal

[‡] CORAL stands for the COmpact Reprocessing of Advanced fuels in Lead shielded facility which is set-up at IGCAR, Kalpakkam, India for demonstrating the feasibility of reprocessing the plutonium rich spent fuel discharged from FBTR. CORAL was formerly known as the Lead Mini Cell (LMC)

needs aggressive conditions for dissolution

- iv. Irradiation renders the fuel more brittle commensurate with the burnup of the fuel due to the gaseous fission products, decay heat and neutron flux.³⁰ Therefore when agitated physically, small fragments of fuel particles is released out of the chopped fuel pin into the acid medium, which dissolve faster than those inside the chopped pin. Additionally, due to the escape of such small particles from the inside the chopped fuel pin pieces, more space is available for ingress of acid. This enhances the dissolution of the fuel particles still intact inside the chopped fuel pin pieces. Thus irradiation enhances dissolution rate³¹
- v. Irradiation also leads to the formation of certain alloys in the spent fuel comprising of the noble metals (Ru, Rh, Pd) and actinides leading to undissolved residues³⁰. This leads to the loss of some fissile materials in these alloys. The amount of actinides, plutonium in particular, present in these undissolvable alloys increases with burnup
- vi. Voloxidation in general enhances dissolution, but also increases the amount of plutonium left in the undissolved residue³²

Owing to the above facts, there has been more attention on the dissolution of high plutonium bearing spent fuel, especially those discharged from a fast reactor. The additional issue of criticality due to the presence of high amount of plutonium in these types of fuel makes it more challenging to develop the process for dissolution.

Until the end of the 20th century, the necessity for developing superior dissolution methods for the spent nuclear fuel and scraps, stemmed predominantly from nuclear waste management. Only in the recent decade owing to plutonium utilization strategies, reprocessing of plutonium containing fuels has taken the center stage wherein dissolution of spent fuel has been an integral part. In the early 1960s, Uriarte and Rainey¹⁸ came out with the recommendations for commercially dissolving irradiated MOX fuel. According to them, nitric acid with traces of HF was the most suitable medium for the dissolution of MOX fuel. But subsequently based on the studies to eliminate corrosive reagents like HF, a method based on cerium(IV)³³ was developed. It was proposed that this method not only is devoid of a corrosive reagent but also enhances plutonium oxide dissolution. Also it was found to be superior to other strong oxidants, including ozone, permanganate, persulphate and Ce(IV). During dissolution, Ce(IV) gets reduced to Ce(III) which needs to be re-oxidized in-situ. The main disadvantage of this method is the increased consumption of Ce(IV) by the other oxidizable fission products like Ru³⁴.

In 1980, Ryan and Bray³⁵ of PNL gave an account of the problem of dissolving plutonium oxide from a thermodynamic and kinetics standpoint. These studies showed that thermodynamically it is impossible to dissolve pure PuO₂ in nitric acid solutions of concentration below about 4 M. Fluoride ion was used based on its ability to complex Pu(IV) in strong acidic solutions, wherein it aids in increasing both the solubility and the rate of PuO₂ dissolution. The formation of the Pu(IV) fluoride complex influences the dissolution process. Hence the fluoride concentration often must exceed the final dissolved plutonium concentration. In irradiated MOX fuels, many scraps and various plutonium contaminated waste, other contaminants such as Si, Zr, U, and various fission products also form fluoride complexes. They virtually prevent the dissolution of PuO₂ when present in large quantity unless a large excess of fluoride is used. Processes for leaching plutonium from various scraps have often employed repeated cycles of leaching by fluoride containing nitric acid solutions. Not only has this produced large volumes of solutions, generating eventually more waste, but significant amounts of Al³⁺ are generally added to the solutions (further increasing waste) to complex the fluoride, both to allow normal plutonium processing by ion exchange or solvent extraction and to minimize fluoride corrosion of equipment. When silica or silicates are present, the volatilization of SiF₄ could produce significant problems in off-gas systems, and silica often precipitates when Al is added to prepare the solution for further processing.

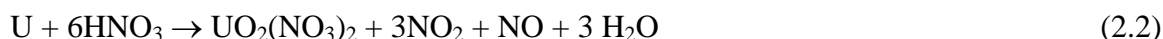
Ryan et.al³⁶, as a follow up to the above findings, proposed a process to dissolve PuO₂ and PuO₂²⁺ ions by using electrical energy and it was named **CEPOD** (Catalyzed Electrolytic Plutonium Oxide Dissolution). In this process, PuO₂ is dissolved in an electrolyte containing small (catalytic) amounts of elements that form kinetically fast, strongly oxidizing ions. The oxidizing ions are regenerated at the anode; they act in a catalytic manner, carrying electrons from the solid PuO₂ surface to the anode of the electrochemical cell.

Among the various methods employed in the studies to enhance the dissolution of spent fuel in nitric acid, voloxidation was expected to be a prominent technique.³⁷ The studies revealed that voloxidation though enhances dissolution and leaves more plutonium in the undissolved residues which are even harder to dissolve.

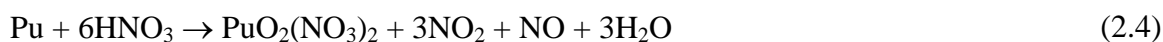
2.4.1.2.1. Dissolution reactions

Various reactions taking place during the dissolution of different types of nuclear fuel materials are summarized in the following few sections.

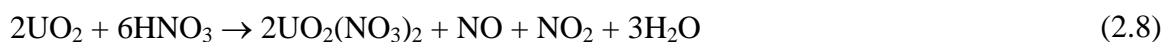
2.4.1.2.1.1. *Dissolution of uranium metal*



2.4.1.2.1.2. *Dissolution of plutonium metal (in the presence of HF)*



2.4.1.2.1.3. *Dissolution of UO₂ with emission of NO_x gases*

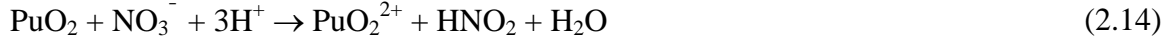
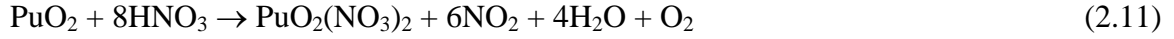


During the dissolution of UO₂, depending on the concentration of the nitric acid, one or more of the above reaction take place. The reaction corresponding to equation 2.6 occurs when the concentration of nitric acid is above 8M. As the acid concentration reduces, the reaction proceeds predominantly through reaction 2.7 and when the acidity reduces below 6M, reaction 2.8 predominates. Though the stoichiometric equations are well established, the detailed mechanism of the reaction has not been completely understood. Though, some of studies in the literature had speculated the role of intermediates like nitrous acid getting generated in-situ during the dissolution process^{38, 39, 40}, no studies have yet been carried out systematically to quantify the role of nitrous acid during dissolution. Hence the present work aims at studying these reactions in detail by determining the quantitative effect of various influencing parameters like initial concentration of nitric acid, temperature, mixing intensity, role of nitrous acid and the surface area of the pellet.

2.4.1.2.1.4. *Dissolution of PuO₂ with emission of NO_x gases*

Unlike UO₂, PuO₂ dissolves in nitric acid very sluggishly¹⁶ as per the following stoichiometric equations.

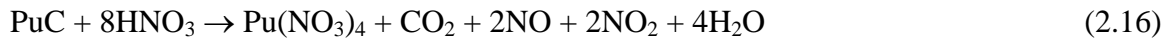
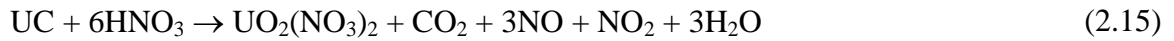




All the above reactions require high concentration of nitric acid at elevated temperatures for quantitative dissolution of plutonia. Generally higher the concentration of the acid used the off-gas NO_x will be dominated by NO_2 . Otherwise it is NO . The reaction 2.12 represents the direct dissolution of PuO_2 in nitric acid whereas equations 2.13 and 2.14 represent the oxidative dissolution of PuO_2 . Thermodynamic calculations presented in the literature have shown that all the above dissolution reactions of PuO_2 in nitric acid are thermodynamically less favorable^{34, 41}.

2.4.1.2.1.5. *Dissolution of UC, PuC and their mixture*

Uranium, plutonium and their mixed carbides are known to dissolve even under mild conditions as compared to their oxide counterparts⁴² with the emission of CO_2 and NO_x gases as per the following reactions.



The earliest studies carried out for the direct dissolution of advanced carbide fuels in nitric acid medium showed the formation of some organics like oxalic and mellitic acids⁴³. In addition to these, some more unidentified compounds were also reported⁴⁴. All these organics generated during the dissolution process were expected to have adverse effect on the subsequent purification of uranium and plutonium by solvent extraction using tributyl phosphate (TBP).

2.4.1.2.2. *Kinetics, mechanism and modeling of dissolution*

Many proposals were brought forward to explain the kinetics and mechanism of dissolution as and when the existing knowledge on the dissolution of spent fuel is being updated by the researchers world over. Some of these proposals were followed by

mathematical modeling for explaining the experimental observations.

Lot of work was carried out to study the kinetics, mechanism and modeling of dissolution of uranium and plutonium oxides in nitric acid for the development of a continuous dissolution equipment and process methodology. Understandably UO₂ dissolution mechanism was studied first which paved way for the evaluation of the reaction mechanism of the dissolution of other actinide oxides. Detailed discussions of literature information on this aspect are presented in Chapter 3 of this thesis.

2.4.1.3. Chemistry of the dissolver off-gas treatment

The dissolver off-gases are cooled and the NO_x gases evolved during the dissolution are scrubbed in DM/distilled water and converted to nitric acid. This is done primarily for two purposes, namely, to reduce the release of NO_x gas into atmosphere and also to minimize the overall consumption of nitric acid during reprocessing by recycling this acid to an appropriate stage within the reprocessing process. The following reactions occur during the dissolver off-gas treatment:

2.4.1.3.1. Gas phase reactions



2.4.1.3.2. Liquid phase reactions



It could be seen that oxygen is required for conversion reactions which is supplied by sparging air¹⁶. Oxygen in air enhances the conversion of NO to NO₂ which has better absorption characteristics with water. The off-gases are then treated for the removal of iodine and then filtered through High Efficiency Particulate Air (HEPA) filters and discharged into the environment through the stack after making sure that the radioactivity of the off-gas stream is within the limits stipulated by the regulatory authority⁴⁵.

2.4.1.4. Decladding chemistry

Decladding is carried out to avoid the clad to be present along with the fuel in further processing since its presence makes the process design very complicated. During the spent nuclear fuel processing by aqueous processes, the cladding material of the fuel would be removed by either of two different ways, viz, mechanical or chemical. The conventional PUREX process removes the clad by mechanical means wherein during the dissolution step, the fuel material inside the chopped fuel pins alone goes into the solution leaving the clad materials undissolved. This undissolved clad after dissolution is termed as the “HULL” and is disposed as solid radioactive waste after appropriate treatment⁴⁶.

The chemical decladding process is adopted in those cases wherein the fuel material is bonded with the clad material as in the case of uranium metal slugs bonded with aluminium-silicon alloy to aluminium cladding during the early production reactions in the US⁴⁷. As the clad and fuel are bonded, mechanical decladding is not feasible here. In the chemical decladding process, the clad materials alone will be dissolved in an alkali leaving out the spent fuel which does not dissolve in that. Then the left over fuel material will be removed and dissolved in nitric acid medium for further processing. The THOREX process adopted for reprocessing the thorium based spent nuclear fuel^{48, 49} employs this method wherein the cladding material is Aluminium. Thus an appropriate decladding method is adopted suitably to avoid the cladding materials being present along with the fuel materials during solvent extraction process. In earlier days when the mechanical decladding process was not developed, the chemical decladding process was used in the zirconium^{50, 51} and sulfur⁵² processes for removing the zircaloy and SS clad materials respectively.

2.4.1.5. Chemistry of feed clarification

Under boiling nitric acid condition, all the fuel material dissolves leaving a small quantity of fine residues^{53, 54} which mainly consists of noble metal alloys with small quantities of plutonium in it. Though the quantity of this undissolved material depends upon the nature of the fuel, burnup and initial plutonium content, it generally increases with the burnup and plutonium composition⁵⁵. Typically this quantity could be as high as 0.74% in FBR fuels⁵⁶. The dissolver solution is filtered to remove these fine particles before subjecting it to solvent extraction. The filtration also removes the clad fines. Though R&D work was conducted with sand bed as well as bag filters, centrifuge filters are more commonly used.

2.4.2. Chemistry involved in feed conditioning

Feed conditioning is the process step carried out to ensure that the chemical conditions of the dissolver solution, viz, acidity and valency of the metal ions of interest, is adjusted for getting the highest possible recovery of uranium and plutonium in an optimum number of extraction stages. While generally 1-3 M is the optimum range of acid concentration employed in the processing of PHWR spent fuels, 4-6 M is used for fast reactor fuels as its plutonium content is higher. This is because the extraction coefficient of plutonium is relatively lower at lower acidities. This range of acid concentration was found to be optimum for the quantitative recovery of both uranium and plutonium as well as for removing bulk of the fission products whose extraction is poor under these conditions. For ensuring quantitative recovery, all the plutonium is converted to its fourth valency state, as the distribution coefficient of Pu(IV) ($D_{\text{Pu(IV)}}$) is the highest among all the plutonium species under PUREX process conditions. Since plutonium co-exists in III, IV and VI oxidation states in nitric acid medium, it is essential to convert all the plutonium species to Pu(IV). It is also well established that Pu(IV) undergoes disproportionation in nitric acid medium by which it gets converted to III and VI valency states partially⁵⁷. Though the kinetics of disproportionation is found to be reasonably slow under PUREX process conditions⁵⁸, it is a general practice to carry out conditioning of the feed solution just before carrying out solvent extraction. Valency adjustment of plutonium could be carried out either chemically or electrolytically.

2.4.2.1. Conditioning by chemical methods

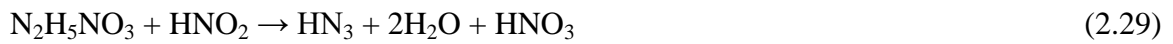
Sparging with NO₂ gas is the most commonly practiced chemical method for conditioning the feed in the PUREX process. The earlier practice of using NaNO₂ for insitu generation of NO₂ for conditioning has been dispensed with in most of the recent plants since this would increase the solid waste quantities by introducing Na⁺ ions in the liquid waste streams. NO₂ gas, when sparged into aqueous solution, produces nitrous acid in-situ by the following reaction.



The nitrous acid (HNO₂ or NO₂⁻) generated in-situ in the solution converts all plutonium species in the dissolver solution to Pu(IV) by the following equations.



Though the most stable oxidation state of uranium in nitric acid medium is VI, presence of any hydrazine (used in its nitrate form as a stabilizing agent of U(IV) in the latter stages of PUREX process) may lead to the reduction of U(VI) to U(IV). The nitrous acid produced in-situ, also takes care of this issue as per the following reaction⁵⁹.



The above reactions takes very rapidly⁶⁰ and destroy hydrazine ions completely in the system thereby avoiding the reduction of U(VI) to U(IV).

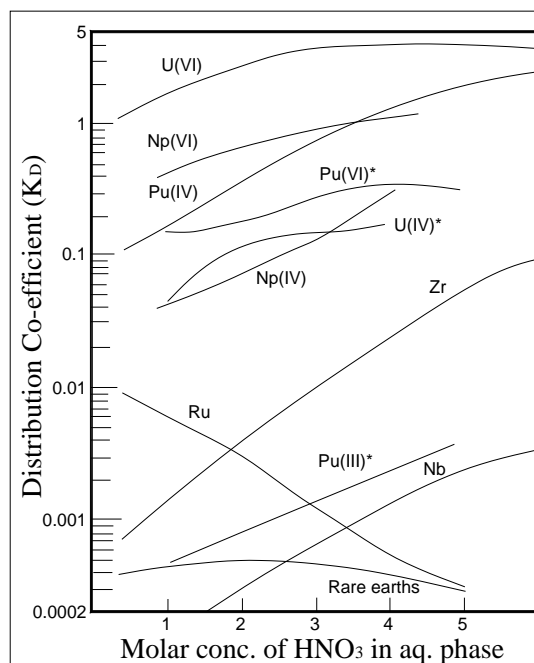
2.4.2.2. Conditioning by electrochemical methods

Alternately, the PUREX process feed conditioning could also be carried out electrochemically using platinum as anode and titanium as cathode. The electrochemical reactions that take place during such an electrochemical conditioning is given by



Though studies have shown that electrolytic conditioning is possible⁶¹, this has not been introduced in any of the plants till date. Most probably this could be due to some of the parasitic electrochemical reactions which could take place simultaneously leading to some undesired changes in the conditioned feed and also in excess consumption of power⁶². The valency of uranium need not be adjusted as its VI valency is the most stable state and hence it remains so by default. The equilibrium acid concentration has a strong effect on the solvent extraction efficiency as shown in Fig. 2.2.

Fig. 2.2. Effect of acidity on the K_D of various species in 30% TBP⁶³



From Fig. 2.2 it could be seen that the D values for U(VI) and Pu(IV) is sufficiently high above 4 M acid concentration when compared with that of the fission products, lanthanides and other actinides. Hence the solvent extraction step is carried out using 30% TBP after conditioning the feed acid concentration to above 4 M during FBR spent fuel reprocessing for achieving the required decontamination for uranium and plutonium from the rest of the species in the spent fuel. Since the FBR spent fuel has higher quantity of Pu, the PUREX process is normally operated with the concentration of nitric acid at or above 4 M. When the spent fuel is short cooled, the concentration of acid is maintained even at 6 M for the first cycle alone to have sufficient decontamination factor (DF) from Ru. Though ⁹⁵Zr has a short half-life of only about 65 days, there will be sufficient amount of it in FBR spent fuel due to the higher burn up. Hence for the decontamination of Zr(IV) whose distribution is sufficiently high at above 4 M acid concentration, an acid scrub of about 3-3.5 M is provided for the loaded organic to strip the extracted Zr(IV), if any.

2.4.3. Chemistry of solvent extraction process

The Organisation for Economic Co-operation and Development (OECD), Nuclear Energy Agency (NEA) has come out with a report prepared by an expert committee in 2012 which is one of the latest compilations as on date on the solvent extraction relevant to spent fuel

reprocessing and recovery of actinides and lanthanides from the high level liquid waste⁶⁴. The conditioned feed solution would then be subjected to solvent extraction using 30% TBP diluted in n-dodecane as solvent for the quantitative recovery of U(VI) and Pu(IV) in the first cycle of solvent extraction. The stoichiometric equation for the extraction of uranium and plutonium by TBP is given in the following equations.



After extraction of U(VI) and Pu(IV) into the organic phase, the loaded organic is separated and contacted with a fresh dilute nitric acid stream. As the Fig. 2.2 indicates, the distribution coefficient of U(VI) and Pu(IV) is lower when the concentration of acid in the aqueous stream in contact with it is less. Hence they get stripped back to the aqueous phase. Pu(IV) is prone for polymerization when the concentration of the acid is low⁶⁵. Since the recovery of the polymerized Pu(IV) is very difficult, care needs to be exercised in choosing the concentration of the strip acid to ensure the prevention of plutonium polymerization. This operation of extraction and stripping is termed as **one cycle of solvent extraction**. Sufficient numbers of such cycles of solvent extraction is carried out during reprocessing to achieve the required levels of decontamination for the final uranium and plutonium products from all the fission products and other impurities.

2.4.4. Chemistry of U/Pu partitioning in the PUREX process

The uranium and plutonium, after being purified from the bulk of fission products and other impurities, is separated from each other in the next cycle which is called the partitioning cycle. The relatively lower distribution co-efficient of Pu(III) into 30% TBP is exploited advantageously for this purpose. As mentioned earlier in section 2.4.2.1, hydrazine stabilized U(IV)⁶⁶ is the commonly used reducing agent for this purpose. U(IV) reduces all Pu(IV) to Pu(III) as per the following reaction⁶⁷.



Thus for every mole of Pu(IV), half the mole of U(IV) is sufficient for effecting the

reduction. Depending on the fuel composition, partitioning could be carried out either in the organic or in the aqueous phase. When the plutonium composition in the spent fuel is relatively low like that in PHWR (typically 0.3 weight %), organic phase partitioning is preferred. In this case, the 1st cycle loaded organic product containing U(VI) and Pu(IV) is contacted with an aqueous scrub stream containing excess amount of hydrazine stabilized U(IV). This U(IV) gets extracted into the loaded organic and it reduces Pu(IV) to Pu(III). In real practice it was found that the quantity of U(IV) required is much higher than the stoichiometry due to various reasons like poor extractability of U(IV), presence of nitrous acid and absence of hydrazine in the organic phase to stabilize U(IV) etc⁶⁸. Since Pu(III) has a very low distribution co-efficient, it immediately strips into the aqueous phase. Thus the loaded organic would retain all the U(VI) and all Pu(III) would strip into the aqueous stream thereby effecting the partitioning.

In the case of FBR spent fuel reprocessing wherein plutonium concentration is higher (typically 20-30 weight %), carrying out partitioning in the organic phase after co-extraction of both uranium and plutonium would lead to unduly higher load of uranium on the plant as very high amount of U(IV) would be required to reduce all plutonium quantitatively in the organic phase. This is because of the combined effects of lower distribution co-efficient of U(IV) in TBP and many side reactions which consumes hydrazine thereby leading to oxidation of U(IV) to some extent in nitric acid medium⁶⁹. Hence while processing plutonium rich spent nuclear fuel, aqueous phase partitioning would be more economical from the overall plant capacity point of view. In aqueous phase partitioning, during the conditioning of the 1st cycle strip product, hydrazine stabilized uranous is added marginally more than the stoichiometric requirement (about 10% in excess) to convert all plutonium to Pu(III). Subsequently when this conditioned feed solution is subjected to solvent extraction, as Pu(III) has a poor distribution co-efficient in TBP, only U(VI) gets extracted leaving out Pu(III) and the excess U(IV) in the aqueous feed itself. The extracted U(VI) is then stripped using dilute nitric acid which is the **partitioned uranium product** stream. The Pu(III) left in the aqueous feed which is referred to as the **partitioned plutonium product** stream, had undergone one cycle of solvent extraction lesser when compared to the uranium stream. Hence it requires more purification from fission products and other associated impurities.

The U(IV) which is the reducing agent used in the partitioning cycle may be added externally or may be generated in-situ by electrolysis. The former method refers to the

chemical partitioning cycle and the latter is referred as the electrolytic/electrochemical partitioning.

2.4.5. Chemistry of the uranium purification cycle

The partitioned uranium product stream may contain some traces of plutonium and fission products which need to be further purified. This is done by solvent extraction using 30% TBP in n-dodecane as the solvent to obtain the purified uranyl nitrate solution (UNS). Depending on the levels of plutonium concentration, hydrazine stabilized uranous is also used to get the required decontamination from plutonium to enable the qualifying of final U_3O_8 product to be handled in fume hood type of containment. The UNS is then taken for reconversion operations for converting them to U_3O_8 through precipitation.

2.4.6. Chemistry of the plutonium purification cycle

The partitioned plutonium product stream depending on whether the partitioning is carried out by organic or aqueous phase partitioning will have certain amount of fission products as contaminants. In the case of aqueous phase partitioning since the plutonium stream is subjected to one cycle of solvent extraction lesser as compared to its uranium counterpart, the plutonium stream will be relative more contaminated with the fission products. Therefore it is taken to the plutonium purification cycles for further decontamination from fission products by employing a 20% TBP solution as the solvent to obtain the purified plutonium nitrate solution (PNS). When the amount of plutonium in the spent fuel is as high as in the case of FBRs, the plutonium purification cycles becomes more essential for not just purifying the plutonium product stream, but also to deliver a concentrated purified plutonium feed to the plutonium reconversion (PuRC) lab. This helps especially in two important ways. One is by making the PuRC feed concentrated and hence the % loss of plutonium during precipitation is reduced and secondly in reducing the work load of the laboratory personnel by reducing the volume of feed to be processed and thereby also leading to a reduction in the manrem expenditure.

The first step in this cycle is to condition the feed with respect to plutonium valency as plutonium is present in its third valency in the partitioned plutonium product stream. This is carried out similar to the feed conditioning step explained in section 2.4.2. The product stream obtained at the end of the plutonium purification cycle is the PNS which would be

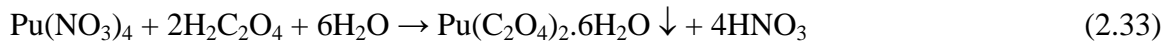
sent to the plutonium reversion lab to obtain the final PuO₂ product.

2.4.7. Chemistry of the tail-end processes during reprocessing

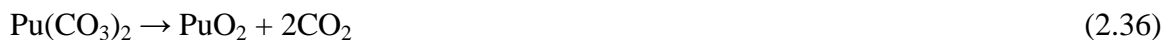
The uranium and plutonium reversion operations wherein the purified nitrate solutions of uranium and plutonium are converted to their respective solid oxide products through precipitation process is referred to as the tail-end processes in a spent nuclear fuel reprocessing plant.

2.4.12.1. Chemistry of plutonium reversion operation

In the plutonium reversion section, the feed PNS is conditioned to a concentration of 3.5 M nitric acid ensuring all the plutonium to be present in their +4 valency for quantitative precipitation. Oxalic acid is the precipitant used which is mixed with the conditioned feed in a definite proportion to precipitate all plutonium as Pu(IV) oxalate hexahydrate quantitatively. The reaction takes place as per the following equation.



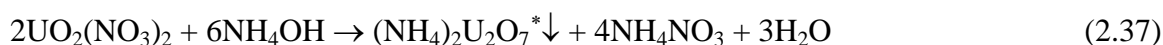
The plutonium oxalate precipitate obtained is then filtered, dried and calcined to obtain the final PuO₂ product. The reactions taking place during calcination are given below.



The rate of addition of feed, precipitant, intensity of mixing and temperature of the reaction mixture plays an important role in deciding the physical properties of the precipitate obtained.

2.4.12.2. Chemistry of the uranium reversion operation

In the uranium reversion operation, the UNS received from the uranium purification cycle is taken for precipitation of uranium as ammonium diuranate (ADU) by using liquid ammonia as the precipitant. The precipitation reaction takes place as per the following stoichiometric equation.



The ADU precipitate is then filtered, dried and calcined to get the final oxide product which is a mixture of UO_3 and UO_2 . The reactions taking place during calcination are given in the following equations.



In reprocessing plants, the calcination of ADU to obtain uranium oxide is normally carried out at about 773 K in the presence of air. Hence it is the reaction 2.38 which takes place predominantly. Thus the final oxide product obtained is a mixture of UO_3 and UO_2 which is normally referred as U_3O_8 ($2\text{UO}_3 + \text{UO}_2$).

2.5. Options for the dissolution of spent nuclear fuel in aqueous media

The primary purpose of the dissolution process step during the reprocessing of the spent nuclear fuel is to convert the spent fuel material to a suitable chemical and physical form that enables easy recovery of the fissile material present in them in the downstream process steps. As liquid is the most preferred physical form for the ease of its handling, dissolution aims at converting the spent fuel into their liquid form.

Among the various techniques available for separation of the species of our interest from a whole lot of material as is the case of spent nuclear fuel reprocessing wherein uranium and plutonium are separated from all the fission products practically comprising of all the elements in the periodic table, solvent extraction is the most preferred technique. This is because the technique is simple and amenable for commercial scale engineering with remote operations⁷⁰.

The next choice to be made is for the medium of dissolution. The oxide form of the nuclear fuel materials are ceramic and are generally known to be chemically inert. Hence to dissolve them we need strong mineral acids. The choices in that sense are limited to hydrochloric acid, nitric acid, and Sulphuric acid. Though there are processes like

* ADU – Ammonium diuranate is a compound of variable composition and is sometimes expressed as $\text{NH}_3(\text{UO}_3)_2 \cdot 3\text{H}_2\text{O}$ or as $\text{UO}_2(\text{OH})_2 \cdot x\text{H}_2\text{O} \cdot y\text{NH}_3$ where x and y depend on production conditions.

Sulfex⁷¹ and Darex⁷² wherein Sulphuric and aquaregia were used respectively during the dissolution either for chemical decladding or the dissolution itself, these processes have their own problems in terms of the stability of the resulting actinide sulphates or the corrosive nature of the solvent in the case of chlorides⁷³. It was also found that TBP does not selectively extract actinides as their chlorides⁷⁴.

One of the main reasons for not employing sulphuric acid as the medium of dissolvent in nuclear fuel reprocessing is the fact that UO_2 has poor solubility in it and also the inextractability of U(VI) sulphates by TBP^{75, 76}. Similarly HF could not be used because of the insolubility of UF_4 . Thus nitric acid turns out to be the most preferred mineral acid for the dissolution of oxide nuclear fuel materials during its reprocessing.

2.6. Importance of studying UO_2 and MOX dissolution kinetics

The INPP is presently in the beginning of the second of its three stages wherein FBRs are going to be the predominant nuclear power producing reactors. As emphasized earlier in this thesis, the success of FBR program is very much dependent on how efficiently and quickly its spent fuel is reprocessed and put back into the reactor for power production. As MOX is going to be the driver fuel at least for the initial FBRs, it is important to study their behavior during reprocessing particularly its dissolution in nitric acid. By understanding the dissolution behavior of these fuel materials in nitric acid, one could get deeper insight into their dissolution kinetics which is the basic input data required for designing the continuous dissolution system for this fuel. For the commercial scale reprocessing of these fuel materials, it is desirable to have continuous process systems as they reduce the overall inventory of the fuel materials outside the reactor in the entire nuclear fuel cycle. This would auger well for the safety of the processing and also would help in having better control over the nuclear material accounting. The continuous dissolution system also increases the overall plant capacity in addition to shrinking the floor space occupancy of the plant in comparison to batch mode of operation.

2.7. References

¹ Dey, P.K., Bansal, N.K., "Spent fuel reprocessing: a vital link in Indian nuclear power program" Nuclear Engineering and Design, Vol. 236, Issues 7-8 (April 2006) 723-729

² IAEA Tecdoc 1587, "Spent fuel reprocessing options", IAEA, Vienna, 2008

-
- ³ Brian. R. T. Frost, Chapter 2 – Fuel types in “Nuclear Fuel Elements – Design, Fabrication and Performance”, 1st Edition, 1982 Pergamon Press, page 18
- ⁴ Yasuo Arai, Atsushi Maeda, Ken-ichi Shiozawa, Toshihiko Ohmichi, “Chemical forms of solid fission products in the irradiated uranium-plutonium mixed nitride fuel”, J Nucl. Mat. 210 (1994) 161-166
- ⁵ Ken Kurosaki, Kosuke Tanaka, Masahiko Osaka, Yuji Ohishi, Hiroaki Muta, Masayoshi Uno and Shinsuke Yamanaka, “Chemical States of Fission Products and Actinides in Irradiated Oxide Fuels Analyzed by Thermodynamic Calculation and Post-Irradiation Examination”, Prog. Nucl. Sci. Tech., Vol. 2, pp.5-8 (2011)
- ⁶ Isamu Sato, Kosuke Tanaka et.al, “Chemical form consideration of released fission products from irradiated fast reactor fuels during overheating”, Prog. Nucl. Ener. 82 (2015) 86-91
- ⁷ Jeff C. Bryan. Introduction to Nuclear Science, 1st ed. Boca Raton, FL, U.S.A: CRC Press, 2009
- ⁸ Briefing to Congress, Office of Nuclear Energy, Science and Technology, U.S. DOE, January 2003
- ⁹ A. V. Bychkov, O. V. Skiba; “Review of Non-Aqueous Nuclear Fuel Reprocessing and Separation Methods”, in Chemical Separation Technologies and Related Methods of Nuclear Waste Management edited by Choppin, Gregory R. and Khankhasayev, Mikhail Kh. Volume 53 of the series NATO Science Series pp 71-98; 1999 Springer
- ¹⁰ J. P. Glatz, “Spent fuel dissolution and reprocessing processes”, Chapter 5.14 in Comprehensive Nuclear Materials Vol. 5, Editors Todd R. Allen, Roger E. Stoller and Shinsuke Yamanaka; Editor in Chief Rudy J. M. Konings
- ¹¹ Starks, J. B. “ The PUREX process”, U.S. Energy Research and Development Administration DPSPU 77-11-1, E.I. du Pont de Nemours and Company, Savannah River Plant, Aiken, SC, 1977
- ¹² Sood, D.; Patil, S. K. “Chemistry of nuclear fuel reprocessing current status”, J. Radioanal. Nuc.Chem. 1996, 203, 547–573.
- ¹³ A. P. Paiva, P. Malik, “Recent advances on the chemistry of solvent extraction applied to the reprocessing of spent nuclear fuels and radioactive waste”, J Radioanal. Nucl. Chem., Vol. 261, No. 2 (2004) 485-496
- ¹⁴ J. Malvyn Mckibben et.al., “Chemistry of the PUREX process”, Radiochimica Acta, 36, 3-15, 1984

-
- ¹⁵ R. Natarajan and Baldev Raj, "Technology development of fast reactor fuel reprocessing in India", *Current Science*, Vol. 108, No. , January 2015, p. 30
- ¹⁶ Blanco, R. E.: "Dissolution and Feed Adjustment," in *Symposium on the Reprocessing of Irradiated Fuels*, Held at Brussels, Belgium, May 20-25, 1957, USAEC Report TID-7534, book 1, pp. 22-44
- ¹⁷ Benedict, M., T. H. Pigford, and H. W. Levi, 1981. *Nuclear Chemical Engineering*, second edition, McGraw-Hill
- ¹⁸ R. Natarajan, "Challenges in Fast Reactor Fuel Reprocessing", *IANCAS Bulletin*, July 1998, pp 27-32
- ¹⁹ Armando L. Uriarte and Robert H. Rainey; "Dissolution of high-density UO₂, PuO₂ and UO₂-PuO₂ pellets in inorganic acids", ORNL-3695, April 1965
- ²⁰ R. Natarajan, Baldev Raj; "Fast Reactor Fuel Reprocessing Technology in India", *J. Nucl. Sci. Tech.*, 44 (3) (2007) pp. 393-397
- ²¹ W. E. Clark, T. A. Gens; "A study of dissolution of reactor fuels containing Zr in a Ti vessel", ORNL-3118, Oct 1961
- ²² W. D. Burch; Oak Ridge National Laboratory; " Advanced concepts under development in the US breeder-fuel-reprocessing program", CONF-811154—1, DE82 003965
- ²³ J. M. Cleveland; "Dissolution of refractory PuO₂", *J. Inorg. Nucl. Chem.* Vol. 26 (1964) pp. 1470-1471
- ²⁴ V. C. A. Vaughen, J. H. Goode; Chemical Technology Division, ORNL; "Dissolution of irradiated MOX fuels", CONF-791086—4, Oct 1979
- ²⁵ J. Bourges, C. Madic, G. Koehly et M. Lecomte; "Dissolution of PuO₂ in HNO₃ medium with electro generated Ag(II)" *J. Less-Common Metals*, 122 (1986) 303-311
- ²⁶ Ewald Veleckis, Joseph C. Hoh; Chemical Technology Division, Argonne National Laboratory; "Dissolution characteristics of mixed UO₂ powders in J-13 water under saturated conditions", ANL—91/8, DE91 010968; March 1991
- ²⁷ H. A. Woltermann, T. L. Ulrick and D. Antion; Monsanto Research Corporation, Ohio, US, "Dissolution of high fired Plutonium Oxide", MLM-2010, TID-4500, UC-4 , March 1973
- ²⁸ R.F. Taylor et al., "Dissolution rates of uranium dioxide sintered pellets in nitric acid systems", *J. Appl. Chem.*, 13, 1963, 32
- ²⁹ S. A. Steward, W. J. Gray; Lawrence Livermore national laboratory; "Comparison of

uranium dissolution rates from spent fuel and uranium dioxide”, UCRL-JC-115355, Jan 1994

³⁰ B. C. Finney, B. A. Hannaford, G. A. West, and C. D. Watson, “Shear-Leach Process: Semi continuous and Batch Leaching of Sheared, Unirradiated Stainless-Steel-Clad and Zircaloy-2-Clad UO₂ and UO₂-ThO₂”, Oak Ridge National Laboratory report ORNL-3984 (July 1969)

³¹ D. O. Campbell, J. C. Mailen, R. L. Fellows; Oak Ridge National Laboratory; “Dissolution behavior of FFTF fuel”; CONF-840802—19, DE85 001854, August 1984

³² V. C. A. Vaughen, J. H. Goode; Chemical Technology Division, ORNL; “Fuel reprocessing tests with short cooled LMFBR type fuel rods”, CONF-720607--16, June 1972

³³ D. E. Horner, D. J. Crouse, J. C. Mailen; “Cerium-promoted dissolution of PuO₂ and PuO₂-UO₂ in nitric acid”, ORNL/TM-4716, August 1977

³⁴ D. Harmon, Aiken, SC, “Dissolution of PuO₂ with cerium(IV) and fluoride promoters”, USAEC Rep. DP-1371, 1975

³⁵ Jack L. Ryan, Lane A. Bray; “Dissolution of Plutonium Dioxide - A Critical Review”, ACS Symposium Series, 1980,117, 449

³⁶ J. L. Ryan, L. A. Bray, E. J. Wheelwright, G. H. Bryan; “Catalyzed Electrolytic Plutonium Oxide Dissolution (CEPOD)”, PNL-SA-18018, DE91 004066, July 1990

³⁷ J. R. Cadieux, J. A. Stone; E. I., “Voloxidation and dissolution of irradiated plutonium recycle fuels”, du Pont de Nemours & Co., Savannah River Laboratory; DP-MS-80-10; CONF-800943—12; Oct 1980

³⁸ Taylor, R. F.; Sharratt, E. W.; Chazal, L. E.; Logsdail, D. H. “Dissolution rate of uranium dioxide sintered pellets in nitric acid systems”, J. Appl. Chem. 1963, 13, 32–40

³⁹ Shabbir, M.; Robbins, R. G. “Kinetics of the dissolution of uranium dioxide in nitric acid-I”, J. Appl. Chem. 1968, 18, 129–134

⁴⁰ Inoue, A.; Tsujino, T. “Dissolution rates of U₃O₈ powders in nitric acid”, Ind. Eng. Chem. Process Des. Dev. 1984, 23, 122–125

⁴¹ Madic, C., Berger, P., Machuronmandard, X., (1992). “Mechanisms of the rapid dissolution of plutonium dioxide in acidic media under oxidizing or reducing conditions”, Morss L. R. and Fuger J.(eds.) *Transuranium Elements – A half century*, pp. 457–468, American Chemical Society

⁴² H. Bokelund et al., “Dissolution of Mixed Carbide Fuels in Nitric Acid”, Radiochim. Acta 30, 49-55 (1982)

-
- ⁴³ J. R. Flanary, J. H. Goode, M. J. Bradley, J. W. Ullmann, L. M. Ferris, G. C. Wall, "Hot-Cell Studies of Aqueous Dissolution Processes for Irradiated Carbide Reactor Fuels", ORNL-3660, Oak Ridge (1964)
- ⁴⁴ L. M. Ferris, M. J. Bradley, "Reactions of the Uranium Carbides with Nitric Acid", J. Am. Chem. Soc. 87, 1710 (1965)
- ⁴⁵ Atomic Energy Act, 1962, GSR-125, Atomic Energy (Safe Disposal of Radioactive Waste), Rule (vi) (1987)
- ⁴⁶ Conditioning and storage of spent fuel element HULLs, "Proceedings of a meeting held in the scope of the R&D Programme of the European Communities on Radioactive Waste Management and Storage Brussels, 19 January 1982", Edited by W. Hebel and G. Cottone
- ⁴⁷ Blanco, R. E.: "Dissolution and Feed Adjustment," in Symposium on the Reprocessing of Irradiated Fuels, Held at Brussels, Belgium, May 20-25, 1957, USAEC Report TID-7534, book 1, pp. 22-44
- ⁴⁸ R. H. Rainey and J. G. Moore, "Laboratory Development of the Acid Thorex Process for Recovery of Consolidated Edison Thorium Reactor Fuel", ORNL-3155, Oak Ridge National Laboratory, Oak Ridge Tennessee, April 27, 1962
- ⁴⁹ Gresky, A.T.; Bennet, M.R.; Brandt, S.S.; McDuffee, W.T.; Savolainen, J.E., "Progress Report on Laboratory Development of the Thorex Process", (1953) USAEC Report, ORNL – 1367
- ⁵⁰ Smith, P. W.: "The Zirflex Process Terminal Development Report," Report HW.65979, Aug. 20, 1960
- ⁵¹ T. A. Gens, "Modified Zirflex Process for dissolution of 1-10% Uranium-Zirconium Alloy Fuels in Aqueous $\text{NH}_4\text{F-NH}_4\text{NO}_3\text{-H}_2\text{O}_2$ ", Laboratory Development, USAEC Report ORNL-2905, Oak Ridge National Laboratory, Mar. 18, 1960
- ⁵² Fisher, F. D.: "The Sulfex Process Terminal Development Report," USAEC Report HW-66439, Aug. 22, 1960
- ⁵³ Z.Kolarik, Handbook on the Physics and Chemistry of the Actinides, Elsevier Sci. Publ. Vol 6 (1991) 181
- ⁵⁴ B.L.Vondra, D.J.Crouse, Proc.AIChE Symposia Series 191, Vol.75 (1979) 207
- ⁵⁵ Bruce K. McNamara, Edgar C. Buck, Chuck Z. Soderquist, Frances N. Smith, Edward J. Mausolf, Randall D. Scheele, "Separation of metallic residues from the dissolution of a high-burnup BWR fuel using nitrogen trifluoride", Journal of Fluorine Chemistry 162 (2014) 1–8

-
- ⁵⁶ B.Anderson, J.D.Frew, O.Pugh, P.J.Thompson, “Reprocessing the fuel from the prototype fast reactor”, *The Nuclear Engineer*, 35(1994)129
- ⁵⁷ G. L. Silver, “Plutonium: disproportionation reactions and acidity changes”, *J Radioanal Nucl Chem* (2016) 308:759–763
- ⁵⁸ John M. Haschke, “Disproportionation of Pu(IV): A reassessment of kinetic and equilibrium properties”, *Journal of Nuclear Materials* 362 (2007) 60–74
- ⁵⁹ Baumgartner, F.; Schmieder, H., “Use of Electrochemical Processes in Aqueous Reprocessing of Nuclear Fuels”, *Radiochimica Acta* 25, 191-210 (1978)
- ⁶⁰ David G Karraker, “Oxidation of hydrazine by nitric acid”, *Inorg. Chem.* 1985, 24, 4470-4471
- ⁶¹ K. M. Goff, J. C. Wass, K. C. Marsden, and G. M. Teske, “Electrochemical processing of used nuclear fuel”, *Nucl. Engg. Tech.*, VOL.43 NO.4 AUGUST 2011, 335
- ⁶² H.Schmieder, G.Petrich, “A concept for an improved Purex process”, *Radiochim. Acta*, 40 (1989) 181
- ⁶³ D.D. Sood, A.V.R. Reddy and N. Ramamoorthy, “Fundamentals of Radiochemistry”, 2nd ed., IANCAS publication, BARC, Mumbai (2004)
- ⁶⁴ OECD-NEA (2012), “Spent Nuclear Fuel Reprocessing Flowsheet”, NEA/NSC/WPFC/DOC(2012)15 June 2012
- ⁶⁵ T. W. Newton and V. L. Rundberg, “Disproportionation and Polymerization of Plutonium(IV) in Dilute Aqueous Solutions”, *Mat. Res. Soc.*, Volume 26 January 1983, 867
- ⁶⁶ Carl S. Schlea, “Uranium(IV) nitrate as a reducing agent for plutonium(IV) in the purex process”, DP808, 1963
- ⁶⁷ V. Reshmi, N.K. Pandey, R. Sivasubramanian, S. Ganesh, M.K. Ahmed, U. Kamachi Mudali and R. Natarajan, “Process modeling of in-situ electrochemical partitioning of uranium and plutonium in purex process: Benchmark results with uranium reduction”, *Desalination and Water Treatment*, 38:1-3, 29-39, 2012
- ⁶⁸ G. Petrich, H. Schmieder, *Proceedings of the International Conference on 'Solvent Extraction', ISEC'83, Denver, Co. Aug. (1983)*
- ⁶⁹ Z. Kolarik, R. Schuler, “Solvent Extraction Recovery of Plutonium from Raffinate Concentrates in the Purex Process”, KFK 3956, August 1985
- ⁷⁰ F. Drain, R. Vinoche, J. Duhamet, “40 years of experience with liquid-liquid extraction equipment in the nuclear industry”, WM'03 Conference, February 23-27, 2003, Tucson, AZ

-
- ⁷¹ B. C. Finney and B. A. Hannaford, "Sulfex process: Engineering scale semicontinuous decladding of unirradiated SS clad UO₂ and UO₂-ThO₂", ORNL-3072, 1961
- ⁷² F. G. Kitts, W. E. Clark, "DAREX Process: Processing of stainless steel containing reactor fuels with dilute aqua regia", ORNL-2712, 1962
- ⁷³ Ahrland, Bagnall et.al., "The Chemistry of the Actinides", Pergamon texts in Inorganic Chemistry, Vol. 10, Pergamon Press 1973
- ⁷⁴ Tomitaro Ishimori, Kenju Watanabe and Eiko Nakamura, "Inorganic Extraction Studies on the System between TBP and HCl", Bulletin of the Chemical Society of Japan, 33, 636, 1960
- ⁷⁵ John F. Flagg (Ed.), "Chemical processing of reactor fuels", Academic Press, New York 1961, p-91
- ⁷⁶ Bhargava, S.K., Ram, R., Pownceby, M., Grocott, S., Ring, B., Tardio, J., et al., "A review of acid leaching of uraninite", Hydrometallurgy 151, 10-24, 2015

CHAPTER 3. Literature review on the dissolution of nuclear fuel materials

3.1 Introduction

The dissolution of nuclear fuel materials in its various chemical forms in different solvent medium under varied conditions has been a topic of research among the entire nuclear technology fraternity world over ever since the nuclear energy was seen as one of the potential option in meeting the ever growing energy demand of the humans. Hence prior to starting any research work in this topic it is important to assimilate the information available in the literature till date to plan the work systematically. This saves a lot of time and energy while trying to achieve the set targets in the research work within the stipulated time. This chapter consolidates the information prevailing in the literature on dissolution behaviour of urania and its mixtures with other actinide oxides in various acid media. As the current topic is more relevant to MOX fuel dissolution in PUREX process, more emphasis is given for urania and (U, Pu) MOX fuel dissolution in nitric acid.

3.2 Aqueous dissolution of urania, plutonia and their powders and pellets

Urania, by far is the widely studied ceramic nuclear fuel material. This is because; several of its properties are favorable for it to be used as a nuclear fuel¹. Most important of these are its stable structure right up to the melting point and excellent compatibility with cladding alloys². The most preferred method of reprocessing a spent/irradiated UO₂ nuclear fuel is the Purex process which is an aqueous based process.

Before getting into the details of the literature relevant to nuclear fuel dissolution, Table 3.1 provides a bird's eye view of the chronological list of major works available in the literature till date along with the primary findings of each of the work as a ready reckoner. Only those works which yielded any major results with respect to the dissolution of nuclear fuel materials in oxide form in inorganic acids are covered in Table 3.1. The text following Table 3.1 provides details of many other works to aid the reader to have a complete picture of the existing literature by extensively covering the information pertaining to oxide fuel dissolution wherein certain special methods were adopted for some specific tasks.

Table 3.1. Chronological list of important literature information relevant to nuclear fuel dissolution as on date

S.No.	Author/s; Main finding/s	Other details					
		Pellets shape	E _a (kcal/mol)	Kinetic expression	[HNO ₃] (M)	Additive	Surface area (m ² /g)
1	Taylor et al (1963) - Dissolution rate of UO ₂ pellets in nitric acid; Order of the reaction w.r.t. nitric acid	UO ₂ pellets	11.47 (unstirred); 13.44 & 14.8±1.3 (unstirred)	-	3-10	-	-
2	Blaine (1960); Dissolution of power reactor fuel cores was studied and the catalytic effect of uranyl ions was investigated						
3	Shabbir and Robins (1968, 1969) - Kinetic studies of dissolution of UO ₂ in nitric acid; U ⁴⁺ aided reaction mechanism	UO ₂ powder(0.003– 0.3 μm)	7.33	-	0.5-2	-	-
		Sphere(100– 500μm)	16.68	-	2-10	-	-
		UO ₂ pellet(D=0.25 in, L=0.75 in)	25.6 (650 psi)	-	4-10	-	-
4	Zimmer and Merz (1984); Reaction mechanism for the dissolution of Th, U MOX in nitric acid was investigated						
5	Inoue et. al. (1984 and 1986) - Kinetic studies of dissolution of UO ₂ and U ₃ O ₈ in nitric acid Reaction mechanism	U ₃ O ₈ powder (4.8 μm)	16.94	-	4-10	-	-
6	Ikeda et.al. (1993); Based on the ¹⁷ O NMR studies on UO ₂ dissolution, U ⁴⁺ aided reaction mechanism was investigated and a one electron transfer mechanism was proposed						
7	Ryan and Bray (1980); Dissolution of PuO ₂ was studied and a thermodynamic explanation for the sluggish dissolution of PuO ₂ over UO ₂ was given						
8	Fukasawa and	Pellet(D=1	-		7.3	-	-

S.No.	Author/s; Main finding/s	Other details					
		Pellets shape	E _a (kcal/mol)	Kinetic expression	[HNO ₃] (M)	Additive	Surface area (m ² /g)
	Ozawa (1986) - Role of porosity on UO ₂ pellets dissolution; Modeling methodology	cm, L=1.1 cm)			(initial)		
9	Ikeda et.al. (1995) - Kinetic studies of dissolution of UO ₂ powders in nitric acid; Speculated the role of nitrous acid and explained the mixing effect	Powder (300–350 μm)	14.22 (18.9±1.6)	-	6-9.5	-	-
	Uriarte and Rainey (1965) - Dissolution of high density MOX pellets in inorganic acids; Instantaneous dissolution rates and order w.r.t. nitric acid	UO ₂ pellets (D=1.06 cm, L=1.59 cm)	-	-	2-10	-	-
10	Uriarte and Rainey (1965) - Dissolution of high density MOX pellets in inorganic acids; Instantaneous dissolution rates and order w.r.t. nitric acid	MOX pellets		$(k C_{\text{HNO}_3}^{4.05} C_{\text{HF},0}^{0.37}) / C_{\text{Al}(\text{NO}_3)_3,0};$ $k C_{\text{HNO}_3}^{0.78}$ $C_{\text{Cd(IV)},0}^{0.58};$ $k C_{\text{HNO}_3}^{-0.13}$ $C_{\text{HCl},0}^{1.01}$	4-14 7-14 2-14	HF(0.005–0.1) Al(NO ₃) ₃ (0.015–0.3) Ce(IV) (0.0005–0.5) HCl (0.1–5)	7.3×10 ⁻⁵
11	Berger (1990, 1992); Electrochemical studies of PuO ₂ dissolution was carried out and the reaction mechanism based on the redox reactions of MOX fuel was determined						
12	Gelis et.al. (2011); Developed a method to dissolve plutonium rich MOX fuels aided by ozone using Am(VI)/Am(III) couple as mediators						

S.No.	Author/s; Main finding/s	Other details					
		Pellets shape	E _a (kcal/mol)	Kinetic expression	[HNO ₃] (M)	Additive	Surface area (m ² /g)
13	Harmon (1975); Dissolution of PuO ₂ aided by Ce(IV) and fluoride ions was investigated to determine the reaction mechanism				8	KF(0.05) Ce(IV) (0.0125- 0.05)	-
14	Barney (1977) - Dissolution kinetics of PuO ₂ in HNO ₃ /HF mixtures; Explanation for the surface attach of PuO ₂ by HF	Powder	13	k C _{HF}	10	HF (0.05- 0.2)	2.9
15	Miner et.al. (1969) - Dissolution of PuO ₂ in nitric acid; Order of the reaction w.r.t. HF	Circular coupons	1.61	k C _{HNO₃} ^{-0.048} C _{HF,0} ^{0.73}	1-5	HF (0.01- 0.13)	8.7x10 ⁻⁵
16	Horner (1977) - Cerium promoted oxidative dissolution of PuO ₂ ; Explored a method to dissolve plutonium rich MOX fuels	Micro spheres	14.5	k C _{Ce}	4	Ce(IV) (0.03- 0.12)	1.2x10 ⁻²
17	Bjorklund and Staritzky (1954); Use of HCl and HI for dissolving PuO ₂ based fuels						
18	Shakila et.al. (1987, 1989); Dissolution of PuO ₂ in HNO ₃ /HF/N ₂ H ₄ medium was carried out to demonstrate the feasibility of reductive dissolution of PuO ₂ using Fe(II)/Fe(III) couple						
19	Fife (1996); Kinetics of PuO ₂ dissolution in HCl was carried out and a non-porous shrinking particle model was developed						
20	Hirotoimo Ikeuchi et.al. (2012); Dissolution behaviour of irradiated MOX fuel was studied and it was found that MOX containing beyond 30-35% of PuO ₂ by weight does not dissolve completely in pure nitric acid						

S.No.	Author/s; Main finding/s	Other details					
		Pellets shape	E _a (kcal/mol)	Kinetic expression	[HNO ₃] (M)	Additive	Surface area (m ² /g)
21	<p>Desigan et. al. (2017);</p> <p>NO_x composition was measured during the course of UO₂ dissolution under typical PUREX conditions for the first time and the reaction mechanism was determined based on this information. The change in surface area of the pellet during dissolution was also estimated for the first time.</p> <p>Dissolution kinetics of simulated urania-ceria MOX was studied and understood under various conditions.</p> <p>MOX fuel dissolution was investigated under various conditions of acidity, temperature and mixing.</p> <p>Penetration and surface area based model equations were developed to explain the dissolution behaviour of all these fuels. The model was validated using the experimental results and were found to explain the reaction satisfactorily.</p>						

One of the earliest reported works on the dissolution of UO₂ was carried out by Taylor et al.³. They had studied the dissolution of sintered uranium dioxide pellets in nitric acid at various temperatures and given the initial rate plots which indicate that, in the range of 2-10 M nitric acid, the logarithm of the rate of dissolution is proportional to the concentration of nitric acid raised to the power 2.3-3.3, the precise value depending on temperature. At concentrations greater than about 10 M, the logarithm of the rate was found to vary directly with the concentration of nitric acid. The latter relationship was attributed to diffusional control. They also reported a decrease in reaction rate with increased stirring speed, reaching constant rate at about 400 RPM, which they conjectured to autocatalysis by nitrous acid formed during the reduction of nitric acid.

Prior to this, Blain⁴ reported similar work on the dissolution of sintered UO₂ pellets in nitric acid in which the logarithm of the rate was found to be proportional to the concentration of nitric acid raised to the power 1.2. An increase in dissolution rate with added uranyl nitrate was also reported.

In 1984 Zimmer and Merz⁵ first speculated the oxidative dissolution of UO₂ in nitric acid to proceed through the oxidation of U(IV) to U(VI) in the solid state. This hypothesis gained momentum with the results published by Inoue et.al,^{6, 7} based on the kinetic studies of dissolution of UO₂ and U₃O₈ in nitric acid. They concluded that the rate determining step was the interfacial electron transfer reaction between solid UO₂ and proton in the nitric acid solution.

Simultaneously there were studies conducted on the plutonium dissolution in nitric acid medium in the presence of fluoride ions⁸. However, it didn't provide much insight and was found to be of mere academic interest and gave very little direction to the plutonium dissolution in nitric acid medium.

Subsequently Fukasawa and Ozawa⁹ of Hitachi, Japan studied the dependence on the acid concentration, temperature and porosity on the initial dissolution rate. It was also found that air oxidation of the spent fuel to U_4O_{9+x} and unirradiated UO_2 to U_3O_7 had no significant effect on the subsequent steady state dissolution rates of uranium¹⁰.

Eary and Cathles¹¹ have studied the dissolution reactions of UO_2 in $H_2O_2-SO_4^{2-}-H_2O$ solution and proposed that a direct two electron transfer process between H_2O_2 and UO_2 is the rate-determining step.

Shabbir and Robins^{12, 13} proposed a mechanism for the dissolution of UO_2 in nitric acid particularly in the lower acid concentration range by making use of the energetics known for the system. They dissolved UO_2 powder in nitric acid of varying concentration and generated the rate curves at different temperatures. Based on thermodynamic considerations and the experimental results, they proposed a reaction mechanism initiated from the formation of U^{4+} ions, followed by the oxidation of U^{4+} to UO^{2+} or UO_2^{2+} with NO_3^- and HNO_2 . They carried out the dissolution reaction in the presence of sodium nitrite to confirm the catalytic role of nitrous acid.

Inspired by all these results, Ikeda et.al¹⁴ carried out more studies to evaluate the mechanism for UO_2 dissolution in nitric acid medium. They ruled out the mechanism aided by the formation of U^{4+} as proposed by Shabbir and Robins based on the ^{17}O NMR studies. They concluded that the dissolution of UO_2 is initiated by the two-electron transfer reaction between UO_2 and oxidants in solid phase. They also emphasized that if the rates of reactions between UO_2^+ and oxidants are faster than that of the disproportionation of UO_2^+ ions and the oxygen in UO_2^+ is extremely inert, then the mechanism that the dissolution of UO_2 is initiated from the one-electron transfer between UO_2 and oxidants in the solid phase is quite reasonable.

Ikeda et.al¹⁵, in 1995 evaluated the dissolution kinetics of UO_2 powder in nitric acid based on the assumption that the particles of UO_2 powder are spherical and dissolves homogeneously from the external surface. They explained the effect of stirring speed and temperature on dissolution rates of UO_2 from the dependence of dissolution rate on the concentration of HNO_2 . The HNO_2 concentration at the surface of UO_2 pellets or powders

is the highest in an unstirred solution and decreases with increasing the stirring speed. Hence, the dissolution rates of UO_2 become slow with an increase in stirring speed. The dissolution rate of UO_2 pellets in boiling HNO_3 was typically found to be one-half to one-fifth of that expected at the same temperature in the absence of boiling. This was explained based on the fact that the HNO_2 concentration in HNO_3 solution becomes very low under boiling condition due to its self-decomposition reaction. They also found that the dissolution rate of UO_2 was not accelerated by UO_2^+ ions.

Keith¹⁶ in his doctoral thesis had come out with detailed explanation for the dissolution rate of PuO_2 in HCl medium using Fe(II) as one electron transfer catalyst as an alternate route to nitric acid dissolution procedure.

Steward and Mones¹⁷ in 1996 have modelled the intrinsic dissolution rates of UO_2 under a variety of well controlled conditions. The study was more relevant to a geologic repository. Hence it didn't gain the attention of the reprocessing domain. But it certainly paved way for better modeling of dissolution rates of spent fuel and also remained to indicate the issues in U/Pu slippage in the waste streams.

In 2004 Mineo et.al¹⁸, made an investigation into the dissolution rate of spent fuel in aqueous reprocessing. They proposed a simple dissolution rate equation for the LWR fuel taking into account of cracks occurred during irradiation to estimate the initial effective dissolution area and the change in the area during dissolution.

Subsequently, Heisbourg et al¹⁹ carried out leaching studies on thoria/urania MOX systems in nitric acid medium whose composition varied very widely. They studied the effect of uranium content on the leaching behaviour.

But all these studies were carried out from the point of view of final disposal of spent fuel rather than reprocessing. Hence not much information could be derived out of them as such in the context of spent fuel reprocessing.

For the plutonium rich MOX which are difficult to dissolve completely in nitric acid medium alone, it was felt that ultrasound is a good alternate method to improve the dissolution kinetics. Hence studies were initiated to dissolve the refractory oxides like CeO_2 and PuO_2 by Sonochemistry²⁰. The initial studies aimed at producing free radicals generated by cavitation (bubble implosion) to obtain either the oxidative or reducing conditions required for PuO_2 dissolution. The results indicated that the dissolution rates were even lesser than employing reagents like Ag(II) and HF . Later more investigation was carried out to test the effect of ultrasound on the dissolution of high fired PuO_2 ²¹.

Overall, the results indicate that applying ultrasound for the dissolution of refractory PuO_2 does not offer any substantial advantage over the conventional “heat and mix” treatment. Mixed oxide (MOX) fuel of urania and plutonia are typically used to drive fast breeder reactors. The plutonium composition in the MOX fuel varies from about 10% to 30% by weight. If plutonium exceeds this amount, it renders the fuel practically insoluble in neat nitric acid medium²².

Most of the literature information on MOX dissolution were a result of investigation of the MOX fuel leaching characteristics during the long term storage of spent MOX fuel^{23, 24, 25, 26} from environmental safety point of view.

3.3 Effect of various parameters on UO_2 dissolution in nitric acid

The factors which are generally expected to affect the dissolution kinetics of UO_2 pellets in nitric acid were initial concentration of nitric acid, temperature, specific surface area of the initial pellets, rate of agitation of the reaction mixture etc. Apart from this, there are many other parameters which tend to alter the dissolution kinetics. Some of these are, the method of fabrication (powder metallurgy route, coprecipitation route etc.), the grain size of the starting material used for fabrication, the fabrication process conditions, the sintering temperature, the burnup etc. The present work aims at understanding the role played by most of these parameters.

The process conditions adopted during the fabrication of nuclear fuel were all well established and standardized. Hence one could assume that these parameters are more or less the same while preparing all the types of nuclear fuel of a given chemical form (oxide or nitride or metallic etc.). Hence we consider only those conditions which the spent fuel is subjected to during its reprocessing. Influences of some of those key parameters are briefly explained in this chapter.

3.3.1 Effect of initial concentration of the acid

In general, the concentration of the acid is directly proportional to the dissolution rate. But as chemical corrosion of the dissolver material is an important factor to be considered²⁷, there has to be a proper balance between the maximum acidity to be used and the corrosion tolerance of the material of construction of the dissolver. Generally for thermal reactor spent fuel (TRSF) processing, maximum concentration of acid used would be around 8 M²⁸ while the plutonium rich FBR fuels demands higher acidity (11.5 M

approx.) due to its relatively sluggish dissolution in nitric acid medium²⁹. The results of the experiments presented in Chapter 5 would further emphasize this fact.

3.3.2 Effect of mixing/agitation rate

Mixing generally increases the rate of dissolution of any solid in liquid. This is due to two reasons. The first is the supply of fresh liquid reactant to the solid surface which enhances the reaction rate (with the exception of auto-catalytic reaction) and the second is the roughening of the solid surface which increases the surface area and thereby the contact area between the solid pellet and nitric acid. The solid surface morphology changes increasing the area of contact between solid and the liquid. In the case of UO₂, as it undergoes oxidative dissolution in nitric acid, the presence of nitrous acid (a strong oxidizing reagent) in equilibrium with nitric acid at all conditions alters the dissolution rate. Many studies in the literature have shown mixing to have a negative effect on UO₂ dissolution rate in nitric acid¹⁰⁻¹⁵. The same was also observed in the present work as reported in detail in Chapter 5. The reason for this observation was found to be the dispersion of nitrous acid from the solid-liquid interphase to the bulk at higher mixing rate which makes nitrous acid to be unavailable at the reaction centre for accelerating it. Nitrous acid aids the dissolution of UO₂ by the following reaction.



The nitrous acid is again produced back in the system by the following reaction between NO₂ and water.



3.3.3 Effect of temperature

Temperature is generally proportional to the rate of dissolution of any solid in liquid. During the dissolution of UO₂ pellets in nitric acid, a similar trend is observed. However since UO₂ undergoes oxidative dissolution, the invariable presence of nitrous acid, a good oxidising agent, whose concentration depends strongly on temperature, makes the dissolution kinetics more complex. This issue is also addressed in detail in Chapter five.

3.3.4 Effect of specific surface area of the pellets

Generally for solids dissolving in any liquid, the area of contact between the dissolving solid and the solvent liquid strongly influences the dissolution rate. The chemical reaction engineering treatment of a heterogeneous reaction between a solid and liquid in terms of shrinking particle model gives a very good account of the relation between the effective surface area of the solid to the rate of the dissolution reaction³⁰. This is dealt in detail in Chapter five.

3.3.5 Effect of the presence of other ions/species

UO₂ dissolves in nitric acid oxidatively. Hence the presence of any ions/species in the solution which accelerates or hampers this oxidation will accordingly influence the rate of the reaction. The presence of nitrous acid along with nitric acid in equilibrium has long been established in the literature³¹. Nitrous acid is a well-known oxidizing agent. Hence its presence in the reaction mixture during the dissolution of UO₂ in nitric acid is expected to accelerate the reaction depending on its concentration which in turn depends on temperature.

3.4 Dissolution of PuO₂ in nitric acid

Pure PuO₂ is never used as such during any operations involved in the nuclear technological industries world over. Hence the dissolution of pure PuO₂ has never existed as a process requirement at any stage of the nuclear technological operations. The dissolution of pure PuO₂ received more attention from the researchers world over only during the recovery of plutonium from undissolved residue from the dissolvers of reprocessing plants and also from some of the scrap materials in the nuclear industries.

In contrast to UO₂, PuO₂ dissolves in HNO₃ very slowly. Uriarte and Rainey³² observed that the instantaneous dissolution rate is proportional the fourth power of concentration of HNO₃. However, in 10 M HNO₃, the instantaneous dissolution rate of UO₂ pellet is 22.22 mg cm⁻² min⁻¹, while that of PuO₂ is 1×10⁻³ mg cm⁻² min⁻¹. It is observed that PuO₂ is practically insoluble in HNO₃. Ryan and Bray³³ supported this observation by showing that PuO₂ is practically insoluble in nitric acid from a thermodynamic analysis. They justified the insolubility of PuO₂ in non-complexing acid media based on the free energy which they had calculated for their dissolution experiments. They computed the standard free energy of the dissolution reaction to be $\Delta G_{313}^{\circ} = 41$ kJ/mol in low acidities

(< 5 M) and at the acid boiling point to be only slightly more favorable at $\Delta G_{373}^{\circ} = -10.5$ kJ/mol. They suggested for more studies to unravel the mechanism of PuO_2 dissolution. Fast reactor fuel typically contains plutonium to about 10 to 30% by weight of the total heavy metal (THM), and for all the other reactors it is less. Thus, for the commercial success of the fast reactor fuel cycle technology, the dissolution of FRSF is a major step to be well explored. From the previous two sections and the references therein, it is well known that uranium based spent fuel dissolves relatively easily in nitric acid with simple heating, whereas addition of PuO_2 (making it a MOX fuel) renders the dissolution more sluggish, which is proportional to its composition. Once plutonium exceeds 35% of the THM, it was found to be difficult to dissolve it completely using nitric acid alone^{32, 34, 35}. To enable the dissolution of such plutonium rich fuel, either electrolytic or addition of any strong oxidizing agents like hydrofluoric acid is normally required³³. When scrap materials with relatively high plutonium is dissolved, which is normally a one-time campaign, dissolver vessel made of special material like Ti or Zr is used to make it chemically strong enough to withstand the highly corrosive nature of the chemicals required to dissolve it.

In the Purex process, Pu(IV) is the most suitable oxidation state for its extraction by TBP solvent from the nitric acid medium. Hence after oxidative dissolution of PuO_2 , one has to reduce the resulting Pu(VI) ions to Pu(IV) which was found to be kinetically hindered in the nitric acid medium. This leads to the exploration of optimal methods to reductively dissolve PuO_2 as oxidation of Pu(III) to Pu(IV) is a single electron transfer process without any bond cleavage and is kinetically more favored. In the following section, various methods of PuO_2 dissolution in HNO_3 with several promoters are described.

3.5 *PuO_2 dissolution in aqueous acids with fluoride promoters*

The addition of small amount of fluoride promoters such as HF or KF in HNO_3 solution is the most widely used method to dissolve PuO_2 rapidly^{32, 33, 36}. Although the addition of HF initially increases the dissolution of PuO_2 by several folds, it slows down as the reaction progresses. One of the reasons might be the precipitation of plutonium tetrafluoride. Moreover, HF is corrosive to the process equipment and interferes in the solvent extraction steps of the reprocessing as found by Kazanjian and Stevens³⁷. Several authors studied the kinetics of dissolution of PuO_2 with fluoride promoters. Barney³⁸ proposed that the reaction on PuO_2 surface with the undissociated HF is the rate-

controlling step. Moreover, it was also observed that HF makes stronger complex with Pu(IV) to produce PuF^+ complexes, and the dissolution rate decreases when the total concentration of Pu(IV) is greater than that of HF. Hence, they concluded that HF is getting consumed in stoichiometric quantity as the reaction proceeds, and its role is beyond a catalyst in the process.

The analysis of the instantaneous dissolution rate (IDR) vs time data for pellet by Uriarte and Rainey³² indicates that the IDR is proportional to the fourth power of concentration of HNO_3 , and the 1.31th power of HF concentration. On other hand, Barney³⁸ studied the dissolution of PuO_2 powder in HNO_3 , and HF mixture using the kinetic data. The experimental data were obtained in the regime of kinetically controlled zone via eliminating the stirring speed as a variable. The experiments were performed above 400 rpm. The effects of surface area, HF and HNO_3 concentrations and temperature on the initial dissolution rate were also studied to develop a rate expression. They observed that the initial rates are the same for different concentrations of HNO_3 and hence, HNO_3 was not considered in the rate-determining reaction step. Further, they noticed that the measurement of fluoride on the PuO_2 surface during the dissolution indicates that some fraction of fluoride gets adsorbed on the surface, and it is not sensitive to the total HF concentration. Hence, it was postulated that the rate of reaction could be expressed as a function of non-complexed HF. The rate equation was given by $r = kC_{\text{HF}}$, where C_{HF} is the concentration of non-complexed HF. Under the assumption that the reaction over the surface proceeds uniformly for the particles of identical size and shape, and temperature data, the activation energy was computed as 13 kcal/mol, which is similar to that reported by Barney³⁸. The analysis of experimental data of Bray et al.³⁹ and Miner et al.⁴⁰ show that the dissolution rate is proportional to 1.2th and 0.73th power of the initial concentration of HNO_3 and HF, respectively. In case of Miner et al., it could be seen that dissolution rate is around zeroth power of concentration of HNO_3 , which is in line of the reasoning of Barney. However, the activation energy value of 1.61 kcal/mol indicates a diffusion controlled process, which is in contrast to the observation of Barney³⁸.

In contrast to the above authors, Kazanjian and Stevens³⁷ found that the dissolution of PuO_2 increases when HF concentration was increased up to 0.2 M. Above 0.2 M, the dissolution rate showed a decrease. The data analysis of Kazanjian and Stevens³⁷ data indicates that the behavior of the experimental data could be described by a rate expression with an inhibiting term as follows.

$$\frac{k_1 \cdot C_{\text{HF},0}}{1 + k_2 \cdot C_{\text{HF},0}} \quad (3.3)$$

The experimental data are used to compute the values of rate constants k_1 and k_2 for 0.05–0.5 M HF concentrations. The obtained values of k_1 and k_2 are 7.38×10^{-5} (m/sec), and 3.56 M^{-1} , respectively. It should be noted that HF concentration is less than 0.2 M for the case of Barney³⁸, Miner et al.⁴⁰, Uriarte and Rainey³² and Harmon^{32, 41}. In this concentration range of HF, the dissolution rate is approximately first order as the inhibition term has negligible influence on the rate. However, above 0.2 M HF, the inhibition term becomes significant and hence, the dissolution rate decreases^{42, 43, 34}. Kazanjian and Stevens³⁷ observed that PuF_4 started to precipitate in the solution above 0.2 M HF. Moreover, at 0.7 and 1 M HF concentrations, high amount of PuF_4 was found in the undissolved residue. This indicates that the PuO_2 dissolves rapidly in the solution, and immediately precipitates as PuF_4 . Barney³⁸ had also observed the precipitation of PuF_4 when the total concentration of HF is greater than 0.1 M. However, they noted that PuF_4 redissolves again with time as more plutonium is dissolved. Moreover, they also observed that PuF^{+2} and PuF^+ complexes are present in significant quantities in the solution for the concentration of HNO_3 below 10 M.

As part of a study to systematically evaluate the dissolution behavior of several different actinide oxides, Berger^{40, 44} utilized carbon paste electrochemical techniques and considered the following general dissolution mechanisms for PuO_2 : (i) with no redox reaction, producing the Pu(IV) species in solution, (ii) by oxidation, producing either Pu(V) or Pu(VI), and (iii) by reduction, producing Pu(III). Although oxidative dissolution of PuO_2 is theoretically observed for the electrochemical electrode potentials above 1.43 V and 1.22 V, respectively leading to the formation of Pu(V) and Pu(VI), only the reductive dissolution path has been shown to be thermodynamically favorable in non-complexing acidic media.

3.6 PuO_2 dissolution in HNO_3 –Ce(IV) solution

The slower dissolution kinetics of PuO_2 is well established. Hence there was a strong need to develop alternative methods to quantitatively dissolve PuO_2 rapidly without opting for any corrosive reagents like HF. Thus, redox chemistry became important and

led to many industrial improvements. Initially, Ce(IV) was used as a promoter to enhance the performance of HF based processes for dissolving plutonium rich scrap materials for the recovery of plutonium^{32, 45}. Berger^{40, 44} experimentally determined the half-cell potential of Ce(IV)-Ce(III) couple which paved way for more exploration of this method for the dissolution of plutonium rich spent nuclear fuel. Harmon⁴¹ noted that oxidization of Pu(IV) to Pu(VI) by Ce(IV) is given by the following mechanism:



Uriarte and Rainey³² also studied the effect of addition of Ce(IV) on the dissolution rate. They added ceric ammonium nitrate as source of Ce(IV). They observed that the dissolution rate increased by the addition of Ce(IV) in 2 M HNO₃ solution. The rate was also found to be proportional to Ce(IV) concentration. However for solutions with higher concentration of HNO₃, the rates were found to be independent of Ce(IV). However, it was noted that the rate of reaction was still low for all practical applications. The analysis of the data shows that the dissolution rate is proportional to the 0.78th power of HNO₃ and the 0.58th power of Ce(IV) concentration.

It has been observed that the addition of Ce(IV) into HNO₃ increases the instantaneous dissolution rate. However, Harmon⁴¹ observed that in HNO₃-KF solution, the dissolution rate was directly proportional to the concentration of Ce(IV) till 0.025 M and the dissolution decreases above the concentration of 0.025 M. This result is in contrast to that obtained by Horner et al⁴⁵. This phenomenon could be attributed to the ratio of KF to Ce(IV). It was observed that at a KF to Ce(IV) ratio of 1, the mixed system dissolves less than with the promoter alone. It was observed that mixed Ce(IV) and KF system at certain KF/Ce(IV) yields better results than with either of additives alone. This indicates the importance of ratio optimization for optimal dissolution rate. Moreover, the stoichiometric amount of Ce(IV) is needed for complete dissolution of PuO₂, which indicates that the Ce(IV) does not behave as a catalyst in the process. Hence, the higher concentration of Ce(IV) is required to dissolve high amount of PuO₂. It was shown that there is marginal effect of Ce(III) on the dissolution of PuO₂. Moreover, hydrothermal precipitation of CeO₂ under pressure and high temperature was observed during the experiments with low concentration of HNO₃ (< 2 M). Using the experimental data of Horner et al.⁴⁵, it was found that the dissolution rate is proportional to the 1st power of

Ce(IV) concentration. The activation energy of 60 kJ/mol was computed from the dissolution rate vs temperature data. This result indicates the intrinsic kinetics is the rate controlling step, which is also the case for HNO₃-HF system.

3.7 *PuO₂ dissolution in HNO₃ with other additives*

Various oxidizing agents, Ag(II)-Ag(I) and Co(III)-Co(II) etc., are added to oxidize Pu(IV) to Pu(VI) to prevent the formation of PuF₄ and to enhance the dissolution rate^{46, 47}. Kazanjian and Stevens³⁷ observed that several oxidizing agents enhance the dissolution rate, particularly, Ce (IV) and Ag(II). They also observed that the dissolution is the kinetically controlled. Gelis et al⁴⁸ investigated Am(V)/Am(III) and Am(VI)/Am(III) couples as mediators of the oxidative dissolution of PuO₂ instead of foreign redox couples. Americium dioxo cations were generated by ozonation of solutions containing Am(III). They found that Am(III) increases the dissolution rate and it may be a promising alternative to the external additives. With ozone as an oxidizing agent, Uriarte and Rainey³² observed that there is a marginal increase in the dissolution rate. However, at higher concentrations of HNO₃, Ce(IV) and ozone were reduced rapidly due to their limited stability and hence were not available for catalyzing the reaction. They also used additives such as H₂O₂, Na₂Cr₂O₇, NaNO₃ and LiNO₃. However, they found that there is no effect of these additives on the dissolution rates.

Bjorklund and Staritzky⁴⁹ in their work on reactivity of PuO₂ had already indicated the feasibility of this method using a mixture of hydrochloric acid and iodide. Berger^{40, 44} estimated the PuO₂(s)/Pu(III)(aq) couple's standard potential which paved way for the studies on Cr(II)/Cr(III) couple in sulphuric acid media to be used for the PuO₂ dissolution. The work of Shakila et al⁵⁰ in HCl media using Fe(II)/Fe(III) couple also demonstrated the feasibility of the reductive dissolution of PuO₂. In this work, it was found that the dissolution took place vigorously as long as Fe(II) was available. Hence, hydrazine was used which prolonged the availability Fe(II) by reducing Fe(III) and thereby the dissolution reaction. Shakila et al⁵¹ also reported the improved dissolution in HNO₃-HF medium in the presence of hydrazine. Fife¹⁶ carried out detailed kinetic study of PuO₂ dissolution in HCl media using ferrous as electron transfer catalyst. They modeled the reaction using the classical non-porous shrinking spherical core model and found the dissolution to be kinetically controlled.

3.8 *Dissolution of PuO₂ in medium other than nitric acid*

Mineral acids other than nitric acid are generally not used in any process steps involved in the nuclear fuel cycle because of various processes and the materials safety related issues. But as mentioned in the preceding section, as PuO₂ does not dissolve completely in nitric acid medium, there was a necessity to check the feasibility of complete dissolution of PuO₂ in other acids, especially when it comes to recovering PuO₂ from certain scrap material wherein the levels of plutonium present are higher than the acceptable limits.

Fife¹⁶ carried out dissolution studies of PuO₂ in a non-traditional HCl-Fe(II) system as an alternate to nitric acid medium for rapid dissolution. Fe(II) here was used as an electron transfer reagent which reduces plutonium in PuO₂ to Pu³⁺ which goes into the solution. Cyclic voltammetry was employed as an in-situ analytical technique to monitor the reaction progress. The work was carried out mainly to separate plutonium from various matrices which has chlorides in them. Hence the study is very specific and could not be applicable in general to the reprocessing of the spent nuclear fuel. The work was an extension to the work carried out by Shakila et al⁵¹ who employed Fe(II) as the reducing agent for the electrolytic dissolution of PuO₂. Hydrazine was used in this work to regenerate the Fe(II) in-situ by reducing Fe(III).

3.9 *Dissolution of MOX fuel in nitric acid*

Primarily two types of MOX fuels are used in the field of nuclear technology, namely, uranium thoria MOX and uranium plutonia MOX. They are also used in various compositions for different purposes. This section provides an account of the dissolution behaviour of these MOX fuels in nitric acid medium.

3.9.1 Dissolution of uranium, plutonia MOX fuel in nitric acid

MOX fuel of uranium and plutonia are typically used to drive fast breeder reactors. The plutonium composition in the MOX fuel varies from about 10% by weight to about 30%. If plutonium exceeds this amount, it renders the fuel practically insoluble in neat nitric acid medium^{22, 51}. Most of the literature articles on MOX dissolution were a result of investigation of the MOX fuel leaching characteristics during the long term storage of spent MOX fuel^{23, 26, 52, 53} from environmental safety point of view.

First detailed work on the dissolution of uranium, plutonia MOX fuel was done by Uriarte et

al³². They have investigated the dissolution behaviour of both unirradiated and irradiated MOX with 20% PuO₂ and rest UO₂ by weight in nitric acid. They have attributed the sluggish kinetics of MOX fuel in nitric acid predominantly to the fuel fabrication methodology and its process conditions. MOX fuel fabricated through coprecipitation route has much faster dissolution kinetics as compared to those fabricated through powder metallurgy methods. Also they have observed that co-precipitated fuel goes to dissolution completely as against the MOX obtained by powder blending route. They have also found that the process conditions like sintering temperature and time influences the dissolution kinetics to a greater extent. They have also found out that under the experimental conditions of their work, the irradiated MOX fuel was found to dissolve about five times faster than their unirradiated counterpart. They have estimated the initial dissolution rates of the above mentioned unirradiated and irradiated MOX fuel in nitric acid to be about 1 mg cm⁻² min⁻¹ and 3 mg cm⁻² min⁻¹ respectively.

3.9.2 Dissolution of urania, thoria MOX fuel in nitric acid

Thoria based MOX nuclear fuels are considered as a potential advanced fuel for generation IV nuclear reactors^{54, 55}. Thoria based driver fuel for nuclear reactors leads to lower production rates of minor actinides⁵⁶. Thoria based fuel also offers many advantages like potential to burn weapon grade plutonium⁵⁷, higher capability to resist aqueous corrosion^{58, 59} and isomorphism with other tetravalent actinide dioxides⁶⁰. Hence the presence of thoria in the MOX fuel coupled with its low solubility, direct disposal of spent fuel in deep geological repository is a viable option.

The relatively low normalized rate of dissolution of thoria based fuels had prompted many groups across the globe to study its dissolution kinetics in a quest to design processes for its acceleration^{61, 62}. In all these, several dissolution experiments were carried out on Th_{1-x}U_xO₂ solid solutions with several mole ratios of uranium and thorium ranging from x=0.24 to x=0.81. All these work emphasized more on the kinetics of dissolution and least priority was given towards the thermodynamics of these fuel systems. Hence slowly after few years these processes were discontinued. Subsequently, Heisbourg et al⁶³ carried out leaching studies on thoria/urania MOX systems in nitric acid media whose composition varied very widely. They studied the effect of uranium content on the leaching behaviour. But all these studies were carried out from the final disposal of spent fuel point of view

and not from the viewpoint of their dissolution during reprocessing. Hence not much information could be derived with respect to spent fuel reprocessing.

3.10 Other means of dissolving nuclear materials

Heating in hot concentrated nitric acid is the most preferred method of dissolving nuclear fuel, especially the plutonium and thorium based MOX fuels, as they are highly inert at ambient conditions. At various juncture in the past, different methods other this has been deployed with an aim to increase their dissolution rate. This section gives a brief account of those methods.

3.10.1 Chemical dissolution using reagents other than nitric acid

Uranium oxide dissolves comparatively easily than its plutonium and thorium counterparts. Therefore during the dissolution of any UO_2 materials, it was never needed to add any foreign reagents in the form of oxidizing or reducing agents for accelerating the dissolution rate. But when UO_2 containing MOX was dissolved wherein one component is either PuO_2 or ThO_2 , some undissolved residue rich in plutonium or thorium as the case may be would always remain. One common mode of dissolving these residues is to heat them in concentrated nitric acid in the presence of strong oxidizing agents like HF ⁶⁴. Generally these left over undissolved residues from the main dissolver vessel will be removed and treated with a strong oxidizing agent in a specially designed vessel called **the super dissolver**⁶⁵. The material of construction of this super dissolver is chosen to withstand the strong corrosive chemical environment during the dissolution of the residues. Hence this method is not employed for regular processing. Generally they are adopted whenever any plutonium rich scrap material had to be dissolved for their processing or prior to the disposal of any material containing some residual plutonium in it that has to be recovered.

For thorium containing fuels, dissolution in 11 M HCl + 0.01 M SiF_6^{2-} was attempted in France⁶⁶ to design an anion exchange separation process feasible, but no satisfactory results could be achieved since a complete dissolution of the fuel could be accomplished only by using the THOREX reagent [13M HNO_3 + 0.05M HF + 0.1M $\text{Al}(\text{NO}_3)_3$]. Prior to this dissolution, catalysts like sulphate and phosphate ions were added for complexation purpose but were discontinued subsequently as their disadvantages outweighed the advantages^{67, 68}.

Whenever the cladding material of the fuel used was other than SS, for (e.g.) Zr and Al alloys, dissolving medium other than nitric acid was proposed primarily to dissolve the clad for exposing the fuel to the dissolvent for their dissolution. This is called the chemical decladding method. Some of such methods were Darex⁶⁹, which uses aqua regia; Zirflex⁷⁰, which uses ammonium fluoride - ammonium nitrate mixture and Sulfex²⁰, which uses sulfuric acid.

3.10.2 Sonochemical or Ultrasound aided dissolution of nuclear fuel materials

A concise and complete account of the potential applications of Sonochemistry in the spent nuclear fuel reprocessing operations have been given recently by Nikitenko et al⁷¹ which also gives a brief account of the ultrasound aided dissolution of spent fuel.

For the plutonium rich MOX or neat PuO₂ materials which are difficult to dissolve completely in nitric acid medium in the absence of any additive, it was felt that ultrasound as an alternate method would improve the dissolution kinetics^{20, 72}. Many previous studies have shown the advantages of ultrasound to over activate the surface of solids⁷²⁻⁸³. The intensification of mass-transfer near the solid-liquid interface and the erosion of solids under ultrasound are explained by the asymmetric collapse of cavitation bubbles that leads to micro jet impact at the solid surface⁷³.

A promising example of sonochemical dissolution was reported for metallic plutonium in HNO₃-HCOOH mixture⁷⁴. Dissolution of plutonium metal in HNO₃ medium is an important process for the preparation of MOX nuclear fuel and plutonium reference solutions⁷⁵. Plutonium metal is known to dissolve very slowly in HNO₃ at any concentration because of passivation⁷⁶. It was reported that plutonium and Pu-Ga alloys could be dissolved in HNO₃-HCOOH mixtures. In a 3.5 M HNO₃-3 M HCOOH mixture at ambient temperature, the dissolution rate under mechanical stirring was found to be 100-200 mg.min⁻¹.cm⁻². However, under these conditions potentially explosive denitration may occur during dissolution. This troublesome effect of denitration is not observed in more dilute HNO₃, but the rate of metal dissolution also decreases considerably at lower concentration of HNO₃. Moreover, significant amount of insoluble sludge is formed after dissolution under these conditions. It was found that plutonium dissolution rate in 0.5 M HNO₃-1 M HCOOH mixture is dramatically accelerated under the effect of 20 kHz ultrasound. Explosive denitration does not occur at such concentrations of acids even under strong heating.

A kinetic study revealed 24-fold acceleration of dissolution at the relatively low ultrasonic intensity of 1Wcm^{-2} and at room temperature. Therefore, ultrasonic treatment not only provides a safe dissolution process, but also significant enhancement of the dissolution rate. Furthermore, it was found that the fresh insoluble residue after plutonium dissolution (-5%) could be dissolved sonochemically by increasing the ultrasonic intensity and concentration of HNO_3 . Sludge dissolution is accompanied by oxidation of Pu(III) to Pu(IV), probably due to the reaction with HNO_2 .

It was concluded that the mechanism of sonochemical plutonium metal dissolution is related to the intensification of mass transfer at the metal–solution interface, caused by acoustic cavitation and removal of passivating film from plutonium surface owing to the surface erosion induced by bubble asymmetric implosions.

Dissolution of PuO_2 , is another notoriously difficult but important process in nuclear fuel recycling. Until the 1980's the primary method for dissolving PuO_2 was based on the long boiling of the oxide in HNO_3 – HF mixture under reflux condition. Such a method suffers from two main drawbacks: (i) the reaction is very slow, especially for high temperature fired oxides with low specific area, and (ii) highly corrosive solutions are generated owing to the presence of fluoride ions, which raises the problems of safe effluent management.

Since PuO_2 could also dissolve in aqueous solutions as oxidized or reduced forms, i.e., as Pu(VI) and Pu(III) respectively, new concepts based on redox reactions were developed subsequently. At present, the best industrial process is consistent with the use of electrogenerated Ag(II) ions which induce an oxidative dissolution of PuO_2 in HNO_3 medium⁷⁷. Unfortunately, such a process is not very efficient for treating PuO_2 bearing organic waste. This drawback has been overcome by using reducing species (Cr(II), Ti(III)) in non-oxidizing acidic media like H_2SO_4 or HCl ⁷⁸. However, these acids are not compatible with the PUREX process.

The effect of ultrasound at 20, 500 and 1700 kHz on the dissolution of CeO_2 and PuO_2 in 4 M HNO_3 solutions was studied subsequently²¹. Cerium oxide was used as a non-radioactive surrogate for PuO_2 ^{79, 80}. The authors have observed a strong reduction of the particle grain size at 20 kHz, which did not take place at 500 kHz but appeared again to a smaller extent, at 1700 kHz. At low frequency the initial dissolution kinetics was accelerated only to about 3–4 times compared to dissolution under mechanical stirring. At high frequency ultrasound the effect on the dissolution rate was even weaker than that at 20 kHz.

The strongest effect of ultrasound (15-fold acceleration) was observed in 1–4 M HCOOH solutions at the frequency of 1700 kHz. This result was attributed to the reductive dissolution of PuO₂ with the species formed after formic acid sonolysis. Hence studies were initiated to dissolve the refractory oxides like CeO₂ and PuO₂ by Sonochemistry⁴¹. The initial studies were aimed at producing free radicals generated by cavitation (bubble implosion) to obtain either the oxidative or reducing conditions required for PuO₂ dissolution. The results though indicated that the dissolution rates were even lesser than employing reagents like Ag(II) and HF.

Later more work was carried out to test the effect of ultrasound on the dissolution of high fired PuO₂²¹. Overall, the results indicate that applying ultrasound for the dissolution of refractory PuO₂ does not offer any substantial advantage over the conventional “heat and mix” treatment.

3.10.3 Photochemical dissolution of nuclear fuel materials

Some researchers have studied the photochemical dissolution of UO₂ powders and pellets in nitric acid medium in an effort to develop an alternate method for dissolution in milder conditions like low concentration of nitric acid and/or at ambient temperature. Based on their studies, Wada et al⁸¹ initially proposed that in the photochemical aided dissolution of UO₂, the nitrate ions present in nitric acid gets excited by absorbing the photochemical radiation whose redox potential is much higher than the unexcited one. This leads to faster dissolution rate than in the dark condition. The work of Sasaki et al⁸² further emphasized these findings. Later, Kim et al⁸³ came up with more elaborate mechanism for the photochemical dissolution of UO₂ in nitric acid. They summed up their findings as follows.

1. Photochemical conditions certainly increase the rate of dissolution of sintered UO₂ pellets in nitric acid than in dark conditions
2. Compared to sintered pellets, sintered particles dissolve much faster due to the increased surface area
3. Presence of other elements such as Cs, Sr, Zr, Mo, Ru and Nd increases the rate of photochemical dissolution further
4. The increased rate is due to the NO₂ radical and nitrite ions that are generated and not due to the excited nitrate ions as suggested by Wada et al⁸¹.

But considering the engineering challenges involved in setting up these photochemical set-ups in radioactive hot cells and the chemical and radiation resistance of all the components involved in this set-up, further studies on photochemical dissolution of nuclear materials weren't pursued seriously. Moreover presence of plutonium in the actual spent fuel will complicate the photochemical dissolution process further.

3.10.4 Microwave assisted dissolution of nuclear materials

Microwave heating has a number of unique advantages over conventional heating^{84, 85}. These include non-contact rapid heating, reduced processing costs, material selective heating, volumetric heating, uniform heating, quick start-up and stopping. The less expensive and easily controllable design and construction of the microwave systems over the conventional methods makes it more suitable for automation with inherently higher level of safety. The easily achievable waveguide makes the industrial scale construction of microwave systems more expedient. Its unique internal heating phenomenon could lead to products and processes that could not be achieved by conventional methods.

When it comes to the nuclear industry, microwave has been primarily employed in fuel fabrication for the sintering of the fuel pellets, conversion of highly enriched uranium to uranium oxides^{86, 87}, co-conversion of mixed nitrate solutions to MOX for better proliferation resistance^{88, 89}, analysis of uranium elements and waste management operations⁹⁰ and so on. In order to explore a new concept of head-end process for the treatment of spent fuel from high temperature gas-cooled reactor (HTGR), the dissolution of UO_2 particles in the nitric acid solution by microwave heating was compared with conventional heating⁹¹. The studies indicated that (1) Microwave heating could promote the dissolution of UO_2 particles in nitric acid 10 to 40% higher compared with conventional heating⁹², (2) the dissolution reaction was consistent with the diffusion control model⁹³ and with the surface control model by conventional heating, (3) The diffusion control model for the dissolution of UO_2 particles by microwave heating could be explained by the diffuseness on the surface of UO_2 particles. The dissolution is so deep on the surface by microwave heating that the products may not diffuse in good time. There were also studies carried out for the microwave assisted dissolution of UO_2 particles in HNO_3 -TBP mixture⁹⁴.

Though the results of the various dissolution studies aided by microwave heating were new, they were only of academic interests as deploying such methods in plant scale is very

premature as on date. The technology needs lot of systematic studies to be carried out in various operating scales before even thinking of them for plant conditions.

3.10.5 Electrochemical dissolution of nuclear fuel materials

For the PHWR type spent fuel where plutonium content is very less, dissolution could be carried out just by reflux heating in nitric acid medium. But when the plutonium levels in the spent fuel increases, like about 30% or so in FBRs, just heating in nitric acid medium does not dissolve them completely. Some plutonium rich residues are always found. Hence for such type of fuels, electrolytic dissolution was proposed as an alternate to dissolve the plutonium rich spent fuel completely in nitric acid medium⁴⁹. There was also another process proposed in which cerium was used to electrolytically catalyze the dissolution of PuO₂⁹⁵. The method was primarily developed to avoid the usage of HF while processing plutonium rich spent nuclear fuel. It was claimed that the cerium added in the process could be electrochemically regenerated which helped in reducing its requirement to a great extent. But later on it was found that the major disadvantage of the process is the consumption of cerium in various other side reactions during dissolution^{96, 97}. Subsequently considering the engineering difficulties in setting up an electrolytic cell inside a highly radioactive environment and their long-term routine operation, not much of work was carried out in the electrolytic dissolution of spent fuel though many refractory scrap materials were processed by this method to recover the small amount of plutonium present in them.

Ryan et al⁹⁸ reported one of the first methods for the electrolytic dissolution of PuO₂ of NpO₂ using electrolytically regenerated reagents. They suggested one of the reagents consisting of Ce, Ag, Co and Am could be used as the regenerating agent. Since these species are also present in the spent fuel, they suggested that they could be used in-situ rather than being added externally. Subsequently J.L. Ryan et al⁴⁸ came up with the process called **CEPOD** (catalyzed electrolytic plutonium oxide dissolution) for the dissolution of PuO₂ using Ce(IV)/Ce(III) couple which is regenerated electrolytically in-situ. The method was found very promising to dissolve the LMFBR (liquid metal cooled FBR) spent fuel which is rich in Pu. There was some speculation that Ru present in the spent fuel could reduce Ce(IV) which would render the method ineffective. But Hylton et al⁹⁹ through their detailed investigation spanning over a period of well over a decade have reported that continuous electrolytic in-situ generation of Ce(IV) would ultimately lead to

the depletion of the reductive state of ruthenium. They have successfully applied this method for the dissolution of Np and plutonium oxides.

Bourges et al¹⁰⁰ carried out oxidative dissolution of PuO₂ with electrogenerated Ag(II) ions. They found that the rate of dissolution is dependent on the rate of electro regeneration of Ag(II) ions. They also opined that, based on their pilot plant test, as silver required for the process is very less and also it is ultimately being reduced quantitatively to Ag(I) at the end, silver aided corrosion is never an issue. Zundelevich¹⁰¹ has proposed the mechanism of this reaction which proceeds through electron transfer reactions between PuO₂ and Ag²⁺ ions. He had concluded that the rate of the reaction is not instantaneous and emphasized the need to carry out the reaction at the limiting current for better efficiency.

In order to demonstrate the feasibility of dissolving UO₂ in mild conditions which will not lead to any long-term corrosion of the dissolver vessel, anodic dissolution of UO₂ in aqueous alkaline solutions were tried¹⁰². In order to avoid precipitation of uranium in alkaline medium, NaHCO₃ was employed by means of anodic oxidation. The results indicated complete dissolution rapidly. Similar studies were also carried out in ammonium carbonate solution which was proposed as an alternate to PUREX process for the recovery of nuclear materials¹⁰³. The rate of dissolution of UO₂ was found to be on par with that in 5 M nitric acid solution containing 0.01M nitrous acid at 323K. Also the simulated fuel dissolution rate was slower than UO₂ which was attributed to the poor electrical conductivity of neat UO₂ particles which was found to be formed at the surface of the simulated fuel pellets during the course of dissolution. This was confirmed by SEM/EDX results. Also the alkaline earth and rare earth elements were found to form precipitates in the ammonium carbonate electrolyte solution. Hence the authors also proposed that these elements could be separated as their carbonate precipitates. The left over U(VI) and Pu(IV) in the aqueous carbonate solution could be separated/purified by ion exchange column using amidoxime resins. The adsorbed uranium and plutonium in the resin could be eluted with dilute nitric acid which is then further purified by conventional precipitation methods. Though the method looks different, the overall decontamination factor achievable appears to be less as it is more prone for carryover of fission products whose solubility product in the carbonate medium is pretty high. Also operating the ion exchange columns on larger scale is pretty difficult.

3.10.6 Electrolytic dissolution of nuclear fuel materials

One of the first works on electrolytic dissolution of power reactor fuels in nitric acid was carried out by Thomas Clark et al¹⁰⁴. They demonstrated the electrolytic oxidation of stainless steel, zirconium, Zircaloy-2, zirconium-uranium alloy, aluminum, and uranium-molybdenum alloy in nitric acid on a laboratory scale. The rate of chemical dissolution of UO₂ in nitric acid was measured. Corrosion of stainless steel by these dissolver solutions was measured and found to be negligible. Electrolytic dissolution was demonstrated to be a practical technique for the first step in processing fuel elements of several types of power reactors. The primary aim of this work was to find a suitable material for dissolver during the electrolytic dissolution of power reactor fuels.

Following this Berry and Miner¹⁰⁵ studied the electrolytic dissolution of plutonium metal in nitric acid medium. They found that the rate of dissolution of plutonium at concentration of nitric acid greater than 5 M could be increased significantly by the addition of a slight amount of fluoride while applying a direct current to the plutonium metal. The effect of the concentration of nitric acid is less significant than the current on the rate of dissolution. Fluoride concentration had little effect on the dissolution rate although its presence was found necessary. Absence of fluoride resulted in an extremely slow dissolution rate. Within the ranges investigated, the fastest rate of dissolution was obtained for 10 amp, 15 M nitric acid and 0.01 M HF. With the experimental equipment and conditions used, the following effects were observed. Direct current was more effective than alternating current; lower acid concentrations dissolved alloyed metal approximately 30% faster than unalloyed metal; in 10% HNO₃ and above, the dissolution rates of the two metals were equal; and very little evolved hydrogen could be detected.

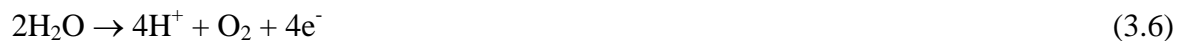
Electrolytic dissolution in nitric acid has been used at the Savannah River and Idaho Chemical Processing plants to dissolve a wide variety of fuels and cladding materials, including uranium alloys, stainless steel, aluminum, zircaloy, and nichrome. The electrolytic dissolver developed by DuPont, uses niobium anodes and cathodes, with the former coated with 0.25 mm of platinum to prevent anodic corrosion. Metallic fuel to be dissolved was held in an alundum insulating frame supported by a niobium basket placed between anode and cathode and electrically insulated from them. Fuel surfaces facing the cathode underwent anodic dissolution according to the following reaction.



At a concentration of nitric acid above 2 M, the cathode reaction was found to be as follows.



This ensures the suppression of hydrogen evolution. The reverse reaction took place at the platinum coated anode, together with evolution of oxygen.



Anodic corrosion of the niobium basket that supports the fuel is inhibited by an electrically conducting oxide film, which forms on the niobium. Advantages of this method were its wide applicability, the absence of anions other than the nitrate and the fact that little hydrogen is evolved. A disadvantage was the presence of cladding metal nitrate in the dissolver solution and its eventual routing to the high-level waste. When applied to zircaloy cladding, most of the zirconium is converted to hydrous ZrO_2 , which could be filtered from the dissolver solution.

3.10.7 Other modes of dissolving nuclear fuel materials

In addition to the above mentioned methods there are also some basic studies carried out world over for the dissolution of nuclear materials in different ways for certain specific tasks. One such method is to dissolve the actinide oxide by employing super critical carbon-dioxide (SC-CO₂) with a suitable complexing agent forming SC-CO₂ soluble complexes with the spent nuclear fuel materials¹⁰⁶. This method was proposed as an alternate to TBP as the solvent so that the amount of organic liquid waste (OLW) could be reduced. Though the method was attractive, it was found that this method does not dissolve NpO_2 and PuO_2 under the similar conditions. Hence when a mechanical mixture of UO_2 with $\text{PuO}_2/\text{NpO}_2$ is treated with TBP-HNO₃, a complex of uranium alone gets dissolved completely leaving the bulk of neptunium and plutonium in the residue.

The kinetics of the dissolution of UO_3 in nitric acid saturated 30% TBP in a hydrocarbon diluent was studied by Dorda et al¹⁰⁷. UO_3 was found to dissolve without the formation of

any gaseous product and reaction followed the contracting sphere equation. The apparent activation energy was estimated to be 45.1 kJ/mol under the experimental conditions and hence the reaction was kinetically controlled.

3.11 Consolidation of literature information on nuclear fuel dissolution

UO₂ is the widely studied nuclear fuel from its dissolution point of view. There are many studies reported in the literature wherein the dissolution kinetics of various physical forms of the fuel, viz pellets and powders; have been reported. The literature information also gives an account of the effect of various parameters which influences the dissolution rate. Some models have been proposed for evaluating the dissolution kinetics. This section consolidates the information available in the literature which will help in sketching the way forward in improving our understanding about the nuclear fuel dissolution behaviour. Following is the summary of the literature review carried out relevant to this PhD thesis work.

3.11.1 Dissolution of UO₂

Lot of work has been carried by researchers world over for understanding the dissolution behaviour of UO₂ fuel both in the form of powder and pellets. Studies have been carried out for both the irradiated and unirradiated fuels. In general the irradiated fuel dissolves easily and completely than the unirradiated ones. This is because; irradiation renders the fuel matrix more porous due to the diffusion of gaseous fission products through the fuel material. Literature also provides information about various factors which influences the dissolution behaviour and how they affect them. Some of the studies have also proposed some model equations to explain the kinetics of the dissolution process. In spite of the large amount of data available in the literature, still there are some gap areas to be understood like the role of nitrous acid generated in-situ and the quantitative effect of pellet surface area on the dissolution rate, measurement of mass transfer co-efficient for the dissolution process under typical PUREX process conditions and so on. Hence this PhD project aims at addressing these aspects of UO₂ dissolution behaviour in nitric acid.

3.11.2 Role of nitrous acid and NO_x gas composition on UO₂ dissolution kinetics

Literature on nuclear fuel dissolution in nitric acid provides some speculation about the role of nitrous acid and NO_x gases generated during the course of dissolution on the

reaction kinetics. But these are not conclusive to arrive at a certain mechanism for the dissolution reaction. This is because; there is a lack of information on the concentration profiles of these species during the dissolution process. Though there are some sporadic work carried out by certain researchers from the US and Japan on the nitrous acid and NO_x gases during dissolution, there are only qualitative. Hence a detailed study is required on the dissolution behaviour of nuclear fuel in nitric acid to extract more authoritative information on these aspects. Once these informations are available, there would be better clarity on the mechanism of UO_2 pellet dissolution in nitric acid which is an important initial input data required for designing a continuous dissolution system relevant to PUREX process. Though the continuous spent fuel dissolution system is not a necessary requirement at the moment for the fuel cycle activities of PHWR fuel in India, it would be the most important and essential information required for the INPP when the second stage of FBR and its associated nuclear fuel cycle technology assumes a larger magnitude in meeting the country's long term energy security.

3.11.3 Nitric acid as the medium for nuclear fuel dissolution

Nuclear fuel dissolution has been carried out in all the mineral acids for various purposes. But when it comes to the operations of nuclear fuel cycle activities, nitric acid is the most preferred and obvious choice. This is because of the availability of compatible material of construction and most importantly the uniqueness of nitric acid medium in offering selectivity towards the recovery of nuclear materials of our interest, namely uranium and plutonium, from the spent nuclear fuel employing the PUREX process. Acids other than nitric acid are employed for certain specific purposes, particularly for the recovery of strategic nuclear materials from the scraps generated during various activities of the nuclear fuel cycle operations. The present work, which aims at providing better understanding of the nuclear fuel dissolution process relevant to PUREX process, will only consider the dissolution process in nitric acid medium.

3.11.4 MOX fuel dissolution

Literature provides some brief understanding on the dissolution behaviour of MOX fuels in nitric acid both in the irradiated and unirradiated form. It has been observed generally that plutonia dissolves comparatively very slowly in nitric acid than urania. Hence as the percentage of plutonia in the MOX fuel is increased, the dissolution rate is expected to be

decreased gradually. It was also reported that when the composition of plutonia in the MOX fuel, prepared by powder metallurgy route, exceeds 35% by weight, complete dissolution of MOX in neat nitric acid is not possible unless plutonium is forced to undergo reductive or oxidative dissolution. Hence for the dissolution of MOX fuel with plutonium above 35% by weight, normally HF or any other strong oxidizing or reducing agents are employed for dissolving them quantitatively. Silver and cerium are other reagents which were suggested to aid rapid and complete dissolution of plutonium rich MOX and PuO_2 fuels. The possible mechanism of the reaction under such conditions are also been explained reasonably in the literature. Also plutonium generally does not undergo any change in its oxidation state during the dissolution of PuO_2 in nitric acid unless it is forced to happen so. Therefore the presence of nitrous acid is not expected to influence its dissolution kinetics of PuO_2 in nitric acid. Though many such works were reported, none of them gives any detailed account of the kinetics and mechanism relevant to PUREX process.

3.11.5 Dissolution behaviour of simulated MOX fuel

The dissolution behaviour of MOX fuel, as explained in the previous section, was not sufficiently explored till date. Since carrying out experiments on plutonium systems has its own safety issues, it was decided to study the dissolution behaviour of a simulated MOX fuel by replacing plutonium with a suitable non-radioactive surrogate. With respect to the chemistry of nuclear fuel fabrication and waste management operations, ceria is the best possible non-radioactive surrogate for plutonium based on the similarities of its relevant solid state structural properties to that of plutonia. As the dissolution of any solid in liquid is dependent on the structural properties of the solid in question when all other factors remain unchanged, the above mentioned similarity between ceria and plutonia could be very well extended to study the dissolution behaviour of plutonia. Hence as a part of this thesis, the dissolution behaviour of simulated MOX fuel of urania-ceria was studied initially. Subsequently based on the results obtained from these studies, similar experimental studies with necessary additional safety precautions and modeling using the experimental results have been carried out for the urania-plutonia MOX fuel system.

3.12 References

- ¹ Gmelin handbook of inorganic chemistry – Behaviour of uranium fuels, Helmut Aßmann et.al., 8th edition, Supplement volume A4, Springer-Verlag 1981
- ² D. D. Sood, “Nuclear Materials”, IANCAS publication 1996, p-57
- ³ Taylor, R. F.; Sharratt, E. W.; Chazal, L. E.; Logsdail, D. H. “Dissolution rate of uranium dioxide sintered pellets in nitric acid systems”. J. Appl. Chem. 1963, 13, 32–40
- ⁴ H. T. Blaine, “Dissolution of power reactor fuel cores” HW-66320, UC-10, Hanford Atomic Products Operation, 1960
- ⁵ E. Zimmer and E. Merz; “Dissolution of thorium-uranium mixed oxides in concentrated nitric acid”, J. Nucl. Mat., 124 (1984) 64-67
- ⁶ A. Inoue and T. Tsujino; “Dissolution Rates of U₃O₈ Powders in Nitric Acid”, Ind. Eng. Chem. Process Des and Dev. 23 (1984) 122-125
- ⁷ A. Inoue; “Mechanism of the oxidative dissolution of UO₂ in HNO₃ solution”, J. Nucl. Mat., 138 (1986) 152-154
- ⁸ D. G. Karraker; “Mechanism of plutonium metal dissolution in HNO₃, -HF-N₂H₄ solution”, J. Less-Common Metals, 122 (1986) 337-341
- ⁹ T. Fukasawa, Y. Ozawa; “Relationship between dissolution rate of uranium dioxide pellets in nitric solutions and their porosity”, J. Radioanal. Nucl. Chem. Letters 106, 6 (1986) 345-356,
- ¹⁰ W. J. Gray, L. E. Thomas, R. E. Einziger; “Dissolution rates of as-received and partially oxidized spent fuel”, PNL-SA--20371, April 1992
- ¹¹ L. E. Eary, L. M. Cathles; “A kinetic model of UO₂ dissolution in acid, H₂O₂ solutions that includes uranium peroxide hydrate precipitation”, Hydrometallurgy, Metallurgical Transactions B, 14, 3, 325-334 (1983)
- ¹² M. Shabbir, R. G. Robins, “Kinetics of the dissolution of uranium dioxide in nitric acid – I”, J. Appl. Chem., 18, 129 (1968)
- ¹³ M. Shabbir, R. G. Robins, “Kinetics of the dissolution of uranium dioxide in nitric acid – II”, J. Appl. Chem., 19, 52 (1969)
- ¹⁴ Y. Ikeda et.al.; “¹⁷O NMR study on dissolution reaction of UO₂ in nitric acid – Mechanism of Electron Transfer”, J. Nucl. Sci. Tech. 30(9) September 1993, pp 962-964
- ¹⁵ Y. Ikeda et.al, “Kinetic study on dissolution of UO₂ powders in nitric acid”, J. Nucl. Mat. 224 (1995) 266-272

-
- ¹⁶ Keith William Fife, “A kinetic study of plutonium dioxide dissolution in hydrochloric acid using iron(II) as an electron transfer catalyst”, PhD Thesis, LA-13188-T; UC-701, September 1996
- ¹⁷ S. A. Steward, E. T. Mones; “Comparison and Modeling of Aqueous Dissolution Rates of Various Uranium Oxides”, UCRL-JC-124602, Nov 1996
- ¹⁸ Mineo, H.; Isogai, H.; Morita, Y.; Uchiyama, G. “An investigation into dissolution rate of spent nuclear fuel in aqueous reprocessing” J. Nucl. Sci. Tech. 2004, 19, 52–56
- ¹⁹ G. Heisbourg, S. Hubert, N. Dacheux, J. Purans, “Kinetic and thermodynamic studies of the dissolution of thoria-urania solid solutions”, J. Nucl. Mat. 335 (2004) 5-13
- ²⁰ S. I. Sinkov, G. J. Lumetta, “Sonochemical Digestion of High-Fired Plutonium Dioxide Samples”, PNNL-16035, October 2006
- ²¹ F. Juillet, J. M. Adnet, M. Gasgnier, “Ultrasound effects on the dissolution of refractory oxides (CeO₂ and PuO₂) in nitric acid”, J Radioanal.Nucl. Chem., VoL 224, Nos 1-2 (1997) 137-143
- ²² Hirotomo Ikeuchi et al., “Dissolution behaviour of irradiated mixed oxide fuels with different plutonium contents”, Procedia Chemistry, 7 (2012), 77-83
- ²³ R. S. Forsyth, L. O. Werme, “Spent fuel corrosion and dissolution”, J. Nucl. Mat. 190 (1992) 3-19
- ²⁴ C. Jegou et.al., “Oxidizing dissolution of spent MOX47 fuel subjected to water radiolysis: Solution chemistry and surface characterization by Raman spectroscopy”, J. Nucl. Mat. 399 (2010) 68-80
- ²⁵ M. Magnin et al., “Oxidizing dissolution mechanism of an irradiated MOX fuel in underwater aerated conditions at slightly acidic pH”, J. Nucl. Mat., 462 (2015) 230-241
- ²⁶ J. A. Serrano et.al., “Influence of low temperature air oxidation on the dissolution behaviour of UO₂ and MOX spent fuel”, J. Alloys Comp. 271-273 (1998) 573-576
- ²⁷ Baldev Raj, U. Kamachi Mudali, “Materials development and corrosion problems in nuclear fuel reprocessing plants”, Prog. Nucl. Ener., Vol 48, Iss 4, May 2006, Pages 283-313
- ²⁸ A. Ramanujam, “An Introduction to Purex Process”, IANCAS Bulletin, July 1998, pp 11
- ²⁹ R. Natarajan, “Challenges in Fast Reactor Fuel Reprocessing”, IANCAS Bulletin, July 1998, pp 27
- ³⁰ Levenspiel, O. (1972) Chemical Reaction Engineering, second edition, John Wiley and Sons, New York.

-
- ³¹ Gilbert N. Lewis, Arthur Edgar, "The equilibrium between nitric acid, nitrous acid and nitric oxide", *J. Am. Chem. Soc.*, 1911, 33 (3), pp 292–299
- ³² Uriarte, A. L.; Rainey, R. H. "Dissolution of high-density UO₂, PuO₂, and UO₂-PuO₂ pellets in inorganic acids", 1965
- ³³ Ryan, J. L.; Bray, L. A. "Dissolution of plutonium dioxide - A critical review", *Actinide Separations*, American Chemical Society USA, 1980
- ³⁴ S. DeMuth, "Conceptual Design for Separation of Plutonium and Gallium by Solvent Extraction", LANL, LA-UR-97-181, 1997
- ³⁵ Polley, G. M. Downblend and Disposition Remote Handled U-233 Material at the WIPP Facility – 9374. WM2009 Conference. Phoenix, AZ, 2009
- ³⁶ Harmon, H. D. "Evaluation of fluoride, cerium (IV), and cerium(IV)-fluoride mixtures as dissolution promoters for PuO₂ scarp recovery processes", Report DP-1383, 1975
- ³⁷ Kazanjian, A. R.; Stevens, J. R. "Dissolution of plutonium oxide in nitric acid at high hydrofluoric acid concentrations", Report RFP-3609, 1984
- ³⁸ Barney, G. S. "The kinetics of plutonium oxide dissolution in nitric/hydrofluoric acid mixtures", *J. Inorg. Nucl. Chem.* 1977, 39, 1665–1669
- ³⁹ Bray, L. A.; Ryan, J. L.; Wheelwright, E. J. "Dissolution of plutonium dioxide using HCl-HF", 1986
- ⁴⁰ Miner, F. J.; Nairn, J. H.; Berry, J. W. "Dissolution of plutonium in dilute nitric acid", *Ind. Eng. Chem. Prod. Res. Dev.* 1969, 8, 402–405
- ⁴¹ Harmon, H. D. "Dissolution of PuO₂ with cerium (IV) and fluoride promoters", Report DP-1371, 1975
- ⁴² J. H. Goode, Hot "Cell Dissolution of Highly Irradiated 20% PuO₂ - 80% UO₂ Fast Reactor Fuel Specimens", ORNL-3754, October 1965
- ⁴³ S. DeMuth, "Technical Basis for Separation of Plutonium from Gallium by Ion Exchange," Los Alamos National Laboratory report LA-UR-97-685, 2/24/97
- ⁴⁴ Berger, P. "A Study of the Dissolution Mechanism by Chemical and Electrochemical Oxidation-Reduction of Actinide Oxides (UO₂, NpO₂, PuO₂ and AmO₂) in an Acid Aqueous Medium", Ph.D. thesis, 1990
- ⁴⁵ Horner, D.; Crouse, D. J.; Mailen, J. C. "Cerium-promoted dissolution of PuO₂ and PuO₂-UO₂ in nitric acid", ORNL/TM-4716, 1977
- ⁴⁶ Zawodzinski, C.; Smith, W. H.; Martinez, K. R. "Kinetic Studies of the Electrochemical

Generation of Ag(II) Ion and the Catalytic Oxidization of Selected Organics”, Proceedings of the Symposium on Environmental Aspects of Electrochemistry and Photoelectrochemistry, Electrochemical Society, 1993

⁴⁷ Ryan J.L., Bray L., Wheelwright E.J., Bryan G.H. “Catalyzed Electrolytic Plutonium Oxide Dissolution (CEPOD): The Past Seventeen Years and Future Potential”, PNL-SA-18018; CONF-900846-5. 1990. –P. 39

⁴⁸ Gelis, V. M.; Shumilova, Y. B.; Ershov, B. G.; Maslennikov, A. G.; Milyutin, V. V.; Kharitonov, O. V.; Logunov, M. V.; Voroshilov, Y. A.; Bobritskii, A. V. “Use of ozone for dissolving high-level plutonium dioxide in nitric acid in the presence of Am (V, VI) ions”, Radiochemistry 2011, 53, 612–618

⁴⁹ Bjorklund, C. W.; Staritzky, E. “Some Observations on the Reactivity of Plutonium Dioxide”; U.S. Document LA-186, 1954

⁵⁰ Shakila, A. M.; Srinivasan, T. G.; Sabharwal, K. N.; Rao, P. R. V. “Dissolution of PuO₂ in HNO₃-HF-N₂H₄ Medium”, Nucl. Technol. 1987, 79, 116

⁵¹ Shakila A. M., Srinivasan T. G., Sabharwal K. N. and P. R. V. Rao, “Dissolution of PuO₂ in hydrochloric acid – Effect of reducing agents”, Nucl. Tech., 88, 290, 1989

⁵² C. Jegou et.al., “Oxidizing dissolution of spent MOX47 fuel subjected to water radiolysis: Solution chemistry and surface characterization by Raman spectroscopy”, J. Nucl. Mat. 399 (2010) 68-80

⁵³ M. Magnin et al., “Oxidizing dissolution mechanism of an irradiated MOX fuel in underwater aerated conditions at slightly acidic pH”, J. Nucl. Mat., 462 (2015) 230-241

⁵⁴ Dasarathi Das, S. R. Bharadwaj (Eds.), “Thoria-based Nuclear Fuels: Thermophysical and Thermodynamic Properties, Fabrication, Reprocessing and Waste Management”, Springer-Verlag London 2013

⁵⁵ Igor Pioro, “Handbook of Generation IV Nuclear Reactors”, Woodhead Publishing in energy no. 103, 2016

⁵⁶ Gruppelaar H. and Schapira J.P. (2000), “Thorium as a Waste Management Option”, Final Report EUR 19142EN, European Commission

⁵⁷ Hiroshi Akie, Tadasumi Muromura, Hideki Takano, Shojiro Matsuura, “A New Fuel Material for Once-Through Weapons Plutonium Burning”, Nucl. Tech. 107 (1994) 182-192

⁵⁸ B. Fourest, T. Vincent, G. Lagarde, S. Hubert and P. Baudoin, “Long-term behaviour of a thorium-based fuel”, J. Nucl. Mat. 282, (2000) 180-185

-
- ⁵⁹ Hubert, S; Barthelet, K; Fourest, B; Lagarde, G; Dacheux, N; Baglan, N; “Influence of the precursor and the calcination temperature on the dissolution of thorium dioxide”, J. Nucl. Mat. 97 (2001) 206-213
- ⁶⁰ W. H. Zachariassen, Manhattan Project Metallurgical Laboratory Report CK-1518, p.3 (March 1994 and Report CN-1807 (June 1944)
- ⁶¹ R.W. Dyck, R. Taylor, D.G. Boase, “Dissolution of (Th,U)O₂ in nitric acid hydrofluoric acid solutions”, Atomic Energy of Canada Limited Report, AECL-5957, 1977
- ⁶² G. Heisbourg, S. Hubert, N. Dacheux, J. Ritt, “The kinetics of dissolution of Th_{1-x}U_xO₂ solid solutions in nitric media”, J. Nucl. Mat. 321 (2003) 141–151
- ⁶³ G. Heisbourg, S. Hubert, N. Dacheux, J. Purans, “Kinetic and thermodynamic studies of the dissolution of thoria-urania solid solutions”, J. Nucl. Mat. 335 (2004) 5-13
- ⁶⁴ G. F. Schiefelbein, R. E. Lerch, “Dissolution properties of UO₂-PuO₂ thermal reactor fuels”, BNWL-1581, AEC R&D report, June 1971
- ⁶⁵ De Regge et.al., “Dissolution of mechanically mixed MOX fuel and insoluble”, FRFR proceedings of a symposium held at UKAEA, 15-18 May 1979, pp 133-143
- ⁶⁶ Helmut Aßmann et al., “Gmelin Handbook of Inorganic Chemistry”, 8th Edition, Uranium supplement volume A4, Springer Verlag 1981, page 298
- ⁶⁷ H. Katz and J. Wagner; Recovery of Uranium from Pyrolytic Carbon-Coated Uranium Carbide Spheroids, BNL-7352, 1963; N.S.A. 18, 1964, No. 3875
- ⁶⁸ M. R. Bomar: Series Electrolytic Dissolver for Nuclear Fuels, I. Scoping Studies; IDO-14563, Nov. 1961; N.S.A.16 [1962] No. 4220
- ⁶⁹ Proceedings of the AEC Symposium for Chemical Processing of Irradiated Fuels from Power, Test, and Research Reactors. Hanford Operations Office, Richland, Wash. AEC Research and Development Report TID-7583, 446 pp. (October 1959)
- ⁷⁰ Smith, P. W. “The Zirflex Process Terminal Development Report”, General Electric Co., Hanford Atomic Products Operation, Richland, Washington. AEC Research and Development Report HW-65979, 51 pp. (August 1960)
- ⁷¹ S. I. Nikitenko et al., “Potential applications of sonochemistry in spent nuclear fuel reprocessing: A short review”, Ultrasonics Sonochemistry 17 (2010) 1033-1040.
- ⁷² L.H. Thompson, L.K. Doraiswamy, “Sonochemistry: science and engineering”, Ind. Eng. Chem. Res. 38 (1999) 1215–1249.
- ⁷³ T.J. Mason, J.P. Lorimer, Applied Sonochemistry, “The Uses of Power Ultrasound in

Chemistry and Processing”, Wiley-VCH, Weinheim, 2002.

⁷⁴ P. Moisy, S.I. Nikitenko, L. Venault, C. Madic, “Sonochemical dissolution of metallic plutonium in a mixture of nitric and formic acid”, *Radiochim. Acta* 75 (1996) 219–225.

⁷⁵ A.S. Polyakov et al, “AIDA/MOX: progress report on the research concerning the aqueous process for allied plutonium conversion to PuO₂ or (U,Pu)O₂”, *Proceedings of Global-95*, September 11–14, Versailles, France, vol. 1, 1995, pp. 640–651.

⁷⁶ J.M. Cleveland, “The Chemistry of Plutonium”, American Nuclear Society, La Grange Park, 1979

⁷⁷ J. Bourges, C. Madic, G. Koehly, M. Lecomte, “Removal of alpha emitters from solid radioactive waste”, *J. Less-Common Met.* 122 (1986) 303–308.

⁷⁸ X. Machuron-Mandard, C. Madic, “Basic studies on the kinetics and mechanism of the rapid dissolution reaction of plutonium dioxide under reducing conditions in acidic media”, *J. Alloys Comp.* 213/214 (1994) 100–105.

⁷⁹ Han Soo Kim, Chang Yong Joung, Byung Ho Lee, Jae Yong Oh, Yang Hyun Koo, Peter Heimgartner; “Applicability of CeO₂ as a surrogate for PuO₂ in a MOX fuel development”, *J. Nucl. Mat.* 378 (2008) 98–104

⁸⁰ J.C. Marra, A. D. Cozzi, R. A. Pierce, J.M. Pareizs, A. R. Jurgensen, and D. M. Missimer; “Cerium as a Surrogate in the Plutonium Immobilized Form”, WSRC-MS-2001-00007; Westinghouse Savannah River Company, Aiken, SC 29808, 2001

⁸¹ Y. Wada, K. Morimoto, H. Tomiyasu, “Photochemical Dissolution of UO₂ Powder in Nitric Acid Solution at Room Temperature”, *Radiochimica Acta*, 72, 83-91 (1996)

⁸² Satoru Sasaki, Yukio Wada, Hiroshi Tomiyasu, “Basic study of photochemistry for application to advanced nuclear fuel cycle technology”, *Progress in Nuclear Energy*. Vol. 32. No. 3/4, pp. 403-410, 1998

⁸³ Eung-Ho Kim, Doo-Sung Hwang, Jae-Hyung Yoo, “Dissolution mechanism of UO₂ in nitric acid solution by photochemical reaction”, *J Radioanal. Nucl. Chem.*, Vol. 245, No. 3, 2000, 567-570

⁸⁴ K. E. Haque, “Microwave energy for mineral treatment processes - A brief review”, *International Journal of Mineral Processing* 57, 1999, 1-24

⁸⁵ D. E. Clark, D. C. Folz and J. K. West, “Processing Materials with Microwave Energy”, *Materials Science and Engineering: A*, Vol. 287, No. 2, 2000, pp. 153-158

⁸⁶ Bao et al., 1991, “The research of technology and equipment for a microwave denitration

process of the uranyl nitrate solution”, in Aesj, Jaif (Eds.), RECOD’91(II), The Third International Conference on Nuclear Fuel Reprocessing and Waste Management, Japan, Sendai, pp. 1075-1080

⁸⁷ Bao et al, “Research on the conversion of highly enriched uranium (HEU) nitrate by using the microwave denitration”, Atomic Energy Science and Technology 29, 268-274, 1995

⁸⁸ Hirofumi Oshima, “Development of Microwave Heating Method for Co-Conversion of Plutonium-Uranium Nitrate to MOX Powder”, J. Nucl. Sci. Tech., 26[1], 1989, pp. 161-166

⁸⁹ K. Asakura, Y. Kato, H. Furuya, “Characteristics and Sinterability of MOX Powder Prepared by the Microwave Heating Denitration Method”, Nucl. Tech. 2008, 162, 265–275

⁹⁰ Yunfeng Zhao, Jing Chen, “Applications of microwaves in nuclear chemistry and engineering”, Prog. in Nucl. Ener. 50 (2008) 1-6

⁹¹ Zhao Yun Feng and Chen Jing, “Kinetics study on the dissolution of UO₂ particles by microwave and conventional heating in 4 mol/L nitric acid”, Sci China Ser B-Chem, Jul. 2008, vol. 51, no. 7, 700-704

⁹² Yunfeng Zhao and Jing Chen, “Comparative studies on the dissolution of ceramic UO₂ pellets in nitric acid by microwave and conventional heating”, Radiochim. Acta 96, 467–471 (2008), DOI 10.1524/ract.2008.1507

⁹³ Yunfeng Zhao, Jing Chen, “Studies on the dissolution kinetics of ceramic uranium dioxide particles in nitric acid by microwave heating”, J. Nucl. Mat. 373 (2008) 53–58

⁹⁴ Yunfeng Zhao and Jing Chen, “Microwave-assisted dissolution of UO₂ with TBP-HNO₃ complex”, Korean J. Chem. Eng., 26(1), 165-167 (2009)

⁹⁵ Cooley, C.R., “Status of electrolytic dissolution for LMFBR fuels”, Report number HEDL-TME--71-123, DOI: 10.2172/4732897, 1971 Jan 01

⁹⁶ Bray, L. A.; Ryan, J. t., in "Actinide Recovery from Waste and Low-Grade Sources", Navratil, J. D. and Schulz, W. W., eds. Harwood Academic Publishers, London; 1982, pp. 129-154

⁹⁷ Ryan, J. L; Bray, L. A.; Boldt, A. L, US Patent 4,686,019, 1987

⁹⁸ Ryan et al., “Dissolution of PuO₂ or NpO₂ using electrolytically regenerated reagents”, US Patent 4686019, Aug 11, 1987

⁹⁹ TD Hylton et al., “Dissolution of Np and Po oxides using catalyzed electrolytic process”, ORNL/TM-2004/211, October 2004

¹⁰⁰ Bourges J, Madic. C, Koehly. G and Leconte. M, “Dissolution of plutonium bioxide in

nitric medium with electrogenerated silver (II)", *J. Less Comm. Met.*, 122 (1986) 303-311

¹⁰¹ Yury Zundeleovich, "The mediated electrochemical dissolution of plutonium oxide: Kinetics and mechanism", *J All. Comp.*, 182 (1992) 115-130

¹⁰² Noriko Asanuma, Hiroshi Tomiyasu, Masayuki Harada, Yasuhisa Ikeda and Shinichi Hasegawa, "Anodic Dissolution of UO₂ in Aqueous Alkaline Solutions", *J Nucl. Sci. Tech.*, Volume 37, Issue 5, 2000, 486-488, DOI:10.1080/18811248.2000.9714921

¹⁰³ Noriko Asanuma, Masayuki Harada, Masanobu Nogami, Kazunori Suzuki, Toshiaki Kikuchi, Hiroshi Tomiyasu and Yasuhisa Ikeda, "Anodic Dissolution of UO₂ Pellet Containing Simulated Fission Products in Ammonium Carbonate Solution", *J Nucl. Sci. Tech.*, Vol. 43, No. 3, p. 255-262 (2006)

¹⁰⁴ Clark, A.T. Jr.; Meyer, L.H.; Owen, J.H.; Rust, F.G., "Electrolytic dissolution of power reactor fuels in nitric acid", Report No. DP - 647, USAEC 1961

¹⁰⁵ Berry, J.W., Miner, F. J.; "Electrolytic dissolution of plutonium in nitric acid", OSTI ID: 4522381; Report No. RFP-1136; USDOE 1968

¹⁰⁶ Yurii M. Kulyako, Trofim I. Trofimov, Maksim D. Samsonov and Boris F. Myasoedov, "Dissolution of uranium, neptunium, plutonium and americium oxides in tri-n-butyl phosphate saturated with nitric acid", *Mendeleev Comm. Electronic Version*, Issue 6, 2003

¹⁰⁷ Dorda F. A., Lazarchuk V. V., Matyukha V. A., Sirotkina M. V., and Tinin V. V., "Kinetics of UO₃ dissolution in nitric acid saturated 30% TBP in a hydrocarbon diluent", *Radiochemistry*, 2010, Vol. 52, No. 5, pp. 469-471

CHAPTER 4. Experimental

4.1. Procurement of UO_2 pellets

The UO_2 fuel pellets that were required for the experimental work reported in this thesis were obtained from the Nuclear Fuel Complex (NFC), Hyderabad, India. The physical and chemical characteristics of these fuel pellets were that of a typical PHWR¹. The pellets were made from natural uranium through powder metallurgy route². The fabrication step consists of dissolution of magnesium diuranate (MDU, which is the purified concentrate of the natural uranium ore) in nitric acid, further purification by solvent extraction using TBP, precipitation of uranium as ammonium diuranate (ADU), calcination to U_3O_8 , reduction in presence of hydrogen to UO_2 powder and finally followed by blending, compaction and sintering to get the UO_2 pellets³. The process is well established for the PHWR fuel pellets of required specification. The pellets used for the dissolution studies reported in this thesis are all dimensionally rejected pellets which are slightly chipped at the edges as shown in Figures 4.1 and 4.2.

Fig. 4.1. Typical PHWR natural UO_2 pellets



In the case of processing the spent fuel by chop leach process, the chopped fuel pins would contain the fuel covered by the SS clad along its curved surfaces. It is open only along the two circular (or oblique/elliptical to be precise) faces. Hence in all the experiments pertaining to this thesis work, the curved surfaces of the pellets are covered using a SS sheet to simulate the presence of clad during the dissolution experiments.

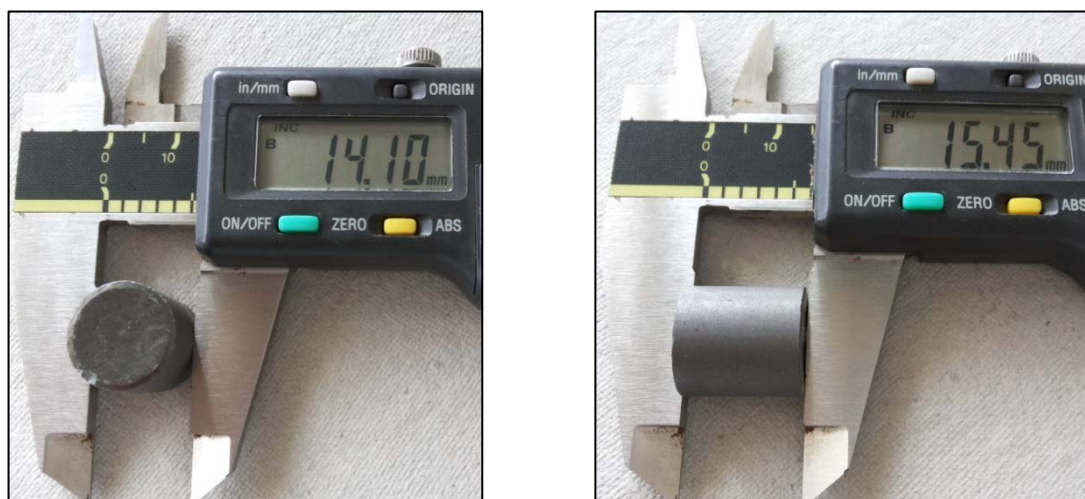
4.2. Physical characterization of UO_2 pellets

The method used in NFC for the production of the UO_2 pellets is well established². Hence the general physical properties of the pellets are all well-known⁴. The typical physical properties which are measured in the present work are given in the Table 4.1.

Table 4.1. Typical physical properties of the UO₂ pellets

No.	Physical Parameter	Details
1	Weight (g)	~16.57-18.29
2	Diameter (mm)	~12.1-12.5
3	Length (mm)	~14.1-15.8
4	Density (g/cc)	~10.3-10.5
5	Nature of the pellet	Sintered and SS cladged

Fig. 4.2. Typical dimensions of sintered UO₂ pellets



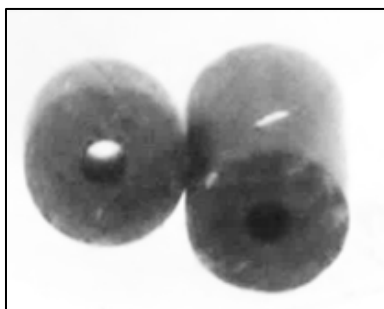
4.3. Physical characterization of MOX pellets

The (U, Pu) MOX pellets used for the dissolution studies were all of Prototype FBR (PFBR) inner core specification containing 21.7% PuO₂ by weight and rest UO₂⁵. They were obtained from BARC, Mumbai. They were all fabricated at the Advanced Fuel Fabrication Facility (AFFF), Tarapur by powder metallurgical route wherein required quantity of UO₂ and PuO₂ powders are mixed in an attritor ball mill, compacted and sintered⁶. These pellets were provided with an annular hole at its center along its length, as shown in Fig. 4.3, so that the MOX fuel pellets will have lower centre line temperature during its irradiation resulting in lower fission gas release and stored energy⁷. The annular pellet design would also provide voidage to accommodate fuel swelling and relieve cladding stresses⁸. The transient behaviour of such pellets has also been reported to be superior⁹. The typical physical properties of these MOX pellets are provided in Table 4.2.

Table 4.2. Typical physical properties of PFBR inner core MOX pellets

S.No.	Parameter	Details
1	Weight (g)	1.5-1.75
2	Diameter (mm)	5-6
3	Length (mm)	10±0.2
4	Other details	Annular hole (3.8±0.2mm) in the middle

Fig. 4.3. Typical FBR MOX pellet



4.4. Reagents used in the experiments

All the reagents used for the experiments were analytical grade chemicals of reputed brands from known suppliers. The following is the list of reagents used.

1. Double distilled water from M/s Millipore
2. Nitric acid from M/s Merck
3. UO₂ pellets from NFC, Hyderabad
4. MOX pellets from BARC
5. UO₂-CeO₂ simulated MOX pellets fabricated in IGCAR
6. Sodium carbonate from M/s Merck for analyzing the concentration of nitric acid
7. Sodium hydroxide from M/s Merck for off-gas scrubbers
8. α -hydroxy isobutyric acid from M/s Alfa Aesar as mobile phase for the analysis of uranium and Ce by HPLC/IC
9. Arsenazo(III) from M/s Sigma Aldrich as chromogenic agent in HPLC analysis
10. Sulfanilamide and N-1-naphthylethylenediamine from M/s Alfa Aesar for the analysis of nitrous acid
11. 4-(2-Pyridylazo)resorcinol (PAR) from M/s Merck as chromogenic agent for the spectrophotometric determination of uranium.

4.5. Free acidity measurement

Measurement of concentration of nitric acid was one of the routine chemical analyses required for this research work. For every dissolution run, it was required to measure the concentration of acid as a function of time to monitor its changes in the dissolution mixture. As there was always uranium/plutonium/cerium present in all the dissolution samples, measurement of concentration of acid in their presence was not straight forward as they would interfere due to the ease with which they get hydrolyzed. Hence it is the free acidity which was required to be measured. Free acidity of a solution containing hydrolysable metal ions is defined as the acidity in excess of the stoichiometrically balanced salts or the acidity without taking into account that contributed by the hydrolysis of such metal ions¹⁰. It could also be simply defined as the acidity of the solution when the hydrolysable metal ions are removed or complexed so as not to interfere during the measurement of the concentration of acid. In all the samples, free acidity was measured by suppressing the hydrolysable metal ions with oxalate ions and titrating with standard sodium carbonate solution. A Metrohm-make model E-526 end point titrator was employed for this purpose.

4.6. Analysis of nitrous acid

The concentration of nitrous acid was determined by both ion chromatography (IC)¹¹ and spectrophotometry employing sulfanilamide and N-1-naphthylethylenediamine as coloring reagents¹². In the analysis by IC, an aliquot of the sample from the reaction mixture was taken and immediately quenched in known excess of sodium hydroxide solution. The nitric and nitrous acids in the sample reacted with sodium hydroxide instantaneously forming sodium nitrate and nitrite respectively¹³. After appropriate dilution of the sample, the concentration of nitrate and nitrite ions were determined by IC. Modular ion-chromatography system from M/s Metrohm equipped with conductivity detector was employed for the analysis. The eluent was a mixture of 3.2 mM Na₂CO₃ and 1.0 mM NaHCO₃ used at a flow rate of 0.7 mL/min. The separation was carried out using an anion exchange column Metrosep A Supp 5-250[250 mm (L) 4.0 mm(ID)] containing polyvinyl alcohol with quaternary ammonium groups as carrier material and a guard column (Metrosep A Supp 4/5). The pH is maintained between 3 and 12 at ambient temperature. Samples and standards were injected manually through a 20 µl PEEK loop fitted with injector. After ion-exchange separation in anionic column followed by suppressed

conductivity detection, chromatograms were obtained. Run time for each sample was 20 min. Concentrations of species of our interest were quantified using peak area. IC net 2.3 Metrohm software was used for instrument control and data acquisition.

4.7. Analysis of the composition of NO_x gas evolved during dissolution

All the dissolution experiments carried out as a part of the current work were under typical PUREX process conditions¹⁴. Hence the NO_x gas emitted during the dissolution experiments contained only NO and NO₂^{15, 16}. The composition of these gases in the NO_x stream during the course of the dissolution runs were determined by trapping them in the NaOH scrubbers connected to the dissolution reactor off-gas lines and analyzing the nitrate and nitrite ions formed by them on reacting with NaOH in the scrubbers. During all the experiments, four such scrubbers were connected in series to the off-gas line. The 1st, 3rd and 4th scrubbers had 2 M NaOH and the 2nd scrubber had 10% H₂O₂ solution at the start of each experiment. The purpose of hydrogen peroxide scrubber was to convert all NO to NO₂, since NO₂ get scrubbed more easily in NaOH than NO¹⁷. It was observed that both the gases were scrubbed quantitatively in the first three scrubbers itself and there was no traces of any nitrate or nitrite ions in the 4th scrubber. The concentration of the NaOH in each of the scrubber was measured before and after each dissolution experiment. Both NO and NO₂ were scrubbed in NaOH and is converted to sodium nitrate and nitrite salts as per the following stoichiometric relations.



The concentrations of the NO and NO₂ gases evolved during each dissolution experiment were back calculated using the above stoichiometric equations. All the connections were made completely airtight to avoid leakage of any gas thereby avoiding errors in the estimation of NO_x gas composition. The nitrate and nitrite ions were estimated by IC similar to the procedure mentioned for the analysis of nitrous acid¹⁸.

4.8. Analysis of uranium in UO₂ and UO₂-PuO₂ MOX fuel dissolution studies

Uranium was analyzed by the standard Davies and Gray method which was based on redox titrimetry¹⁹. But as titrimetric methods were not accurate enough at lower

concentration of the analytes²⁰, spectrophotometric method using pyridyl-azo-resorcinol as the chromogenic reagent was employed to analyze samples which contain low concentrations of uranium²¹. The later method was predominantly used for the samples generated at the beginning of the dissolution experiments when the concentration of uranium was less than 1 g/L.

4.9. Analysis of uranium and cerium in UO₂-CeO₂ simulated MOX fuel dissolution studies

Analyzing uranium by Davies and Gray method, in the presence of cerium, would lead to erroneous results due to the interference of cerium ions in the redox titrations^{22, 23}. Similarly Ce(IV) was also found to interfere in the spectrophotometry method using PAR²⁴. Hence reverse phase HPLC with UV-Vis detection was chosen which enables the determination of both U(VI) and Ce(IV) concentration simultaneously^{25, 26, 27}. The reverse phase HPLC separates the cerium ions and uranyl ions by employing a C₁₈ 10 cm monolith (M/s Merck) column. The mobile phase used was 0.1 M alpha hydroxy isobutyric acid (pH adjusted to 4 with dil. NH₃). The mobile phase flow rate used was 2 mL/min. The post-column detection of metal ions was done by mixing the column effluent with Arsenazo (III) as the chromogenic agent with a flowrate of 1 mL/min at a concentration of 10⁻⁴ M. The detection was based on UV-Vis spectrometry at 655 nm.

4.10. Analysis of plutonium

Analysis of plutonium in all the samples generated during the dissolution of UO₂-PuO₂ MOX pellets were carried out by radiometric methods²⁸. Though there are numerous methods available for the determination of plutonium²⁹, radiometric methods are the most simplest, rapid and easy to execute³⁰. Necessary and proper care was exercised during all the radiometric analysis for obtaining the best results³¹.

4.11. Analytical techniques and instruments used

The various analytical techniques and the instruments used for the analysis of all the samples generated in the experiments carried out as a part of the current work are provided in Table 4.3.

Table 4.3. Analytical techniques and instruments used

S. No.	Technique	Purpose	Instruments used
1	Spectrophotometry	Analysis of uranium in UO ₂ dissolution samples using PAR, backup analysis of nitrous acid using sulphanilamide and N-1-naphthylethylenediamine,	Double beam UV-Vis spectrometer from M/s Thermoscientific
2	Liquid chromatography (HPLC)	Analysis of uranium and Ce in UO ₂ -CeO ₂ dissolution samples	HPLC instruments from M/s Metrohm and M/s Jasco
3	Radiometry	Analysis of plutonium in MOX dissolution samples	Alpha detector from M/s ECIL
4	Redox titrimetry	Analysis of uranium in UO ₂ dissolution samples wherein uranium concentrations are higher	Auto titrator from M/s Metrohm
5	Titrimetry	Free acidity analysis in all the dissolution samples	

4.12. References

¹ N. Desigan, Elizabeth Augustine, Remya Murali, N.K. Pandey, U. Kamachi Mudali, R. Natarajan, J.B. Joshi, “Dissolution kinetics of Indian PHWR natural UO₂ fuel pellets in nitric acid - Effect of initial acidity and temperature”, Prog. Nucl. Ener. 83 (2015) 52-58

² D. Pramanik, M. Ravindran, G.V.S.H. Rao, R.N. Jayaraj, “Innovative Process Techniques to Optimize Quality and Microstructure of UO₂ Fuel for PHWRs in India”, in IAEA-TECDOC-1654 on Advanced Fuel Pellet Materials And Fuel Rod Design For Water Cooled Reactors, Proceedings of a Technical Committee Meeting Held in Villigen, 23–26 NOVEMBER 2009, p13

³ Abe, T.; Asakura, K.; “Uranium Oxide and MOX Production”, Compr. Nucl. Mater. 2012, 2, 393– 422

⁴ a.) H. Assmann, H., et al., “Control of UO₂ microstructure by oxidative sintering”, J. Nucl. Mat., 140, (1986), p.1–6

b.) Wolfrey, J.L., “Surface area changes during the calcinations of ammonium urinate”,

Australian Atomic Energy Commission, AAEC/E329

c.) Glodeanu, F., et al., “Correlation between UO_2 powder and pellet quality in PHWR fuel manufacturing”, *J. Nucl. Mat.*, 153, (1988), p.156–159

d.) Muromura, T., et al., “Formation of uranium mono nitride by the reaction of uranium dioxide with carbon in ammonia and a mixture of hydrogen and nitrogen”, *J. Nucl. Mat.*, 71, (1977), p.65

e.) Kutty, T.R.G., et al., “Densification behaviour of UO_2 in six different atmospheres”, *J. Nucl. Mat.*, 305, (2002), p.159–168

f.) Zawidzki, T.W., et al., “Effect of sulfur on grain growth in UO_2 pellets”, *J. Am. Cer. Soc.*, 31st Pacific coast regional meeting, (1978), Paper No. 38–N–78p

g.) Kun Woo Song, et al., “Grain size control of UO_2 pellets by adding heat-treated U_3O_8 particles to UO_2 powder”, *J. Nucl. Mat.*, 317, Issues 2–3, (2003), p.204–211

⁵ A. Kumar, “Development, fabrication and characterization of fuels for the Indian fast reactor programme”, Proceedings of An International Conference on Fast Reactors and Related Fuel Cycles: Safe Technologies and Sustainable Scenarios (FR13) organized by The International Atomic Energy Agency, Paris, 4–7 March 2013, p 17-32

⁶ H.S. Kamath, “Recycle Fuel Fabrication for Closed Fuel Cycle in India”, *Energy Procedia*, Volume 7, 2011, 110-119

⁷ H.S. Kamath, D.S.C. Purushotham, “Mixed Oxide (MOX) Fuel”, Reference Module in Materials Science and Materials Engineering, from *Encyclopedia of Materials: Science and Technology* (Second Edition), 2001, Pages 5687-5689, Current as of 16 February 2017, DOI: 10.1016/B0-08-043152-6/00991-8

⁸ Brian R. T. Frost, Chapter 8 – “Water Reactor Fuel Performance”, page 190 in *Nuclear Fuel Elements: Design, Fabrication and Performance*, Pergamon Press 1982

⁹ Plutonium utilization in BWR — Phase II — Semi-Annual report, Jan-June 1970, NEDC-12152, General Electric Company (1970)

¹⁰ T. G. Srinivasan, P. R. Vasudeva Rao; “Free acidity measurement – A review”, *Talanta*, 119, 2014, 162-171

¹¹ N. Desigan, P. Velavendan, Remya Murali, Elizabeth Augustine, N. K. Pandey, U. Kamachi Mudali and R. Natarajan, Determination of the composition of NO_x gases during the reprocessing of spent nuclear fuel, CHEMENT-2014, 06-07 March 2014 at Kalpakkam, India

-
- ¹² Schneider, R. A., Harmon, K. M., Analytical Technical Manual 1961, HW-53368
- ¹³ M. P. Pradhan and J. B. Joshi, “Absorption of NO_x Gases in Aqueous NaOH Solutions: Selectivity and Optimization”, *AIChE Journal*, January 1999, Vol. 45, No. 1, pp 38-50
- ¹⁴ W. B. Lanham, T. C. Runion,, “Purex process for plutonium and uranium recovery”, USAEC, ORNL-479, 1949
- ¹⁵ J.-P. Glatz, H. Bokelund, S. Zierfuß, “Analysis of the off-gas from dissolution of nuclear oxide- and carbide fuels in nitric acid”, *Radiochim. Acta* 51, 17 (1990)
- ¹⁶ Tsutomu Sakurai et al, “The composition of the NO_x generated in the dissolution of Uranium Dioxide”, *Nucl. Tech.*, Vol.83, 1988, 24-30
- ¹⁷ John M. Kasper, Christian A. Clausen III and C. David Cooper, “Control of Nitrogen Oxide Emissions by Hydrogen Peroxide-Enhanced Gas-Phase Oxidation Of Nitric Oxide”, *Journal of the Air and Waste Management Association*, 46:2, 127-133, 1996
- ¹⁸ N. Desigan, P. Velavendan, Remya Murali, Elizabeth Augustine, N. K. Pandey, U. Kamachi Mudali and R. Natarajan, “Development of an analytical method for estimating the composition of NO_x gas using ion chromatography”, Poster presentation in NUCAR 2015 held at Mumbai from Feb 09-13 2015
- ¹⁹ W. Davies and W. Gray, “A rapid and specific titrimetric method for the precise determination of uranium using iron(II) sulphate as reductant”, *Talanta*, 1964, Vol. 11, pp. 1203 to 1211
- ²⁰ Wisconsin Department of Natural Resources, "LOD/LOQ Technical Advisory Committee Report", February 21, 1994
- ²¹ Florence T. M., Yvonne. Farrar, “Spectrophotometric Determination of Uranium with 4-(2-Pyridylazo) resorcinol”, *Anal. Chem.* 1963, 35 (11), pp 1613–1616
- ²² W. J. Maeck, G. L. Booman, M. C. Elliott, and J. E. Rein, “Spectrophotometric Extraction Methods Specific for Uranium”, *Anal. Chem.*, 1959, 31 (7), pp 1130–1134
- ²³ Khan, M.H., Warwick, P. and Evans, N., “Spectrophotometric determination of uranium with arsenazo-III in perchloric acid”, *Chemosphere*, 63, 2006, pp. 1165-1169
- ²⁴ Gholamreza Khayatian; Shahed Hassanpoor; Amir R. J. Azar; Sajjad Mohebbi, “Spectrophotometric determination of trace amounts of uranium(VI) using modified magnetic iron oxide nanoparticles in environmental and biological samples”, *J. Braz. Chem. Soc.* vol.24 no.11, Nov. 2013

-
- ²⁵ Akhila Maheswari, D. Prabhakaran, M.S. Subramanian, N. Sivaraman, T.G. Srinivasan, P.R. Vasudeva Rao, “High performance liquid chromatographic studies on lanthanides, uranium and thorium on amide modified reversed phase supports”, *Talanta* 72 (2007) 730–740
- ²⁶ P.G.Jaison, Vijay M.Telmore, PranawKumar, Suresh K.Aggarwal, “Reversed-phase liquid chromatography using mandelic acid as an eluent for the determination of uranium in presence of large amounts of thorium”, *Journal of Chromatography A*, Volume 1216, Issue 9, 27 February 2009, Pages 1383-1389
- ²⁷ Narendra M.Raut, P.G.Jaison, Suresh K.Aggarwal, “Separation and determination of lanthanides, thorium and uranium using a dual gradient in reversed-phase liquid chromatography”, *Journal of Chromatography A*, Volume 1052, Issues 1–2, 15 October 2004, 131-136
- ²⁸ J. Parus and W. Raab, “Analysis of Uranium and Plutonium Materials by Radiometric Methods”, *Int. J. Radiat. Appl. Instrum. Part A, Appl. Radiat. Isot. Vol. 39, No. 4*, pp. 315-322, 1988
- ²⁹ Milner, G.W.C.; Phillips, G., “An Appraisal of Analytical Methods for Plutonium and their Applications to the Analysis of Nuclear Materials”, *Proceedings of the Symposium on Nuclear Materials Management, International Atomic Energy Agency, Vienna (Austria)*; 905 p, Feb 1966, p. 691-704
- ³⁰ Xiaolin Hou, Per Roos, “Critical comparison of radiometric and mass spectrometric methods for the determination of radionuclides in environmental, biological and nuclear waste samples”, *Anal. Chim. Acta* 608, (2008), 105–139
- ³¹ Nora Vajda and Chang-Kyu Kim, “Determination of Transuranium Isotopes (Pu, Np, Am) by Radiometric Techniques: A Review of Analytical Methodology”, *Anal. Chem.* 2011, 83, 4688–4719

CHAPTER 5. Dissolution kinetics of UO_2 pellets in nitric acid medium

5.1 Design of reactor for UO_2 dissolution

During the course of the dissolution experiments, it is always desirable to have the option for live visual inspection into the reactor vessel to notice any interesting and/or unintended event at its onset itself, if it so happens. Hence it was decided to use only glass reactors for all the dissolution experiments. Hard borosilicate glass materials only were used for this purpose. Additionally, as a solution of uranium in nitric acid medium has its own characteristic colour in the visible region of the electromagnetic spectrum depending on its oxidation state, a glass reactor would help in monitoring the visual progress of the reaction from the intensity of the colour of the reaction mixture.

Subsequently when it came to the design of the dissolution reactor, after various trials with different design, it was finally decided to employ only cylindrical reactors with sufficient nozzles for various requirements like sampling, condenser for off-gas cooling and sampling, thermowell for measuring the temperature of the reaction mixture, glass impeller for stirring the reaction mixture at various preset speed and so on. Though a thermosyphon design was initially thought off, its construction and operation with glass as the material of construction (MOC) is practically very difficult. Moreover as the ultimate goal of this work is to generate only intrinsic dissolution data which is independent of the design and dimensions of the reactor¹, it was found prudent to adopt a simple, elegant and well proven design based on cylindrical geometry. For the initial dissolution experiments on UO_2 , cylindrical glass vessel with provision for air sparging was used. Air sparging served the purpose of mixing in place of mechanical mixing. The pellets to be dissolved would be placed on a zero size glass frit provided at the bottom of the reactor whose other end is a thin glass tube meant for purging air. The dissolver is then connected to required numbers of scrubbers in series for off-gas treatment cum sampling. The other end of the scrubbers is connected to the suction nozzle of an air ejector which creates the negative pressure and thereby sucks air through the reaction mixture in the dissolution reactor into the scrubber. The air is then scrubbed and exhausted in to the atmosphere through a fume

hood. Figures 5.1 to 5.4 provide the schematic sketches and the photographs of the dissolution reactors employed in this work.

Fig. 5.1. Schematic sketch of the experimental dissolver with mechanical mixing

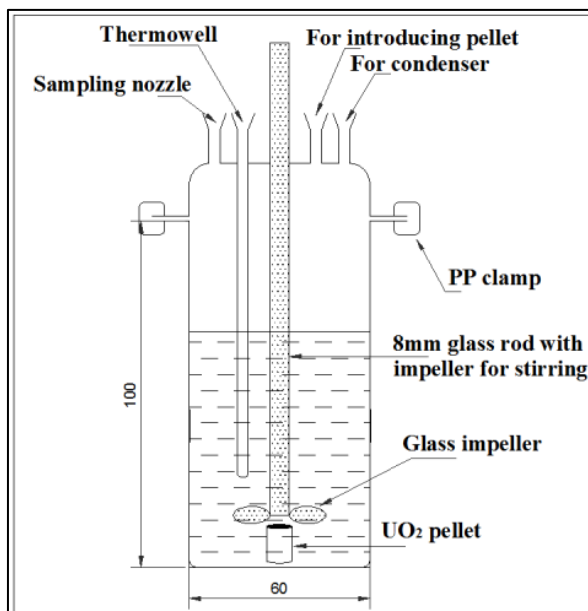
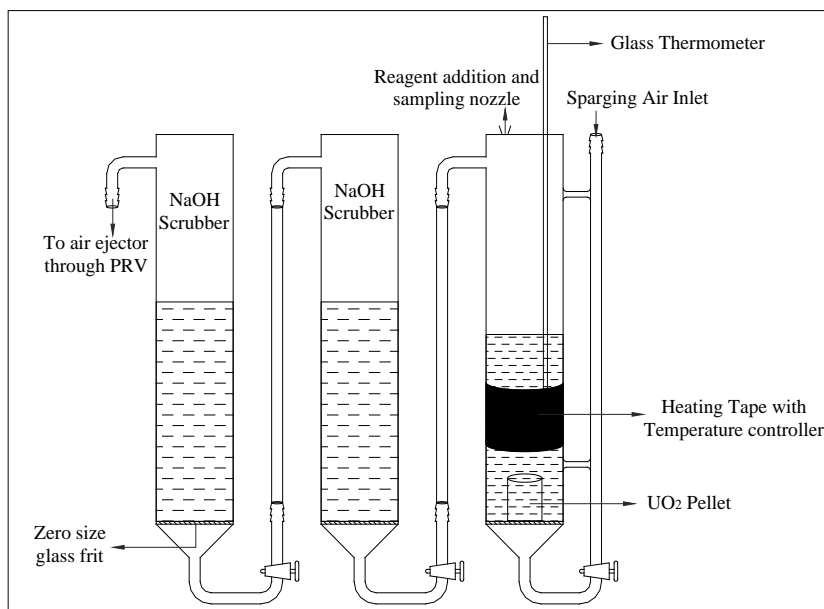


Fig. 5.2. Schematic sketch of air sparging dissolution set-up



5.2 Choice of the concentration of nitric acid

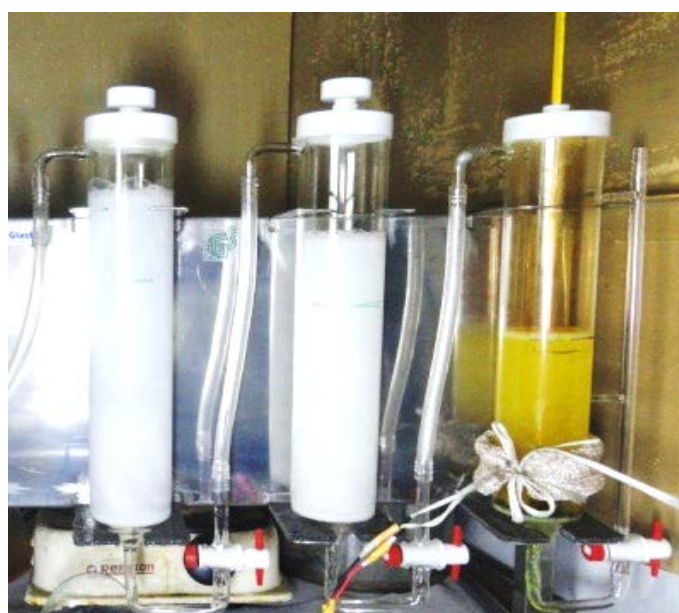
For studying the dissolution reaction relevant to PUREX process, there is not much of choice available when it came to the concentration of acid. Typically the initial

concentration of the nitric acid employed worldwide in the dissolution of nuclear fuel during reprocessing is about 8 M². Hence in all the experiments where the acidity needs to be constant, the concentration of nitric acid was chosen to be 8 M. The amount of fuel pellets required for each experiment was carefully chosen to ensure sufficient decrease in the concentration of acid during the course of the reaction so that the reaction could be modeled at a later stage.

Fig. 5.3. Cylindrical glass dissolver with mechanical mixing



Fig. 5.4. Glass bubble dissolver with air sparging



Also in Purex process, the dissolution step is immediately followed by solvent extraction for which the preferred concentration of the acid is between 3.5 and 4 M³. Hence care was taken in choosing the quantities of 8 M nitric acid and fuel pellets for each experiments so that the final acidity of the dissolver solution is around 4 M. For this purpose the connections in the dissolution set-up leading up to the off-gas condenser and scrubbers were made air tight using vacuum grease for avoiding the leakage of any acid vapors. For the experiments involving simulated MOX and (U, Pu) MOX fuel pellet dissolution in nitric acid (Chapters 6 and 7 respectively), whose dissolution is sluggish as compared to UO₂⁴, it is desirable to have the initial concentration of the acids to be higher⁵. But for the sake of comparison of the dissolution behaviour of different fuel materials, the initial concentration of nitric acid is retained at 8 M for these MOX fuel pellets also. But for comparing the effect of initial concentration of acid on the dissolution kinetics, the acidity was increased up to 11.5 M nitric acid for MOX pellet dissolution experiments which is the typical acid concentration used in FBR fuel reprocessing⁶.

5.3 Choice of temperature for the dissolution experiments

The average temperature maintained during the dissolution in the spent fuel reprocessing plants varies depending on the type and nature of the spent fuel. Generally, for oxide fuels which are more ceramic in nature⁷, the dissolution temperature would be on the higher side due to their relatively sluggish dissolution behaviour⁸. Among oxide fuels, temperature required is more for MOX fuel dissolution than UO₂ since PuO₂ is known to dissolve relatively slowly under similar conditions in nitric acid⁹. Hence higher the temperature better would be the dissolution rate. At the same time, the rate of corrosion of the dissolver materials in the reprocessing plants¹⁰ and the rate of evaporation of the solvent is directly proportional to the temperature. Hence there has to be an optimization. As SS is the MOC of the dissolvers in thermal reactor fuel reprocessing plant, generally the temperature is maintained around 353 K as the corrosion rates of SS under that condition is acceptable for its long term operation¹¹. In the case of FBR spent fuel reprocessing, where plutonium rich MOX/MC is the fuel, around 373-383 K is maintained to increase the dissolution rate¹². To overcome the corrosion related issues, the dissolver in FBR spent fuel reprocessing plant is made of titanium whose corrosion resistance is better and acceptable in that temperature range¹³. As mentioned earlier, it was already decided to make the dissolution reactor of hard borosilicate glass for the experiments to be

carried out as a part of this thesis work. Hence corrosion of the reactor is never an issue. But in order to compare the dissolution rates of simulated MOX and uranium plutonium MOX fuel with UO₂ dissolution behaviour, it was decided to carry out all the dissolution experiments at 353 K. For all those experiments where the effect of temperature needs to be studied, it would be varied between 333 and 373 K.

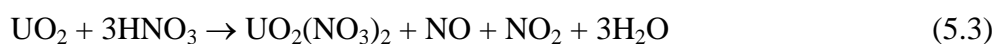
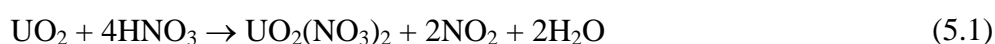
5.4 Effect of initial concentration of nitric acid and temperature on UO₂ dissolution

Experiments on the dissolution behaviour of unirradiated sintered UO₂ pellets were conducted under typical PUREX process conditions to study the effect of initial concentration of nitric acid and temperature on the rate of the reaction in cylindrical glass reactors. The results of these studies and their detailed discussions are presented in this section.

5.4.1 Experimental Procedure

The initial concentration of the acid is known to influence the rate of dissolution proportionately. The qualitative effect of acidity on the dissolution rate has been well understood from many works reported in the literature over the past five decades or so (references 3, 6, 7, 9, 11-15 given in Chapter 3). But for developing a working model for the dissolution process, it is required to establish the quantitative effect of the concentration of acid on the dissolution rate. For this purpose, initial dissolution experiments on unirradiated sintered UO₂ pellets in nitric acid with varying starting concentration was carried out in a glass bubble dissolver shown in Fig. 13.

There are many stoichiometric chemical equations for the dissolution of UO₂ in nitric acid medium¹⁴. Among them the following are the predominant reactions under typical PUREX process conditions^{15, 16, 17}:



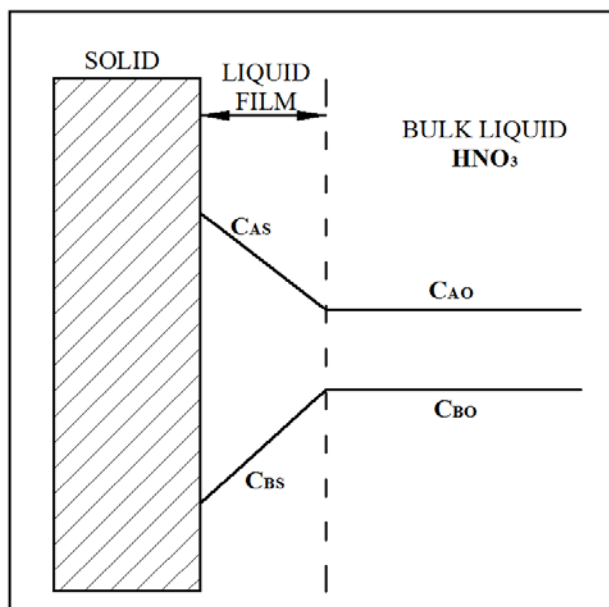
The stoichiometry of the dissolution reaction of UO₂ in nitric acid is variable and it depends on the reaction conditions¹⁸. All the three reactions given above occur to some extent and the predominance of one over the other depends on various conditions like

acidity and temperature¹⁹. The first reaction predominates at concentrations of acid greater than 8 M and the third below 6 M²⁰. In the present investigation, initial concentrations of nitric acid in all our experiments were always more than 8 M. Hence, analysis of experimental data was based on first reaction, (i.e.) for the calculation of the rate parameters.

5.4.2 Modeling of the dissolution of UO_2 in nitric acid by SPM

Nuclear fuel dissolution could be categorized as solid-liquid reaction under the domain of chemical reaction engineering. There are two common approaches for studying the behaviour of fluid-solid interaction²¹. They are the shrinking particle model (SPM)²² and the progressive conversion model (PCM)²³. Among these, for obvious reasons the former is the most suited methodology for studying the dissolution behaviour of solids in liquid solvents²⁴. Hence SPM was chosen to correlate the experimental data. The general approach for formulating the model equations is given by Levenspiel (1972)²¹ for spherical geometry. But with respect to the cylindrical geometry, the equations are accordingly modified and used in this study. A general schematic representation of the solid-liquid heterogeneous reaction is given in Fig. 5.5.

Fig. 5.5. General schematic representation of a solid-fluid reaction



The dissolution of UO_2 pellet in nitric acid medium is a heterogeneous reaction and could be generally represented by the model equations given below. In Fig. 5.5, solid represents

the UO_2 pellets denoted by “A” and liquid represents nitric acid denoted by “B”. The same representations are used in the reactions explained below.

Any solid-liquid reaction proceeds through three main stages, namely, (i) diffusion of reactant B (nitric acid molecules in this case) through the film, (ii) reaction of the reactant B with the solid A (UO_2 in this case) at the solid surface and (iii) diffusion of the product formed (UO_2^{2+} in this case) at the solid surface back to the bulk liquid through the diffusion film.



The reaction is either diffusion controlled wherein stages 1 and/or 3 would be the rate determining step or chemical reaction controlled wherein the stage 2 would be the rate controlling step. The rate of the reaction is directly proportional to the available surface of the unreacted core of the solid particle. Thus the rate expression for the stoichiometric equation 1 is given by

$$-\frac{1}{(2\pi r l + 2\pi r^2)} \frac{dN_A}{dt} = \frac{1}{b} k C_B = k_L (C_{B0} - C_{Bs}) \quad (5.5)$$

Where N_A is the amount of solid A reacting, C_A is the concentration of solute (A) in the liquid at time t, C_B is the concentration of solvent molecules (B), C_{B0} is the concentration of solvent molecules in the bulk liquid, C_{Bs} is the concentration of solvent molecules at the solid surface, b is the stoichiometric coefficient of reactant A, r is the radius of the shrinking particle and k is the first order rate constant.

Though the pellet was covered with a SS plate along the curved surface area, during the subsequent data analysis it was found that unless the curved surface area is included, the model was not able to predict the experimental values satisfactorily. This shows that the curve surface area also takes part in the dissolution reaction. Later on detailed analysis it was found that, though the SS plate covers the curved surface of the pellet tightly, the moment the pellet with the SS cover is dropped into hot concentrated nitric acid solution, there is some ingress of acid in between the pellet and SS sheet. Hence the dissolution starts happening along the curved surface also.

To confirm this, the aspect ratio (L/R) of the pellet was measured during the process of dissolution and was found to decrease initially and became constant by around 15-20% of dissolution. Hence the inclusion of the curved surface area in the model equation in spite of the pellets being covered by SS plate along the curved surface was justified.

As the reaction is carried out with air sparging under sufficiently high temperature, one could expect the diffusion to be sufficiently fast enough and hence as a first approximation, the dissolution is assumed to be predominantly chemical reaction controlled.

For a cylindrical particle whose dissolution is chemical reaction controlled, the rate could be determined by the following computations. As the amount of acid taken initially during the experiments is very high, its concentration remains practically constant all through the reaction. Hence we have

$$C_{B0} \approx C_{BS} \approx C_{B,initial} \quad (5.6)$$

$$-\frac{1}{(2\pi rl + 2\pi r^2)} \frac{dN_A}{dt} = \frac{1}{b} k C_B \quad (5.7)$$

As per the assumptions of SPM, we have

$$N_A = \rho_A V \text{ and } L/R = l/r = x \quad (5.8)$$

Where ρ_A is the molar density of A in solid and V is its volume, L and R are the initial length and radius of the cylindrical particle, l and r are the length and radius of the shrinking particle at any given time and x is the aspect ratio of the dissolving cylindrical particle at any instant. N_A could be rewritten in terms of r as

$$-dN_A = -bdN_B = -\rho_A dV = -\rho_A d(\pi r^2 l) = -\pi \rho_A d(x.r^3) = -3\pi \rho_A x.r^2 \quad (5.9)$$

Substituting equations (5.6) and (5.9) in (5.7), the rate of the reaction in terms of shrinking radius of the unreacted core is given by

$$-\frac{3\pi\rho_A x.r^2}{(2\pi.x.r^2 + 2\pi.r^2)} \frac{dr}{dt} = \frac{1}{b} kC_B \quad (5.10)$$

On integrating and rearranging the above equation, we get

$$\frac{r}{R} = (1 - X_A)^{1/3} = 1 - \frac{2}{3} \frac{(x+1).k.C_B}{b.x.\rho_A.R} t \quad (5.11)$$

This is the rate equation for chemical reaction controlled dissolution of cylindrical solid particles in a liquid. Here X_A is fraction of moles of reactant “A” that has reacted at time t , or in other words, $(1 - X_A)$ is the unreacted fraction of reactant “A” at time t . Equation 5.11 could be specifically rewritten for the dissolution of UO_2 in nitric acid as follows.

$$\left(1 - \frac{[U]_t}{[U]_f}\right)^{1/3} = 1 - \frac{2}{3} \frac{k.(x+1).C_{HNO_3}}{\rho_A.x.b.R} t \quad (5.12)$$

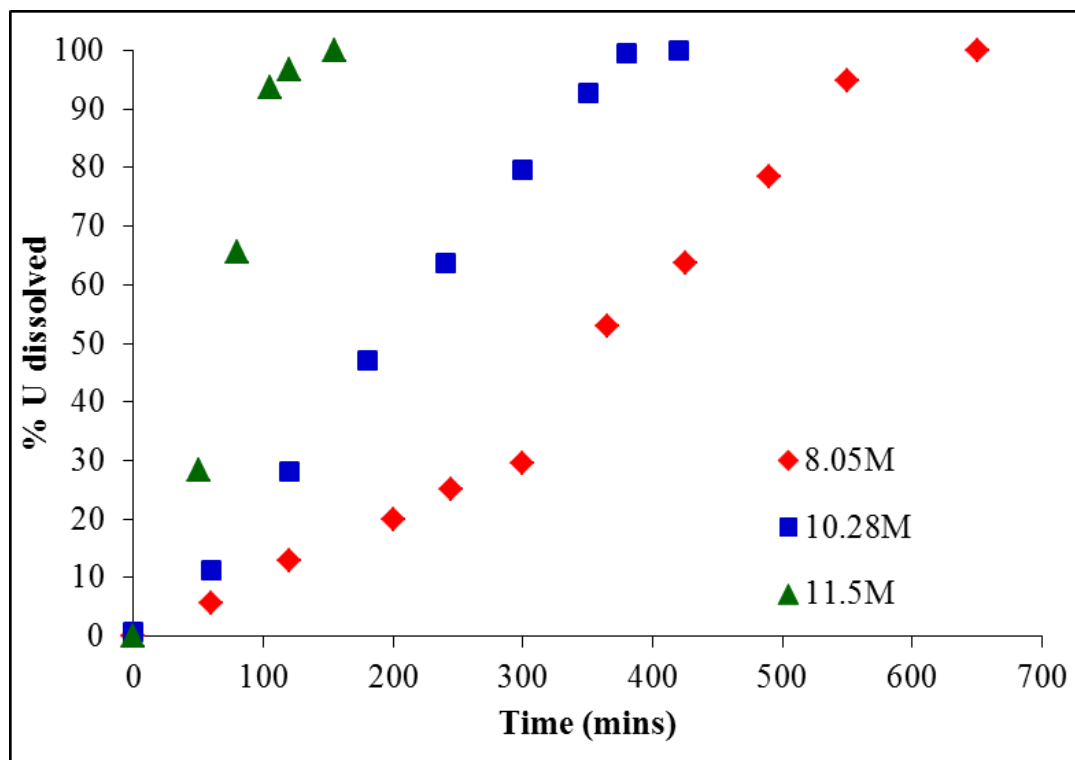
$[U]_t$ and $[U]_f$ are the molar concentration of U(VI) at any time t and at the end of the reaction respectively. Thus by plotting $(1 - ([U]_t/[U]_f))^{1/3}$ against t , we get a straight line and from its slope, the rate constant could be determined since all other parameters contributing to the slope (x , C_{HNO_3} , ρ_A , b and R) are known. It could be seen from equations (5.12) that the stoichiometric co-efficient is in the denominator of the equation which would have an inverse effect on the rate of dissolution of UO_2 pellets.

5.4.3 Results and Discussion

5.4.3.1. Effect of concentration of nitric acid

The experimental set-up used for studying the influence of initial concentration of nitric acid on the dissolution rate of UO_2 pellets was used for probing the effect of temperature also. The experiment was carried out in three different initial concentrations of nitric acid namely 8.05, 10.3 and 11.5 M. Temperature was maintained at 353 K during these experiments. The dissolution curve for the sintered UO_2 pellets in nitric acid of initial concentrations 8.05, 10.3 and 11.5M at 353 K is given in Fig. 5.6.

Fig. 5.6. Dissolution of UO₂ pellets in 8.05, 10.3 and 11.5 M HNO₃ at 353 K



It could be seen from Fig. 5.6 that the rate of dissolution is directly proportional to initial concentration of nitric acid at a given temperature. The experimental data in Fig. 5.6 was used to compute the rate constant for the dissolution using SPM as explained in section 5.4.2. The SPM assumes that the reaction takes place at the surface of the solid being dissolved and also the aspect ratio of the solid is retained till the end of dissolution. Since the dissolution of UO₂ pellets in nitric acid is a solid-liquid reaction, the above assumptions of SPM is reasonably valid as a first approximation towards the computing of rate parameters. The validity of these assumptions, especially of that of the constancy of aspect ratio, was cross checked in our experiment by measuring the length and diameter of the dissolving pellet. It was found that the aspect ratio of the pellet was almost constant till the pellet crumbled and lost its shape. This happened only after about 60% of the dissolution was complete under the experimental conditions.

5.4.3.2. Effect of temperature

Experiments, similar to that explained in previous section (5.4.3.1), were carried out at different temperatures to probe the effect of temperature on the dissolution rate of UO₂ in

nitric acid. In all these experiments, the initial concentration of nitric acid was maintained at 8 M. The results are plotted in Figures 5.7 and 5.8 for the nitric acid concentrations of 8.05 and 10.3 M respectively. These plots clearly show how the rate of the dissolution reaction increases with increase in the temperature when all other parameters are kept constant. The results of these experiments are then subjected to SPM treatment as explained before to evaluate the kinetic parameters.

Figures 5.9 and 5.10 represent comparison between experimental and calculated results using SPM Eq. (5.12) and they are found to be in good agreement. It should be noted that for the purpose of modeling the reaction using SPM, only those data were considered that were generated till the pellet crumbled. This is because; the SPM assumptions are not valid beyond this point.

Since nitric acid is taken in large excess than the stoichiometric requirement in these experiments, the dissolution of UO_2 is pseudo first order with respect to nitric acid. The apparent first order rate constant calculated using the model equation (5.12) for the various initial concentration of nitric acid is given in Table 5.1²⁵.

Fig. 5.7. Effect of temperature on the dissolution of UO_2 pellets in 8.05 M HNO_3

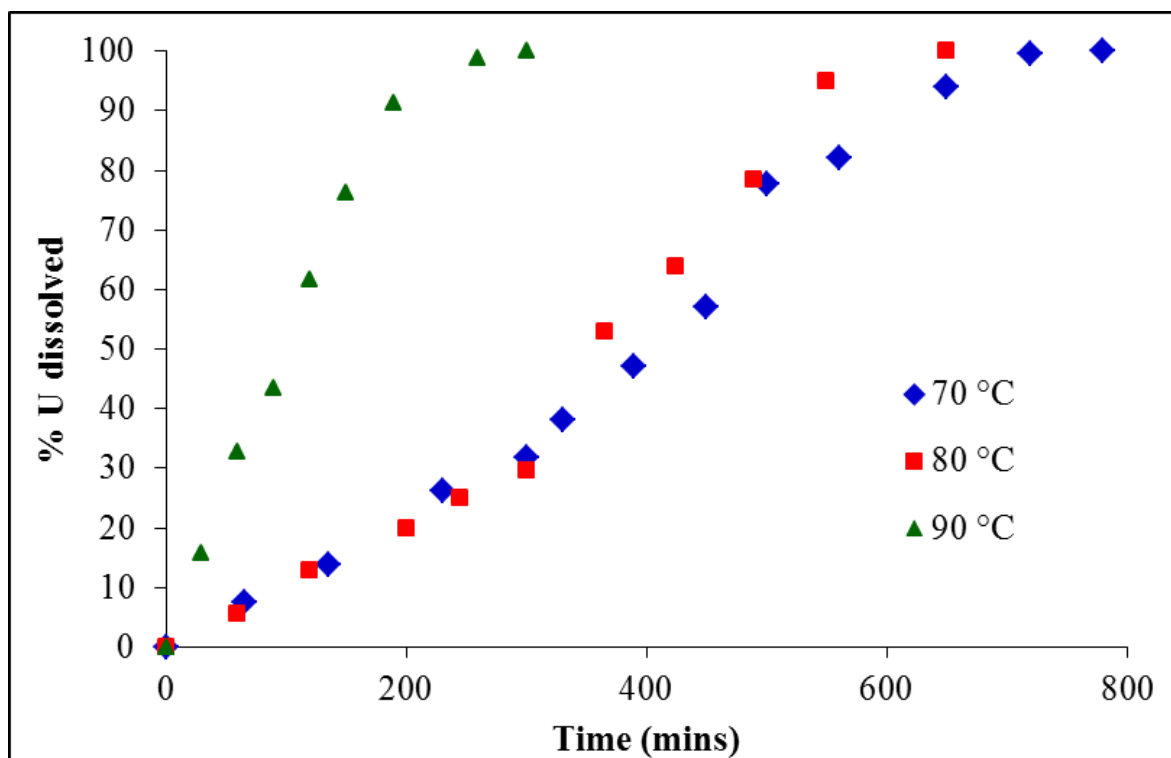


Fig. 5.8. Effect of temperature on the dissolution of UO_2 pellets in 10.3 M HNO_3

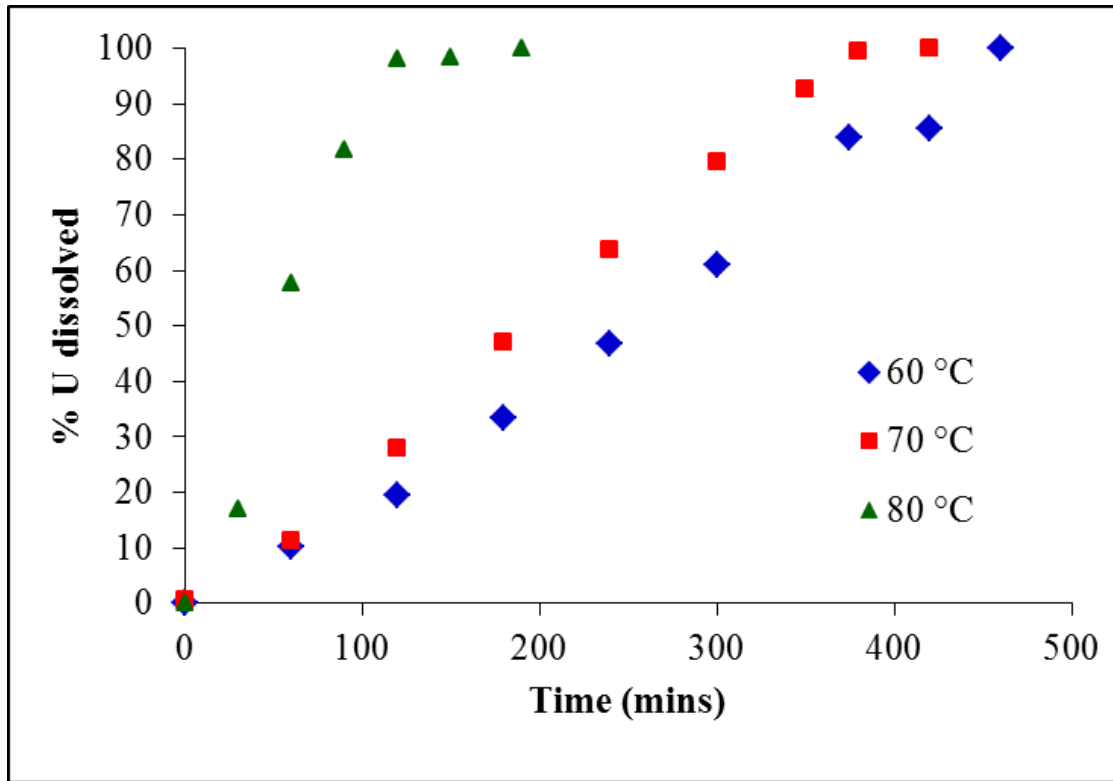


Fig. 5.9. Experimental and modelled UO_2 dissolution curves in 8.05 M HNO_3 at various temperatures

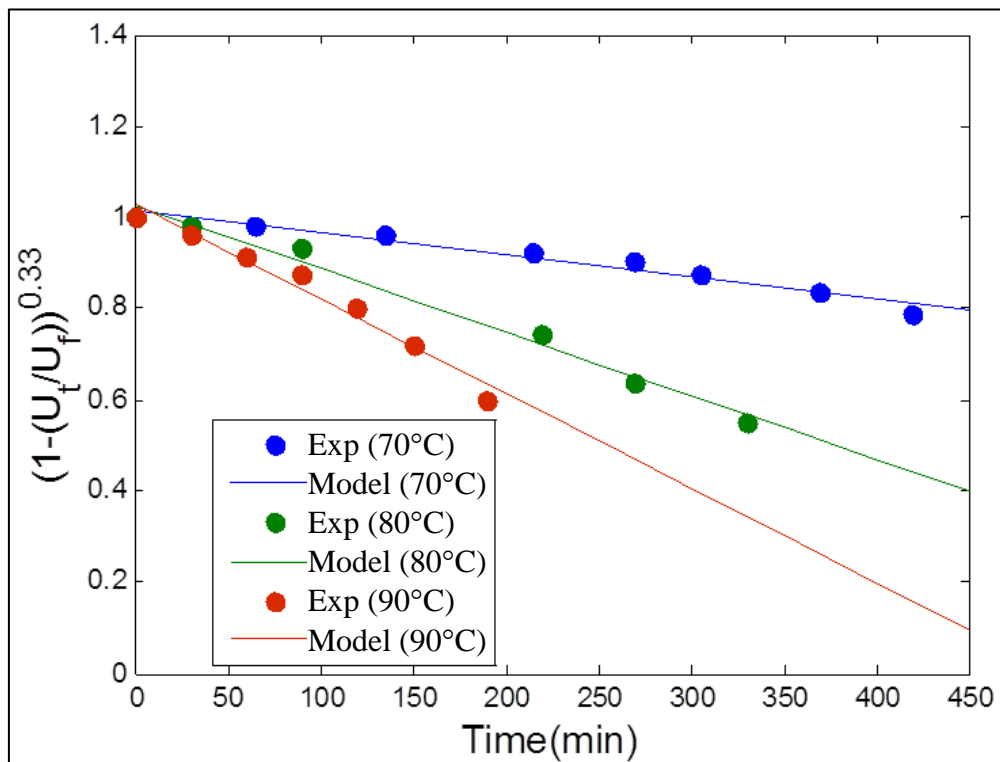


Fig. 5.10. Experimental and calculated dissolution curves for UO₂ pellets in 10.3 M nitric acid at various temperatures

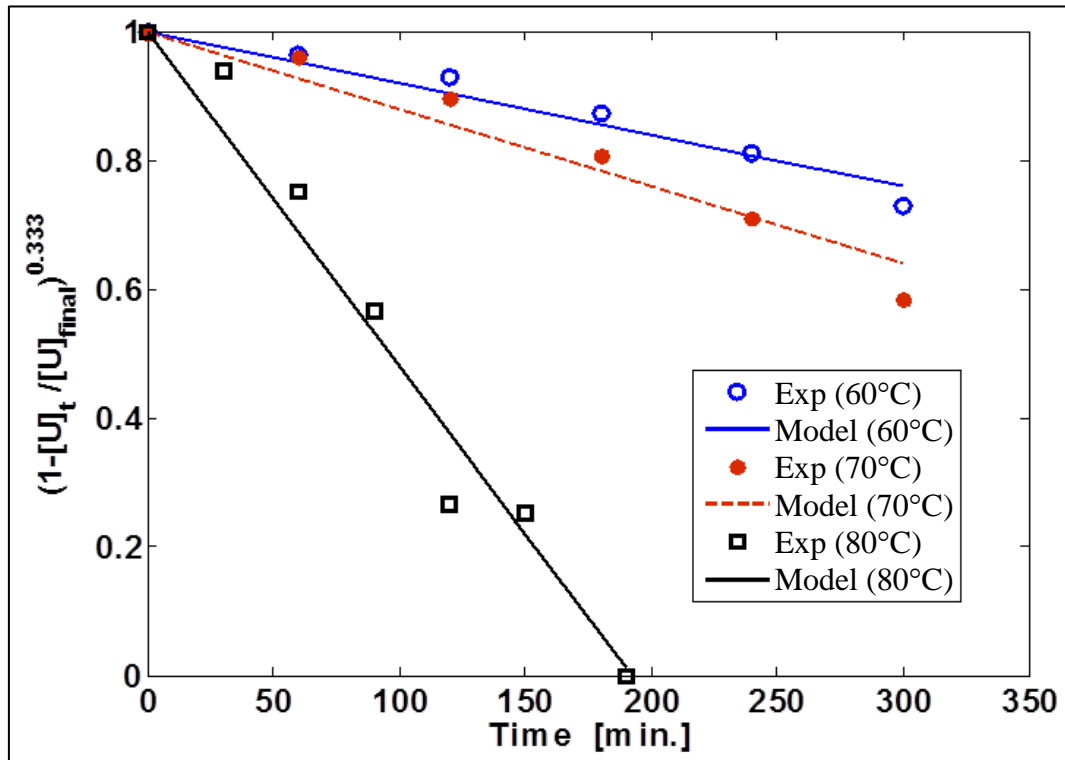


Table 5.1. Pseudo 1st order rate constant for UO₂ dissolution in HNO₃

Rate constant	[HNO ₃]						
	8.05 M			10.3 M		11.5 M	
	Temperature (K)						
	343	353	363	333	343	353	
k(m/s)	1.57E-03	3.19E-03	7.29E-03	2.02E-03	3.08E-03	1.30E-02	8.73E-02

From the pseudo first order rate constant values in Table 5.1, it could be seen that on increasing the initial concentration of nitric acid from 8.05 to 10.3 M, the rate constant increases to above four folds and two folds at 353 and 343 K respectively. The temperature dependency of the dissolution rate is governed by the Arrhenius equation²⁶ which is given by;

$$\ln(k) = \ln(A) - E_a/RT \quad (5.13)$$

Where “A” is the pre exponential factor, E_a is the activation energy, R is the universal gas constant and T is the experimental temperature in kelvin. Thus the plot of $\ln(k)$ vs $1/T$ gives a straight line with the slope E_a/R . The Arrhenius plot for the dissolution reaction at 8.05 and 10.3 M initial concentrations of acid are given in Figures 5.11 and 5.12 respectively.

Fig. 5.11. Arrhenius plot of $\ln(k)$ vs $1/T$ for UO_2 dissolution in 8.05 M HNO_3

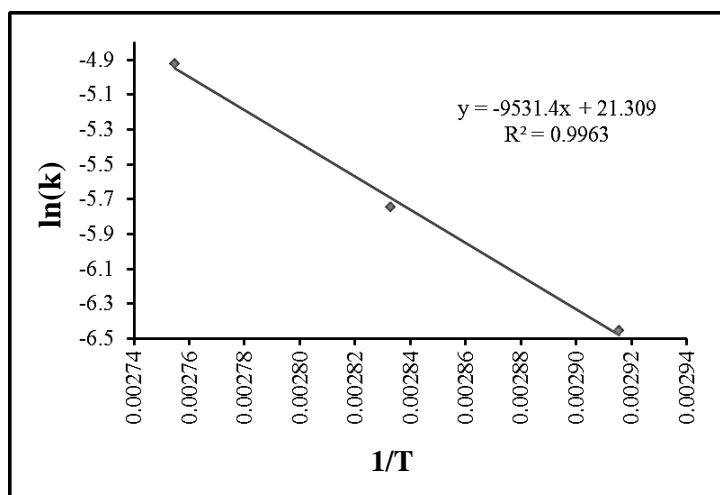
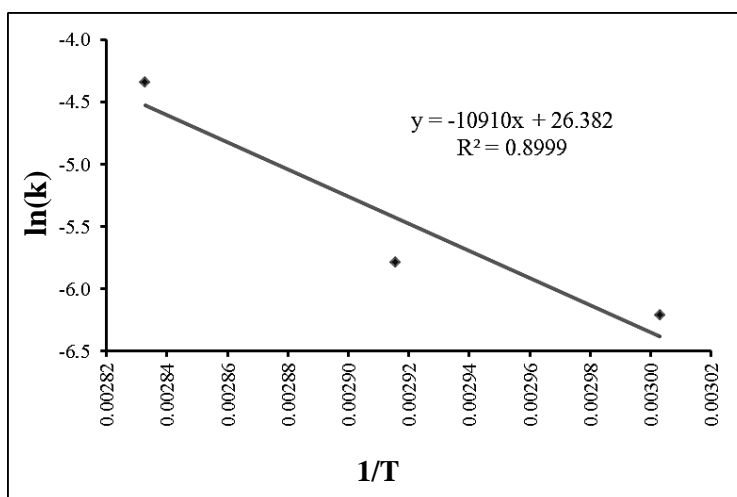


Fig. 5.12. Arrhenius plot of $\ln(k)$ vs $1/T$ for UO_2 dissolution in 10.3 M HNO_3



The E_a for the dissolution reaction at the initial concentration of nitric acid being 8.05 and 10.3 M as calculated from Figures 5.11 and 5.12 were about 80 and 90 kJ/mol respectively²⁷. The calculation of the activation energy in this entire thesis (wherever applicable) was done using the standard MS Excel 2010 software with the confidence levels set at 95% by default.

In general, if the rate of the reaction is controlled by chemical reaction, E_a is more than 40 kJ/mol and if the rate is controlled by diffusional process, E_a is less than 20 kJ/mol, and the E_a value between 40 and 20 kJ/mol is expected for a mixed controlled regime²⁸. The obtained value of E_a suggests a possible chemical reaction controlled regime in the temperature range of 233–363 K. Hence the contribution of diffusion process on dissolution rate of UO_2 pellet could be assumed to be negligible under these experimental conditions.

5.4.4 Conclusion based on the initial experiments on UO_2 dissolution in nitric acid

The dissolution behaviour of the typical Indian PHWR natural UO_2 pellets in nitric acid medium has been studied at conditions relevant to FBR fuel reprocessing. The reaction was modeled using the shrinking particle approach coupled with chemical reaction control. The experimental and the calculated values are in good agreement thereby justifying the applicability of the model to study the dissolution reaction under the given conditions. The model was also used to evaluate the pseudo first order rate constant. The determined rate constant suggests a fourfold increase in the reaction rate on changing the initial concentration of nitric acid from 8.05 to 11.5 M at 353 K. The reaction was carried out at different temperatures and the activation energy of the dissolution reaction was also estimated as a function of the initial concentration of acid. The estimated activation energy indicates the reaction to be predominantly chemical reaction controlled²⁹. The approach would be further extended to evaluate the effect of other parameters like mixing speed and the surface area of the pellet on the rate of dissolution. The exercise and methodology employed to study the dissolution behaviour of UO_2 fuel system, with added necessary safety precautions, would be adopted to study the dissolution behaviour of simulated urania ceria MOX and urania plutonia MOX pellets in nitric acid medium.

5.5 Effect of mixing on the dissolution kinetics of UO_2 pellets in nitric acid

5.5.1 Introduction

The rate of the reaction of a solid-liquid reaction system in a mechanically mixed Stirred Batch Reactor (SBR) type vessel is generally proportional to the mixing intensity³⁰. This observation generally holds good except for any change in the reaction mechanism or an autocatalytic reaction wherein one of the products formed catalyzes the reaction. Thus in

general, for any solid-liquid reaction system, as the mixing intensity is increased, the rate keeps changing. A stage would come wherein further increase in the mixing intensity does not affect the reaction rate practically any further³¹. At this juncture, the diffusion control of the reaction is either at its bare minimum or absent and the rate of the reaction determined under such condition would be intrinsic in nature. One of the objectives of the present work is to determine the intrinsic kinetics of the dissolution of nuclear fuel in nitric acid. Hence the dissolution of UO₂ pellets in nitric acid was carried out with different agitation rate to study the effect of mixing on the reaction rate.

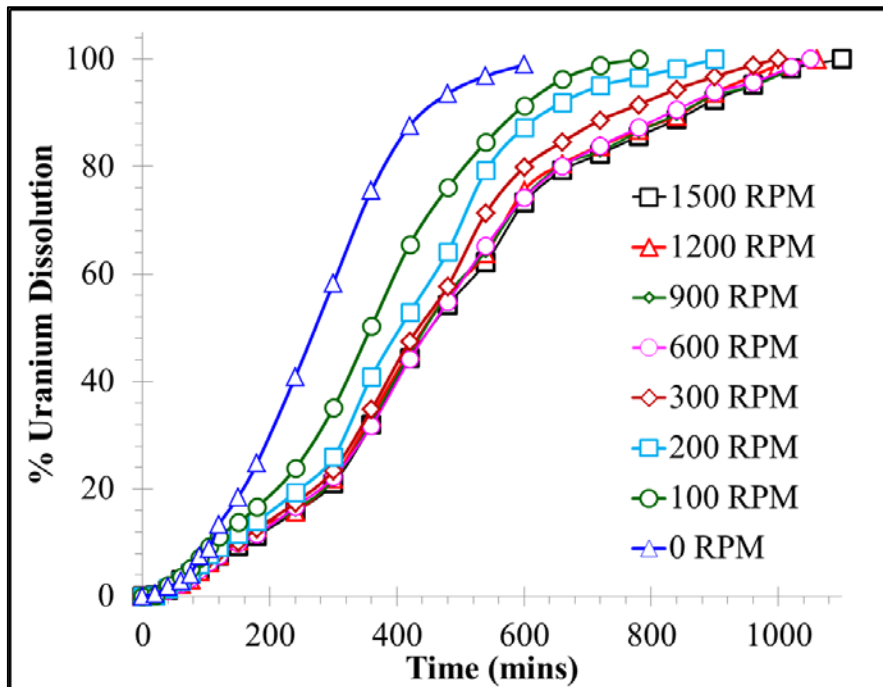
5.5.2 Experimental procedure

The dissolution of sintered UO₂ pellets in nitric acid was conducted in cylindrical glass reactor, shown in Figures 5.1 and 5.3, with varying rates of mechanical mixing using glass impeller. The initial concentration of acid and temperature for each of this experiment was maintained at 8 M and 353 K respectively as justified in sections 5.2 and 5.3. In each experiment, calculated amount of nitric acid was used to achieve uranium concentration levels of around 1.2 to 1.3 M at the end of dissolution which is adopted in typical reprocessing plants². For every experimental run, required volume of 8 M nitric acid was taken in the reaction vessel and was first heated to a preset temperature (353 K in the present case). Once that temperature is reached, an UO₂ pellet whose dimensions and weight were measured and recorded accurately and which is SS clad was immersed carefully and placed at the bottom of the reactor as shown in Fig. 5.1. The glass impeller was set to rotate at a known fixed RPM and the timer was started. Periodical samples were taken from the reaction mixture to analyze the concentrations of uranium, nitric acid and nitrous acid. Heating at the constant set temperature was continued till the pellet dissolved completely. Similar experiments were carried out at different mixing rates to evaluate its effect on the rate of dissolution. The various mixing rates employed during the experiments were 0, 100, 200, 300, 600, 900, 1200 and 1500 RPM.

5.5.3 Results and discussion

The plot of percentage dissolution as a function of time at various mixing intensity is provided in Fig. 5.13.

Fig. 5.13. Percentage UO₂ dissolution in nitric acid at various mixing rate

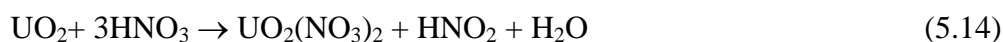


From Fig. 5.13, it could be observed that when the reaction mixture is stirred vigorously, the rate of UO₂ dissolution in nitric acid decreases significantly till 600 RPM and remains almost constant on increasing it further³². In other words, the time taken for the complete dissolution of same starting mass of sintered UO₂ pellet under similar conditions increases from 600 to about 1100 mins as the stirring rate is increased from 0 to 600 RPM respectively³³. For all mixing rates from and above 600 RPM, the time taken for the complete dissolution is more or less same. Thus for all the experiments where the mixing rate needs to be fixed constantly for studying the effect of any other parameter, 600 RPM was employed. This observation is against the general perception that for any solid dissolving in a liquid, the rate of dissolution is directly proportional to the mixing rate. This is a fair indication that the mechanism operating in this reaction is different as against any solid dissolving in a liquid. It should also be noted that, the dissolution curve at all mixing rates employed in this study has a sigmoidal or S shape³⁴. Autocatalytic reactions are generally found to exhibit sigmoidal or S shaped curve for the conversion of reactant/s to product/s³⁵. Hence as a first approximation, one could conclude that dissolution of UO₂ pellets in nitric acid is an autocatalytic reaction. In literature, it has been postulated that the inverse relation between the mixing intensity and the rate of dissolution of UO₂ fuel system in nitric acid medium is due to the autocatalytic action aided by nitrous acid^{36, 37}.

It should be noted here that figures 5.7 and 5.8 does show a sigmoidal behaviour. But it was not so prominent. This is because, the set of experiments corresponding to figures 5.7 and 5.8 were carried out under air sparged condition as shown in figures 5.2 and 5.4. As a result, the nitrous acid produced in-situ at the pellet solution interface was dispersed into the bulk of the reaction mixture along the direction of the air flow thereby reducing the diffusional resistance offered to the reaction. The slight sigmoidal shape of the curve indicates that the air flow rate is not high enough to eliminate the diffusional resistance completely.

5.5.3.1 Role of nitrous acid

The dissolution of UO_2 fuel system in nitric acid is an oxidative dissolution process as U(IV) in the solid (UO_2) is oxidized to U(VI) in the aqueous medium (UO_2^{2+} ions). Therefore the presence of any oxidizing agent in the reaction mixture during the course of dissolution would accelerate/catalyze the reaction. It is well established in the literature that nitrous acid is produced in-situ during the dissolution of UO_2 in nitric acid at the pellet-solution interface as per the stoichiometric equation given below,^{37, 38}.



Thus the presence of nitrous acid, a good oxidizing agent, greatly enhances the dissolution rate of UO_2 by oxidizing UO_2 at the solid surface to UO_2^{2+} through the following reaction³⁹.



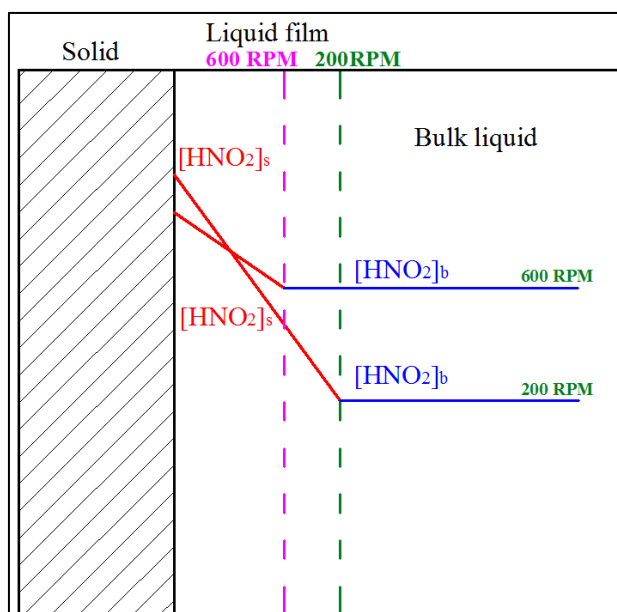
The nitrous acid so produced, finally decomposes as per the following reaction.



Thus the equation 5.3 mentioned earlier is the algebraic addition of equations 5.14 and 5.16. When the reaction mixture is stirred vigorously, there is a decrease in the concentration of nitrous acid at the pellet-solution interface due to the dispersal of nitrous acid into the bulk solution. This tends to reduce the availability of nitrous acid at the

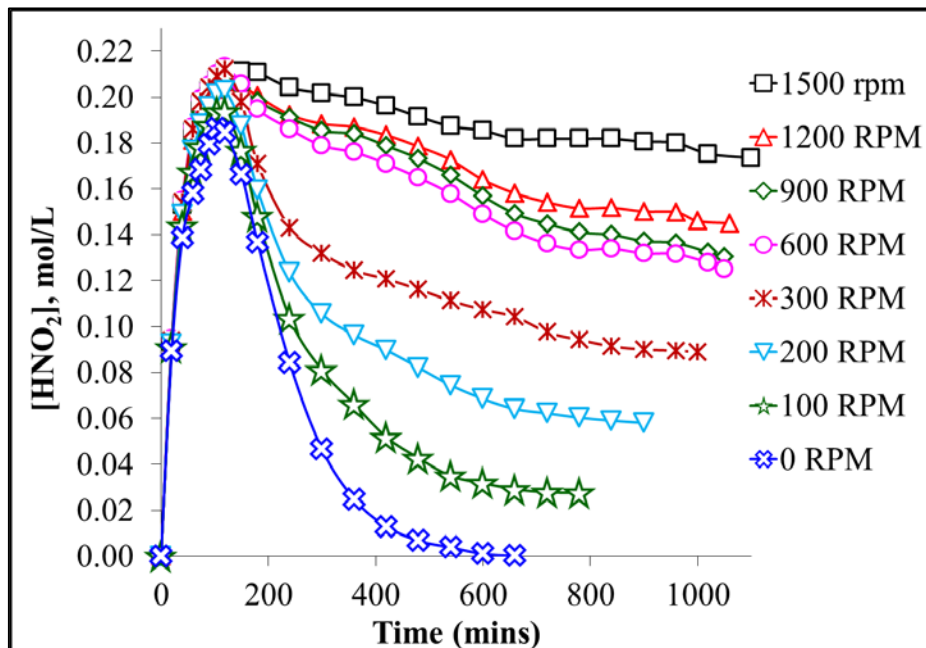
interphase, thereby leading to a decrease of the oxidative dissolution reaction in equation 5.15. Thus under agitated condition, UO_2 dissolves only by equation 5.14 as against in the unstirred condition where it dissolves by both equations 5.14 and 5.15. As an added effect, the rate of decomposition of nitrous acid is also enhanced with mixing⁴⁰, resulting in further decrease in dissolution of UO_2 by equation 5.15. This explanation is schematically represented in Fig. 5.14.

Fig. 5.14. Schematic representation of the effect of mixing intensity on the nitrous acid concentration profiles in the reaction system



Experiments were formulated to test this hypothesis by monitoring the concentration of nitrous acid in the bulk reaction mixture along with uranium during the course of dissolution⁴¹. The results are plotted in Fig. 5.15. Fig. 5.15 indicates that, during the course of UO_2 dissolution in nitric acid, upto 150 mins the concentration of nitrous acid increases and reaches its maximum irrespective of the mixing rate, gradually reduces from there and stabilizes at various levels depending on the intensity of agitation. Nitrous acid once generated, is consumed in two ways, (i) its self-decomposition as per equation 5.16 and (ii) its reaction with UO_2 at the solid surface to generate UO_2^{2+} ions in the liquid as per the reaction 5.15⁴². When the mixing rate is higher, nitrous acid gets dispersed faster and its self-decomposition rate is also higher⁴³. Hence its availability for the UO_2 dissolution reaction as per equation 5.15 is reduced.

Fig. 5.15. Concentration profile of nitrous acid in the reaction mixture during the dissolution of UO_2 in nitric acid at various mixing rates



Thus the overall dissolution rate is decreased now as the dissolution takes place only by the reaction 5.14. At lower mixing intensity, nitrous acid spends more time at the vicinity of the interface and thereby its consumption by reaction 5.16 to dissolve more UO_2 dominates over its self-decomposition. This behaviour is further emphasized by an increase in dissolution rate at lower mixing rate as shown in Fig. 5.13⁴⁴.

To further ascertain the catalytic role of nitrous acid on the oxidative dissolution of UO_2 in nitric acid, the reaction was carried out in the presence of hydrazine (0.5M hydrazine added at a rate of 1 mL/min) which reacts with nitrous acid and consumes it instantaneously⁴⁵. The concentration profiles of uranium and nitrous acid are shown in Figures 5.16 and 5.17 respectively in the presence and absence of hydrazine.

The results, as shown in Figures 5.16 and 5.17, clearly indicate that when there is no hydrazine in the reaction mixture, there is a steady increase in the concentration of both uranium and nitrous acid in it. In its presence, hydrazine reacts with nitrous acid instantaneously and consumes it thereby reducing the availability of nitrous acid for the oxidative dissolution of uranium (refer equations 28-30 of Chapter 2 for the reactions between hydrazine and nitrous acid). When the addition of hydrazine is stopped, the dissolution reaction starts taking place at an increased rate as indicated by the increase in the slope of the concentration profile curves of uranium and nitrous acid in the reaction

mixture in Figures 5.16 and 5.17 respectively. This confirms the autocatalytic role of nitrous acid during the oxidative dissolution of UO_2 in nitric acid medium.

Fig. 5.16. Effect of hydrazine on the uranium concentration profile during UO_2 dissolution in nitric acid

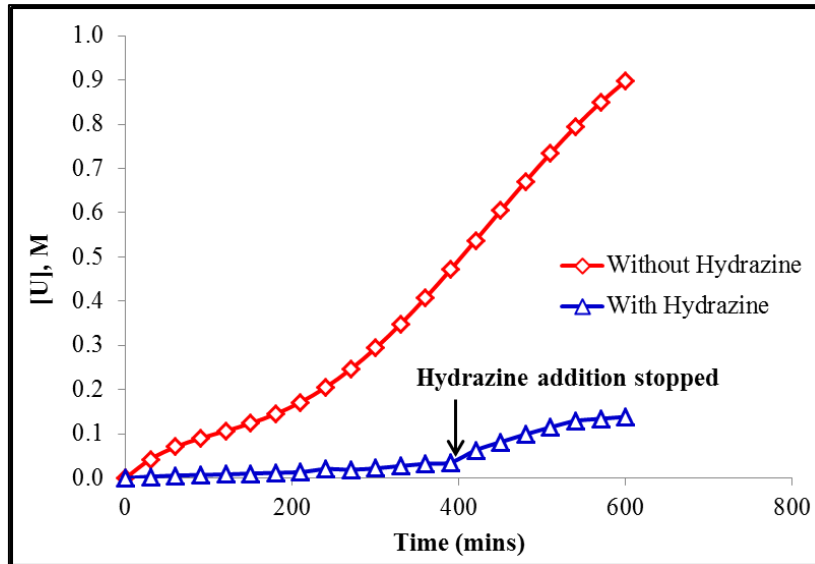
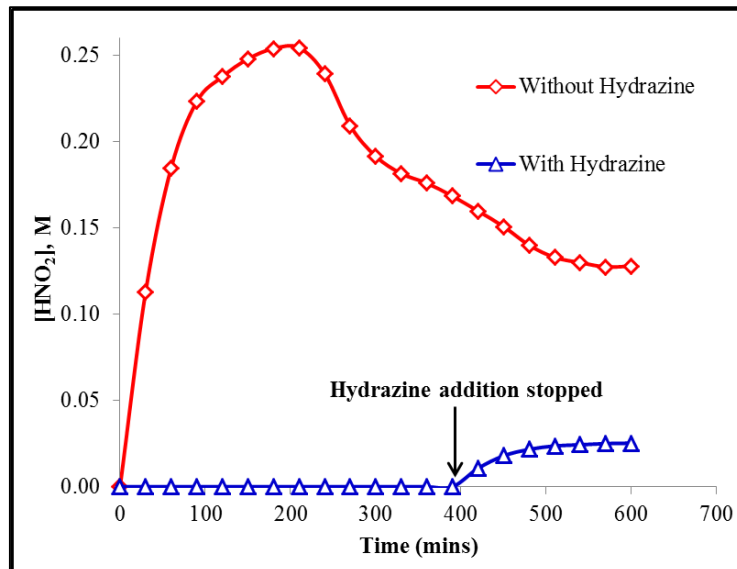


Fig. 5.17. Effect of hydrazine on the nitrous acid concentration profile during UO_2 dissolution in nitric acid



The results also indicate that during the dissolution of TRSF in nitric acid wherein uranium constitutes more than 99% of actinide elements, the dissolution would be faster under unstirred condition. Though agitation of the spent fuel is required to break down the

solid fuel particles and establish better contact between nitric acid and the spent fuel particles, the above results translates into the fact that if excess nitrous acid is supplied into the dissolver solution either by the addition of sodium nitrite or by sparging NO_2 gas, the reaction would proceed faster thereby increasing the overall plant production rates. Thus the optimization of dissolution process with respect to agitation and sparging with NO_2 gas would greatly enhance the TRSF dissolution rates during its reprocessing.

5.5.4 Conclusions of experiments on the effect of mixing on UO_2 dissolution rate

Various parameters which influence the dissolution kinetics of UO_2 in nitric acid, particularly the effect of mixing intensity and the role of nitrous acid were studied in detail. The retarding effect of the intensity of mixing the reaction mixture on the rate of dissolution of UO_2 was explained based on the autocatalytic role of nitrous acid. The explanation was justified by the reduction in the dissolution rate in presence of hydrazine, a masking reagent for hydrazine. These results and their explanations clearly emphasizes the necessity to optimize the operating parameters like stirring rate and sparging of NO_2 gas into the spent nuclear fuel dissolution mixture to improve the throughput of the dissolution process in a TRSF reprocessing plant.

5.6 Effect of temperature on the intrinsic kinetics of UO_2 dissolution

5.6.1 Introduction

In the previous section, it has been brought out that the rate of dissolution of sintered UO_2 pellets in nitric acid under the given experimental conditions, does not vary much starting from 600 RPM and beyond. Hence 600 RPM has been fixed as the mixing rate for studying the effect of temperature on the intrinsic kinetics of UO_2 pellet dissolution in nitric acid. The cylindrical glass dissolver which was used to study the effect of mixing was used for evaluating the effect of temperature on the reaction kinetics.

5.6.2 Experimental details and procedure

Experiments were conducted in same/similar cylindrical glass reactor, shown in Figures 5.1 and 5.3, that was used for studying the effect of rate of mixing. The initial concentration of nitric acid and mixing rate for each of this experiment was maintained constantly at 8 M and 600 RPM respectively as explained earlier in sections 5.2 and 5.5.3

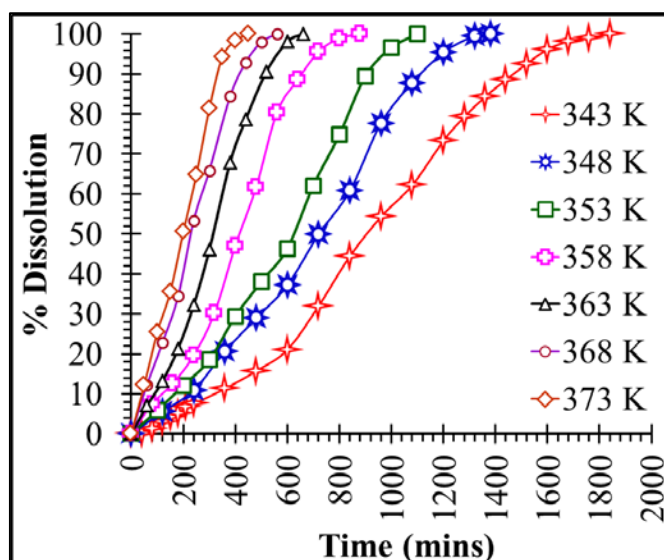
respectively. The temperature was varied from 343 to 373 K in steps of 5 K. In each of the experiment, required numbers of standard UO_2 pellets and 8 M nitric acid was used to achieve a uranium concentration of about 1 M at the end of each experiment. Pellets were chosen such that the cumulative starting weight of all the pellets put together is almost the same in all the experiments. The initial volume of nitric acid was chosen to ensure the proper immersion of the glass impeller into the liquid mixture right till the end of each experiment, taking into account the amount of nitric acid that would be lost in each of the entire experiment in the form of periodic samples.

For every experimental run, nitric acid was taken in the reaction vessel and was first heated to a preset temperature. Once the set temperature is reached, required numbers of UO_2 pellet/s, whose dimensions and weight were measured and recorded accurately and which were SS clad, were immersed carefully and placed at the bottom of the reactor as shown in Fig. 5.1. The glass impeller was set to rotate at 600 RPM constantly using a DC motor and the timer was set. Periodical samples were taken from the reaction mixture to analyze uranium, nitric acid and nitrous acid concentrations. To the extent possible, the sampling frequencies were maintained constant across all experiments for the ease of comparing the results. Heating at the constant set temperature was continued till the pellet dissolved completely. All the connections were ensured to be sufficiently air tight to avoid the loss of nitric acid vapors and also for effectively scrubbing and determining the composition of the off gases evolved. Similar experiments were carried out at different temperature to evaluate its effect on the rate of dissolution.

5.6.3 Results and discussion

The results of the experiments carried out to study the effect of temperature on the dissolution kinetics of UO_2 pellets in nitric acid is presented in Fig. 5.18. It has to be noted that the data in Fig. 5.18 is much different from that in Fig. 5.7 though both correspond to UO_2 dissolution at 353K and 8 M starting nitric acid concentration. The earlier experiment was carried out with excess nitric acid. Hence the concentration of acid practically remained constant and hence the reaction rate was relatively higher. But in the latter, the amount of acid taken initially was much lower (but sufficiently more than the required stoichiometry). Hence the rate was relatively lower. The amount of acid required was calculated such that, the final concentration of uranium is in line with a typical PUREX process flowsheet.

Fig. 5.18. Effect of temperature on the dissolution kinetics of UO_2 pellets in HNO_3

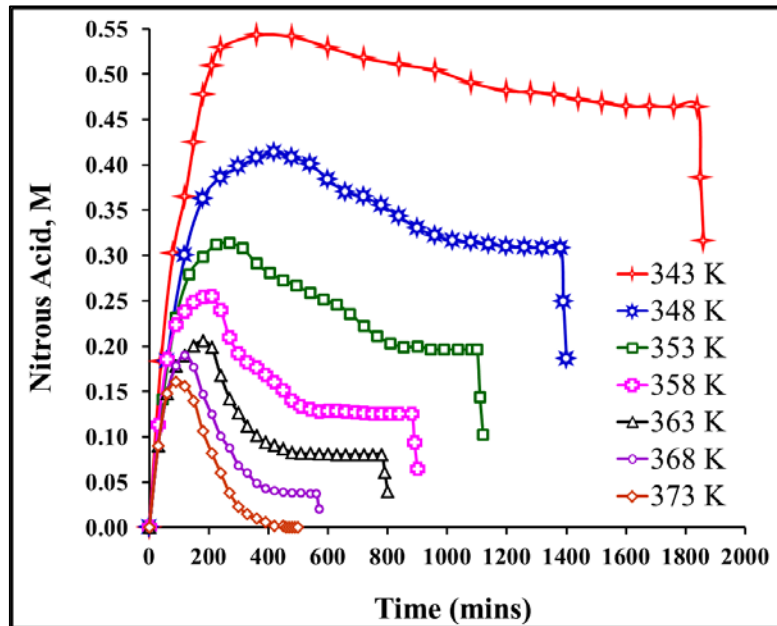


As reported earlier in this thesis (section 5.5.3), all the dissolution curves in Fig. 5.18 has an ‘S’ shape indicating the autocatalytic nature of the reaction. It could also be noted that as the temperature increases, the rate of the reaction also increases which is indicated by the reduced time taken for the complete dissolution of similar starting amount of UO_2 pellet/s at higher temperatures. This data is subsequently used in determining the rate constant as a function of temperature and the apparent activation energy of the dissolution reaction using Arrhenius relation.

To understand the role played by nitrous acid on the dissolution kinetics of UO_2 pellets at various temperatures of the studies, the concentration of nitrous acid was also measured during all these dissolution experiments. The concentration profile of nitrous acid as a function of time during the UO_2 dissolution experiments at various temperatures indicated in Fig.5.18 are plotted in Fig. 5.19.

The most striking and important feature of Fig. 5.19 is the abrupt decrease in the nitrous acid concentration profiles at all conditions at the end of dissolution. As soon as the last spec of the pellet dissolved, the nitrous acid concentration suddenly decreased indicating that it is produced in-situ during the dissolution of UO_2 in nitric acid. Though there would be some amount of nitrous acid always associated with nitric acid⁴⁶, the observations of Fig.5.19 shows that the concentration of nitrous acid produced in-situ during the dissolution of UO_2 pellet in nitric acid is far higher than that presently inherently in equilibrium with nitric acid at that temperature.

Fig. 5.19. Nitrous acid concentration profile during UO₂ dissolution at various temperatures



Nitrous acid is very reactive and decomposes to NO_x gases during UO₂ dissolution in nitric acid medium³⁹ which is highly favored at higher temperatures. Hence the amount of nitrous acid found in the bulk of the reaction mixture as indicated in Fig. 5.19 is lower at higher temperatures. Therefore the catalytic effect of nitrous acid towards the dissolution of UO₂ pellets is limited at higher temperatures. But still the rate of the dissolution reaction is found to be higher at higher temperatures. Thus it could be concluded that the positive effect of higher temperatures towards the rate of dissolution of UO₂ in nitric acid medium overrides the absence of the autocatalytic effect of nitrous acid whose decomposition rate increases with increase in temperature.

5.7 Determination of the composition of NO_x gas evolved during dissolution

5.7.1 Importance of the measurement of NO_x gas composition during dissolution

Nitric acid is the medium of choice for processing the spent nuclear fuel through aqueous route by employing PUREX process for various reasons⁴⁷. Hence NO_x gases are generated during most of the process steps in reprocessing, especially during dissolution where concentrated nitric acid is employed at high temperatures. The NO_x gases are generated during the dissolution of UO₂ in nitric acid predominantly due to the

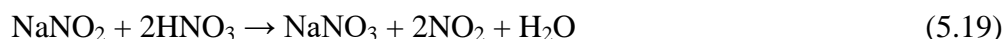
decomposition of nitrous acid³⁸. Due to the chemical conditions that prevail in a typical PUREX process^{14, 48}, only NO and NO₂ gases gets generated⁴⁶. The composition of these NO_x gases depends on the initial concentration of the nitric acid used during the dissolution process step⁴⁹. As explained in the section 5.3.3.1, nitrous acid plays an important role in the dissolution reaction³⁶⁻⁴⁵. Therefore to determine the mechanism of the dissolution reaction, it is mandatory to know the profiles of the NO_x gases during the course of the reaction to understand the behaviour of nitrous acid. Also the composition of NO_x gases plays an important role on the reaction mechanism of dissolution of nuclear fuel in nitric acid⁵⁰. Hence by measuring the composition of the NO_x gases, one could get to know about the mechanism and thereby the intrinsic rate of dissolution of nuclear fuel in nitric acid which is the fundamental data required for designing a continuous dissolution process for spent nuclear fuel reprocessing applications⁵¹.

5.7.2 Principle of analysis

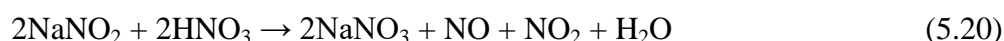
For the purpose of this study, NO_x gases were generated by reacting a known amount of sodium nitrite with nitric acid in a closed stirred reaction chamber. This reaction was chosen as it is fast and is more amenable with the analytical methods adopted for the determination of the off-gas composition⁵². The NO_x gases evolved during the reaction were scrubbed in two NaOH scrubbers in series before exhausting them into the atmosphere. The NO and NO₂ gases evolved in the reaction, react with NaOH in the scrubbers forming sodium nitrite and nitrate whose stoichiometry is well established⁵⁵. By measuring the concentration of the nitrate and nitrite ions in the scrubber solution before and after scrubbing, the composition of the NO_x gas was back calculated from the overall stoichiometric reactions. Though there were many methods reported in the literature for the measurement of NO_x composition in radioactive environment⁵³, the present method is the simplest, straight forward and easily adaptable⁵⁴.

5.7.3 Reactions involved

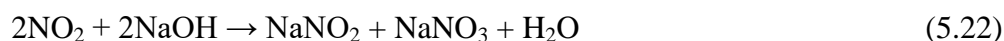
The reaction between sodium nitrite (NaNO₂) and nitric acid happens through any of the following three stoichiometric equations depending on the conditions⁵². Assuming that all the mechanisms are equally probable, the overall reaction stoichiometry could be arrived as follows.



The overall reaction could be represented as follows.



When the NO_x gases are scrubbed in sodium hydroxide, sodium nitrite and nitrate are formed as per the following stoichiometric reactions⁵⁵.



By estimating the amount of nitrite and nitrate ions formed in the sodium hydroxide scrubbers, the composition of the NO_x gas could be back calculated using the above stoichiometric reactions.

5.7.4 Experimental setup and procedure

The experimental set-up (fig.5.1 and fig.5.3) consists of a cylindrical glass reaction chamber that is closed to sufficient leak tightness and is connected with a reflux condenser. The condenser is connected to two NaOH glass scrubbers in series for the purpose of absorbing the NO_x gases quantitatively after which the off-gas is exhausted to the atmosphere. The initial concentration of the NaOH scrub solution is 2 M. To the reaction chamber containing known quantity of nitric acid, calculated quantity of sodium nitrate of known concentration is added to generate NO_x gases which are then bubbled through sodium hydroxide scrubbers. The generated NO_x gases are completely absorbed in the two scrubbers by maintaining a slight negative pressure inside them using an air ejector set-up. After ensuring the completion of reaction and total absorption of the NO_x gases as indicated by the absence of any brown fumes, samples from the two scrubbers are taken and analysed by ion chromatographic method for the concentration of total nitrate

and nitrite ions. From these values and from the stoichiometric equations for the scrubbing of NO_x gases in NaOH as given in equations 5.21 and 5.22, the compositions of the NO_x gases are back calculated.

5.7.5 Analytical instruments

The details of the analytical instruments used for the NO_x measurement studies are already explained in section 4.7. the analytical procedure is discussed in detail in the following sections.

5.7.6 Analytical procedure

An analytical method for the determination of the composition of NO_x gas was standardized using mixtures of solution of standard sodium nitrite and sodium nitrate of various proportions. 2 M sodium hydroxide was used as the scrub solution to trap the NO_x gases evolved from the reaction mixture. Hence, appropriately diluted 2 M sodium hydroxide is used to generate the blank/base line of the chromatogram. Figures 5.20 and 5.21 shows the calibration graphs for nitrate and nitrite ion determinations respectively by IC.

Fig. 5.20. Calibration graph for the nitrate concentration varies from 10-100 ppm

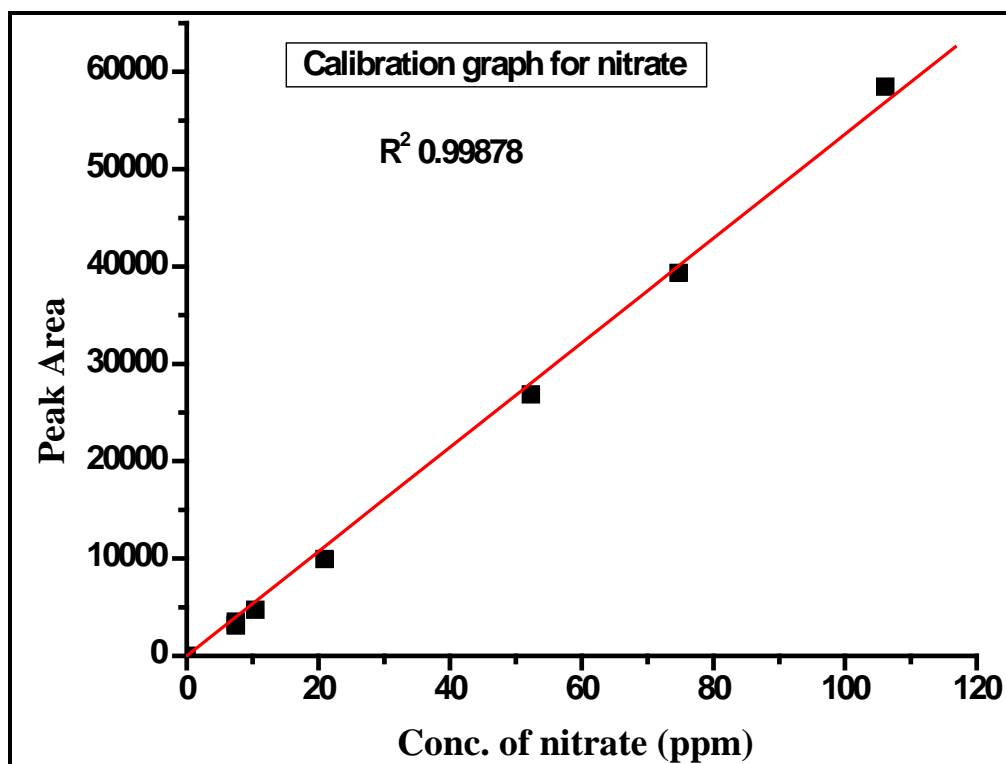
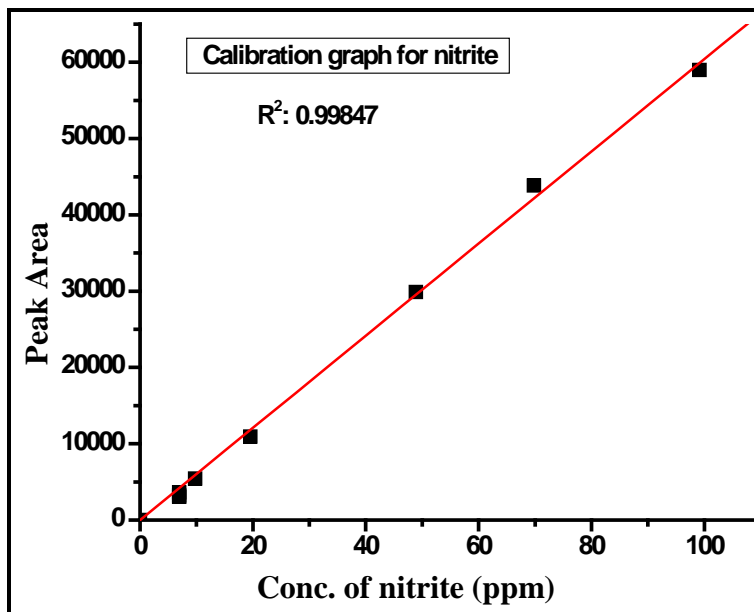
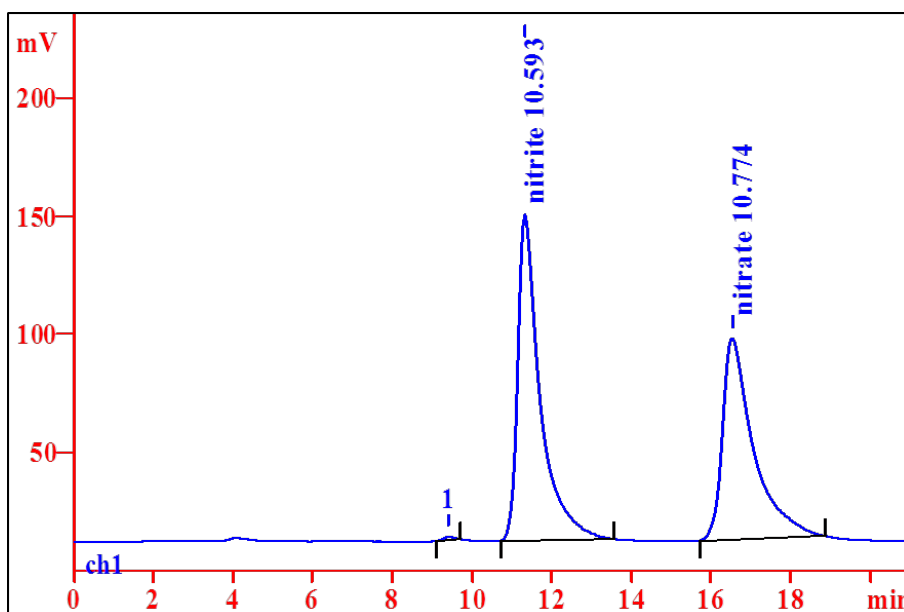


Fig. 5.21. Calibration graph for the nitrite concentration varies from 10-100 ppm



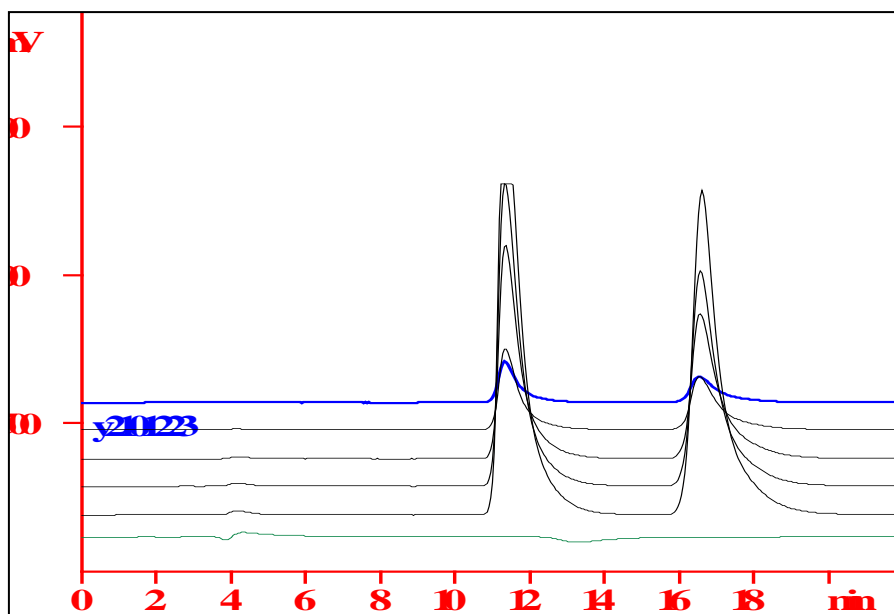
During the analysis of any unknown sample, the response of the analytes in the unknown samples (NO_x) was compared with the calibration curves in Figures 5.20 and 5.21 and the concentrations of nitrite and nitrate ions generated by the unknown samples of NO_x gas in the NaOH scrubber were determined. Typical Ion-Chromatogram of nitrite and nitrate ions (10 ppm) is shown in Fig. 5.22.

Fig. 5.22. Typical Ion –Chromatogram of nitrite and nitrate ions (10 ppm)



The overlay of the two chromatogram peaks at various concentrations against the base line is given in Fig. 5.23.

Fig. 5.23. Overlay view of the chromatogram peaks of nitrite and nitrate ions from 10 -100 ppm against the base line



5.7.7 Results and conclusion on NO_x gas compositions measurements

Nitrogen oxide gases were generated using standard reaction and an IC based analytical method was developed for the estimation of the composition of the gases. The method is amenable to be adopted for radiochemical plant applications. The composition of the NO_x gases generated during the dissolution experiments of all fuel materials as a part of this thesis work was estimated based on this method only.

5.8 Mechanism of UO_2 dissolution relevant to PUREX process

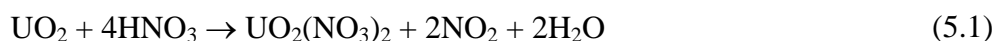
5.8.1 Introduction

The mechanism and kinetics of the dissolution of the nuclear fuel under consideration is the most important and foremost input data required for the design of a continuous dissolution system in a spent fuel reprocessing plant. Hence it is desirable to determine these data for a typical FBR fuel under PUREX process conditions. As UO_2 is the major component of a typical FBR fuel (20-30 wt % PuO_2 and the rest UO_2), it was felt prudent to first systematically evaluate the dissolution kinetics of UO_2 fuel under typical PUREX

process conditions and then gradually fine tune the experimental methodology for determining the dissolution kinetics of plutonium rich MOX fuel in nitric acid. This section of the thesis explains how the mechanism of dissolution of unirradiated sintered UO₂ fuel pellets under typical PUREX conditions has been unraveled from the knowledge of the concentration profiles of nitric and nitrous acids and NO_x gases that are determined during the course of its dissolution in nitric acid under various process conditions⁵⁶.

5.8.2 Consolidation of experimental observations

The stoichiometric dissolution reactions of UO₂ in nitric acid could be represented by equations 5.1, 5.2 and 5.3 mentioned in section 5.4.1. These equations are reproduced here for ease of reference.



Reaction 5.1 occurs predominantly when the acid concentration is above 8 M and the rest of the two reactions take place predominantly below 8 M acidity. The ratio of the amount of nitric acid consumed to the amount of uranium dissolved during the course of UO₂ dissolution experiments under typical Purex process conditions (8 M nitric acid and 353 K), as a function of stirring speed is given in Fig. 5.24.

Analysis of Fig. 5.24 shows that the ratio of [H⁺] reacted to [U(VI)] dissolved is always between 2.7 to 3 all through the dissolution process. This indicates that it is the reactions given in equations 5.2 and 5.3 which are taking place predominantly. The experimental data was plotted and the reaction mechanism was proposed by analyzing the plots of formation of UO₂(NO₃)₂, NO, NO₂, HNO₂ and depletion of HNO₃ with respect to time. These concentration profiles for the UO₂ pellet dissolution carried out at 600 RPM in 8 M nitric acid are given in Fig. 5.25.

For the ease of understanding, the profile of half of uranium ([U(VI)]/2) in the reaction mixture is also plotted along the profiles of NO_x gases in Fig. 5.25 and 5.26. Fig. 5.24 indicates that the formation of NO is almost 0.5 to 0.6 times the formation of uranium product. This further confirms that reaction 2 and 3 might be possible.

Fig. 5.24. Ratio of HNO₃ consumed to uranium dissolved

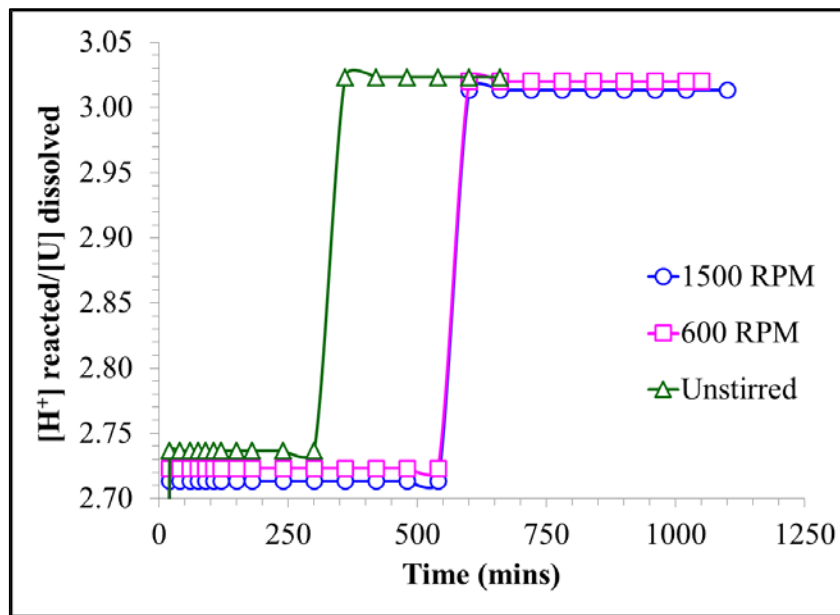
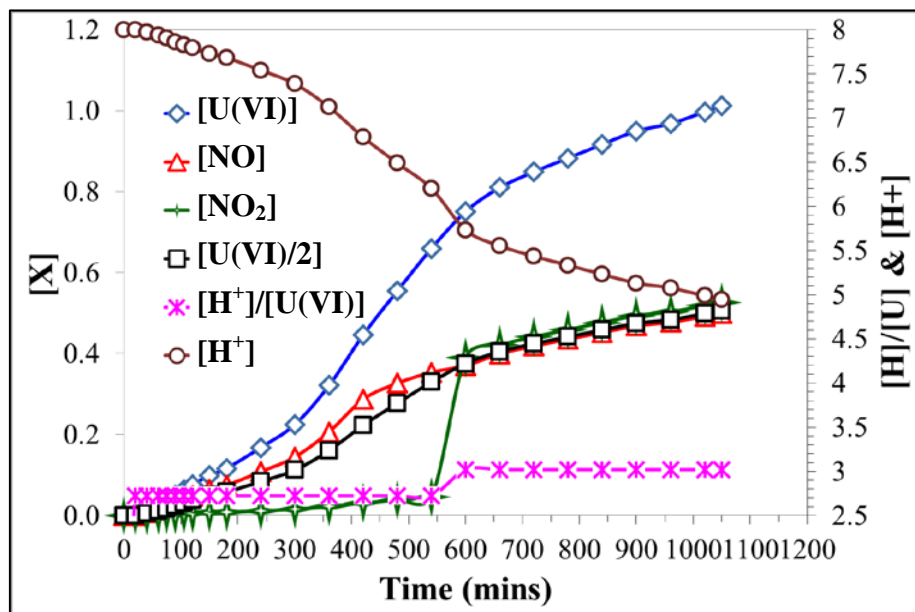
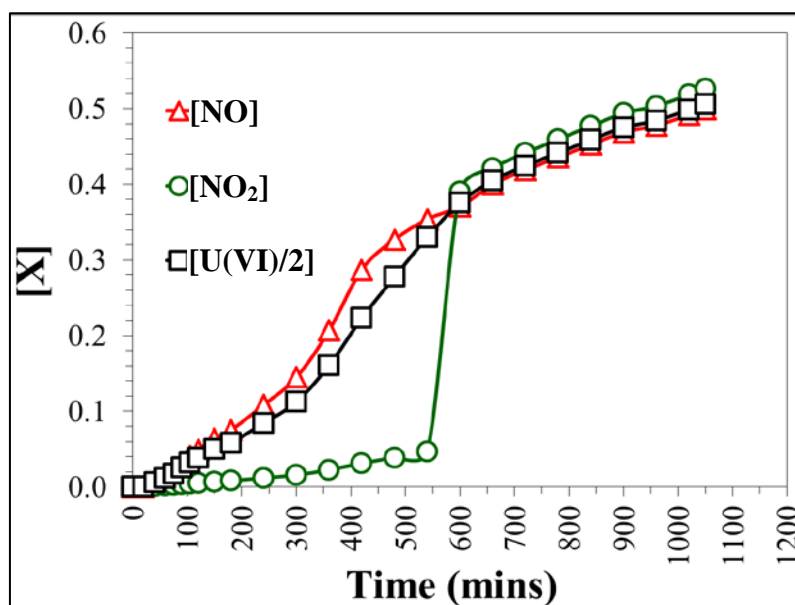


Fig. 5.25. Profiles of [U(VI)], [NO], [NO₂], [HNO₃] and ([H⁺] consumed / [U(VI)] dissolved) ratio during UO₂ dissolution



Unlike NO, NO₂ concentration is very low initially. At around 550 mins, it becomes equal to NO concentration which is almost half of the concentration of uranium ([U(VI)]/2). This shows that dissolution proceeds according to reaction 3 after 600 mins. From Fig. 5.15, it could be seen that the formation rate of nitrous acid is rapid initially, then reaches a maximum and finally decreases gradually at a rate depending on the intensity of mixing.

Fig. 5.26. Profiles of [NO], [NO₂] and [U(VI)/2] during dissolution



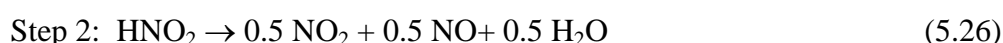
At higher stirring intensity, the rate of decrease after the maximum value is steady and very slow. But as the agitation rate is reduced, this decrease in the concentration of nitrous acid is very abrupt indicating that the consumption of nitrous acid is faster at lower mixing rates. Also the amount of nitrous acid formed towards the later part of the reaction is high, which could not be explained by reaction 5.2. Hence it could be assumed that it is reaction 5.3 which takes place predominantly rather than reaction 5.2 during this period.

5.8.3 Proposed mechanism for UO₂ dissolution in nitric acid under PUREX conditions

The mechanism of the dissolution of UO₂ could be explained by dividing the dissolution process into three different time zones as given in Fig. 5.27.

5.8.3.1. Time zone 1: (0 to 300 min)

The dissolution of UO₂ is initiated in this time zone and the reaction takes place according to the equation 5.3 in two steps as given below⁵⁷.



Hence, whatever nitrous acid that is formed initially during the dissolution reaction, immediately diffuses into the bulk, and attains a steady state concentration depending on

the mixing rate.

Fig. 5.27. Various time zones during the dissolution of UO_2 in nitric acid

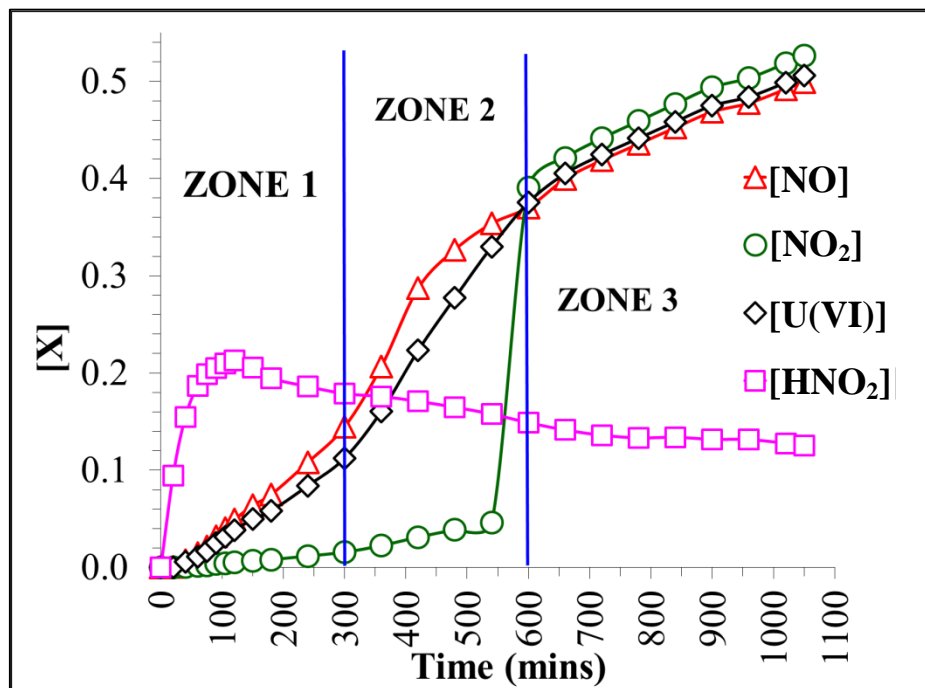
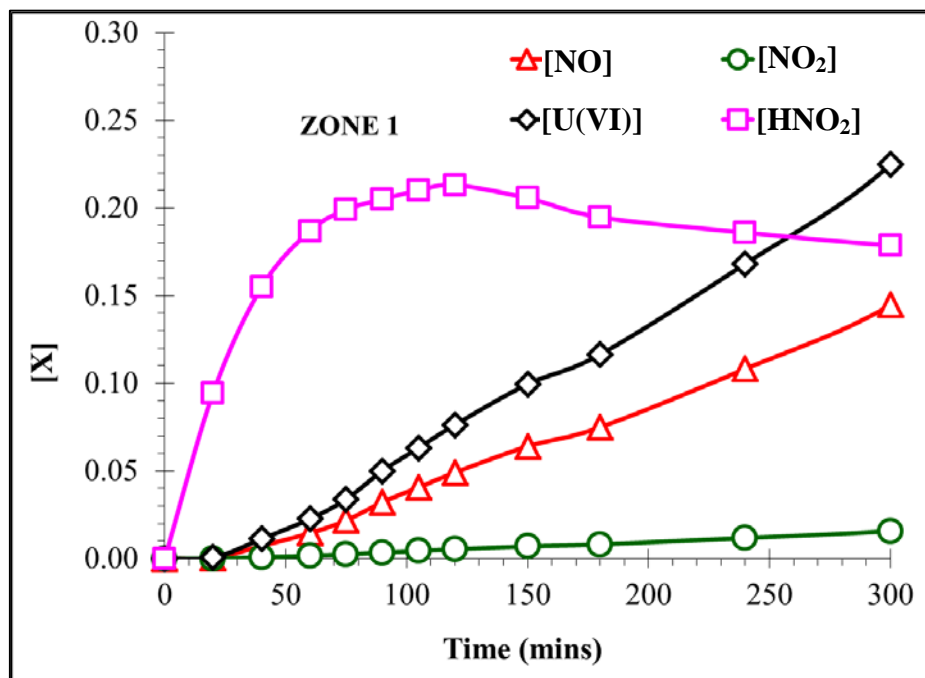


Fig. 5.28. Concentration profiles of NO, NO₂, HNO₂ and uranium in time zone 1



Subsequently it dissociates into NO and NO₂. NO being less soluble in water escapes out⁵⁸ and hence its concentration is higher in the off-gas stream as indicated in the plot.

NO₂ reacts with water to form HNO₂ and HNO₃ as per equation 5.27. Thus NO₂ profile in the off-gas stream is pretty low in this time zone.



For better clarity, the expanded view of the concentration profiles of all the species involved in the reaction during the time zone 1 is given in Fig. 5.28.

5.8.3.2. *Time zone 2: (300-600 min)*

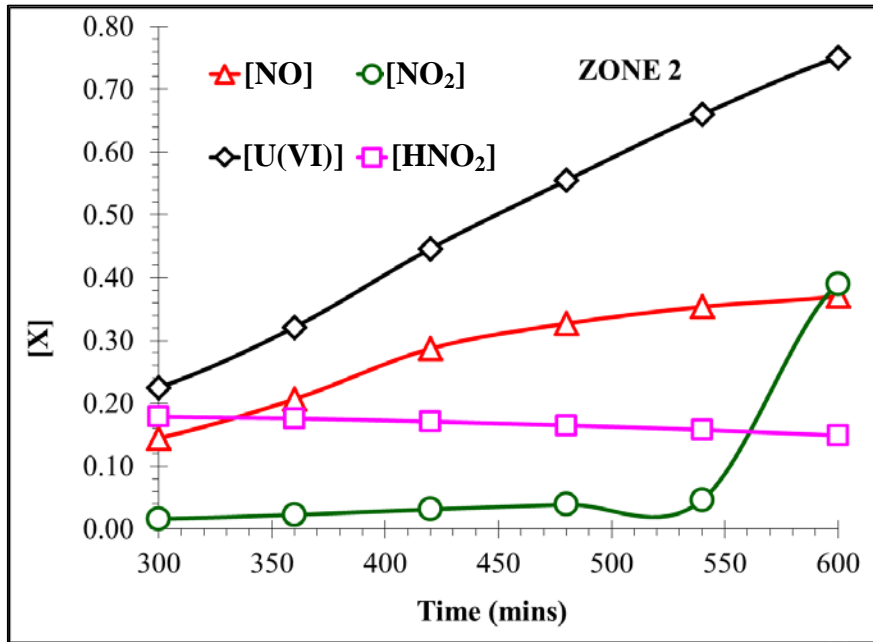
In this time zone, the concentration of nitrous acid reaches an equilibrium value as it is almost constant. Thus, the nitrous acid produced instantaneously dissociates into NO and NO₂. Due to the dissolution of UO₂ from the external layer of the pellet/s, new surface gets generated. Some amount of nitrous acid gets adsorbed on this newly generated surface of UO₂ and this further catalyzes the dissolution of UO₂. This leads to an increase in the rate of reaction as indicated by an increase and decrease in the slopes of [U(VI)] and [HNO₂] plots respectively. In the case of experiments with lower mixing rate, since nitrous acid dispersion to the bulk of the liquid is relatively slow, it spends more time at the vicinity of the pellet surface. Hence its consumption is more towards dissolution. This could be inferred from the higher slope of uranium concentration profile and the decrease in the slope of the NO line. Also there is a faster decrease in the concentration of nitrous acid in the time zone 2 of Fig. 5.27 as the mixing intensity is decreased. This further reinstates the fact that at lower mixing rate, the consumption of nitrous acid towards the dissolution is predominant rather than towards its self-decomposition. For better clarity, the expanded view of the concentration profiles of all the species involved in the reaction during this time zone is given in Fig. 5.29.

5.8.3.1. *Time zone 3: (above 600 mins)*

The autocatalytic effect of nitrous acid in time zone 2 had resulted in the dissolution of more UO₂. Hence the pellet surface area available for the reaction had sufficiently decreased by the time the reaction reaches the time zone 3. Therefore the catalytic effect of nitrous acid also decreases. At the same time the reaction of NO₂ with water (reaction 5.27) had reached equilibrium and hence its concentration profile follows the same trend as that of NO. For better clarity, the expanded view of the concentration profiles of all the

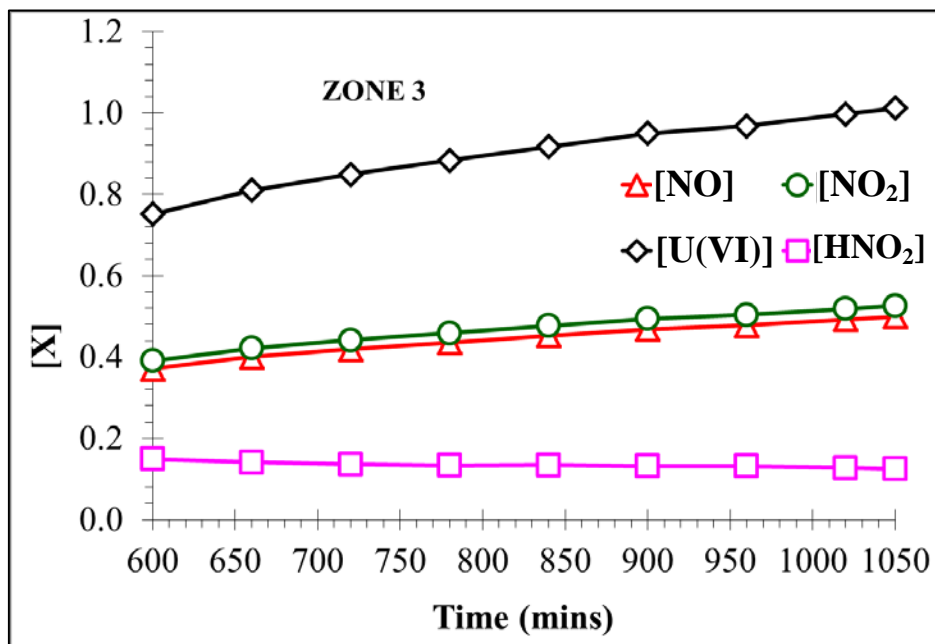
species involved in the reaction during this time zone is given in Fig. 5.30.

Fig. 5.29. Concentration profiles of NO, NO₂, HNO₂ and uranium in time zone 2



To sum up, it could be concluded that the dissolution of UO₂ under typical PUREX process conditions proceeds predominantly by equation 5.3 which takes place in two steps as depicted in equations 5.25 and 5.26.

Fig. 5.30. Concentration profiles of NO, NO₂, HNO₂ and uranium in time zone 3



In the first reaction, nitrous acid is produced directly by the dissolution of UO_2 . Due to its high reactivity in aqueous solution, nitrous acid self decomposes to NO and NO_2 . Subsequently the NO_2 produced, reacts with water as per equation 5.27 and forms nitrous and nitric acids. Hence the overall stoichiometric reaction is the algebraic sum of these three equations (5.25 to 5.27) which is given as equation 5.28.



This overall stoichiometric consumption of nitric acid is what is observed in all our dissolution runs irrespective of the stirring speed which indicates that this mechanism holds good under all conditions of a typical PUREX process^{51,55}.

5.8.4 Conclusion on the proposal of UO_2 dissolution mechanism

The mechanism of UO_2 dissolution was established by analyzing the data obtained from the experiment. It was seen that UO_2 initially reacts with nitric acid to form nitrous acid which quickly diffuses into the bulk of the reaction mixture and then dissociates to form NO_x . NO_2 formed from the dissociation reaction, reacts with water to form nitrous acid again which settles down on the surface of the reactant particle and catalyzes the dissolution reaction further, before attaining equilibrium. The catalytic effect reduces as the concentration of the reactant and surface area decrease until all of UO_2 is reacted.

5.9 Effect of surface area

5.9.1. Basis for studying the surface area effect on dissolution kinetics

The dissolution of nuclear fuel in nitric acid is a solid-liquid heterogeneous reaction, for which, the surface area of the solid is an important parameter that would influence the reaction kinetics. Since the nuclear fuel dissolution is a surface phenomenon, the surface area should be directly proportional to the reaction rate. Hence qualitatively it is well established that more the availability of the solid surface area at any given time, faster would be the dissolution reaction rate. In order to quantify this, experiments were conducted to evaluate the effect of surface area on the rate of UO_2 dissolution reaction rate in nitric acid.

5.9.2. *Experimental procedure*

The initial concentration of nitric acid and temperature were fixed at 8 M and 353 K, as justified in sections 5.2 and 5.5.3 respectively for all the experiments to be carried out to evaluate the surface area effect on the reaction rate. The mixing rate was maintained constantly at 600 RPM as mentioned in section 5.5.3. Three experiments were conducted wherein the pellet was dissolved as such in the 1st experiment. In the 2nd and 3rd experiments, the pellet was cut into two and three parts respectively. A diamond wheel cutter was employed to cut the pellets along the curved surface area such that the resulting pieces are 2 or 3 small discs of same height as the case may be. In the case of the pellet being cut into two pieces, the height of each piece was about 7.6 ± 0.2 mm. In the case of three pieces they were about 4.9 ± 0.2 mm. The diameter of the original pellet remained the same as it was not altered.

The initial surface area of all UO_2 pellets as well as the cut pieces were measured by nitrogen adsorption technique based on BET method⁵⁹. The cylindrical glass dissolver shown in Figures 10 and 11 was employed. In each of the experiment, the mass of the starting UO_2 pellet or all the pieces put together, as the case may be, was almost maintained constant. Same volume of 8 M nitric acid was taken at the beginning of each of the dissolution experiment.

5.9.3. *Surface area measurements during the course of dissolution of UO_2 in HNO_3*

During the course of all the dissolution experiments, samples were taken from the reaction mixture at regular intervals of time for the analysis of uranium and acidity. During the sampling time, the heating of the reaction mixture was stopped. All the nitric acid from the reaction vessel was drained carefully and slowly without disturbing the UO_2 pellets/pieces so that their dimensions does not get altered significantly. Then these pellets/pieces were washed carefully with distilled water thoroughly to remove all the residual nitric acid sticking to their surface and also that trapped inside the open pores of the pieces. Finally they are washed with acetone to remove the traces of water in them. Later they were placed on a clean dry wash glass and dried in an oven at around 333-343 K for about 1 hour. After cooling, the surface area of the samples was measured by BET method. In the BET method, a known composition of N_2 -He gaseous mixture is allowed to pass through the pellet in a close path during which some amount of He gets adsorbed

on to the surface of the pellet and in the open pores. The conductivity of the gaseous mixture is measured before and after passing through the solid sample which will be different due to the preferential adsorption of He. This difference is then correlated to the total surface area of the pellet including the open pores.

Once the surface area and dimensions of the pellet/pieces were measured, the nitric acid mother dissolver solution from which the dissolving pellet/pieces were removed was restored back to the glass dissolution set. All the connections to the glass dissolution set-up were given again and services like chilled water for the off-gas condenser were restored. The original nitric acid (containing the partially dissolved uranium in it) is heated back to the original set temperature (353 K in this case). When the set temperature was reached, the pellet/pieces whose surface area was measured, was replaced back into the hot nitric acid and the timer was continued. This exercise was repeated at every sampling point and the surface area profile of the dissolving solid as a function of time was generated.

5.9.4. Principle of surface area measurements

Brunauer–Emmett–Teller (BET) theory aims to explain the physical adsorption of gas molecules on a solid surface and serves as the basis for an important analysis technique for the measurement of the specific surface area of materials. The BET theory applies to systems of multi-layer adsorption, and usually utilizes probing gases that do not chemically react with material surfaces as adsorbates to quantify specific surface area. Nitrogen is the most commonly employed gaseous adsorbate used for surface probing by BET methods. For this reason, standard BET analysis is most often conducted at the boiling temperature of N₂ (77 K).

The concept of BET theory is an extension of the Langmuir theory of monolayer molecular adsorption to multilayer adsorption with the following hypotheses: (a) gas molecules physically adsorb on a solid in layers infinitely; (b) there is no interaction between each adsorption layer; and (c) the Langmuir theory could be applied to each layer. The resulting BET equation is expressed by equation (5.29):

$$\frac{1}{v[(P_0/P) - 1]} = \frac{c - 1}{v_m c} \left(\frac{P}{P_0} \right) + \frac{1}{v_m c} \quad (5.29)$$

P and P_0 are the equilibrium and the saturation pressure of adsorbates at the temperature of adsorption, v is the adsorbed gas quantity (for example, in volume units), and v_m is the monolayer adsorbed gas quantity. 'c' is the BET constant, which is expressed by equation (5.30):

$$c = \exp\left(\frac{E_1 - E_L}{RT}\right) \quad (5.30)$$

where E_1 is the heat of adsorption for the first layer, and E_L is that for the second and higher layers and is equal to the heat of liquefaction.

Equation (5.29) is the adsorption isotherm and could be plotted as a straight line with $1/v[(P_0/P)-1]$ on the y-axis and P/P_0 on the x-axis from the experimental results. This plot is called a BET plot. The linear relationship of this equation is maintained only in the range of $0.05 < P/P_0 < 0.35$. The value of the slope (A) and the y- intercept of the line (I) are used to calculate the monolayer adsorbed gas quantity v_m and the BET constant c using equations 5.31 and 5.32.

$$v_m = 1 / (A+I) \quad (5.31)$$

$$C = 1+ (A/I) \quad (5.32)$$

The BET method is widely used in surface science for the calculation of surface areas of solids by physical adsorption of gas molecules. A total surface area S_{total} and a specific surface area S_{BET} are evaluated by the following equations.

$$S_{total} = (v_m \cdot N \cdot s) / V \quad (5.33)$$

$$S_{BET} = S_{total} / a \quad (5.34)$$

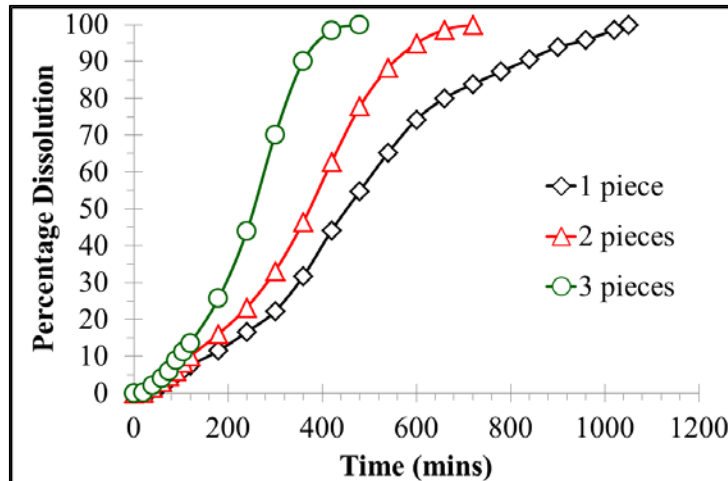
Here N is the Avogadro's number, s is the adsorption cross section of the adsorbing species, V is the molar volume of adsorbent gas and 'a' is the mass of adsorbent (in g).

5.9.5. Results and discussion for the surface area measurements

The dissolution profile for the three experiments with one, two and three pieces of the UO_2

pellet/s in nitric acid in terms of percentage dissolved is given in Fig. 5.31. It should be noted that the mass of initial UO_2 is almost the same in each of these experiments.

Fig. 5.31. Dissolution of UO_2 in nitric acid as a function of initial surface area



The results are along the line of expectation that more the surface area of the initial mass of UO_2 , higher would be the rate of dissolution reaction. Again, irrespective of the starting surface area, all the dissolution curves are “S” shaped as reported earlier in section 5.5.3. This further confirms the autocatalytic role of nitrous acid.

The plots of surface area of the pellet/pieces put together in each of these three cases as a function of time during the course of the dissolution reaction were measured and are given in Fig. 5.32.

Fig. 5.32. Surface area profile for UO_2 dissolution in nitric acid as a function of initial surface area

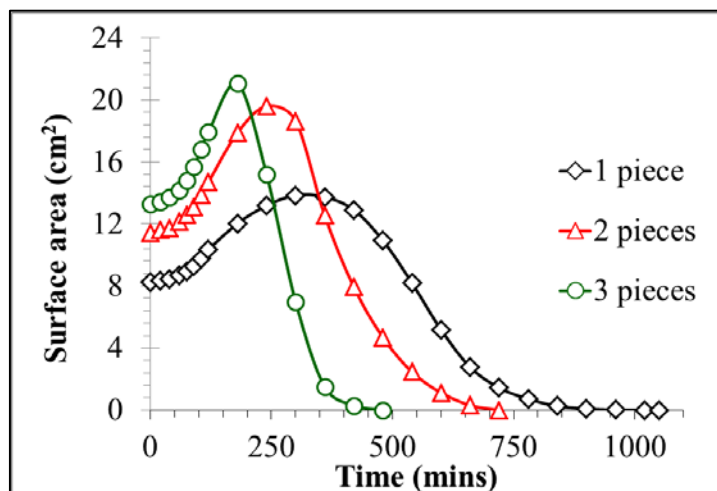
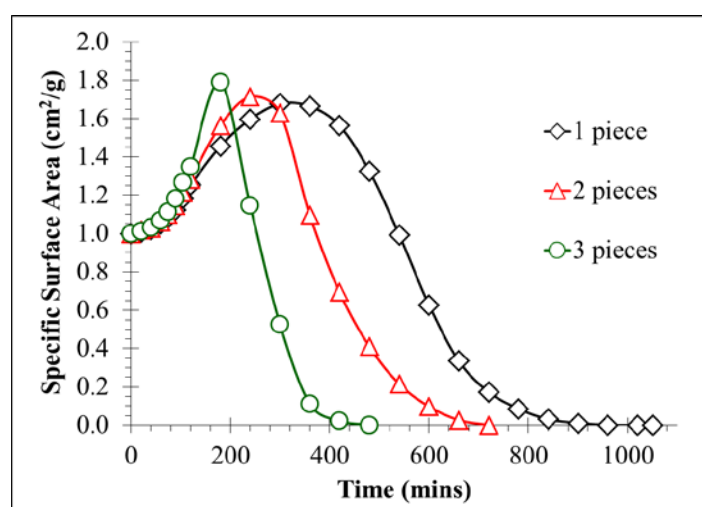


Fig. 5.32 indicates that the surface area profile follows the same trend in all the cases. That is, it starts from a specific value, reaches a maximum and falls down to zero when the dissolution is completed. As the pellet starts dissolving, its surface gradually roughens becomes more porous leading to the increase in the total surface area. As the pellet continues to dissolve, the surface area gradually reaches a maximum when the roughness of the pellet is at its highest.

Subsequently, due to further dissolution, the pellet dissolves and the surface area gradually reduces to zero at the completion of the reaction. It also shows that as the pellet is cut into more number of pieces; the peak of the curve also increases. This is understandable since the initial surface area also increases with increase in the number of pieces for almost the same starting mass of UO_2 . But what is more interesting is that, the slope of the rise and fall of this curve is steeper with increase in the initial surface area. This indicates that the reaction happens rapidly as the initial surface area is increased.

A similar trend is seen in the slope of the percentage dissolution curve in Fig. 5.31. Thus, as the initial surface area is higher for same initial mass, the dissolution rate is also higher. The information in Fig. 5.32 is normalized in terms of specific surface area and is plotted in Fig. 5.33 which clearly indicates the positive influence of the initial surface area on the dissolution rate.

Fig. 5.33. Variation of specific surface area for UO_2 dissolution in nitric acid as a function of initial surface area



All the data presented in this thesis were used for modeling the reaction to arrive at a generalized rate expression for the dissolution of UO_2 pellets in nitric acid.

5.10 Modeling of UO_2 dissolution reaction

5.10.1. Introduction to solid-liquid reactions

Solid-liquid reactions are commonly encountered in industries as well as in everyday life. In industry, very large volumes of products are synthesized via solid-liquid reaction routes. The starting point in designing an industrial process should be a detailed understanding of the thermodynamics and kinetics of the chemical reactions involved in the process. The detailed understanding of the reaction kinetics and thermodynamics is also crucial for optimizing the already existing plant processes. Thermodynamics limits the extent of any chemical reaction, by setting the boundaries of chemical equilibria. The major factors governing the rates of chemical reactions are the concentrations or activities of the reactants, temperature, pressure and mass and heat transfer properties.

5.10.2. Basis of modeling

The knowledge of the kinetics is crucial for the design and development of the industrial processes. Quantitative modeling of the behaviour of reactive solids in liquids is a big challenge⁶⁰. The reaction mechanism could be a very complex one, often comprising several unknown elementary steps. The structure and structural changes of the solid material are also often difficult to determine. Kinetics and mass transfer effects are always coupled. Hence to determine the intrinsic kinetics, the experiments should be free from mass transfer limitations. External mass transfer resistance could be suppressed by creating sufficient turbulent effects around the solid particles, but internal mass transfer effects could be present for porous particles. A common methodology in investigating the kinetics of a chemical reaction is to carry out experiments in a batch reactor and follow the product and/or reactant concentrations as a function of time. The influence of external mass transfer could be experimentally determined by performing experiments at sufficiently high stirring rate such that further increase in stirring speed has no influence on the reaction rate⁶¹. Internal mass transfer is relevant only for porous solids and this could be experimentally investigated, for example, by performing experiments with different particle sizes. In the present case, no investigation on the internal mass transfer

could be carried out since the particle size of the dissolving UO_2 pellets is a function of its extent of damage by irradiation. Hence, one needs to generate data on the nature and characteristics of the surface and particles of UO_2 pellets as a function of different burnups. As this involves more sophisticated and dedicated analytical facilities, it is not carried out as a part of the thesis. Studies on the changes in the surface morphology and particle size of the spent nuclear fuel are itself a separate topic and needs detailed investigation. After evaluating mass transfer effects, systematic kinetic experiments were performed at different temperatures and other relevant conditions to determine their influence on the rate.

In the present study, dissolution of sintered UO_2 pellet in nitric acid is the solid-liquid reaction under consideration. The dissolution experiments are conducted at different stirring speeds to study the effect of mass transfer on dissolution rate. As reported already, the time taken for the complete dissolution of the given mass of UO_2 pellets in nitric acid under similar conditions, increases with stirring speed until 600 rpm and thereafter the rate of dissolution is not much influenced by stirring speed on. That is the rate of dissolution is inversely related to the stirring speed till 600 RPM and almost remains constant with further increase in stirring rate. Thus the influence of external mass transfer is at its barest minimum at and beyond 600 RPM. Hence to study the intrinsic kinetics, the experiments were conducted at different conditions of acidity and temperature at a stirring speed of 600 rpm. Hence, in these experiments, the external mass and heat transfer could be neglected since the mixing was efficient and the reaction rate also being sufficiently slow.

As reported in the previous section, experiments were conducted by taking 4 pellets together with almost similar cumulative average weight and diameter. The dissolution was conducted with 8 M HNO_3 at 343, 348, 353, 358, 363, 368 and 373 K. Concentration of HNO_3 , uranium and total surface area of pellets were measured at different intervals of time. The objective of the current work is to explore different approaches for modeling solid-liquid reaction, (dissolution of solid in liquid).

5.10.3. Methodologies of modeling

For modeling the dissolution reactions of UO_2 pellets in nitric acid, three different approaches were undertaken as explained in the following sections.

5.10.3.1 Method 1 – Based on surface penetration phenomenon

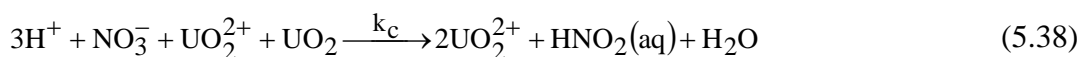
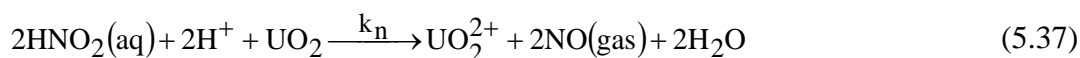
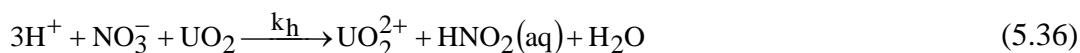
In a similar fashion to investigating the homogeneous reactions, studying of solid-liquid reaction kinetics could be performed in batch reactors. The progress of the reaction is often measured by observing the change in the weight of the solid phase, or by measuring the product concentrations in the liquid phase.

In this method, dissolution model is expressed by a two-step scheme as given below⁶².



Where W_{ue} is the unexposed mass of fuel, W_e is the exposed mass and W_d the dissolved mass. The first process in the above equation is the penetration process and its rate may be proportional to the concentration of nitric acid in the solution. The second process is considered as the chemical reaction.

The reactions between UO_2 and ions in the nitric acid solution under these experimental conditions were assumed as follows^{36, 37}.



The stoichiometric equation (5.36) denotes the dissolution of due to the effect of nitric acid whose rate constant is denoted as k_h ($[L/mol]^2/min$) where the subscript 'h' stands for HNO_3 . The process in equation (5.37) designates the dissolution of UO_2 pellets aided by nitrous acid which plays an autocatalytic role in the dissolution reaction as established earlier in this thesis. The rate constant of this process is denoted by k_n where the subscript 'n' stands for nitrous acid. The equation (5.38) denotes the chemical reaction process of the dissolution of UO_2 pellets. Hence the rate constant of this step is denoted by k_c ($[L/mol]^3/min$) with the subscript 'c' denoting the catalytic effect of chemical reaction controlled step. Uranyl ion (UO_2^{2+}) is included in the stoichiometric equation here as it was reported that presence of any uranyl ion in the reaction system prior to the dissolution of UO_2 pellets has an accelerating effect on the dissolution process⁶³. Though this observation was never found in any of the experiment carried out as a part of this thesis work, it has been included to make the modeling complete in all sense. This could be

because, the maximum concentrations of UO_2^{2+} ions encountered in the present study (about 240 g/L) is much less than the solubility limit of the ions in 4-11 M nitric acid (typically greater than 500 g/L). But it could be certainly said that the UO_2^{2+} ions present in the solution indirectly catalyzed the reaction. This is because; it is the UO_2 in solid ($\text{U}^{4+}_{\text{solid}}$) which first comes to the aqueous as U^{4+} in liquid ($\text{U}^{4+}_{\text{liq}}$). This $\text{U}^{4+}_{\text{liq}}$ is then oxidized to UO_2^{2+} by the nitrous acid present in the liquid. This oxidation disturbs the $\text{U}^{4+}_{\text{solid}} \rightleftharpoons \text{U}^{4+}_{\text{liq}}$ equilibrium. To negate this disturbance and restore the equilibrium, more $\text{U}^{4+}_{\text{solid}}$ would dissolve to form $\text{U}^{4+}_{\text{liq}}$ thereby enhancing the dissolution.

During the derivation of the dissolution rate equation based on both the penetration process and the above reaction schemes, the steady state approximation was applied to the nitrous acid concentration⁶⁴. Consequently, nitrous acid concentration and rate constant k_n were eliminated in the rate equations. The derivation is given in the appendix of the thesis for further details.

Following the derivation (refer appendix for derivation), the rate equations obtained are as follows

$$\frac{dW_{ue}}{dt} = -k_p [\text{HNO}_3] W_{ue} \quad (5.39)$$

$$\frac{dW_e}{dt} = k_p [\text{HNO}_3] W_{ue} - 1.5 \left(k_h [\text{HNO}_3]^2 + k_c [\text{HNO}_3]^2 [\text{UO}_2^{2+}] \right) W_e \quad (5.40)$$

$$\frac{d[\text{UO}_2^{2+}]}{dt} = 1.5 \left(M_{\text{UO}_2} V^{-1} \right) \left(k_h [\text{HNO}_3] + k_c [\text{HNO}_3] [\text{UO}_2^{2+}] \right) W_e \quad (5.41)$$

$$\frac{d[\text{HNO}_3]}{dt} = -4 \left(M_{\text{UO}_2} V^{-1} \right) \left(k_h [\text{HNO}_3] + k_c [\text{HNO}_3] [\text{UO}_2^{2+}] \right) W_e \quad (5.42)$$

Where k_p ([L/mol]/min) is the rate constant of penetration process, M_{UO_2} the molecular weight of UO_2 and V the volume of reacting solution.

5.10.3.1.1 Case-I: Considering the effect of nitrous acid

The experimental data of concentrations of nitric acid and uranium as a function of time explained in section 5.6 of this thesis were fitted into the above rate equations using a nonlinear regression technique to obtain rate constant that best correlates the experimental

data. The best values were obtained by minimizing the following objective function

$$f = \sum_1^n 20 * (C_{U_{exp}} - C_{U_{calc}})^2 + \sum_1^n (C_{HNO_3_{exp}} - C_{HNO_3_{calc}})^2 \quad (5.43)$$

The model equations derived were applied to all the experimental conditions and the concentration profiles of uranium and nitric acid were predicted. The comparison between the experimental and the calculated concentration profiles of uranium and nitric acid (predicted using the model equations) in the reaction mixture during the course of the dissolution reaction as a function of time were plotted on a semi log plot and are shown in the Figures 5.34 to 5.40 for all the temperatures employed in the experiment. The profiles were generated by plotting the ratio of the concentration of the species under consideration at any given time over the concentration of the same species at the end of the dissolution reaction. Hence it was $[U(VI)]_t/[U(VI)]_f$ and $[HNO_3]_t/[HNO_3]_f$ for uranium and nitric acid respectively. Here the subscripts 't' and 'f' denotes the values at time t and the final value.

Fig. 5.34. Experimental and calculated profiles of [U] and [HNO₃] at 343 K

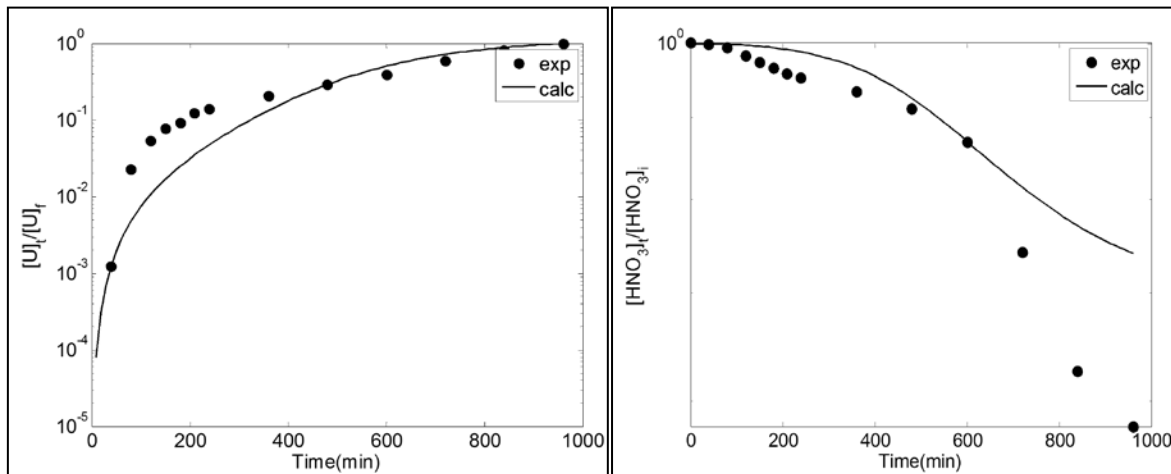


Fig. 5.35. Experimental and calculated profiles of [U] and [HNO₃] at 348 K

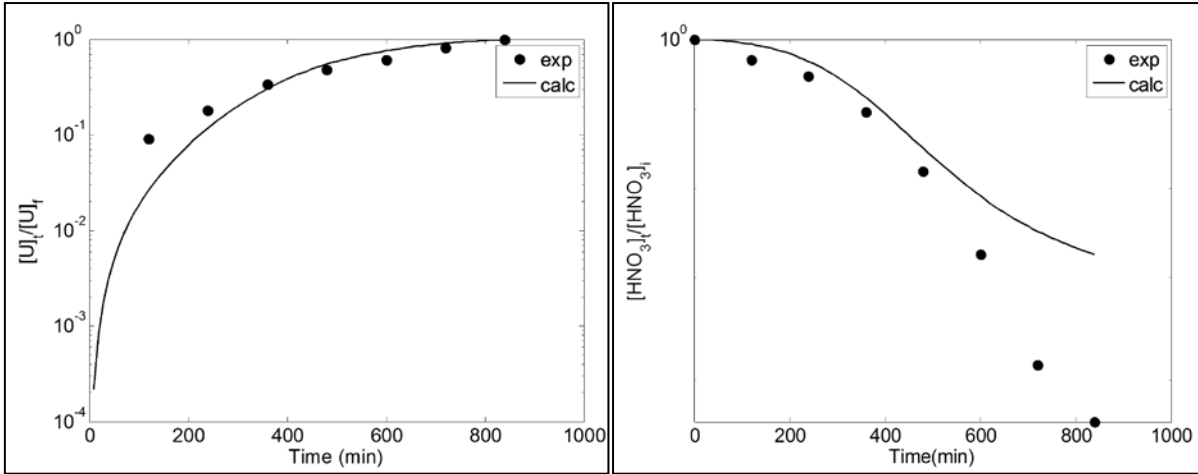


Fig. 5.36. Experimental and calculated profiles of [U] and [HNO₃] at 353K

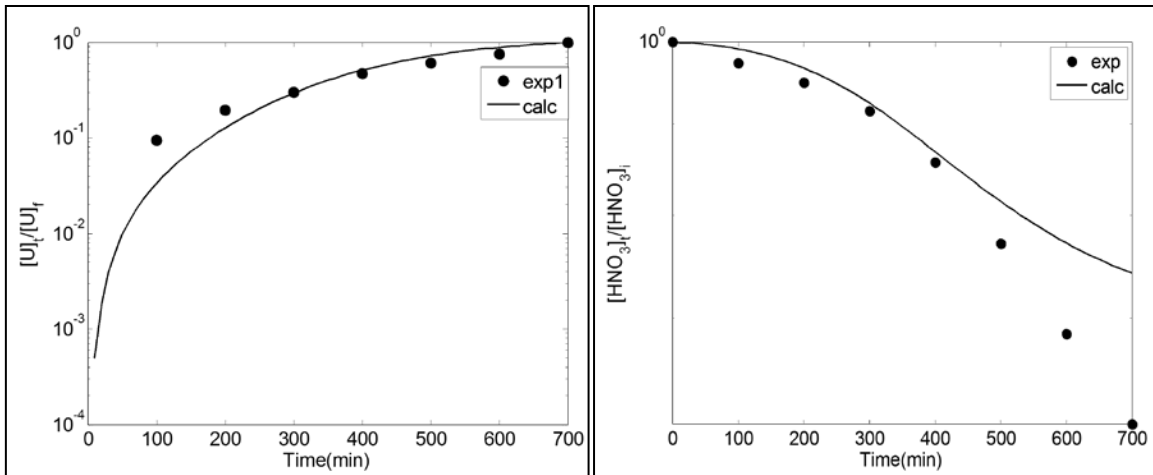


Fig. 5.37. Experimental and calculated profiles of [U] and [HNO₃] at 358 K

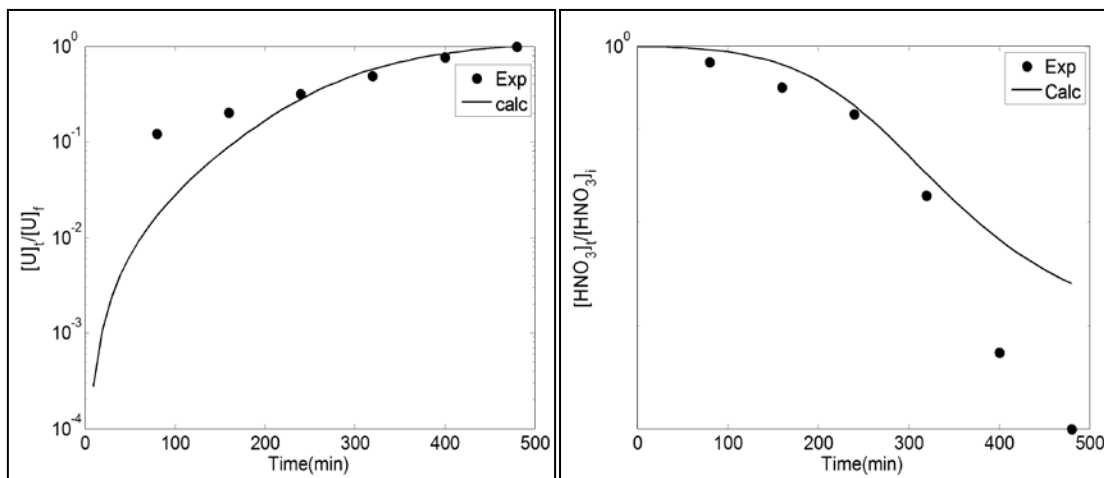


Fig. 5.38. Experimental and calculated profiles of [U] and [HNO₃] at 363 K

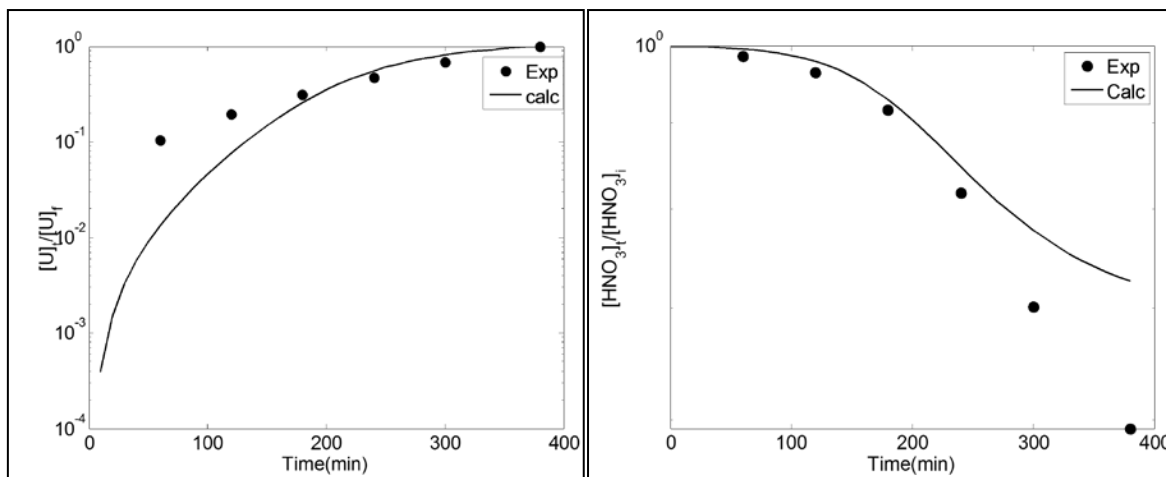


Fig. 5.39. Experimental and calculated profiles of [U] and [HNO₃] at 368 K

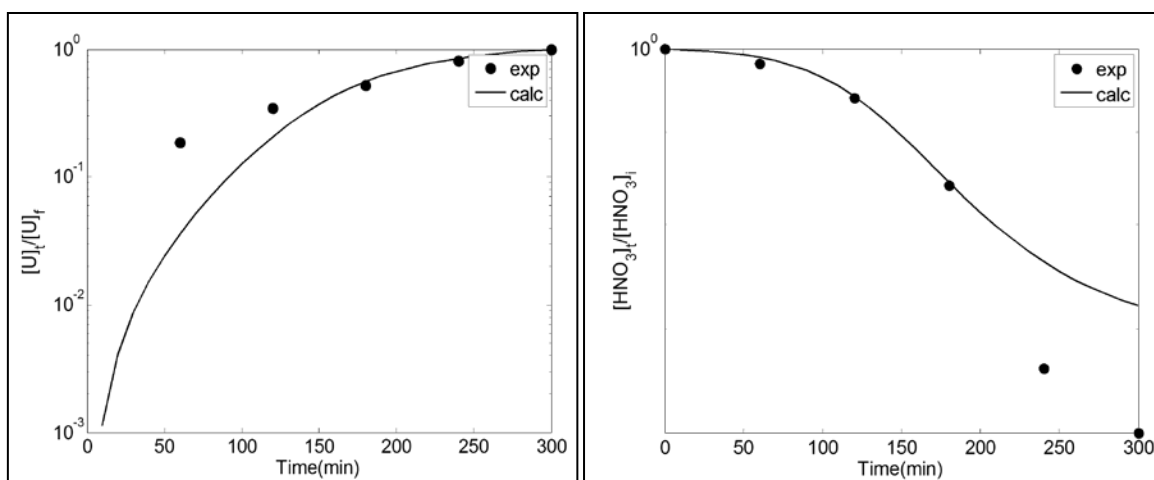
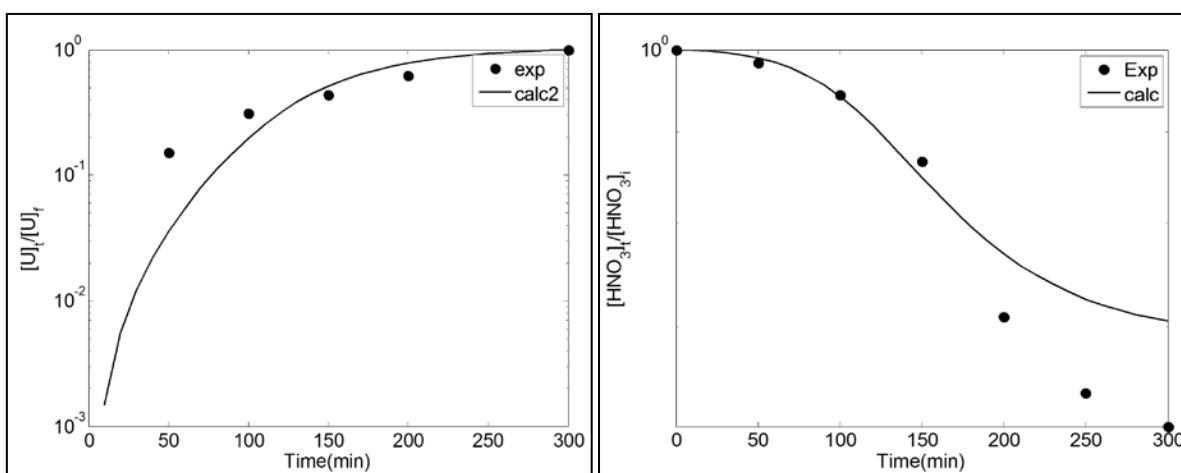


Fig. 5.40. Experimental and calculated profiles of [U] and [HNO₃] at 373 K



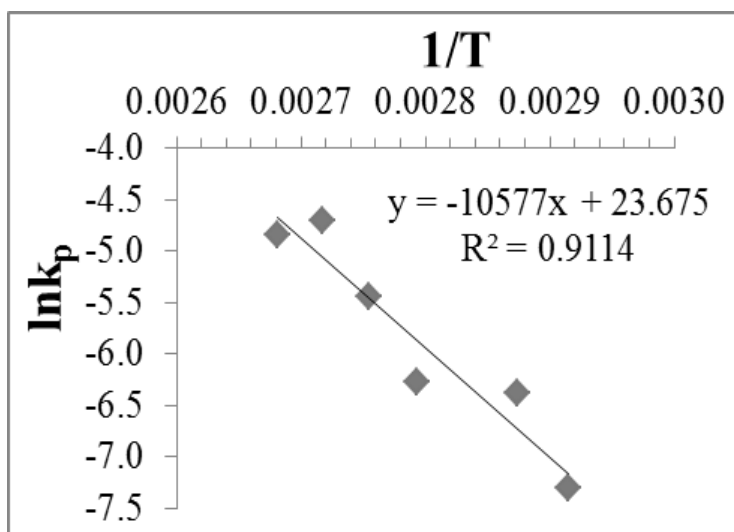
The rate constants k_p , k_h and k_c were calculated at different conditions of temperature and

are given in Table 5.2. Using the data given in Table 5.2, the activation energy for each of the processes namely penetration, nitric acid aided dissolution and the chemical reaction process were calculated using the Arrhenius plot. For this purpose, the values of $\ln(k)$ were least-square fitted against $1/T$ for the above three rate constants. The slope of the line corresponds to E_a/R , where E_a is the apparent activation energy of the process and R is the universal gas constant. The Arrhenius plots for the three rate constants are given in Figures 50 to 52.

Table 5.2. The values of k_p , k_h and k_c as a function of temperature

Temperature (K)	Rate constants for		
	Penetration process (k_p) ([L/mol]/min)	Nitric acid aided dissolution process (k_h) ([L/mol] ² /min)	Chemical reaction process (k_c) ([L/mol] ³ /min)
343	6.7071×10^{-04}	2.5630×10^{-06}	9.5021×10^{-05}
348	1.7000×10^{-03}	3.0067×10^{-06}	1.0302×10^{-04}
353	3.7000×10^{-03}	3.1279×10^{-06}	1.0348×10^{-04}
358	1.9000×10^{-03}	3.3594×10^{-06}	1.8781×10^{-04}
363	4.3000×10^{-03}	2.2978×10^{-06}	2.6859×10^{-04}
368	9.0000×10^{-03}	3.4506×10^{-06}	3.3064×10^{-04}
373	7.9000×10^{-03}	4.0543×10^{-06}	4.0980×10^{-04}

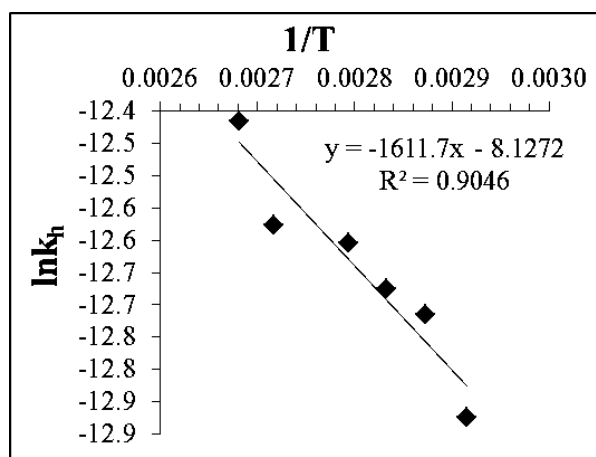
Fig. 5.41. Arrhenius plot for the penetration process



The apparent energy of activation for the penetration process from the above equation was

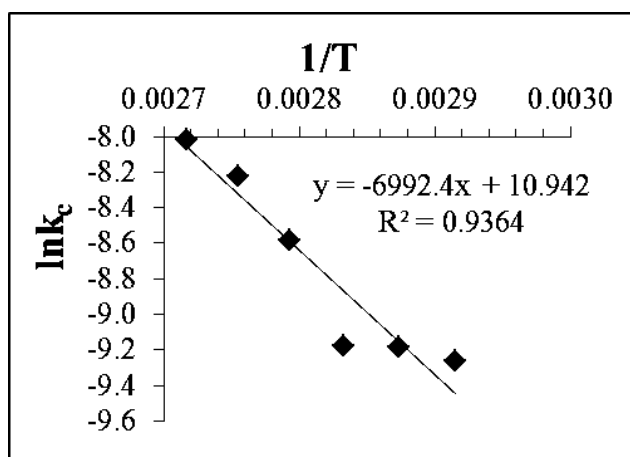
estimated to be about **88.2 kJ/mol**. The calculation of the activation energy in this entire thesis (wherever applicable) was done using the standard MS Excel 2010 software with the confidence levels set at 95% by default.

Fig. 5.42. Arrhenius plot for nitric acid aided dissolution process



The apparent activation energy for the nitric acid aided dissolution process was estimated to be about **13.4 kJ/mol**.

Fig. 5.43. Arrhenius plot for chemical reaction controlled dissolution process



The apparent activation energy for the chemical reaction controlled dissolution process was estimated to be about **58.1 kJ/mol**.

5.10.3.1.2 Case II: Neglecting the effect of HNO₂ due to the elimination of diffusion control

As justified earlier in the thesis, all the experiments for studying the effect of temperature on the dissolution of UO₂ pellets in nitric acid (section 5.6) was conducted at a stirring speed of 600 rpm. Hence the concentration of HNO₂ at the pellet liquid interface would be very less as seen in Fig. 5.15. Therefore the stoichiometric equation for the nitrous acid aided dissolution of UO₂ given in equation 5.37 is not considered in this figure. The reactions between UO₂ pellet and ions in the nitric acid solution considered for modeling under these conditions are only 5.36 and 5.37. The reaction 5.38 which is due to the effect of nitrous acid is omitted. The derivations for arriving at the rate equations are given in the appendix. The rate equations arrived at after derivation are given by

$$\frac{dW_{ue}}{dt} = -k_p [\text{HNO}_3] W_{ue} \quad (5.46)$$

$$\frac{dW_e}{dt} = k_p [\text{HNO}_3] W_{ue} - \left(k_h [\text{HNO}_3]^2 + k_c [\text{HNO}_3]^2 [\text{UO}_2^{2+}] \right) W_e \quad (5.47)$$

$$\frac{d[\text{UO}_2^{2+}]}{dt} = (M_{\text{UO}_2} V)^{-1} \left(k_h [\text{HNO}_3]^2 + k_c [\text{HNO}_3]^2 [\text{UO}_2^{2+}] \right) W_e \quad (5.48)$$

$$\frac{d[\text{HNO}_3]}{dt} = -3(M_{\text{UO}_2} V)^{-1} \left(k_h [\text{HNO}_3]^2 + k_c [\text{HNO}_3]^2 [\text{UO}_2^{2+}] \right) W_e \quad (5.49)$$

Where k_p is the rate constant for the penetration process, M_{UO_2} is the molecular weight of UO₂ and V is the volume of reacting solution.

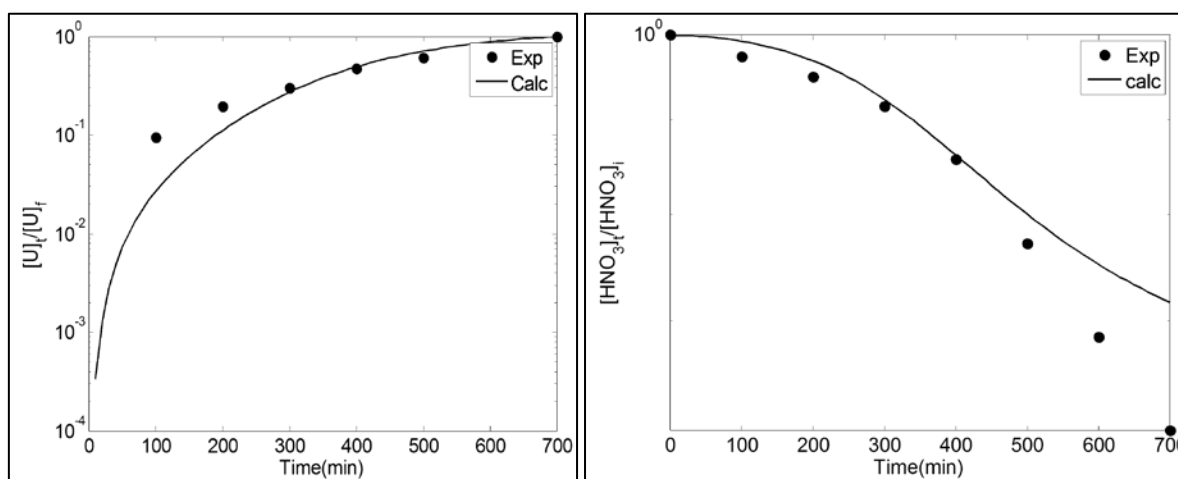
The experimental data of concentrations of nitric acid and uranium as a function of time were fitted into the above rate equations using a nonlinear regression technique to obtain rate constant that best correlates the experimental data. The best values were obtained by minimizing the following objective function.

$$f = \sum_1^n 20 * \left(C_{\text{Uexp}} - C_{\text{Ucalc}} \right)^2 + \sum_1^n \left(C_{\text{HNO}_3\text{exp}} - C_{\text{HNO}_3\text{calc}} \right)^2 \quad (5.50)$$

The model equations derived were applied to all the experimental conditions and the concentration profiles of uranium and nitric acid were predicted. The comparison between

the experimental and the calculated concentration profiles of uranium and nitric acid (predicted using the model equations) in the reaction mixture during the course of the dissolution reaction as a function of time were generated as a semi log plot for all temperatures. Fig. 5.44 shows this plot at 353K. The profiles were generated by plotting the ratio of the concentration of the species under consideration at any given time to the concentration of the same species at the end of the dissolution reaction.

Fig. 5.44. Experimental and calculated profiles of [U] and [HNO₃] at 353 K



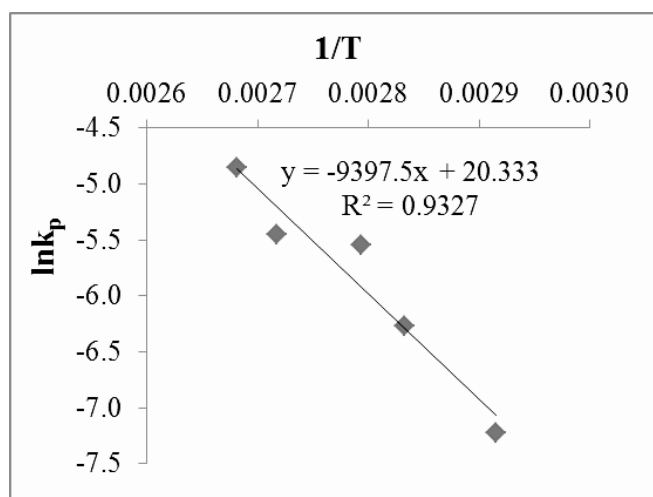
The rate constants k_p , k_h and k_c were calculated at different conditions of temperature and are given in Table 5.3.

Table 5.3. The values of the rate constants k_p , k_h and k_c as a function of temperature without nitrous acid effect

Temperature (K)	Rate constants for		
	k_p ([L/mol]/min)	k_h ([L/mol] ² /min)	k_c ([L/mol] ³ /min)
343	7.3335×10^{-04}	1.9402×10^{-06}	1.6836×10^{-04}
348	2.5000×10^{-03}	3.2862×10^{-06}	1.5757×10^{-04}
353	1.9000×10^{-03}	4.9532×10^{-06}	2.4199×10^{-04}
358	3.9000×10^{-03}	2.4847×10^{-06}	2.8786×10^{-04}
363	3.2000×10^{-03}	3.8593×10^{-06}	4.1007×10^{-04}
368	4.3000×10^{-03}	8.0309×10^{-06}	4.9215×10^{-04}
373	7.8000×10^{-03}	1.2453×10^{-05}	4.8196×10^{-04}

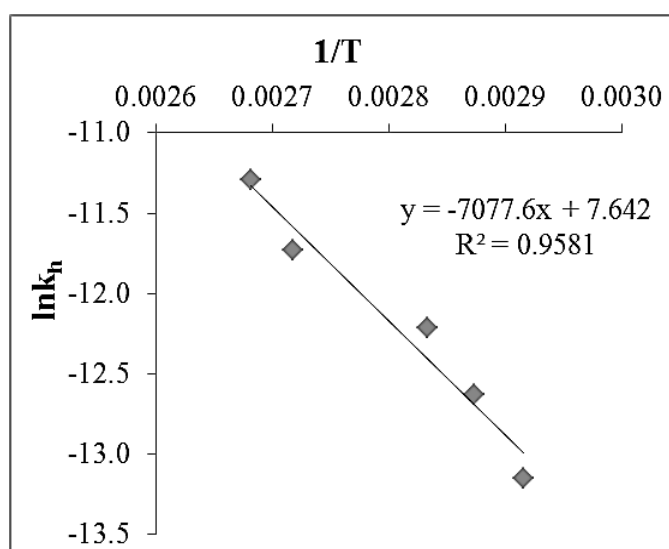
Using the data given in Table 5.3, the apparent activation energy for each of the processes namely penetration, nitric acid aided dissolution and the chemical reaction process were calculated using the Arrhenius plot as explained in case 1. The Arrhenius plots for the three rate constants are given below.

Fig. 5.45. Arrhenius plot for the penetration process without the effect of HNO₂



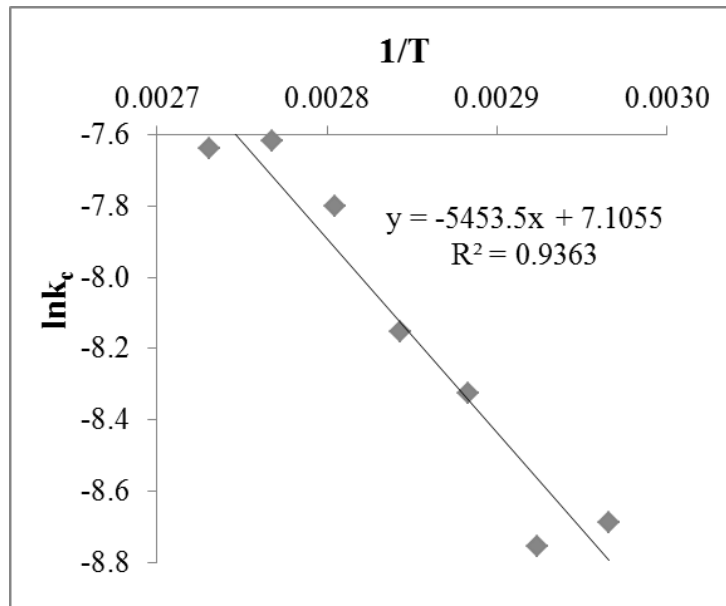
The apparent activation energy for the penetration process was estimated from the above plot to be about **78.13 kJ/mol**.

Fig. 5.46. Arrhenius plot for nitric acid aided dissolution process neglecting the effect of nitrous acid



The apparent activation energy for this process was deduced as **58.84 kJ/mol**.

Fig. 5.47. Arrhenius plot for the chemical reaction controlled dissolution process in the absence of the influence of nitrous acid



The apparent activation energy for this process was deduced as **45.34 kJ/mol**.

5.10.3.2 Method 2 – Based on surface area measurements

The kinetics of solid-liquid reactions and homogeneous reactions has some fundamental differences. Contrary to homogeneous reaction, the reaction rate of a solid compound dispersed in the liquid does not directly depend on the concentration of the solid in the liquid phase, but rather on the reactive surface area of the solid. This fact complicates the work very much as compared to homogeneous reactions, as the quantification of the surface area is not as straightforward as the concentration measurements. This is because; unlike concentrations the surface area of the solid dispersed in the liquid does not usually decrease linearly with the conversion⁶⁵. This could also be inferred from Figures 41 and 42 wherein the surface area and specific surface area of the dissolving UO₂ pellets were shown as a function of time respectively. This makes the kinetics behave differently and complicates the interpretation of experimental data.

Basically there are two ways to model the solid-liquid heterogeneous reactions by following the surface area profile. They are,

- Based on the correlation of the surface area to the conversion
- Based on the surface area estimations

5.10.3.2.1 Method – 2A: Correlation of the surface area to the conversion

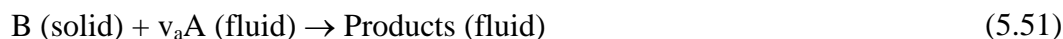
The behaviour of solids in liquids is not straight forward. Hence certain assumptions are needed to be made about the behavior of the solid for modeling purposes, if the surface area during the reaction could not be quantified directly. The most commonly used assumptions are based on relating the change in surface area to the reactant conversion, which could be more easily measured than the surface area. This correlation is based on the morphological changes of the solid during the reaction. The particle morphology is typically assumed to be uniform and of some ideal shapes like sphere, cylinder or slab. The correlation of the surface area to the conversion could be derived for different cases based on geometry. All these expressions are valid for isothermal batch reactors and the liquid phase concentrations are assumed to be constant. These expressions for various shapes of solids could be tested by plotting the experimental data versus the reaction time. If the plot is a straight line, it is usually considered to be the appropriate model to explain the reaction. One major challenge in this methodology is that solid particles seldom follow ideal morphology. Moreover, the discrimination of the models could be challenging, as several models could fit the experimental data when the parameter values are adjusted, especially if considerable experimental scattering exists. These traditional models do not allow flexible implementation of non-ideal behavior and more complex kinetics. Therefore this model based on the correlation of the surface area of the solid to the conversion ratio was considered not so appropriate to study the dissolution reactions of nuclear fuel in nitric acid and hence is not pursued in this research work.

5.10.3.2.2 Method – 2B: Based on surface area estimations

In contrary to measuring the surface area online during the course of the dissolution which as explained in the previous para is highly unreliable, the measurement of the surface area under static conditions is more reliable and reproducible⁶⁶. This could be done using techniques like nitrogen physisorption and mercury porosimetry. In the current work, the total surface area of the dissolving UO₂ pellet is assumed to react with nitric acid. The basis of this assumption is the fact that for most crystalline solids, since some crystal surfaces tend to be more reactive than others, the overall surface area could be assumed to correspond to the reactive area. No product layer formation was observed during the reaction. In these experiments, the external mass and heat transfer could be neglected due to the efficient agitation. It is to be noted that, as reported earlier in this thesis, a mixing

rate of 600 RPM under the given experimental conditions was sufficient to reduce the external mass and heat transfer effects to its bare minimum. Consequently, the concentration of nitric acid at the solid surface is assumed to be same as bulk concentration and hence the kinetics is purely chemically controlled. The total surface area is expressed as dA/dt as a function of C_{Ab} , the concentration of nitric acid in the bulk.

Consider the stoichiometric equation for the dissolution reaction as follows.



Here B represents the UO_2 pellet, A denotes nitric acid and v_a is the stoichiometric co-efficient of nitric acid in the reaction.

The rate expression for the stoichiometric equation (5.51) is given as follows.

$$\frac{dC_{Ab}}{dt} = -v_a k A_t C_{Ab}^m \quad (5.52)$$

$$\frac{dC_B}{dt} = -v_b k A_t C_{Ab}^m \quad (5.53)$$

Where, A_t is the surface area measured by nitrogen physisorption method under static conditions (refer section 5.9 of this thesis), C_{Ab} is the concentration of nitric acid in bulk phase (mol m^{-3}), C_B is the concentration of uranium in solid phase (mol.m^{-3}), k is the rate constant ($\text{m}^{-2}.\text{s}^{-1}$), v_a is the stoichiometric co-efficient with respect to nitric acid, v_b is the stoichiometric co-efficient with respect to UO_2 which is unity in this case and m is the order of the reaction with respect to nitric acid.

In a general, the concentration profiles as a function of the reaction time could be obtained by solving the above rate equations. The experimental data of concentration of nitric acid and solid phase uranium concentration vs time were fitted into the rate equation using a nonlinear regression technique to obtain rate constant that best correlates the experimental data.

The rate constant is estimated at different temperature. Comparison between experimental and calculated values of solid phase uranium concentration vs. time, concentration of nitric acid vs time and total area vs time are generated for various cases and the explanations are given at the respectively places. The temperature dependence of the

dissolution rate is governed by the Arrhenius equation. The plot of $\ln(k)$ vs $1/T$ gives a slope equal to $(-E_a/R)$ where E_a is the apparent activation energy of the reaction.

In order to find the order of the reaction with respect to nitric acid that best explains the experimental data, various cases were considered. The information available in the literature as reported in Chapter 3 of this thesis describes different orders with respect to nitric acid. The values range from about 1.3 to about 2.5. Also during each of the experiments it was found that between about 40 to 60% of dissolution, the physical integrity of the pellet is lost and the pellet crumbles. Hence the surface area measurements, even though carried out under static condition, are not reliable and reproducible. Therefore the experimental data points obtained till the pellet crumbles are only considered for the modeling purpose.

5.10.3.2.2.1 Case 1

The order of the reaction and stoichiometric co-efficient with respect to nitric acid was considered as 1 and 4 respectively. The dissolution experimental data upto 60% was only considered as the pellets crumbled beyond that point. The base values of the estimated rate constants were obtained by minimizing the objective function given in the following equations.

$$f = \sum_1^n 20 * (C_{B\text{exp}} - C_{B\text{calc}})^2 + \sum_1^n (C_{A\text{bexp}} - C_{A\text{bcalc}})^2 + \sum_1^n (A_{t\text{exp}} - A_{t\text{calc}})^2 \quad (5.54)$$

Each term in equation 5.54 corresponds to the square of the difference between the experimental and modelled value of a given parameter. The constant which is multiplied to this in the first term of the equation is the weightage factor. Higher the weightage factor, the difference between the experimental and calculated values would be that much less. But at the same time, higher weightage factor also increases the computational time and requirement more. Hence the weightage factor has to be optimum. The comparisons between the experimental and predicted values of the concentration profiles of nitric acid, uranium and the total surface area of the dissolving pellet as a function of time at 353 K are given in Figures 5.48 to 5.50.

Fig. 5.48. Comparison of experimental and calculated [HNO₃] profile at 353 k

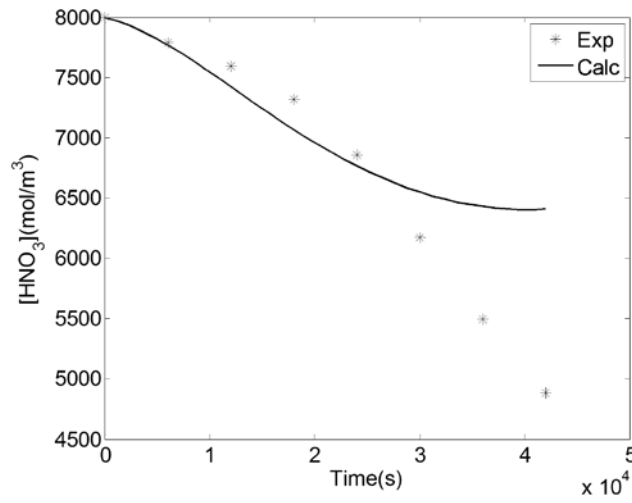


Fig. 5.49. Comparison of experimental and calculated [U] profile at 353 K

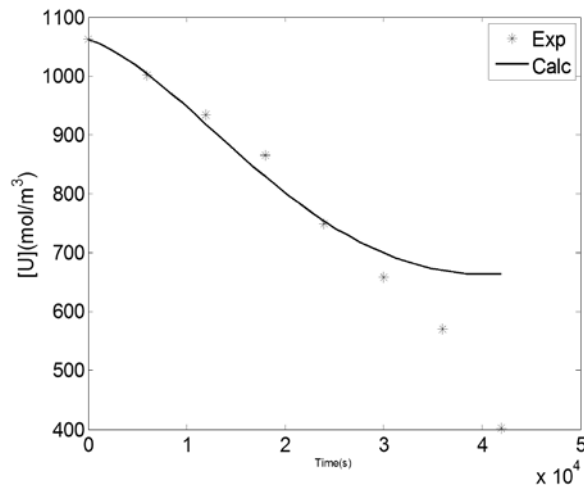
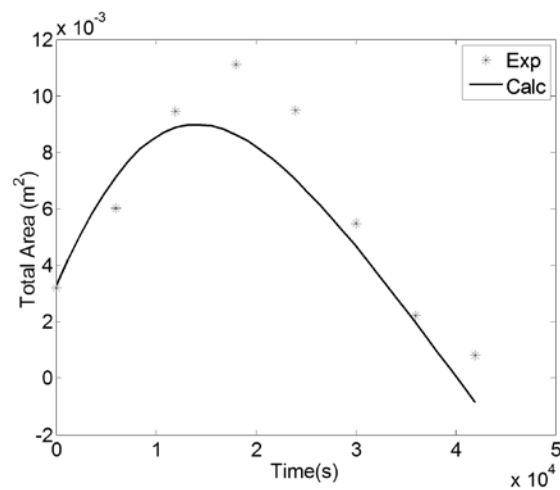


Fig. 5.50. Comparison of experimental and calculated pellet surface area profile during UO₂ dissolution at 353 K



The rate constants estimated using the model equations at various temperatures is given in the Table 5.4.

Table 5.4. Estimated values of rate constant at different temperature

T(K)	k (m⁻² sec⁻¹)
343	2.1661 x 10 ⁻⁰⁴
348	2.6050 x 10 ⁻⁰⁴
353	2.2997 x 10 ⁻⁰⁴
358	4.3579 x 10 ⁻⁰⁴
363	6.4740 x 10 ⁻⁰⁴

The activation energy for the process was calculated using Arrhenius equation and its value was found to be **55.9 kJ/mol** in the temperature range of 343-363 K.

5.10.3.2.2.2 Case 2

The order of the reaction and the stoichiometric co-efficient with respect to nitric acid was considered as 1 and 2.75 respectively. The value of 2.75 was based on the mechanism that was proposed for the dissolution of UO₂ in nitric acid under typical PUREX process conditions (section 5.8). The dissolution experimental data up to 60% was only considered as the pellets crumbled beyond that point. The base values of the estimated rate constants were obtained by minimizing the objective function given in equation 5.55.

$$f = \sum_1^n 50 * (C_{Bexp} - C_{Bcalc})^2 + \sum_1^n (C_{Abexp} - C_{Abcalc})^2 + \sum_1^n (A_{texp} - A_{tcalc})^2 \quad (5.55)$$

The comparisons between the experimental and predicted values at 353 K are given in Figures 5.51 to 5.53.

Fig. 5.51. Comparison of experimental and calculated $[\text{HNO}_3]$ profile at 353 K

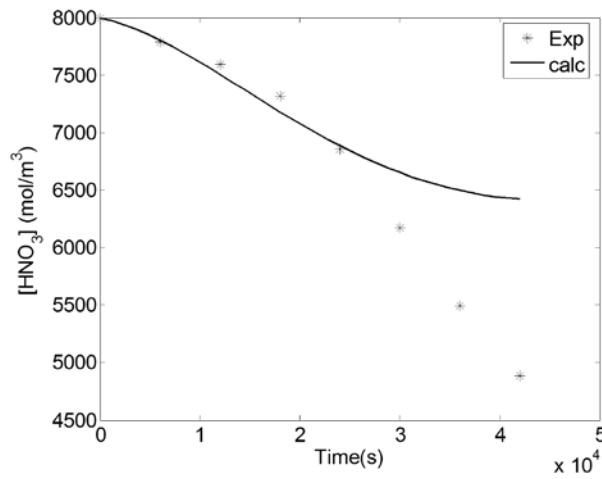


Fig. 5.52. Comparison of experimental and calculated $[\text{U}]$ profile at 353 K

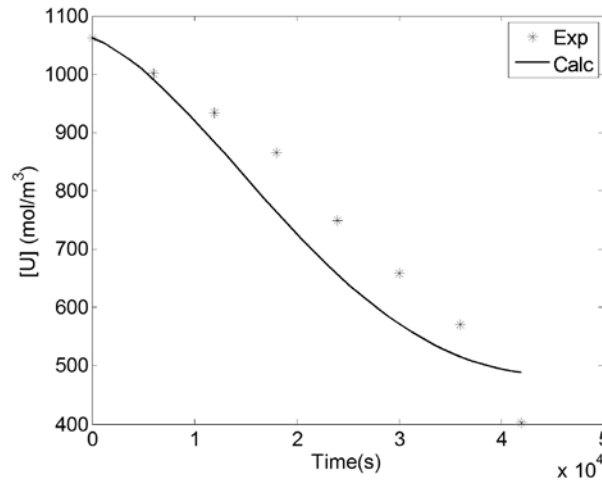
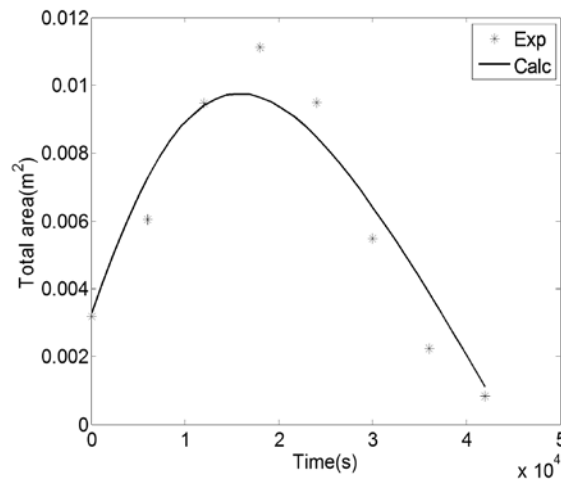


Fig. 5.53. Comparison of experimental and calculated pellet surface area profile during UO_2 dissolution at 353 K



The rate constant estimated using the model equations at various temperatures is given in the Table 5.5.

Table 5.5. Estimated values of rate constant at different temperature

T(K)	k (m ⁻² sec ⁻¹)
343	2.3186 x 10 ⁻⁰⁴
348	2.5506 x 10 ⁻⁰⁴
353	2.7791 x 10 ⁻⁰⁴
358	3.7027 x 10 ⁻⁰⁴
363	5.4439 x 10 ⁻⁰⁴

The activation energy for the process was calculated from Arrhenius equation and it was found to be about **42.8 kJ/mol** in the temperature range of 343-363 K.

5.10.3.2.2.3 Case 3

The order of the reaction and stoichiometric co-efficient with respect to nitric acid was considered as 2 and 4 respectively. The dissolution experimental data up to 60% was only considered as the pellets started to crumble at that point. The base values of the estimated rate constants were obtained by minimizing the objective function given below.

$$f = \sum_1^n 50 * (C_{Bexp} - C_{Bcalc})^2 + \sum_1^n (C_{Abexp} - C_{Abcalc})^2 + \sum_1^n (A_{texp} - A_{tcalc})^2 \quad (5.56)$$

The comparisons between the experimental and predicted values at 353 K are given in Figures 5.54 to 5.56.

Fig. 5.54. Comparison of experimental and calculated $[\text{HNO}_3]$ profile at 353 K

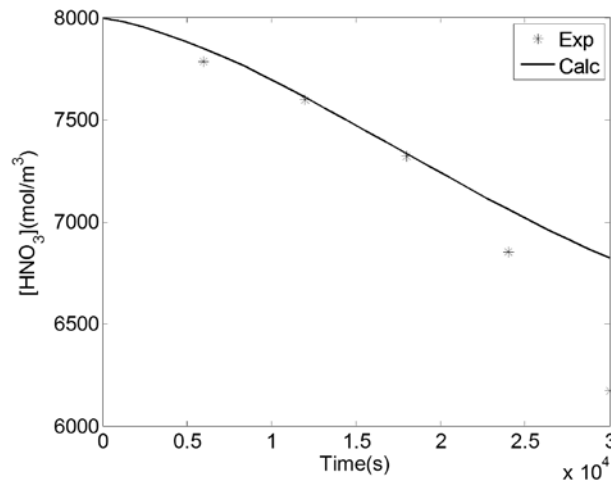


Fig. 5.55. Comparison of experimental and calculated $[\text{U}]$ profile at 353 K

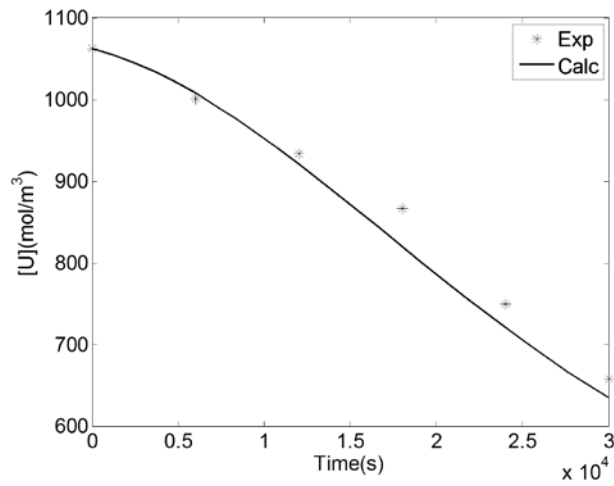


Fig. 5.56. Comparison of experimental and calculated pellet surface area profile during UO_2 dissolution at 353 K

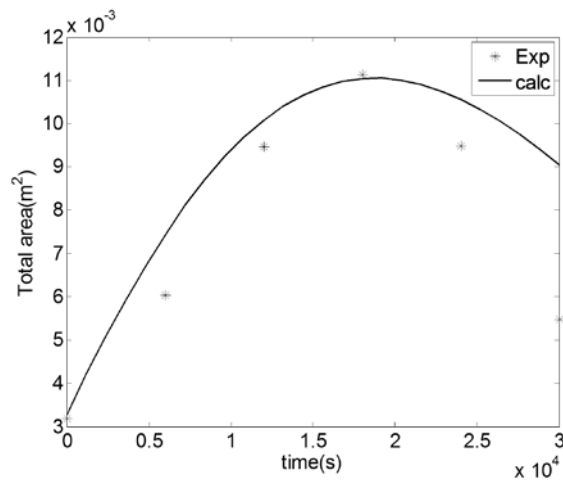


Table 5.6 gives the rate constant estimated at various temperatures.

Table 5.6. Estimated values of rate constant at different temperature

T(K)	k (m ⁻² sec ⁻¹)
343	1.5257 x 10 ⁻⁰⁴
348	1.9043 x 10 ⁻⁰⁴
353	2.1047 x 10 ⁻⁰⁴
358	3.2511 x 10 ⁻⁰⁴
363	3.9479 x 10 ⁻⁰⁴

The activation energy for the dissolution process was calculated from Arrhenius equation and it was found to be about **50.4 kJ/mol** in the temperature range of 343-363 K.

5.10.3.2.2.4 Case 4

The order of the reaction and stoichiometric co-efficient with respect to nitric acid was considered as 2 and 2.75 respectively. The dissolution experimental data upto 60% was only considered as the pellets started to crumble at that point. The base values of the estimated rate constants were obtained by minimizing the objective function given below.

$$f = \sum_1^n 50 * (C_{Bexp} - C_{Bcalc})^2 + \sum_1^n (C_{Abexp} - C_{Abcalc})^2 + \sum_1^n (A_{texp} - A_{tcalc})^2 \quad (5.57)$$

The comparisons between the experimental and predicted values at 353 K are given in Figures 5.57 to 5.59.

Fig. 5.57. Comparison of experimental and calculated [HNO₃]profile at 353 K

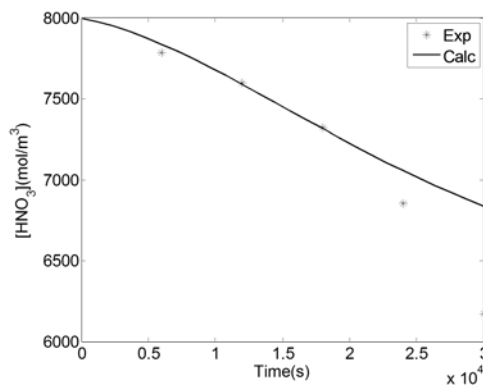


Fig. 5.58. Comparison of experimental and calculated [U] profile at 353 K

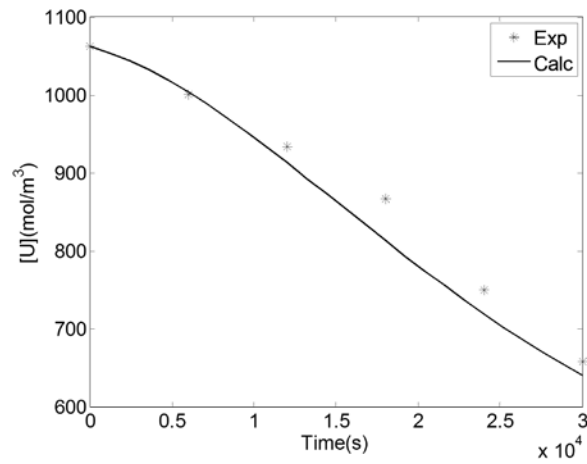
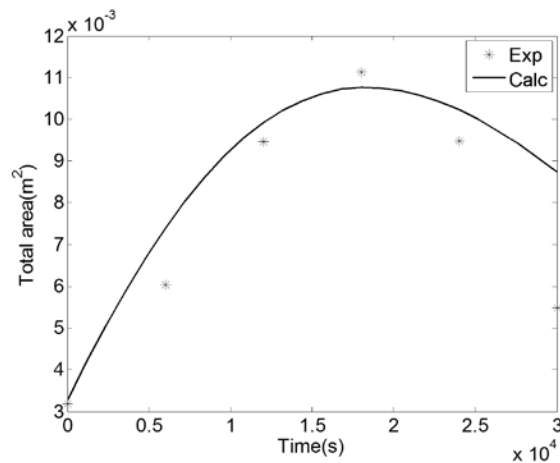


Fig. 5.59. Comparison of experimental and calculated pellet surface area profile during UO₂ dissolution at 353 K



The rate constant estimated using the model equations at various temperatures is given in the Table 5.7.

Table 5.7. Estimated values of rate constant at different temperature

T(K)	k (m⁻² sec⁻¹)
343	2.0452×10^{-08}
348	2.6264×10^{-08}
353	2.8701×10^{-08}
358	4.4786×10^{-08}
363	5.2895×10^{-08}

The activation energy for the rate constant was calculated from Arrhenius equation and its value was found to be **50.3 kJ/mol** in the temperature range of 343-363 K.

Thus in all the cases, the values of rate constant at different temperature and the apparent activation energy does not vary much. Also the experimental and estimated values are very closely fitting. Hence it could be concluded that the model equations derived here were satisfactorily explaining the reaction kinetics. As the apparent activation energy is comparable in all the cases here, the order of the reaction with respect to nitric acid does not vary the reaction kinetics much in the range of 1 to 2.

5.10.3.3 *Method 3 - Considering non-ideal nature of particle during reaction*

5.10.3.3.1 Introduction

A common feature for the models described so far is the hypothesis of ideal geometry, i.e. slab, infinitely long cylinder and spherical particle and so on. This is not true in many cases. The main reason for the deviation from the ideality is often the highly non-ideal structure of the solid material. Surface defects, such as cracks and craters, as well as porosity affect the particle structure and the observed reaction kinetics. Thus, there is a risk that assuming an ideal geometry for a solid particle, a wrong reaction order with respect to the solid substance is predicted. For example, the hypothesis of a perfect, non-porous spherical particle free from any defects implies the reaction order $2/3$ with respect to the solid component but a higher reaction order is expected, if the surface is rough and/or the particle contains some pores. The measurements of specific surface areas by gas adsorption (physisorption) have also revealed that the surface areas of reactive solids could clearly exceed the areas predicted by ideal surfaces. This could also be inferred from Figures 41 and 42.

5.10.3.3.2 Generalized characteristics of the shrinking particle model

In the case of dissolution of UO_2 in nitric acid, all the products formed dissolves into liquid phase and no undissolved residue was left. Hence the shrinking particle theory is the most appropriate model that could be employed to explain the reaction. In the present case, as and when the product is formed, it gets dispersed into the bulk of the reaction mixture and does not form any layer. Hence in the model equations it is sufficient to

consider the chemical reaction resistance and diffusion resistance alone. For incorporating the non-ideal behaviour of the solid, a parameter called “**Shape Factor**” (α) is introduced in the model which could be ascertained with any value for accounting any shape. This would be explained in detail later. A pseudo steady state is assumed on the reaction surface.

5.10.3.3.3 Interaction of chemical reaction and diffusion

The mass balance equation for each fluid-phase component (HNO_3 -A) at the reaction surface could be written as follows, provided the mass transfer through the fluid film could be described with Fick’s law,

$$k_{LA} \left(C_{LA}^b - C_{LA}^s \right) + v_A \text{Ra} \left(C_{LA}^s \right) = 0 \quad (5.58)$$

Where A denotes the fluid phase component (here HNO_3) and Ra is the chemical reaction rate in terms of concentration of fluid component in the solid surface and k_{LA} represents the mass transfer coefficient between solid phase and bulk fluid phase.

Dissolution of UO_2 in HNO_3 is represented by rate equation, as shown below.

$$\text{Ra} \left(C_{LA}^s \right) = k C_{LA}^s \quad (5.59)$$

Considering, that $y_A = \frac{C_{LA}^s}{C_{LA}^b}$, then equation 5.58 could be rewritten as

$$1 - y_A + \frac{v_A \text{Ra}(y_A)}{k_{LA} C_{LA}^b} = 0, \quad \text{Ra}(y_A) = k C_{LA}^b y_A \quad (5.60)$$

By using a generalized Mear’s criterion, we get

$$\varphi' = \frac{-v_A \text{Ra}(y_A = 1)}{k_{LA} C_{LA}^b} \quad (5.61)$$

This is the ratio of the rate of the reaction to the rate of external mass transfer.

Thus the equations 5.60 could be modified as

$$1 - y_A + \frac{\phi' Ra(y_A)}{Ra(y_A = 1)} = 0 \quad (5.62)$$

The rate equation for UO_2 dissolution is considered as first order with respect to concentration of nitric acid. Therefore the rate equation is

$$y_A = 1, C_{LA}^s = C_{LA}^b; \quad Ra(y_A = 1) = k C_{LA}^b \quad (5.63)$$

Substituting equation 5.63 into 5.62, we get

$$1 - y_A - \phi' y_A = 0 \quad (5.64)$$

The solution for the above equation is as follows

$$y_A = \frac{1}{\phi' + 1} \quad (5.65)$$

$$C_{LA}^s = \frac{1}{\phi' + 1} C_{LA}^b \quad (5.66)$$

If order of reaction with respect to HNO_3 is 2, then

$$\phi' = \frac{-v_A k (C_{LA}^b)^2}{k_{LA} C_{LA}^b} \quad (5.67)$$

$$C_{LA}^s = \frac{2 * C_{ab}}{(1 + 4 * \phi')^2 + 1} \quad (5.68)$$

5.10.3.3.4 Fluid–solid mass transfer coefficients

The fluid–solid mass transfer coefficient (k_{LA}) is included in the model considered here.

For the shrinking particle model, the numerical value of the mass transfer coefficient changes during the reaction, since the radii of the solid particles diminishes. A generally accepted correlation for the mass transfer around solid particles is

$$sh = a' + b' Re^{1/2} Sc^{1/3} \quad (5.69)$$

where Sh, Re and Sc denote Sherwood, Reynolds and Schmidt numbers respectively. The parameters a' and b' have various values, depending on the literature source. Usually a'=2 and b'=0.6 but it is claimed that the values a'=0 and b'=1 are sufficient to describe tank reactors with impellers for not too low Reynolds number which is given as follows.

$$Re = \left(\frac{\varepsilon d^4}{\nu^3} \right)^{1/3} \quad \varepsilon = \frac{N_p \rho_L N^3 D^5}{V_L \rho_L} \quad (5.70)$$

Where ε is the energy dissipated to the system, d is the particle diameter, ν is the kinematic viscosity, N_p is the power number, N is the speed of impeller, D is the diameter of impeller and V_L is volume of liquid . The Schmidt number is given as follows.

$$Sc = \frac{\nu}{D_A} \quad (5.71)$$

where D_A is diffusivity. The Sherwood number is given by

$$sh = \frac{k_{LA}}{D_A} \quad (5.72)$$

Inserting equations 5.70 to 5.72 in 5.69, we get

$$k_{LA} = \frac{D_A}{d} \left(a' + b' \left(\frac{\varepsilon d^4}{\nu^3} \right)^{1/6} \left(\frac{\nu}{D_A} \right)^{1/3} \right) \quad (5.73)$$

For shrinking particle model, the particle diameter changes as the reaction proceeds. In general R/R_0 could be written as $(V_p/V_{p0})^{1/a}$, where R_0 and V_{p0} are the initial radius and initial volume respectively. In addition, it could be shown that $V_p/V_{p0} = n_j/n_{j0}$ or C_j/C_{j0} for constant volume. These relations are inserted into equation 5.73 and we obtain the final form for the correlation of the mass transfer coefficient under reaction conditions.

$$k_{Li} = \frac{D_i}{d_0 z^{1/a}} \left(a' + b' \left(\frac{\varepsilon d_0^4 z^{4/3}}{v^3} \right)^{1/6} \left(\frac{v}{D_i} \right)^{1/3} \right) \quad (5.74)$$

Where $z = C_j/C_{j0}$. In the present case, $j = \text{Uranium in solid phase (B)}$ and $i = \text{HNO}_3 \text{ (A)}$. As the reaction progresses, the mass transfer coefficients increase for the shrinking particle model.

5.10.3.3.4.1 Reaction area and reaction order with respect to solid phase component

For fluid–solid processes, the overall rate is assumed to be proportional to the accessible surface area (A). For instance, for a dissolved component (i) in a perfectly mixed, batch wise operated tank reactor, the balance equation could be written as

$$\frac{dn_i}{dt} = v_i R_a(C_{Li}^s) A \quad (5.75)$$

The specific rates (R_a) are expressed as $\text{mol}/(\text{m}^2 \cdot \text{s})$. The total accessible surface area (A) is related to the number of particles (n_p) and the specific surface area (σ). The relation between the available particle surface area and the specific surface area for general particle geometry will be derived in this section. By assuming equal-size particles, the accessible total surface area is given as follows

$$A = n_p \cdot A_p \quad (5.76)$$

The volume of a particle is given by

$$V_P = \frac{m_P}{\rho} = \frac{nM}{n_P \rho_P} \quad (5.77)$$

Where M and n denote the molar mass and the total molar amount, respectively. The number of particles could be obtained from the initial state (0) as follows.

$$V_{0P} = \frac{n_0 M}{n_P \rho_P} \quad (5.78)$$

Combining the above two equations, we get,

$$n_P = \frac{n_0 M}{V_{0P} \rho_P} \quad (5.79)$$

Substituting equation 5.79 into 5.76, the accessible area becomes

$$A = \frac{n_0 M}{\rho_P} \frac{A_{0P}}{V_{0P}} \frac{A_P}{A_{0P}} \quad (5.80)$$

The area-to-volume ratio (A_{0P}/V_{0P}) expressed by the shape factor (a) and the characteristic dimension (R_0) as given below.

$$a = \left(\frac{A_{0P}}{V_{0P}} \right) R_0 \quad (5.81)$$

Now substituting equation 5.81 into 5.80, we get

$$A = \frac{n_0 M}{\rho_P} \frac{a}{R_0} \frac{A_P}{A_{0P}} \Rightarrow A = \frac{aM}{\rho_P R_0} n_0 \frac{A_P}{A_{0P}} \quad (5.82)$$

The ratio A_P/A_{0P} is expressed in terms of the radius of ideal geometries as follows.

$A_P/A_{0P} = (R/R_0)^2$ for a sphere; $(R/R_0)^1$ for an infinitely long cylinder and $(R/R_0)^0$ for a slab.

In terms of particle volumes we obtain the following relations for this ratio.

$A_P/A_{0P} = (V_P/V_{0P})^{2/3}$ for a sphere; $(V_P/V_{0P})^{1/2}$ for an infinitely long cylinder and $(V_P/V_{0P})^0$ for a slab.

Thus the relation could be generalized for an arbitrary geometry as given below.

$$\frac{A_P}{A_{0P}} = \left(\frac{V_P}{V_{0P}} \right)^{\frac{(a-1)}{a}} \quad (5.83)$$

Combining equations 5.77 and 5.78 we get

$$\frac{V_P}{V_{0P}} = \frac{n}{n_0} \quad (5.84)$$

Substituting the above relation in equation 5.83 we get,

$$\frac{A_P}{A_{0P}} = \left(\frac{n}{n_0} \right)^{\frac{(a-1)}{a}} \quad (5.85)$$

Thus equation 5.82 now becomes,

$$A = \frac{aM}{\rho_P R_0} n_0^{1/a} n^{1-1/a} \quad (5.86)$$

But we know that $\frac{a}{R_0} = \frac{A_{0P}}{V_{0P}}$ and specific surface area is given by $\sigma = \frac{A_{0P}}{m_{0P}}$.

Thus we have $\frac{a}{R_0} = \frac{\sigma m_{0P}}{V_{0P}} = \sigma \rho_P$

$$\frac{a}{R_0} = \frac{\sigma m_{0P}}{V_{0P}} = \sigma \rho_P \quad (5.87)$$

And the total accessible surface area now becomes

$$A = \sigma M n_0^{1/a} n^{1-1/a} \quad (5.88)$$

If the mole fraction of the solid material is constant (x_{0B}), the amounts of substance are given by

$$n_{0B} = x_{0B} n_0 \text{ at } (t = 0) \text{ and}$$

$$n_B = x_{0B} n \text{ at } (t > 0)$$

Inserting these expressions in equation 5.88, we get

$$A = \frac{\sigma M}{x_{0B}} n_{0B}^x n_B^{1-x} \quad (5.88)$$

Where $x=1/a$. This expression for the area is used in the bulk-phase mass balances of the fluid and solid components in equation 5.75. Thus for the mass balance equation for a solid component (j), the equation 5.75 gets modified as

$$\frac{dn_j}{dt} = \frac{v_j \sigma M}{x_{0j}} n_{0j}^x n_j^{1-x} R_a \quad (5.89)$$

In the present case of UO_2 dissolution studies, this equation becomes

$$\frac{dn_A}{dt} = \frac{v_A \sigma M}{x_{0B}} n_{0B}^x n_B^{1-x} k_{LA}^S \quad (5.90)$$

Here the fluid volume could be considered to remain constant, and thus the above two

equations become

$$\frac{dC_B}{dt} = \frac{v_B \sigma M}{x_{0B}} C_{0B}^x C_B^{1-x} k C_{LA}^s \quad (5.91)$$

$$\frac{dC_A}{dt} = \frac{v_A \sigma M}{x_{0B}} C_{0B}^x C_B^{1-x} k C_{LA}^s \quad (5.92)$$

Here $v_A = -4$, $v_B = -1$ and $x_B = 0.333$. The experimentally observed reaction order thus depends on the particle geometry. For a long cylinder, $x = 1/2$ and for a perfect, non-porous sphere $x = 1/3$. Thus reaction orders of $(1 - x)$, $1/2$ and $2/3$ are predicted for these particles. For a slab, $x = 1$ and the observed reaction order approaches zero. However, as the real particles deviate from the ideal ones, the accessible surface area for the chemical reactions is higher. So in the present case the value of shape factor (a) is calculated from experimentally determined specific surface area as given below.

We know that shape factor is given by equation 5.81 as $a = \frac{A_{0P}}{V_{0P}} R_0$, we also know that

$V_{0P} = \frac{m_P}{\rho_P}$ and $A_{0P} = \sigma m_P$. Thus the shape factor now becomes

$$a = \sigma \rho_P R_0 \quad (5.93)$$

In a general, the concentration profiles as a function of the reaction time could be obtained by solving equations 5.91 and 5.92 numerically. The concentrations at the reaction surface are calculated iteratively or analytically from equation 5.63. The experimental data of concentration of nitric acid and solid phase uranium concentration vs time were fitted into equations 5.91 and 5.92 using a nonlinear regression technique to obtain rate constant that best correlate the experimental data. As reported earlier in this thesis, the pellet starts crumbling into small fragments generally at around 60% of dissolution during most of the experiments. So the value of shape factor is not constant from this point in time onwards. So in the current modeling method, experimental data points only up to 60% of uranium

dissolution was considered for the mathematical analysis.

The rate constants were estimated at different temperatures. Comparison between experimental and calculated values of solid phase uranium concentration vs. time and bulk phase concentration of nitric acid vs time were generated graphically and are shown in the following sections for various conditions as the cases may be. The temperature dependency of the dissolution rate is governed by the Arrhenius equation. Thus the plot of $\ln(k)$ vs $1/T$ gives a slope equal to $(-E_a/R)$ from which the apparent activation energy of the dissolution reaction under the experimental conditions were estimated

5.10.3.3.4.1.1. Case 1

Consider the order with respect to HNO_3 is 1 and the stoichiometric coefficient with respect to HNO_3 is 4. Considering the experimental data up to 40 % dissolution as indicated before, the best values of rate constants were obtained by minimizing the objective function given below.

$$f = \sum_1^n 20 * (C_{B\text{exp}} - C_{B\text{calc}})^2 + \sum_1^n (C_{A\text{bexp}} - C_{A\text{bcalc}})^2 \quad (5.94)$$

The comparison between the experimental and calculated concentration profiles using the model equations are given in Figures 5.60 and 5.61..

Fig. 5.60. Comparison of experimental and calculated [U(VI)] profile at 353 K

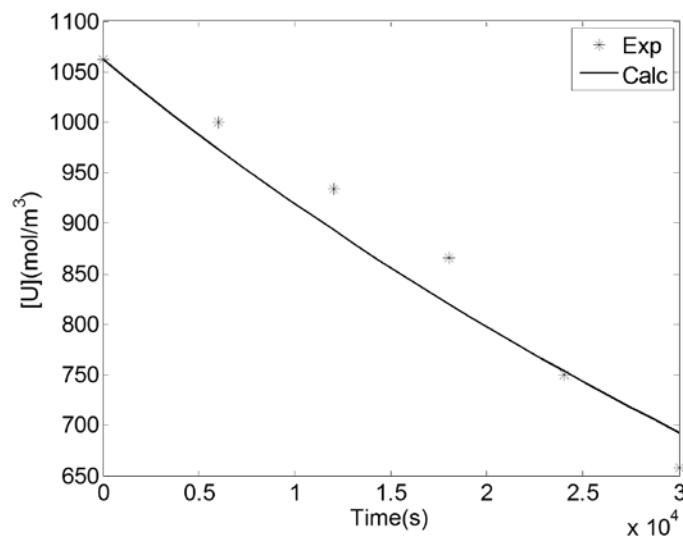
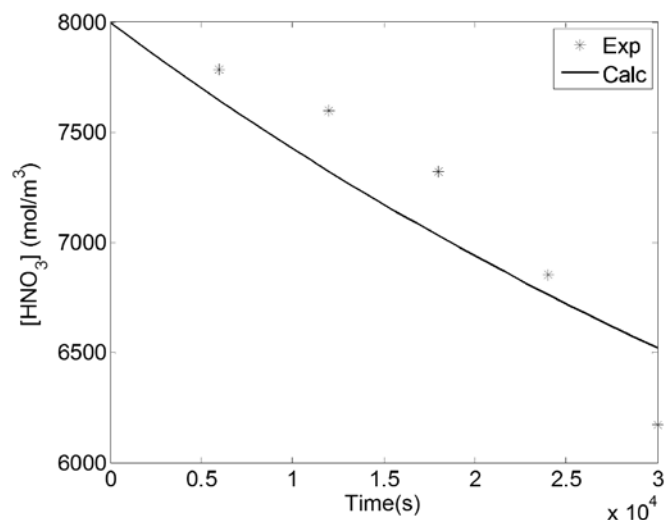


Fig. 5.61. Comparison of experimental and calculated [HNO₃] profile at 353 K



The values of the rate constant estimated at various temperatures of the experiment are provided in table 5.8.

Table 5.8. Estimated rate constants at various temperatures

T(K)	k (m/s)
343	3.4045 X 10 ⁻⁰⁸
348	4.8920 X 10 ⁻⁰⁸
353	5.1405 X 10 ⁻⁰⁸
358	5.8389 X 10 ⁻⁰⁸
363	7.7638 X 10 ⁻⁰⁸

The activation energy for the dissolution process was calculated from Arrhenius equation and its value was found to be about **37.8 kJ/mol** in the temperature range of 343-363 K.

5.10.3.3.4.1.2. Case 2

Consider the order with respect to HNO₃ is 1 and the stoichiometric coefficient with respect to HNO₃ is 2.75. Considering the experimental data up to 40 % dissolution as indicated before, the best values of rate constants were obtained by minimizing the objective function given below.

$$f = \sum_1^n 20 * (C_{Bexp} - C_{Bcalc})^2 + \sum_1^n (C_{Abexp} - C_{Abcalc})^2 \quad (5.95)$$

The comparison between the experimental and calculated concentration profiles using the model equations were given graphically in Figures 5.62 and 5.63.

Fig. 5.62. Comparison of experimental and calculated [U(VI)] profile at 353 K

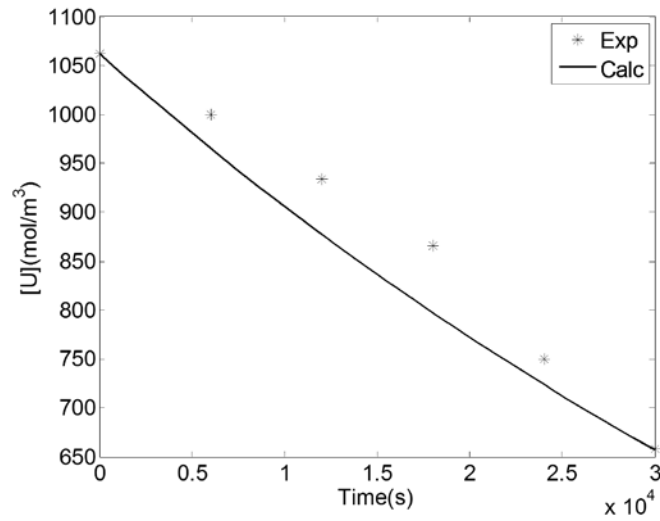
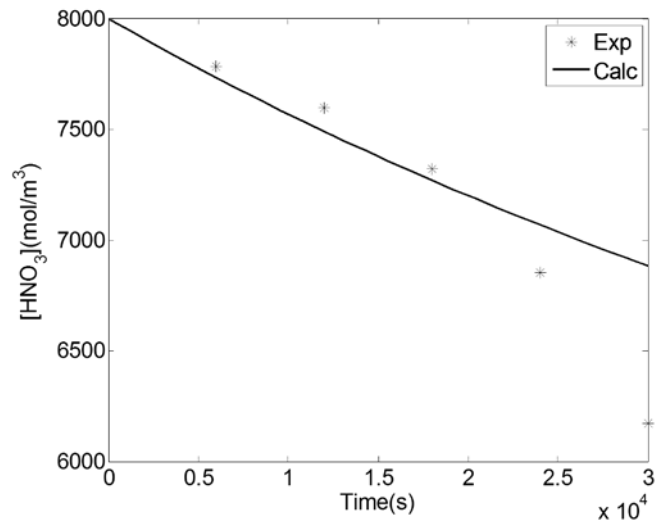


Fig. 5.63. Comparison of experimental and calculated [HNO₃] profile at 353 K



The values of the rate constant estimated at various temperatures of the are provided in table 5.9.

Table 5.9. Estimated rate constants at various temperatures

T(K)	k (m/s)
343	3.3153×10^{-08}
348	4.8880×10^{-08}
353	5.5705×10^{-08}
358	6.3988×10^{-08}
363	8.8924×10^{-08}

The activation energy for the process was calculated from Arrhenius equation and it was found to be about **46.5 kJ/mol** in the temperature range of 343-363 K.

5.10.4. Conclusion on modeling of UO₂ dissolution reaction

Two different models have been chosen for explaining the dissolution reaction of UO₂ pellets in nitric acid under various experimental conditions. First model is based on the penetration of nitric acid into the solid pellets and undergoing reaction at the pellet acid interface. The latter model is based on the surface area estimations. Both the models employed the shrinking particle theory in deriving the rate equations from which the rate parameter and the apparent activation energy was estimated. Both the models seem to be predicting the experimental data satisfactorily. The latter model has the provision to incorporate the non-ideal behaviour of the surface morphology of the dissolving solid while determining the kinetics. This is carried out by introducing the concept of “shape factor” which takes into account of the surface morphology of all geometries. Thus the model appeals to be more realistic. Hence, when it comes to determining the kinetics of the actual spent fuel dissolution, the surface morphology of the irradiated fuel will be extremely rough and irregular. Hence the latter model seems to be of more value in explaining their dissolution behaviour.

As for as the order of the reaction with respect to nitric acid is concerned, the results of the modelling shows, that the 2nd order model fits well with the experimental results. Similarly the stoichiometric co-efficient of 2.75 for nitric acid in its reaction with UO₂ seems to be predicting the experimental values more satisfactorily than 4. This further justifies the proposed mechanism for the dissolution of UO₂ pellets under typical PUREX process conditions as given in section 5.8.

The model equations generated were based on the dissolution results of unirradiated fuel

pellets. It has been well established in the literature that under similar conditions, irradiated pellets dissolve faster than their unirradiated counterparts⁶⁷. This is because of the surface defects created in the irradiated fuel matrix due to the presence of fission gases which makes the solid fuel more porous thereby increasing its effective specific surface area⁶⁸. Thus during dissolution there is a better contact between the fuel and the solvent enabling faster dissolution. Hence the rate equations developed and presented in this work, when used for designing the dissolution system for processing the spent nuclear fuel will be conservative and will definitely ensure a better performance of the process system. Therefore further studies of similar kind and approach is required to be carried out using nuclear fuel irradiated to different burn up levels to realistically model the dissolution process for an irradiated UO₂ fuel system in nitric acid. The results of the present thesis would pave way for further development of this work.

5.11 References

-
- ¹ Vishwas Govind Pangarkar, “Design of Multiphase Reactors”, First Edition, 2015 John Wiley & Sons, Inc
- ² OECD-NEA (2012), “Spent Nuclear Fuel Reprocessing Flowsheet”, NEA/NSC/WPFC/DOC(2012)15 June 2012
- ³ R. Natarajan, N. K. Pandey, V. Vijayakumar, R. V. Subbarao, “Modeling and Simulation of Extraction Flowsheet for FBR Fuel Reprocessing”, *Procedia Chemistry*, Volume 7, 2012, pp 302-308
- ⁴ F. L. Culler and R. E. Blanco, Dissolution and Feed Preparation for Aqueous Radiochemical Separation Processes, in *Proceedings of the Second international conference on the Peaceful Uses of Atomic Energy*, Geneva, 1958, Vol. 17, p. 285, United Nations, New York, 1959
- ⁵ W. D. Bond, Dissolution of Sintered Thorium-Uranium Oxide Fuel in Nitric Acid Fluoride Solutions, USAEC Report ORNL-2519, Oak Ridge National Laboratory, Nov. 14, 1958
- ⁶ Natarajan R. and Baldev Raj, “Fast Reactor Fuel Reprocessing Technology: Successes and Challenges”, *Energy Procedia*, 2011, Vol. 7, pp 414-420
- ⁷ J. T. A. Roberts, “High temperature plasticity of oxide nuclear fuel”, in *Deformation of Ceramic Materials* edited by R. C. Bradt and R. E. Tressler, 1975 Plenum Press New York, p-325

-
- ⁸ G. F. Kessinger and M. C. Thompson, Dissolution of Dresden Reactor Fuel, WSRC-TR-2002-00448, Westinghouse Savannah River Company, Aiken, SC (2002)
- ⁹ Dieter Vollath, Horst Wedemeyer, Helmut Elbel, Elmar Günther; “On the Dissolution of (U,Pu)O₂ Solid Solutions with Different Plutonium Contents in Boiling Nitric Acid”, Nucl. Tech., Vol 71, Number 1, October 1985, pp 240-245
- ¹⁰ Charles L. Peterson, Paul D. Miller, Earl L. White, Walter E. Clark, “Materials of Construction for Head-End Processes - Aqueous Reprocessing of Nuclear Fuels”, Ind. Eng. Chem., 1959, 51 (1), pp 32–37
- ¹¹ Baldev Raj, U. Kamachi Mudali, “Materials development and corrosion problems in nuclear fuel reprocessing plants”, Progress in Nuclear Energy 48 (2006) 283–313
- ¹² R. Natarajan and Baldev Raj, “Technology development of fast reactor fuel reprocessing in India”, Current Science, Vol. 108, No. , January 2015, p. 30
- ¹³ Geetha Manivasagam, V. Anbarasan, U. Kamachi Mudali, Baldev Raj; “Corrosion-Resistant Ti-xNb-xZr Alloys for Nitric Acid Applications in Spent Nuclear Fuel Reprocessing Plants”, Metall. and Mat. Trans. A (2011) 42: 2685
- ¹⁴ Justin T. Long, “Engineering for Nuclear Fuel Reprocessing”, The American Nuclear Society (1978)
- ¹⁵ Davidson J. K., Haas W. O., Jr., Meroherter J. L., Miller R. S., and Smith D. J., (1959) “The Fast Oxide Breeder: The Fuel Cycle”, KAPL-1757
- ¹⁶ Flagg J. F. (1960), “Chemical Processing of Reactor Fuels”, Academic Press, N.Y., P 90
- ¹⁷ Ferris L. M. and Kibbey A. H., “Sulfex-Thorex and Darex-Thorex Processes for the Dissolution of Consolidated Edison Power Reactor Fuel: Laboratory Development”, ORNL-2934 (October 1960)
- ¹⁸ P. Marc et al.: “Dissolution of uranium dioxide in nitric acid media: what do we know?”, EPJ Nuclear Sci. Technol. 3, 13 (2017)
- ¹⁹ Benedict, M., T. H. Pigford, and H. W. Levi, 1981. Nuclear Chemical Engineering, second edition, McGraw-Hill
- ²⁰ Tsutomu Sakurai et al, “The composition of the NO_x generated in the dissolution of Uranium Dioxide”, Nucl. Tech., Vol.83, 1988, 24-30
- ²¹ Levenspiel, O. (1972) Chemical Reaction Engineering, second edition, John Wiley and Sons, New York
- ²² Nils Lindman, Daniel Simonsson; “On the application of the shrinking core model to

liquid—solid reactions”, *Chemical Engineering Science*, Volume 34, Issue 1, 1979, Pages 31-35

²³ C. Y. Wen; “Non-catalytic heterogeneous solid-fluid reaction models”, *Ind. Eng. Chem.*, 1968, 60 (9), pp 34–54

²⁴ Jeff Y. Gao; “Studying Dissolution with a Model Integrating Solid–Liquid Interface Kinetics and Diffusion Kinetics”, *Anal. Chem.*, 2012, 84 (24), pp 10671–10678

²⁵ N. Desigan, Elizabeth Augustine, Remya Murali, N. K. Pandey, U. Kamachi Mudali, R. Natarajan, Nirav Bhatt and J. B. Joshi, “Kinetic study on the dissolution of sintered UO₂ pellet in HNO₃”, Poster presentation in CHEMCON 2013 held at ICT Mumbai from December 27-30, 2013

²⁶ Arrhenius, S.A. "Über die Dissociationswärme und den Einfluß der Temperatur auf den Dissociationsgrad der Elektrolyte". *Z. Phys. Chem.* 4: 96–116, 1889

²⁷ N.Desigan, Elizabeth Augustine, Remya Murali, N.K.Pandey, U.Kamachi Mudali, R.Natarajan, “Determination of activation energy for the Dissolution of sintered UO₂ Pellet in Nitric Acid”, Poster presentation in SESTEC 2014 conference, BARC from Feb 25-28, 2014

²⁸ Yu. J.F., Ji. C., “Interfacial chemistry and kinetics-controlled reaction mechanism of organophosphoric acid mixed extraction systems”, *Chem. J. Chin. Univ.* 13, 1992, 224–226

²⁹ N. Desigan, Elizabeth Augustine, Remya Murali, N.K. Pandey, U. Kamachi Mudali, R. Natarajan, J.B. Joshi, “Dissolution kinetics of Indian PHWR natural UO₂ fuel pellets in nitric acid - Effect of initial acidity and temperature”, *Prog. Nucl. Ener.* 83 (2015) 52-58

³⁰ Ryutaro Shiba, Md. Azhar Uddin, Yoshiei Kato and Shin-ya Kitamura, “Solid/liquid Mass Transfer Correlated to Mixing Pattern in a Mechanically-stirred Vessel”, *ISIJ International*, Vol. 54 (2014), No. 12, pp. 2754–2760

³¹ L.K. Doraiswamy, M.M. Sharma, “Heterogeneous reactions: analysis, examples, and reactor design”, Wiley, NY 1984

³² N. Desigan, Nirav P Bhatt, N. K. Pandey, U. Kamachi Mudali, R. Natarajan, J. B. Joshi, “Dissolution kinetics of UO₂ in nitric acid – Effect of mixing”, Poster presentation in NUCAR 2015 held at Mumbai from Feb 09-13 2015

³³ N. Desigan, Nirav P Bhatt, N. K. Pandey, U. Kamachi Mudali, R. Natarajan and J. B. Joshi, “Reducing effect of mixing on the dissolution kinetics of UO₂ pellets in nitric acid”, Poster presentation in International Conference on Sustainable Chemistry and Engineering (SusChemE 2015), Hotel Lalit, Mumbai Organized by ICT, Mumbai from 8-9 Oct, 2015

-
- ³⁴ von Seggern, D. CRC Standard Curves and Surfaces with Mathematics, 2nd ed. Boca Raton, FL: CRC Press, 2007.
- ³⁵ Levenspiel, O. (1972) Chemical Reaction Engineering, 3rd edition, Chapter 3: Interpretation of batch reactor data, page 52-53, John Wiley and Sons, New York
- ³⁶ Taylor, R. F.; Sharratt, E. W.; Chazal, L. E.; Logsdail, D. H. Dissolution rate of uranium dioxide sintered pellets in nitric acid systems. *J. Appl. Chem.* 1963, 13, 32–40
- ³⁷ Shabbir, M.; Robbins, R. G. Kinetics of the dissolution of uranium dioxide in nitric acid. I. *J. Appl. Chem.* 1968, 18, 139–134
- ³⁸ Tetsuo Fukasawa et al. (1991), “Generation and decomposition behaviour of nitrous acid during dissolution of UO₂ pellets by nitric acid”, Vol 94, 108-113
- ³⁹ Kenji Nishimura, Takahiro Chikazawa, Shinichi Hasegawa, Hiroshi Tanaka, Yasuhisa Ikeda, Yoshiyuki Yasuie and Yoichi Takashima, “Effect of nitrous acid on dissolution of UO₂ powders in nitric acid”, *J. Nucl. Sci. Tech.*, 32(2), pp 157-159, 1995
- ⁴⁰ H. Kobayashi et al. (1976), “The mechanism of nitrous acid decomposition”, *Nippon Kagaku Kaishi*, 3, 383; doi: <http://doi.org/10.1246/nikkashi.1976.383>
- ⁴¹ N. Desigan, N.K. Pandey, U. Kamachi Mudali, J.B. Joshi, “Role of nitrous acid during the dissolution of UO₂ in nitric acid”, SESTEC 2016 Proceedings, page 198, SESTEC 2016 held at IIT Guwahati from May 17-20, 2016
- ⁴² Ikeda. Y., Yasuie. Y., Takashima. Y., Park. Y. Y., Asano. Y., Tomiyasu. H.; “¹⁷O NMR study on the dissolution of UO₂ in nitric acid”, *J. Nucl. Sci. Technol.*, 30 (9), 962, 1993
- ⁴³ Jong Yoon Park, Yin Nan Lee, “Solubility and decomposition kinetics of nitrous acid in aqueous solution”, *J. Phys. Chem.*, 1988, 92 (22), pp 6294–6302, DOI: 10.1021/j100333a025
- ⁴⁴ N. Desigan, N. K. Pandey, U. Kamachi Mudali, “Effect of nitrous acid on the dissolution kinetics of UO₂ pellets in nitric acid”, Poster presentation at CHEMNUT 2015 organized in IGCAR on 30th and 31st July 2015
- ⁴⁵ David G Karraker (1985), “Oxidation of hydrazine by HNO₃”, *Inorg. Chem.* 24, 4470-4477
- ⁴⁶ L. Venault, Ph. Moisy, S. I. Nikitenko, C. Madic, “Kinetics of nitrous acid formation in nitric acid solutions under the effect of power ultrasound”, *Ultrasonics Sonochemistry*, 4 (1997) 195-204
- ⁴⁷ Steven B. Krivit (Editor-in-chief), Jay H. Lehr (Series Editor), Thomas B. Kingery (Editor) “Nuclear energy encyclopaedia: Science , Technology and Applications”, John Wiley & Sons, Inc., 2011

-
- ⁴⁸ A. Ramanujam, "An Introduction to Purex Process", IANCAS Bulletin, July 1998
- ⁴⁹ A. T. Gresky, "Recovery of nitrogen oxides and rare gas fission products from the nitric acid dissolution of irradiated uranium", ORNL-1208, 1952
- ⁵⁰ Y. Ikeda et al., "Kinetic study on the dissolution of UO₂ powders in nitric acid", J. Nucl. Mat. 224(1995) 266-272
- ⁵¹ N. Desigan, Nirav P. Bhatt, N. K. Pandey, U. Kamachi Mudali, R. Natarajan, J. B. Joshi, "Mechanism of dissolution of nuclear fuel in nitric acid relevant to nuclear fuel reprocessing", J Radioanal Nucl Chem 2017, DOI 10.1007/s10967-017-5208-z
- ⁵² Jerzy Piotrowski, Krzysztof Piotrowski, "Kinetic analysis of sodium nitrite inversion with nitric acid", Chemical Engineering Journal, Vol.95, pp 95-99, 2003
- ⁵³ Chang H. Oh. (Editor), "Hazardous and radioactive waste treatment technologies handbook", 2001 by CRC Press
- ⁵⁴ N. Desigan, P. Velavendan, Remya Murali, Elizabeth Augustine, N. K. Pandey, U. Kamachi Mudali, R. Natarajan and J.B. Joshi, "Determination of the composition of NO_x gases during the reprocessing of spent nuclear fuel", Poster presentation in CHEMENT-2014, 06 – 07 MARCH – 2014, Kalpakkam
- ⁵⁵ M. P. Pradhan and J. B. Joshi, "Absorption of NO_x Gases in Aqueous NaOH Solutions: Selectivity and Optimization", AIChE Journal, January 1999, Vol. 45, No. 1, pp 38-50
- ⁵⁶ N. Desigan, N. K. Pandey, C. Mallika, U. Kamachi Mudali, R. Natarajan and J. B. Joshi, "Mechanism of dissolution of UO₂ pellets in nitric acid – New insights", Poster presentation in Pu-75 theme meeting to be organized in IGCAR from 23-25 May, 2016
- ⁵⁷ Tetsuo Fukasawa, Yoshihiro Ozawa and Fumio Kawamura, "Generation and decomposition behaviour of HNO₂ during UO₂ dissolution", Nuc. Tech., Vol. 94, pp 108-113, 1991
- ⁵⁸ Zacharia, I.G. and Deen, W.M., "Diffusivity and Solubility of Nitric Oxide in water and saline", Ann. Biomed. Eng. (2005) 33: 214-222, doi:10.1007/s10439-005-8980-9
- ⁵⁹ Brunauer Stephen, Emmett P. H.; Teller Edward, "Adsorption of Gases in Multimolecular Layers" J Am. Chem. Soc., 60 (2), 1938, 309–319
- ⁶⁰ Salmi, T., Lehtonen, J., "Modeling of reaction kinetics in complex systems". Kemia 25, 311–316, 1998
- ⁶¹ Dickinson, C.F., Heal, G.R., "Solid-liquid diffusion controlled rate equations". Thermochemica Acta 340, 89–103, 1999

-
- ⁶² Hodgson, T. D.: RECOD'87, Vol. 2, 591 (1987)
- ⁶³ Shunji Homma, Jiro Koga, Shiro Matsumoto, Tomio Kawata, "Dissolution rate equation of UO₂ pellet", J. Nucl. Sci. Tech., 30(9), pp.959-961, 1963
- ⁶⁴ Koga. J., Homma. S., Kanehira. O., Matsu Moto. S., Goto. M., Yasu. T., Kawata. T.; RECOD □91, Vol. II. 687 (1991)
- ⁶⁵ Henrik Grenman, Malin Ingves, Johan Warna, Jukka Corander, Dmitry Yu. Murzin, Tapio Salmi, "Common pot holes in modeling solid-liquid reactions—methods for avoiding them", Chem. Engg. Sci. 66 (2011) 4459–4467
- ⁶⁶ Tapio Salmi, Henrik Grenman, Johan Warna, Dmitry Yu. Murzin, "New modeling approach to liquid-solid reaction kinetics: From ideal particles to real particles", Chem. Engng. Res. Des., 91 (2013) 1876-1889
- ⁶⁷ Hirotomo Ikeuchia, Atsuhiko Shibata, Yuichi Sano, Tsutomu Koizumi, "Dissolution behavior of irradiated mixed-oxide fuels with different plutonium contents", Procedia Chemistry 7 (2012) 77 – 83
- ⁶⁸ Yasuhisa Ikeda, Yoshiyuki Yasuike, Kenji Nishimura, Shinichi Hasegawa, Chris Mason, Richard Bush and Yoichi Takashima (1999), "Dissolution Behavior of Pulverized Irradiated Fuels in Nitric Acid Solutions", J. Nucl. Sci. Tech., 36:4, 358-363

CHAPTER 6. Fabrication and dissolution studies of $\text{UO}_2\text{-CeO}_2$ simulated MOX pellets

6.1 Introduction

The previous chapter described the dissolution of UO_2 in nitric acid under typical PUREX process conditions. This explains the behaviour of the major component of FBR MOX fuel in nitric acid system. The next step naturally is to study the dissolution behaviour of the minor component, PuO_2 , in the FBR MOX. But plutonium being a highly alpha radioactive species, needs special experimental facilities to handle them safely. Moreover as plutonium is a fissile material which is not available naturally, its quantity at given time is very less. Hence carrying out more experiments with PuO_2 containing MOX system should be well thought out and preplanned. Therefore it was found necessary to carry out the bulk of the dissolution experiments using a non-radioactive surrogate species in place of Pu. This species should be a true representative of plutonium in terms of its chemistry towards its dissolution behaviour in nitric acid. After detailed review of the literature it was decided to use Ce as the surrogate of plutonium in a (U, Ce) simulated MOX fuel. Once the bulk of the studies are carried out with this fuel, limited number of experiments will be carried out using the actual U, plutonium MOX to justify the use of Ce and to determine the kinetics of its dissolution in nitric acid under typical PUREX conditions.

6.2 Justification for using Ce as the surrogate for Pu

A surrogate system is a species which is chemically a true representative of the original species under the conditions of the experiments. Under the current research scheme, dissolution of a solid substance being the reaction under consideration, the major chemical properties under consideration are the solid state structure and the ionic radii. Both Ce and plutonium oxides crystalize in the same fluorite type structures. This is due to the similarity in the ionic radii of Ce^{4+} and Pu^{4+} species¹. During the MOX fuel fabrication, $\text{UO}_2\text{+CeO}_2$ MOX forms a cubic fluorite-type (U, Ce) O_2 solid solution during sintering at a high temperature of around 1873 K. Both the thermal and material properties of this solid solution are similar to those of (U, Pu) O_2 ². The thermodynamic properties of both CeO_2 and PuO_2 are also similar³. The dissolution behaviour of both these oxides was also reported to be similar in the context of development of an immobilized form of them for long term storage under typical deep geological conditions⁴.

6.3 Fabrication of UO_2 - CeO_2 simulated MOX pellets

6.3.1. Introduction

Gel combustion synthesis route was chosen for fabricating the simulated UO_2 - CeO_2 MOX powder⁵. Citric acid was used as the combustion fuel⁶. Sintering of the solid solutions was carried out at 1873 K under reducing atmosphere. As the primary objective of the current research work is to study the dissolution behaviour of typical FBR MOX fuel, PFBR fuel compositions were chosen. Hence simulated UO_2 - CeO_2 MOX of compositions $(U_{1-x}Ce_x)O_2$ with $x=0.22$ and 0.28 were fabricated. In order to study the influence of Ce composition on the dissolution behaviour of this MOX, two more compositions of MOX (one above and one below the PFBR compositions) were also prepared with $x=0.15$ and 0.35 . Thus a total of four different compositions of simulated UO_2 - CeO_2 MOX fuels were chosen and fabricated for studying their dissolution behaviour in nitric acid medium under the conditions same as that carried out for UO_2 pellets described in the previous chapter.

6.3.2. Chemicals used

Nuclear grade UO_2 was obtained from Nuclear Fuel Complex, Hyderabad. Cerium (IV) oxide was procured from M/s. Indian Rare Earths Ltd., Mumbai. Analytical reagent grade nitric acid was supplied by M/s. Rankem Laboratory Chemicals Pvt. Ltd., Chennai. Citric acid was procured from M/s. Fischer Inorganics and Aromatics Ltd., Chennai, India.

6.3.3. Preparation of simulated MOX powder by gel combustion synthesis

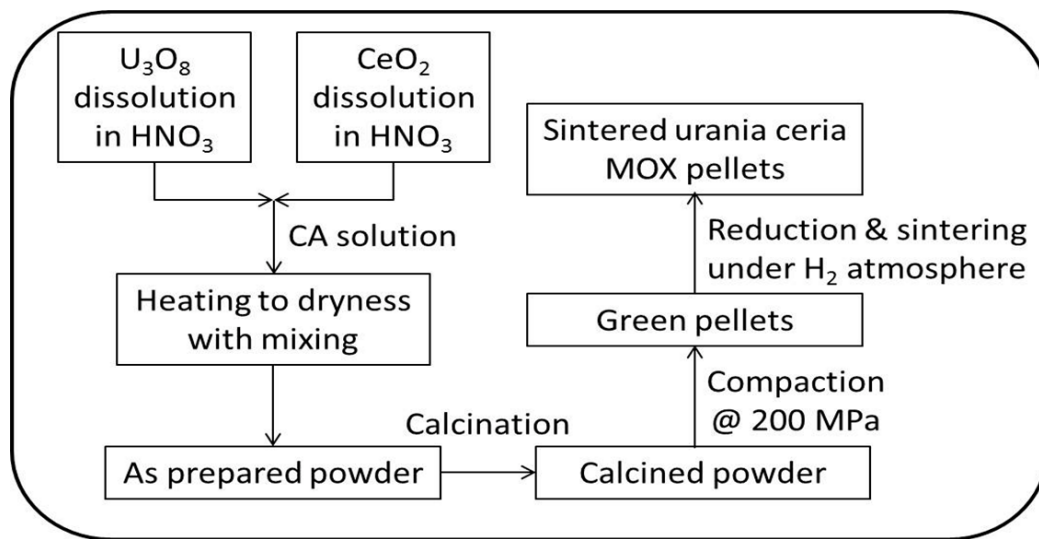
For each composition of the simulated MOX fuel, uranyl nitrate solution was prepared by dissolving appropriate quantity of U_3O_8 powder in concentrated nitric acid followed by evaporation of the excess acid. U_3O_8 was prepared by oxidizing nuclear grade uranium dioxide powder in air at 1073 K for 4 h with intermediate grinding and homogenization. Cerium nitrate solution was prepared by dissolving cerium(IV) oxide in nitric acid with few drops of HF. The combustion mixture was prepared by mixing the above solutions with an appropriate quantity of citric acid. The quantity of citric acid was so chosen that the ratio of citrate ions to that of nitrate ions in the solution was unity⁷. This mixture was heated with stirring in a glass bowl using hot plate. Gradually with the evaporation of all the moisture, the contents became a jelly mass. On further heating the gel hardened forming a charred mass. The combustion reaction was taken to completion by heating the charred mass which burns leading to a blackish powder.

6.3.4. Calcination and sintering

The combustion product will have some carbon in it and hence was calcined at 1023 K for 5 h in air using a resistance heating furnace fitted with silicon carbide heating elements. The mixed oxide powders obtained after calcination were compacted to form the green pellets. All the pellets are of almost uniform dimensions with an average diameter of 9.7 mm and average height of 6 mm. Tools made out of hardened tool-steel were used for the compaction. A double action hydraulic press was used for the above purpose with a pressure of about 200 MPa. The green pellets were sintered at 1873 K for 4 h in a stream of flowing gas mixture containing 92% argon and 8% hydrogen in a furnace fitted with molybdenum wire heating elements. A typical heating/cooling rate of 0.05 K/s was employed.

The schematic flow diagram for the fabrication of the simulated (U, Ce) MOX pellets is presented in Fig. 6.1.

Fig. 6.1. Schematic flow diagram for the fabrication of simulated (U, Ce) MOX pellets

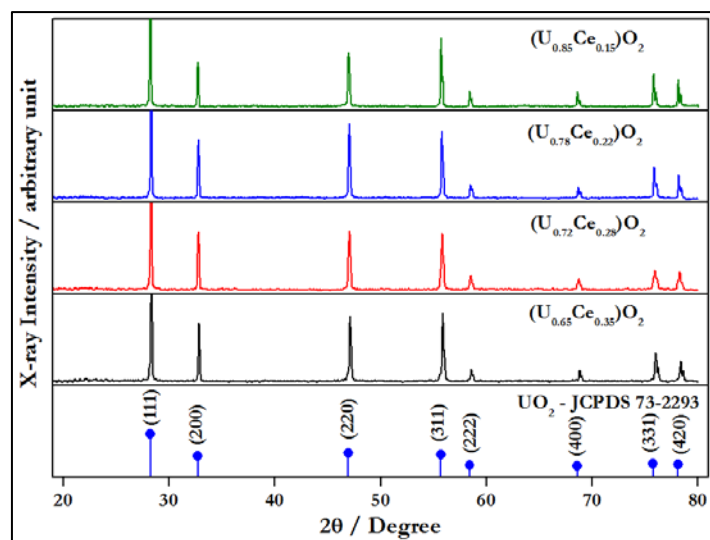


6.4 Characterisation of powders and compacts

The impurities present in the starting materials were analyzed using an inductively coupled plasma mass spectrometer (ICPMS). The surface area of the powders was measured by the BET method. The particle size distribution was analyzed using Mastersizer, supplied by M/s. Malvern, Worcestershire, UK. Simulated UO_2 - CeO_2 MOX pellets of all compositions were powdered and characterized by powder X-ray diffraction

(XRD). The XRD pattern of the solid solutions (Fig. 6.2) showed the absence of peaks due to neat UO_2 and neat CeO_2 , confirming the formation of solid solution.

Fig. 6.2. XRD pattern of the sintered urania-ceria simulated MOX pellets of all compositions



Lattice parameters were derived from the XRD patterns of the uranium–cerium MOX and also computed from the lattice parameters of UO_2 and CeO_2 from literature⁸, using Vegard’s law⁹. The two sets of lattice parameters are in good agreement with each other and with those available in the literature¹⁰. The average crystallite size of the powders was measured by X-ray line broadening technique using the Scherer formula¹¹. The instrumental broadening was obtained using standard silicon sample. The density of the green as well as sintered compacts was measured by using the Archimedes principle with di-butyl phthalate as the pycnometric liquid.

Compositional characterization was done by HPLC. Accurately weighed amounts of pellets of all the MOX compositions were dissolved in nitric acid. After appropriate dilution, their compositions was measured by HPLC which was pre-calibrated with known standards of U(VI) and Ce(IV). Separation of cerium ions and uranyl ions by Reverse phase HPLC. C18 10 cm monolith (M/s Merck) column was employed. The mobile phase used was 0.1 M alpha hydroxy isobutyric acid (pH adjusted to 4 with dil. NH_3) at a flow rate of 2 mL/min. Post-column detection of metal ions was done by mixing with Arsenazo(III) (1 mL/min) at 655 nm. The concentration of Arsenazo(III) was 10^{-4} M.

6.5 Effect of initial acidity on the dissolution kinetics of simulated U, Ce MOX pellets

6.5.1. Introduction

The simulated $\text{UO}_2\text{-CeO}_2$ MOX pellets of all the compositions fabricated were subjected to dissolution in nitric acid under the same conditions as carried out for UO_2 pellets described in the previous chapter. First studies were carried out to evaluate the effect of initial concentration of nitric acid on the dissolution kinetics of these pellets. For this purpose, the simulated $\text{UO}_2\text{-CeO}_2$ MOX pellet composition $(\text{U}_{0.78}\text{Ce}_{0.22})\text{O}_2$ was chosen. The same cylindrical glass reactor which was used for UO_2 pellet dissolution studies was used for studying the dissolution of simulated MOX pellets (Figures 10 and 11 in Chapter 5). The amount of nitric acid and the number of pellets required for each dissolution run was chosen such that the end total metal ion concentration is in the range of 240 g/L as it was done in the UO_2 dissolution experiments. Mixing rate was fixed at 600 RPM and the temperature at 353 K. The initial concentrations of acid chosen for the experiments were 6, 8, 10 and 11.5. The concentration of uranium and cerium were measured using HPLC as described earlier in the thesis (section 4.9).

6.5.2. Results and discussion

The dissolution curve for all the experiments were given pictorially in the following figures. Fig. 6.3 clearly indicates the effect of initial concentration of nitric acid which is directly proportional to the dissolution rate. The time taken for the complete dissolution of the (U, Ce) MOX pellets at 8 M initial concentration of acid is around 1020 mins. Under similar conditions the time taken for the complete dissolution of almost similar quantity of sintered UO_2 pellets fabricated through powder metallurgical route is about 1050 mins (Fig. 5.18, section 5.6.3). That is, the simulated uranium ceria MOX pellets containing 22 atom percent of Ce fabricated by combustion synthesis route dissolves faster than the pure sintered UO_2 pellets fabricated by the conventional powder metallurgical route. This clearly shows the effect of fabrication route on the dissolution kinetics of the nuclear fuel pellets in nitric acid which is very much comparable. Another feature of the above dissolution curve that needs attention is its typical 'S' shape which was also found in the dissolution curve of UO_2 pellets. This is because the major component of the fuel being uranium here, its behaviour is also same.

Fig. 6.3. Effect of initial concentration of acid on the dissolution of $(U_{0.78}Ce_{0.22})O_2$

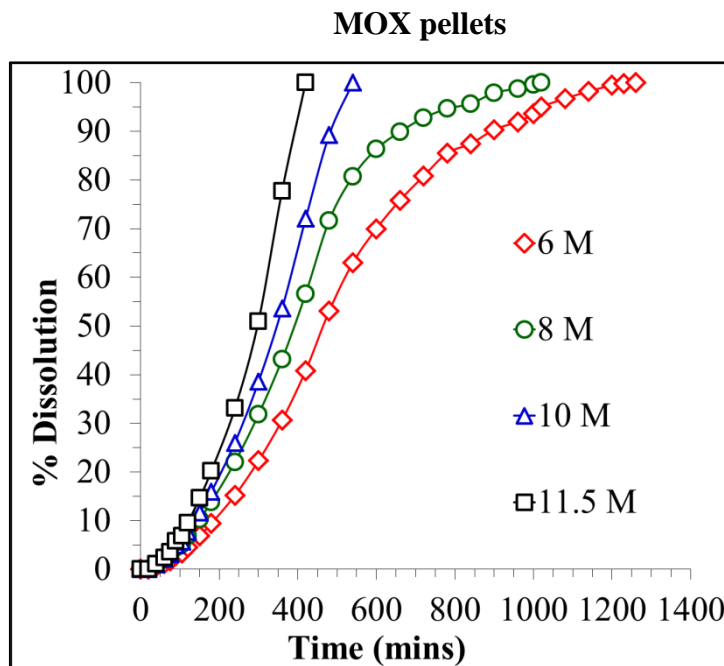
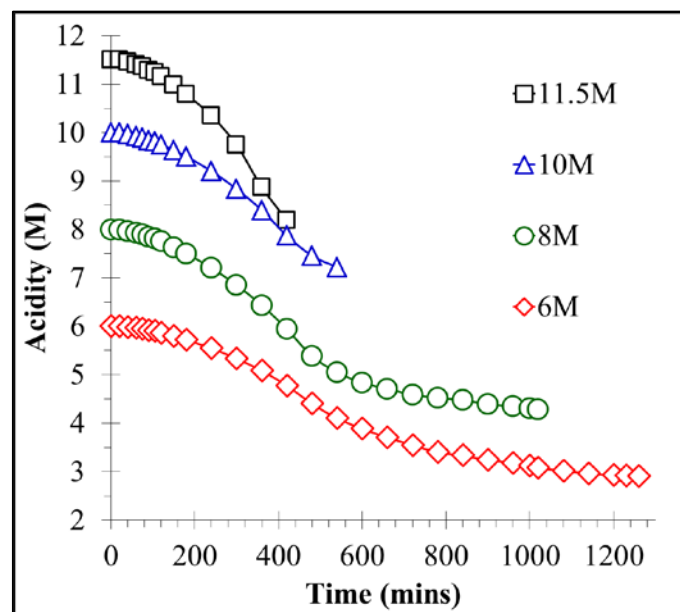


Fig. 6.4. Acidity profile for the dissolution of $(U_{0.78}Ce_{0.22})O_2$ MOX pellets at different acidities

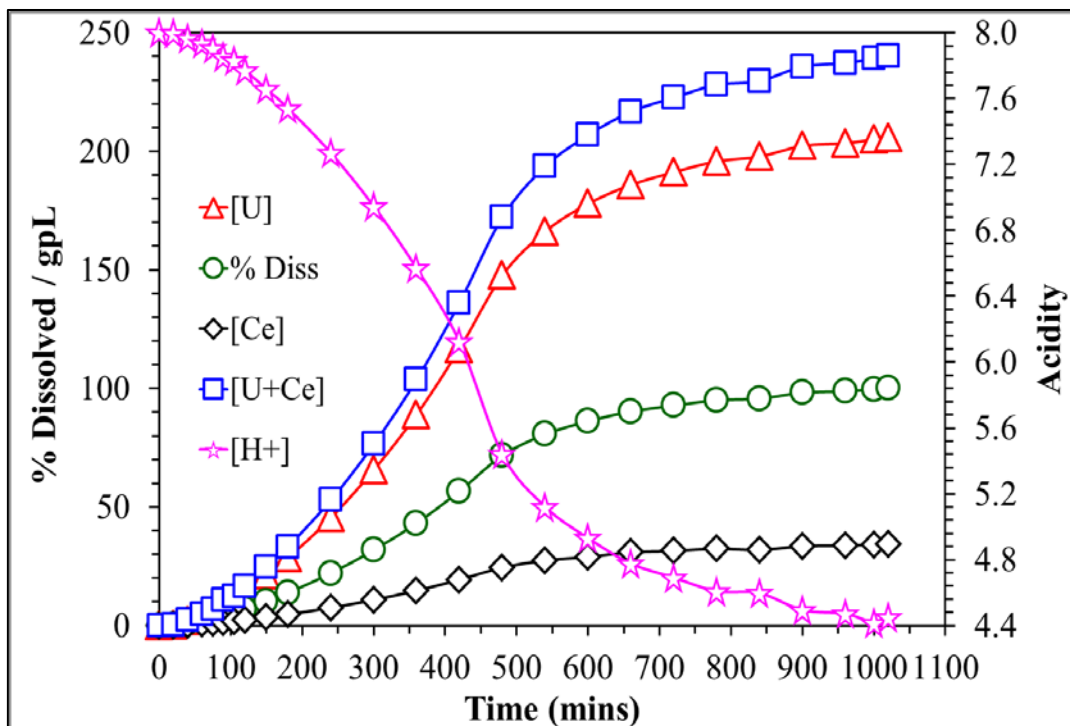


The profile of the acidity during the course of dissolution of the simulated MOX pellet is given in Fig. 6.4. During the analysis of the samples of these experiments, it was also found that, the composition of uranium and cerium did not vary in the liquid phase all through each of the dissolution run of all the compositions of the simulated MOX pellets.

And the composition of uranium and cerium in the liquid was always same as that of the dissolving solid pellet. This is indicated in Fig. 6.6 wherein the percentage dissolution of uranium and Ce were plotted as a function of time for the dissolution of $(U_{0.78}Ce_{0.22})O_2$ MOX pellets in 8 M nitric acid at 353 K. This is a fair indication of the formation of the solid solution in the pellets during its sintering.

Fig. 6.5 provides the typical concentration profiles of uranium, cerium and nitric acid as a function of time for the dissolution of $(U_{0.78}Ce_{0.22})O_2$ MOX pellets in 8 M nitric acid at 353 K. Fig. 6.5 also shows the variation in percentage dissolution of uranium, cerium and the total heavy metal (uranium and cerium put together). As the range of values for the acidity profile alone is very different, it is plotted on a different scale which is given in the right side y axis in the figure.

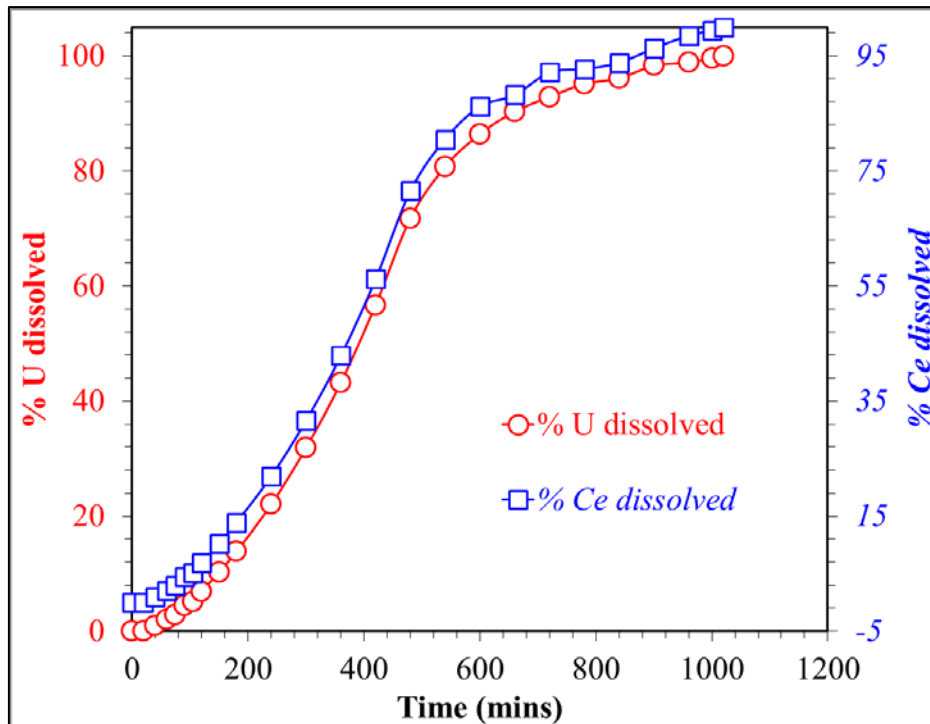
Fig. 6.5. U and Ce dissolved during the dissolution of $(U_{0.78}Ce_{0.22})O_2$ MOX pellets in 8 M HNO_3 at 353 K



In Fig. 6.6 both uranium and cerium percentage dissolution profile was plotted as a function of time in different y-axis on either side vertically. As the values of both the profiles are same, the two y axes are staggered by 5% so that both the curves lie parallel to each other clearly depicting their similarity. This is done for the ease of understanding.

The profiles of metal ion concentrations and nitric acid concentration generated in these experiments were later used for modeling this reaction and arriving at its rate equation.

Fig. 6.6. U and Ce percentage during the dissolution of $(U_{0.78}Ce_{0.22})O_2$ MOX pellets in 8 M HNO_3 at 353 K



6.6 Effect of cerium composition

6.6.1. Preamble

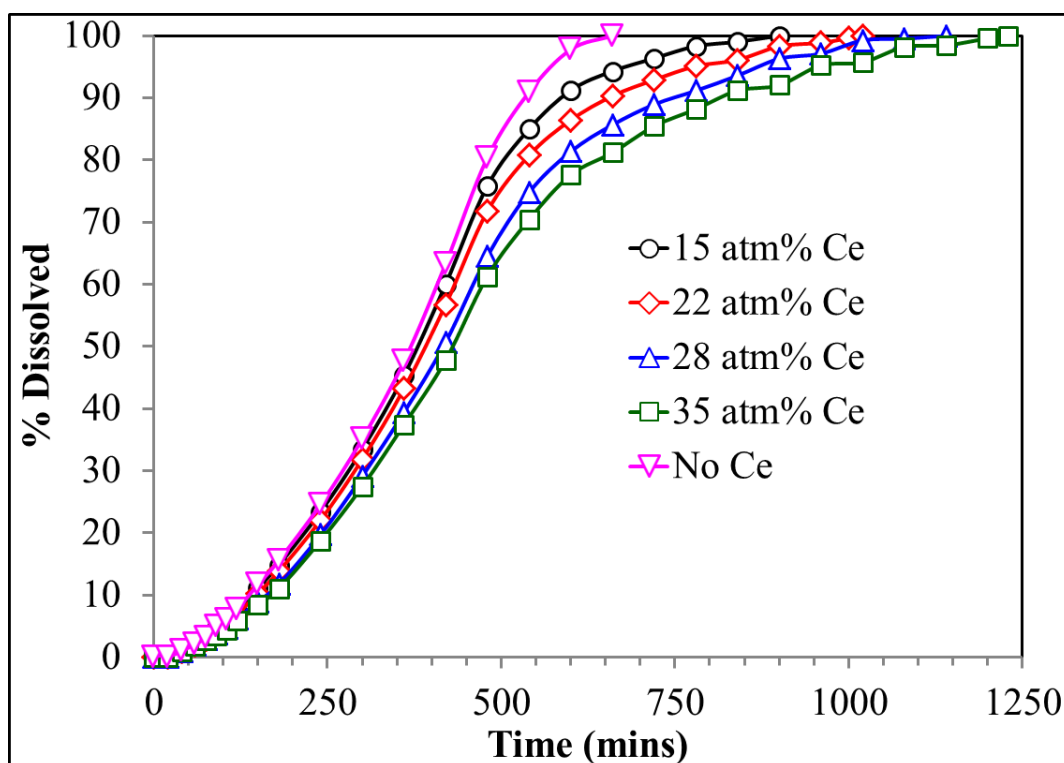
The effect of plutonium concentration in the MOX fuel on its dissolution kinetics in nitric acid medium is well documented in the literature¹². MOX fuel with various compositions of plutonium has been proposed and used as driver fuel in nuclear reactors world over till date. Hence it is required to study the dissolution behaviour of nuclear fuels as a function of plutonium composition. As Ce is employed as the non-radioactive surrogate of plutonium, it is logical and mandatory to study the influence of its composition on the dissolution kinetics of the simulated MOX fuel pellets in nitric acid.

6.6.2. Experiments, results and discussion

Simulated urania ceria MOX pellets of all the four compositions that were fabricated were subjected to dissolution in nitric acid under similar conditions. The initial concentration of

nitric acid and the mixing rate for all these dissolution experiments were fixed at 8 M and 600 RPM respectively. The number of pellets and the amount of nitric acid employed in each of this experiment were chosen such that the final metal ion concentration (uranium and cerium put together) is around 240 g/L. The concentrations of uranium and cerium were analyzed by HPLC as reported earlier in this chapter. The result is given pictorially in Fig. 6.7 which clearly depicts the effect of Ce composition on the dissolution kinetics of simulated MOX pellets. As Ce increases in the MOX fuel pellet, it renders its dissolution sluggish in nitric acid. This is very similar to the effect of plutonium composition in the MOX pellet. Again in all the above experiments, the dissolution curve features the ‘S’ shape indicating the autocatalytic effect of nitrous acid

Fig. 6.7. Effect of Ce composition on the dissolution kinetics of simulated uranium ceria MOX pellets in nitric acid



The concentration profiles of all the species in the reaction namely U(VI), Ce(IV) and nitric acid for the dissolution of $(U_{0.78}Ce_{0.22})O_2$ MOX pellet is shown in Fig. 6.8. Though it is a well-documented fact that uranium in the MOX dissolves faster than Ce or Pu, the above results clearly indicates that the rate at which both uranium and cerium comes into the solution is exactly the same. That is the composition of the pellet and solution with

respect to uranium and cerium was same all through the dissolution reaction. This was the case in the dissolution of simulated urania ceria MOX pellets of all the compositions prepared in this work.

This indicates that preferential leaching of uranium in the MOX pellets over cerium is not seen unlike in the case of U, plutonium MOX pellets which will be discussed in the next chapter of this thesis. This further reiterates the formation of solid solution in all these pellets during its fabrication. This result makes it an interesting case to study the effect of mixing on the dissolution kinetics of all these pellets which was the next set of experiments carried out.

6.7 Effect of mixing on the dissolution kinetics of simulated MOX pellets

6.7.1. Introduction

In Chapter 5 the effect of mixing rate on the dissolution kinetics of UO_2 in nitric acid has been discussed in detail. As UO_2 being the predominant fuel component of simulated urania ceria MOX pellets of all compositions, it becomes interesting and important to the study the effect of mixing intensity on the dissolution of all these simulated MOX pellets in nitric acid under similar conditions.

6.7.2. Experiments, results and discussion

Simulated urania ceria MOX pellets of all the four compositions were subjected to dissolution in 8 M nitric acid and 353 K with mixing intensities of 100 and 600 RPM very similar to the dissolution runs carried out for UO_2 pellets. Figures 6.8 and 6.9 shows the concentration profiles of all the species present in solution as a function of RPM for two of the simulated urania ceria MOX pellets of PFBR fuel compositions, namely, $(\text{U}_{0.78}\text{Ce}_{0.22})\text{O}_2$ and $(\text{U}_{0.72}\text{Ce}_{0.28})\text{O}_2$.

Both Figures 6.7 and 6.8 clearly bring out the retarding effect of mixing on the dissolution kinetics of simulated urania ceria MOX fuel pellets in nitric acid. This behaviour of the simulated MOX pellet is similar to that of UO_2 pellets under similar conditions. This is because the major component of the fuel in the simulated MOX fuel is uranium (72 and 78 atom percent). But it is interesting to note that there is no preferential leaching of uranium over cerium in the simulated MOX pellet during its dissolution.

Fig. 6.8. Concentration profiles of all the species during the dissolution of $(U_{0.78}Ce_{0.22})O_2$ MOX pellet in 8 M HNO_3 at 100 and 600 RPM

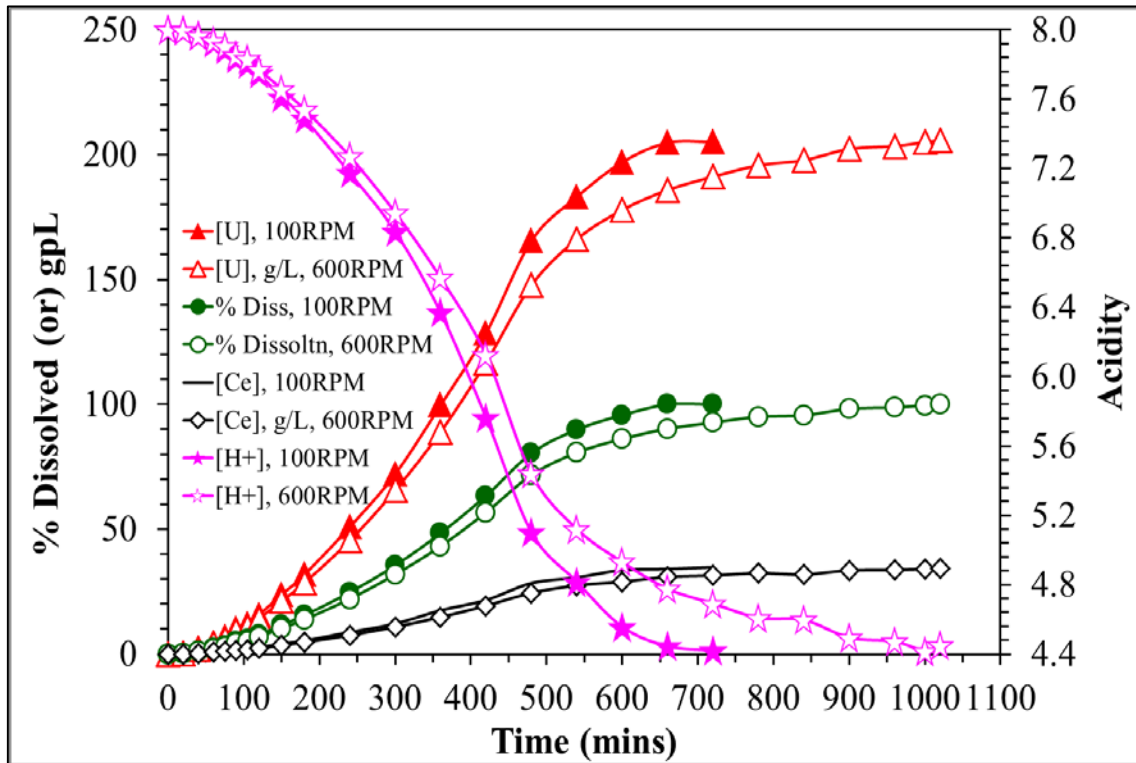
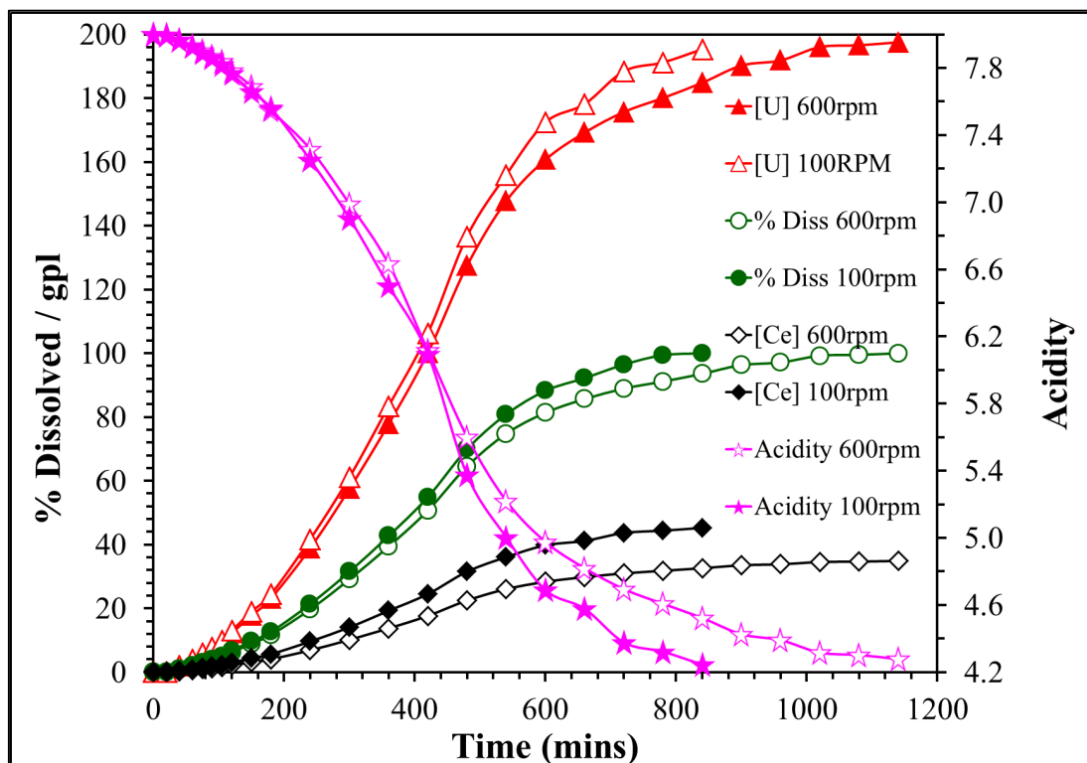


Fig. 6.9. Concentration profiles of all the species during the dissolution of $(U_{0.72}Ce_{0.28})O_2$ MOX pellet in 8 M HNO_3 at 100 and 600 RPM



This justifies the formation of solid solution in these MOX pellets completely. Within the errors of the experimental results, the composition of uranium and cerium in the solution was found to be always the same as that of the dissolving simulated MOX pellet.

6.8 *Effect of temperature on the dissolution kinetics of simulated MOX pellets*

6.8.1 *Introduction*

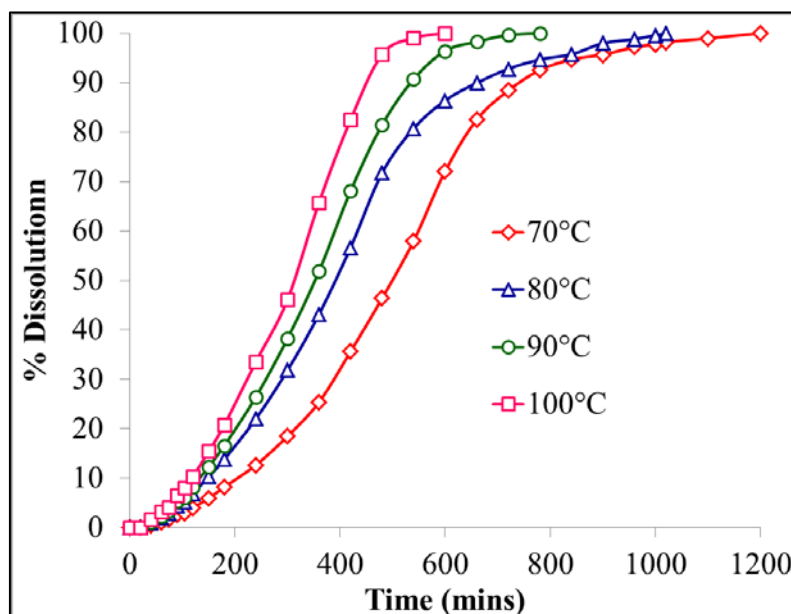
The effect of temperature is one of the fundamental parameter required to be generated to model any chemical reaction. Hence the effect of temperature on the dissolution kinetics of the simulated urania ceria MOX pellets in nitric acid was investigated.

6.8.2 *Experiments, results and discussion*

The same cylindrical glass reactor which was used for UO₂ pellet dissolution was employed for these experiments. The initial concentration of nitric acid and the mixing intensity were fixed at 8 M and 600 RPM respectively for this set of experiments. In all the experiments about 100 mL of nitric acid was employed. The temperatures chosen were 343, 353, 363 and 373 K. The numbers of pellets were chosen such that the final concentration including both U and Ce at the end of each run is about 240 g/L. In each experiment, nitric acid of required concentration and quantity will first be taken in the cylindrical glass dissolver and heated to a preset temperature. Once the set temperature is reached, the pellets were carefully lowered into the hot nitric acid and the mechanical glass impeller was set at 600 RPM simultaneously initiating the timer. At periodic intervals of time, samples were taken and analyzed for acidity, uranium and cerium ion concentrations. As indicated earlier in this chapter, uranium and cerium were analyzed simultaneously by HPLC.

The plot of percentage dissolution against time as a function of various temperature is given in Fig. 6.10 for (U_{0.72}Ce_{0.28})O₂ simulated MOX pellet. Similar trends were seen for all the compositions of the simulated MOX pellet. Some of the most prominent features of these plots are the curve is 'S' shaped indicating the autocatalytic nature of UO₂ dissolution. Further, temperature has a positive effect on the dissolution kinetics of simulated urania ceria MOX like most of the reactions.

Fig. 6.10. Effect of temperature on the dissolution rate of simulated urania ceria MOX pellets in nitric acid

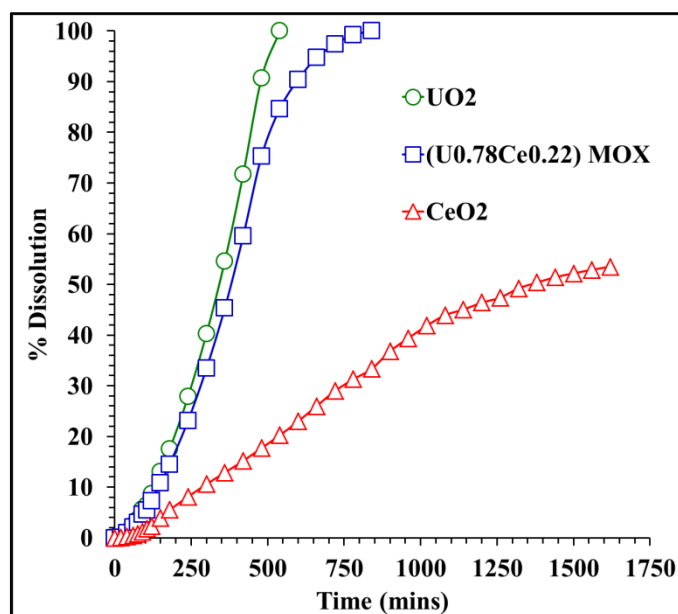


6.8.3. Role of nitrous acid on the dissolution of simulated MOX pellets

The effect of nitrous acid on the dissolution kinetics of UO_2 fuel pellets in nitric acid had been investigated and well established in the previous chapter. Hence experiments were conducted with UO_2 , $(\text{U}_{0.72}\text{Ce}_{0.28})\text{O}_2$ simulated MOX pellet and pure sintered ceria pellets (fabricated in the same way as the simulated MOX pellet) under similar conditions. These dissolution runs were conducted in the same cylindrical glass dissolver used for all the experiments till date. The temperature was fixed at 353 K and a mixing rate of 600 RPM. NO_2 gas (5000 PPM) was constantly purged into the reaction mixture during dissolution to ensure sufficient availability of nitrous acid during the reaction. In order to compare the results, the initial amount of pellets (in terms of moles of metal atoms) was kept same in all the above experiments. Around 100 mL of nitric acid with an initial concentration 8 M was used in all these experiments. The results of the above experiment are presented in Fig. 6.11.

The result presented in Fig. 6.11 clearly indicates that as more cerium is added to UO_2 pellets to make it a MOX, the dissolution rate decreases finally leading to CeO_2 pellet with the least rate of dissolution under similar conditions. This along the expected lines of thinking that as uranium composition in the MOX is reduced, the rate of its dissolution in nitric acid also gets reduced accordingly.

Fig. 6.11. Effect of cerium on the dissolution of (U, Ce)MOX pellets in nitric acid

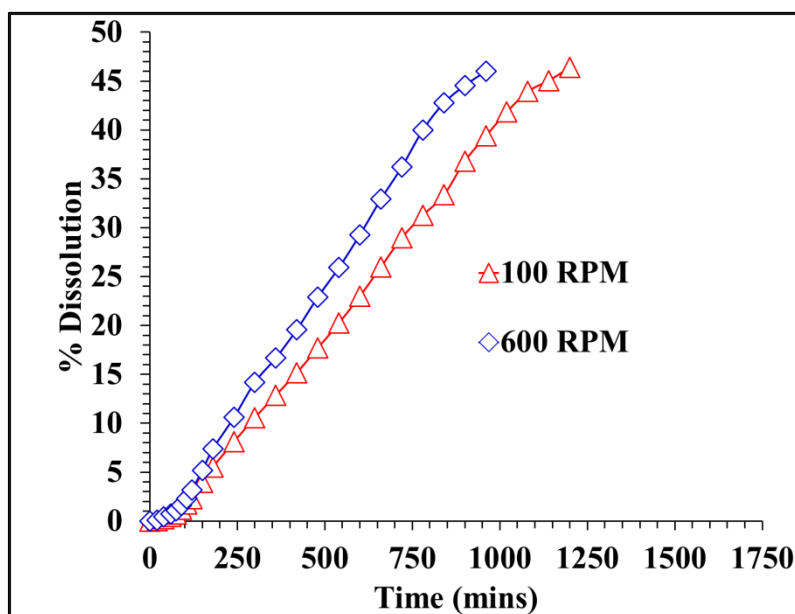


It was also found that when NO₂ gas is purged into the reaction mixture during dissolution, both UO₂ and the simulated urania ceria MOX pellets dissolved faster than in the absence of NO₂ gas. But in the case of CeO₂ pellets, time taken for the complete dissolution of the same mass of pellet in nitric acid under similar conditions was almost the same irrespective of the presence of absence of NO₂ gas. This is because, as uranium undergoes oxidative dissolution, presence of NO₂ gas catalyzes the reaction by producing nitrous acid in-situ. But cerium is present in the same oxidation state of 4 both in solid and liquid. Hence NO₂ gas did not influence the rate of dissolution of CeO₂.

In order to study the effect of mixing on the dissolution kinetics of CeO₂, ceria pellets fabricated by similar procedure as that of simulated urania ceria MOX pellets was subjected to dissolution in a similar cylindrical glass dissolver in 8 M initial concentration of nitric acid at 353 K under two different mixing rates of 100 and 600 RPM. Since CeO₂ is independent of the presence of NO₂ gas, these pellets were expected to exhibit increased dissolution rate when the mixing intensity is increased. The results of these experiments are presented in Fig. 6.12 which clearly confirms that ceria dissolution rate in nitric acid is proportional to the rate of mixing. But a similar effect of mixing is not seen in the simulated urania ceria MOX pellets. This is because; uranium (major component in the simulated MOX pellets) undergoes oxidative dissolution in nitric acid whose rate is inversely related to mixing due to the dispersion of nitrous acid away from the pellet solution interface. As cerium is the minor component of the solid solution, the overall rate

is dictated by the chemical behaviour of urania, whereas in the case of dissolution of pure ceria pellets, such constraints are not present..

Fig. 6.12. Effect of mixing on CeO₂ dissolution rate in nitric acid



All the results presented in this chapter so far, were used for modeling the dissolution reaction of simulated urania ceria MOX fuel pellets in nitric acid which is presented in the following section.

6.9 Modeling of simulated MOX dissolution behavior

6.9.1. Introduction

The methodology adopted for modeling the dissolution of simulated urania ceria MOX pellets in nitric acid was similar to the methods which were already developed for understanding the dissolution behavior of UO₂ pellets in nitric acid presented in section 5.10.

6.9.2. Methodologies

The analytical methods employed for analyzing the dissolution behavior of UO₂ pellets in nitric acid was employed for evaluating the kinetics of dissolution urania ceria MOX pellets in nitric acid also.

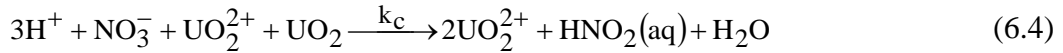
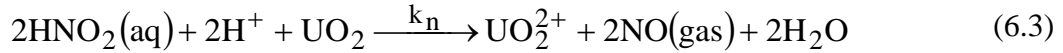
6.9.2.1. Method 1 – Based on surface penetration of nitric acid into pellets

In this method, dissolution reaction is expressed by a two-step scheme as given below¹³.



Where W_{ue} is the unexposed mass of fuel, W_e is the exposed mass and W_d the dissolved mass. The first process in the above equation is the penetration process and its rate may be proportional to the concentration of nitric acid in the solution. While the latter process in the above equation is the chemical reaction.

The reactions between UO_2 and ions in the nitric acid solution under these experimental conditions were assumed as follows^{14, 15}.



The reactions between CeO_2 and ions in the nitric acid solution under these experimental conditions was assumed as



Where k_{ce} is the rate constant for the nitric acid aided dissolution reaction of ceria pellets.

6.9.2.1.1. Case-I: Considering the effect of nitrous acid to be negligible

The dissolution experiments on simulated urania ceria MOX pellets in nitric acid was conducted at high stirring speed (600 rpm). Hence the concentration of HNO_2 at solid-liquid interface is very much less. So the dissolution of UO_2 due to nitrous acid could be neglected (equation 6.3 is not considered).

The rate equations obtained based on eqn (6.2).eqn (6.4) and eqn (6.5) neglecting eqn (6.3) are given as follows.

$$\frac{dW_{ue}}{dt} = -k_p [\text{HNO}_3] W_{ue} \quad (6.6)$$

$$\frac{dW_e}{dt} = k_p [\text{HNO}_3] W_{ue} - (k_h [\text{HNO}_3]^2 + k_c [\text{HNO}_3]^2 [\text{UO}_2^{2+}] + k_{ce} [\text{HNO}_3]^2) W_e \quad (6.7)$$

$$\frac{d[\text{UO}_2^{2+}]}{dt} = (MV)^{-1} (k_h [\text{HNO}_3]^2 + k_c [\text{HNO}_3]^2 [\text{UO}_2^{2+}]) W_e \quad (6.8)$$

$$\frac{d[\text{Ce}^{4+}]}{dt} = (MV)^{-1} (k_{ce} [\text{HNO}_3]^2) W_e \quad (6.9)$$

$$\frac{d[\text{HNO}_3]}{dt} = -(M V)^{-1} (3k_h [\text{HNO}_3]^2 + 3k_c [\text{HNO}_3]^2 [\text{UO}_2^{2+}] + 4k_{ce} [\text{HNO}_3]^2) W_e \quad (6.10)$$

Where k_p is the rate constant for the penetration process, M is the molecular weight of mixed oxide and V is the volume of the reacting solution.

The experimental data of concentrations of nitric acid, uranium and cerium as a function of time were fitted into above rate equations using a nonlinear regression technique to obtain rate constant that best correlates the experimental data. The best values were obtained by minimizing the following objective function.

$$f = \sum_1^n 20 * (C_{U_{exp}} - C_{U_{calc}})^2 + \sum_1^n (C_{\text{HNO}_3_{exp}} - C_{\text{HNO}_3_{calc}})^2 + \sum_1^n 20 * (C_{\text{Ce}_{exp}} - C_{\text{Ce}_{calc}})^2 \quad (6.11)$$

The rate constants k_p , k_h , k_c and k_{ce} were calculated at different conditions of temperature and acidity. The values of rate constants and corresponding standard deviation are given in tables 6.1 and 6.2 respectively for different temperatures and acidity.

Table 6.1. Rate constants for simulated MOX fuel dissolution at different temperatures

T(K)	343	353	363	373
k_p ([L/mol]/min)	4.05E-04	4.97E-04	7.95E-04	7.39E-04
k_h ([L/mol]²/min)	3.17E-05	2.43E-05	1.81E-05	2.54E-05
k_c ([L/mol]³/min)	1.05E-04	2.54E-04	2.98E-04	3.83E-04
k_{ce} ([L/mol]³/min)	1.06E-05	1.46E-05	1.42E-05	1.88E-05
sd(U)	0.0176	0.0083	0.0099	0.0109
sd(HNO₃)	0.0832	0.0359	0.0449	0.0472
sd(Ce)	0.0085	0.0092	0.0094	0.0088

Table 6.2. Rate constants for the dissolution of simulated MOX fuel

[HNO ₃] (M)	6	8	10	11.5
k_p ([L/mol]/min)	5.30E-03	4.97E-04	4.11E-04	4.03E-04
k_h ([L/mol] ² /min)	5.13E-06	2.43E-05	1.98E-05	1.48E-05
k_c ([L/mol] ³ /min)	3.57E-04	2.54E-04	2.53E-04	2.77E-04
k_{ce} ([L/mol] ³ /min)	5.25E-06	1.46E-05	1.24E-05	1.21E-05
sd(U)	0.0108	0.0083	0.008	0.0105
sd(HNO ₃)	0.0298	0.0359	0.0312	0.0385
sd(Ce)	0.0063	0.0092	0.0068	0.0089

The concentration profiles of uranium, nitric acid and cerium during the course of dissolution were determined using the model equations 6.6 to 6.10. The comparison between experimental and calculated values of [U(VI)], [HNO₃] and [Ce] vs time at 343 K are shown as semi log plots in the Figures 6.13 to 6.15. Similar plots were also generated for each of the conditions mentioned in the tables 6.2 and 6.3.

From the data given in Table 6.1, the activation energy for all the processes were estimated from Arrhenius equation to be about 34.8, 29, 43.5 and 18.3 kJ/mol for rate constants k_p , k_h , k_c and k_{ce} respectively in the temperature range 343-373 K.

Fig. 6.13. Modelled uranium concentration profile for the dissolution of (U_{0.78}Ce_{0.22})O₂ MOX pellet in 8 M HNO₃ at 343 K and 600 RPM

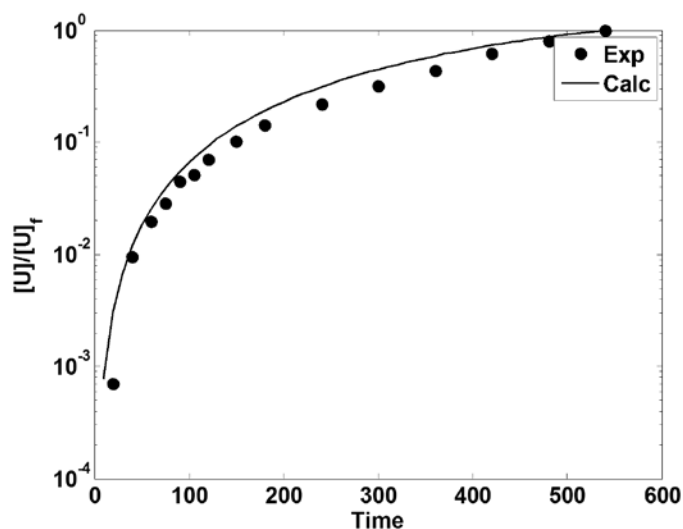


Fig. 6.14. Modelled nitric acid concentration profile for the dissolution of $(U_{0.78}Ce_{0.22})O_2$ MOX pellet in 8 M HNO_3 at $70^\circ C$ and 600 RPM

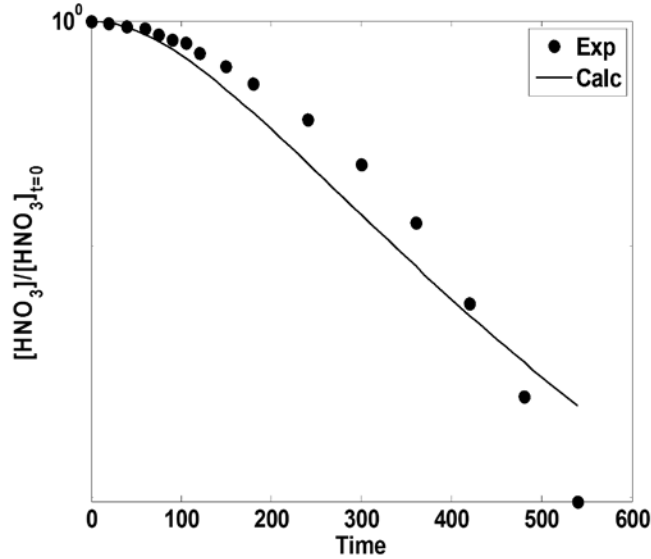
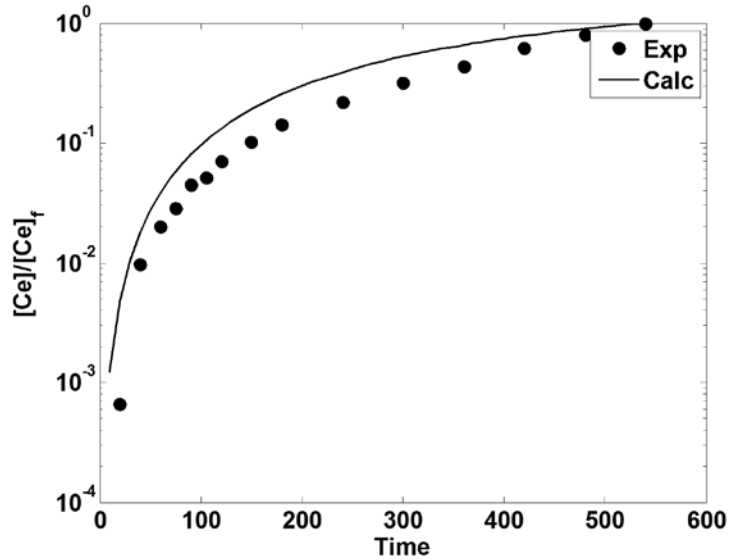


Fig. 6.15. Modelled cerium concentration profile for the dissolution of $(U_{0.78}Ce_{0.22})O_2$ MOX pellet in 8 M HNO_3 at $70^\circ C$ and 600 RPM



6.9.2.1.2. Case II: Neglecting the autocatalytic effect of uranyl ion in solution

If autocatalytic effect of uranyl ion is not considered over and above the effect of nitrous acid, then eqn (6.4) also need not be considered for deriving the rate equations along with eqn (6.3). In that case, the rate equation gets modified as follows.

$$\frac{dW_{ue}}{dt} = -k_p [\text{HNO}_3] W_{ue} \quad (6.12)$$

$$\frac{dW_e}{dt} = k_p [\text{HNO}_3] W_{ue} - (k_h [\text{HNO}_3]^2 + k_{ce} [\text{HNO}_3]^2) W_e \quad (6.13)$$

$$\frac{d[\text{UO}_2^{2+}]}{dt} = (MV)^{-1} (k_h [\text{HNO}_3]^2) W_e \quad (6.14)$$

$$\frac{d[\text{Ce}^{4+}]}{dt} = (MV)^{-1} (k_{ce} [\text{HNO}_3]^2) W_e \quad (6.15)$$

$$\frac{d[\text{HNO}_3]}{dt} = -(M V)^{-1} (3k_h [\text{HNO}_3]^2 + 4k_{ce} [\text{HNO}_3]^2) W_e \quad (6.16)$$

The experimental data of concentrations of nitric acid, uranium and cerium as a function of time were fitted into above rate equations using a nonlinear regression technique to obtain rate constant that best correlates the experimental data. The best values were obtained by minimizing the following objective function.

$$f = \sum_1^n 20 * (C_{U_{exp}} - C_{U_{calc}})^2 + \sum_1^n (C_{\text{HNO}_3_{exp}} - C_{\text{HNO}_3_{calc}})^2 + \sum_1^n 20 * (C_{\text{Ce}_{exp}} - C_{\text{Ce}_{calc}})^2 \quad (6.17)$$

The rate constants k_p , k_h and k_{ce} were calculated at different conditions of temperature and acidity. The values of rate constants and corresponding standard deviation for different temperatures and acidity are given in Tables 6.3 and 6.4 respectively.

Table 6.3. Rate constants for the dissolution of simulated MOX fuel at different temperatures

T(K)	343	353	363	373
k_p ([L/mol]/min)	4.12E-04	5.25E-04	6.32E-04	7.02E-04
k_h ([L/mol]²/min)	4.60E-05	6.21E-05	7.35E-05	8.30E-05
k_{ce} ([L/mol]³/min)	1.11E-05	1.29E-05	1.68E-05	1.88E-05
sd(U)	0.027	0.0278	0.0311	0.0293
sd(HNO₃)	0.1114	0.1059	0.134	0.1267
sd(Ce)	0.0082	0.0123	0.0108	0.0104

Table 6.4. Rate constants for simulated MOX fuel dissolution at different acidity

[HNO ₃] (M)	6	8	10	11.5
k_p ([L/mol]/min)	5.87E-04	5.17E-04	4.89E-04	5.38E-04
k_h ([L/mol] ² /min)	1.02E-04	6.32E-05	4.23E-05	4.05E-05
k_{ce} ([L/mol] ³ /min)	1.35E-05	1.32E-05	1.02E-05	1.02E-05
sd(U)	0.0294	0.0277	0.0208	0.0235
sd(HNO₃)	0.1248	0.1059	0.0997	0.1277
sd(Ce)	0.0037	0.0124	0.0046	0.0053

The concentration profiles of uranium, nitric acid and cerium during the course of dissolution were determined using the model equations 6.12 to 6.16. The comparison between experimental and calculated values of [U(VI)], [HNO₃] and [Ce] vs time at 343 K are shown as semi log plot in the Figures 6.16 to 6.18. Similar plots were also generated for each of the conditions mentioned in the tables 6.3 and 6.4.

Fig. 6.16. Modelled uranium concentration profile for the dissolution of (U_{0.78}Ce_{0.22})O₂ MOX pellet in 8 M HNO₃ at 70°C and 600 RPM

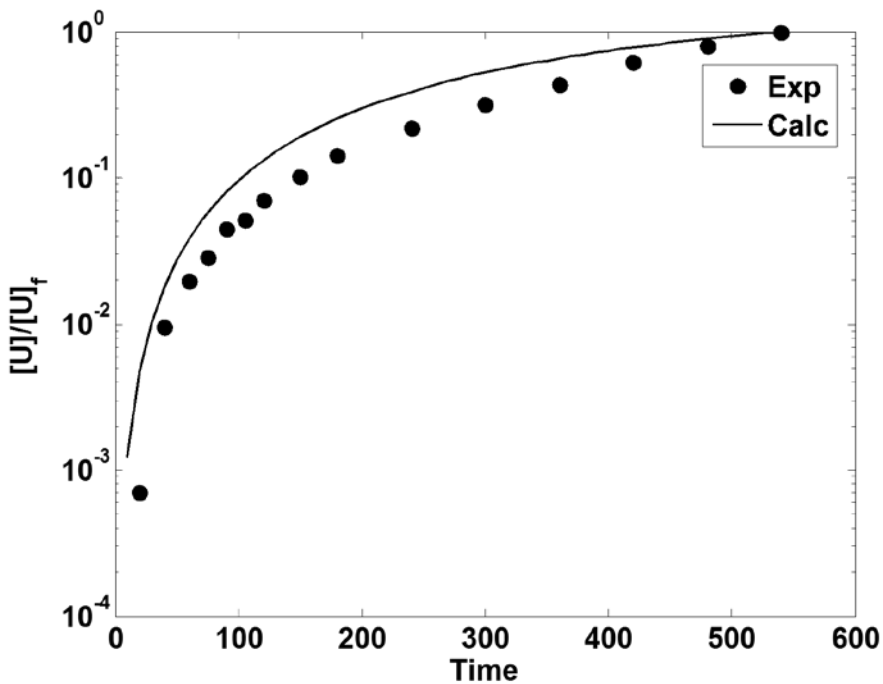


Fig. 6.17. Modelled nitric acid concentration profile for the dissolution of $(U_{0.78}Ce_{0.22})O_2$ MOX pellet in 8 M HNO_3 at $70^\circ C$ and 600 RPM

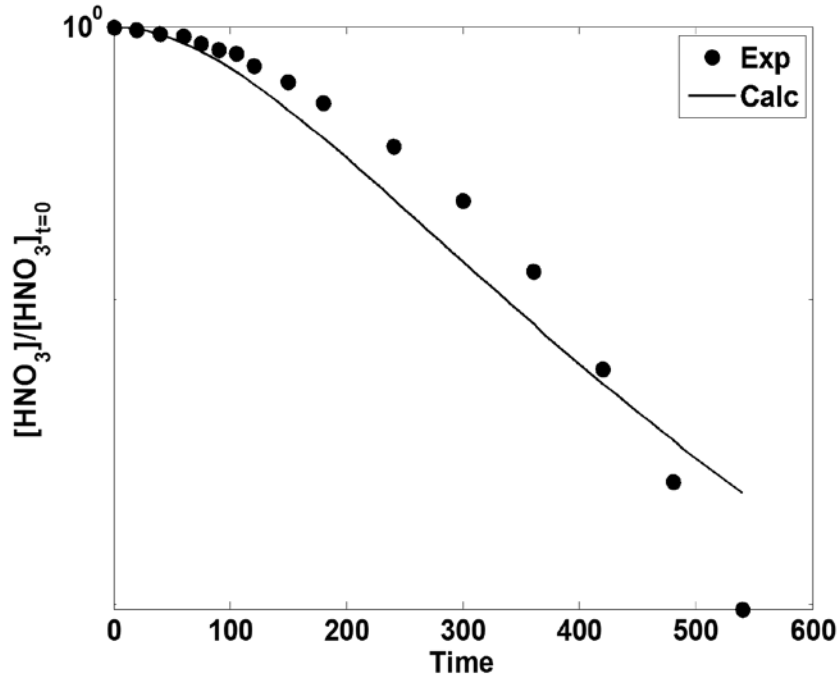
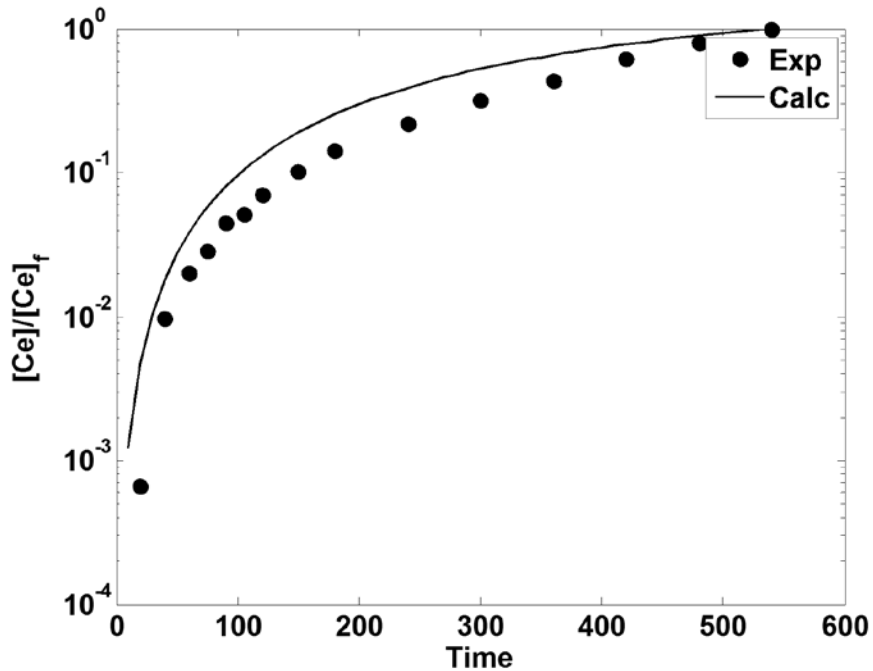


Fig. 6.18. Modelled cerium concentration profile for the dissolution of $(U_{0.78}Ce_{0.22})O_2$ MOX pellet in 8 M HNO_3 at $70^\circ C$ and 600 RPM



From the data given in Table 6.3, the activation energy for all the processes were calculated from Arrhenius equation and the values were found to be about 19.1, 20.7 and

19.6 kJ/mol for the rate constants k_p , k_h and k_{ce} respectively in the temperature range 343-373 K.

6.9.2.2. Method 2: Considering non-ideal nature of particle during the reaction

6.9.2.2.1. Introduction

Similar to the data analysis carried out for the dissolution of UO_2 pellets in section 5.10.3.3, the experimental data of the U, Ce MOX dissolution experiments was also analyzed considering the non-ideal nature of the particle during the reaction for the determinations of its kinetics.

6.9.2.2.2. Model equations

Here also the shrinking particle model was invoked by including the interaction of chemical reaction and diffusion together. Model equations were derived in the same way as that of UO_2 pellets dissolution. As this is a MOX pellet, while deriving the rate equation, the reaction of ceria with nitric acid also needs to be considered. Due to the presence of Ce as an additional species here, we will be ending up with three rate equations unlike in the case of UO_2 (where it was only 2), i.e. one each for predicting the concentration profile of nitric acid, uranyl ion and ceric ion in the solution as a function of time. In this derivation, the subscript 'A', 'B' and 'E' were used respectively to denote nitric acid, uranyl ion and ceric ion respectively. Here also the accessible surface area was taken into account and is denoted by A. It is calculated as per equation 5.88 given in the section 5.10.c.v in the previous chapter. The surface area (A) and the subscript A denoting nitric acid (X_A) are differentiated sufficiently all through the derivation. As the derivations are already explained in detail in section 5.10 of this thesis, the same is not repeated here. The final rate equations for determining the concentration profiles of various species are given in the following equations.

$$\text{for nitric acid, } \frac{dC_A}{dt} = (v_{AB}k_B C_{LA}^S + v_{AE}k_E C_{LA}^S) \cdot A \quad (6.18)$$

$$\text{For uranium, } \frac{dC_B}{dt} = v_B k_B C_{LA}^S \cdot A \quad (6.19)$$

$$\text{For cerium, } \frac{dC_E}{dt} = v_E k_E C_{LA}^s \cdot A \quad (6.20)$$

Here the values for the stoichiometric coefficients used are $v_{AB} = 2.75$, $v_{AE} = 4$, $v_B = v_E = 1$.

The rate constants were estimated at different temperatures. Comparison between experimental and calculated values of the concentration profiles of uranyl ion, ceric ion and bulk phase nitric acid were generated graphically as a function of time are shown in the figures in the following sections for various conditions as the case may be. The temperature dependency of the dissolution rate is governed by the Arrhenius equation. Thus the plot of $\ln(k)$ vs $1/T$ gives a slope equal to $(-E_a/R)$ from which the apparent activation energy of the dissolution reaction under the experimental conditions were estimated. The best values of the rate constants were obtained by minimizing the objective function given below.

$$f = \sum_1^n 20 * (C_{Bexp} - C_{Bcalc})^2 + \sum_1^n 50 * (C_{Abexp} - C_{Abcalc})^2 + \sum_1^n 50 * (C_{Eexp} - C_{Ecalc})^2 \quad (6.21)$$

The comparison between the experimental and calculated concentration profiles using the model equations were given graphically in the following sections for different cases.

The above model equations are applied for all the experimental data generated to study the effect of initial concentration of nitric acid, mixing rate (RPM) and temperature. For each of the above experiment, model equations were used to determine the rate constants for two different situations namely the order with respect to nitric acid being 1 and 2.

6.9.2.2.2.1. Case 1: Order w.r.t. nitric acid is 1

Figures 6.19 to 6.21 shows the comparison between the experimental and the predicted concentration profiles of nitric acid, uranium and cerium for the dissolution of $U_{0.78}Ce_{0.22}O_2$ MOX pellets in 8 M nitric acid at 353 K with the assumption that the order w.r.t. to nitric acid is unity. The experimental data only up to 60% of the dissolution was considered for modeling as the pellets crumble beyond that point beyond which the value of the shape factor is no more constant and changes very drastically.

Fig. 6.19. Comparison of experimental and calculated profiles of [U(VI)] at 353 K for $U_{0.78}Ce_{0.22}O_2$ MOX pellet dissolution assuming 1st order w.r.t. HNO_3

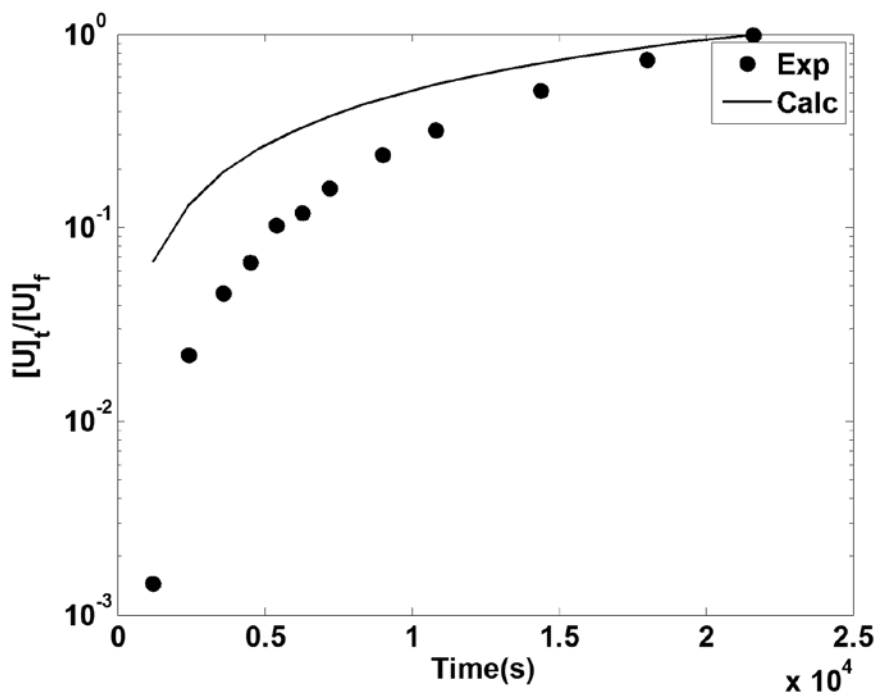


Fig. 6.20. Comparison of experimental and calculated 1st order $[HNO_3]$ profiles at 353 K for $U_{0.78}Ce_{0.22}O_2$ MOX pellet dissolution

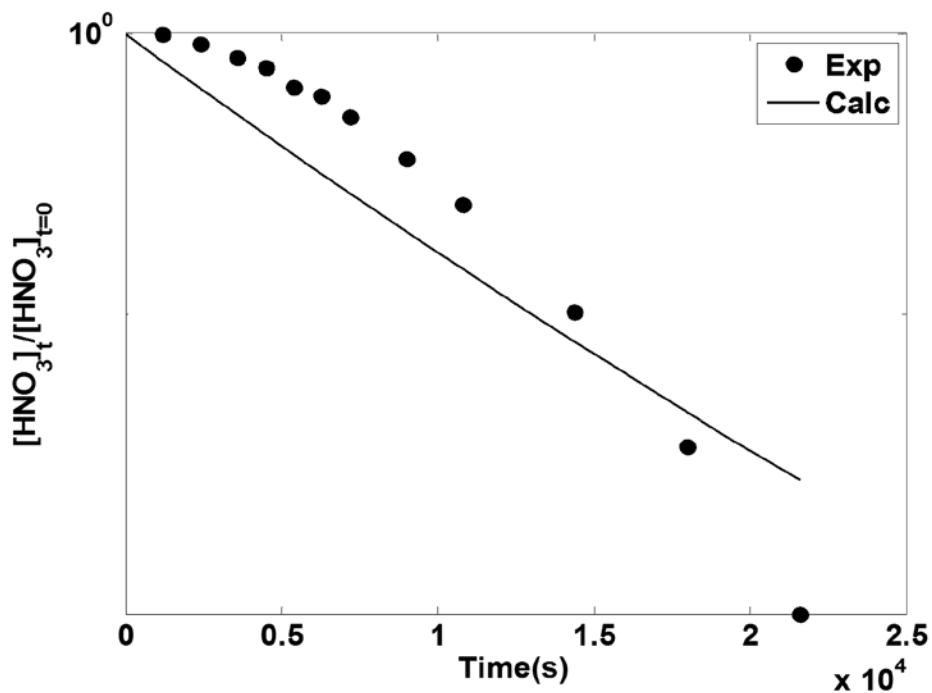
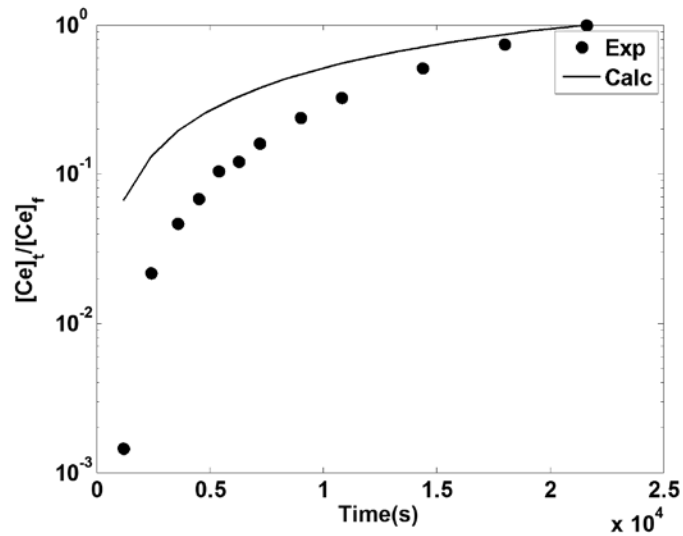


Fig. 6.21. Comparison of experimental and calculated profiles of [Ce(IV)] at 353 K for $U_{0.78}Ce_{0.22}O_2$ MOX pellet dissolution assuming 1st order w.r.t. HNO_3



6.9.2.2.2. Case 2: Order w.r.t. nitric acid is 2

Figures 6.22 to 6.24 shows the comparison between the experimental and the predicted concentration profiles of nitric acid, uranium and cerium for the dissolution of $U_{0.78}Ce_{0.22}O_2$ MOX pellets in 8 M nitric acid at 353 K with the assumption that the order w.r.t. to nitric acid is two. The experimental data only upto 60% of the dissolution was considered for modeling as the pellets crumble beyond that point beyond which the value of the shape factor is no more constant and changes very drastically.

Fig. 6.22. Comparison of experimental and calculated profiles of [U(VI)] at 353 K for $U_{0.78}Ce_{0.22}O_2$ MOX pellet dissolution assuming 2nd order w.r.t. HNO_3

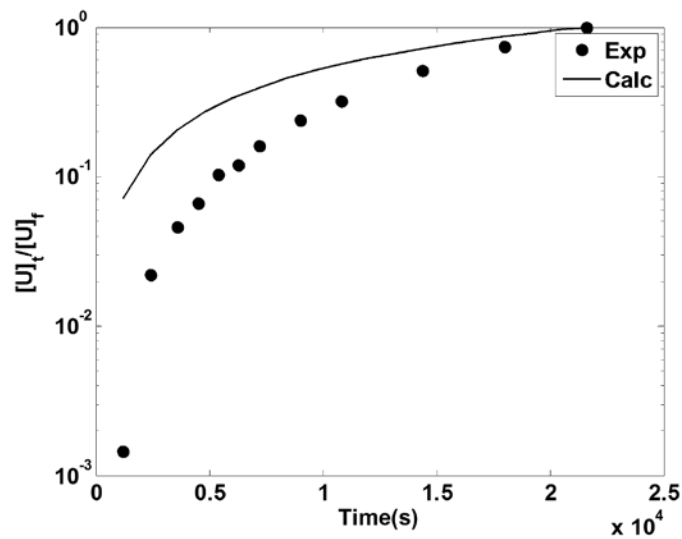


Fig. 6.23. Comparison of experimental and calculated 2nd order [HNO₃] profiles at 353 K for U_{0.78}Ce_{0.22}O₂ MOX pellet dissolution

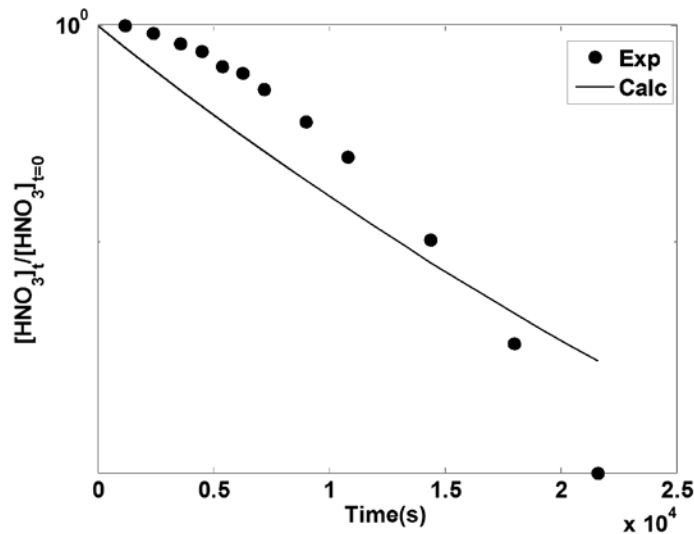
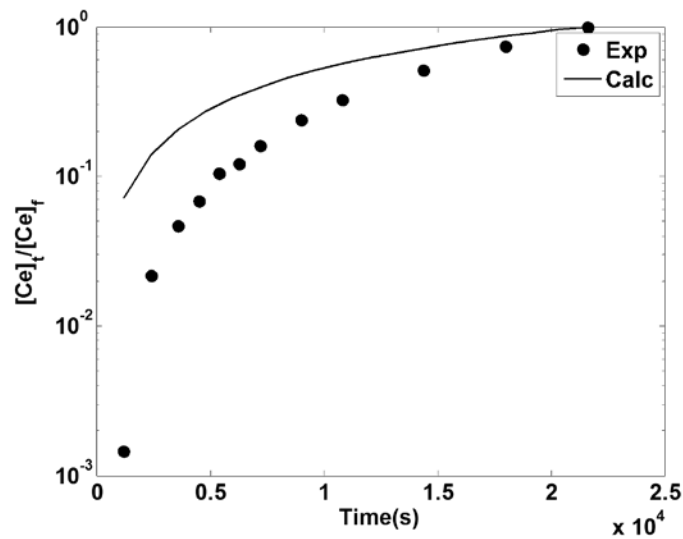


Fig. 6.24. Comparison of experimental and calculated profiles of [Ce(IV)] at 353 K for U_{0.78}Ce_{0.22}O₂ MOX pellet dissolution assuming 2nd order w.r.t. HNO₃



6.10 Conclusion on the modeling of simulated U, Ce MOX pellet dissolution

The modeling of the experimental data on the dissolution of simulated urania ceria MOX pellets in nitric acid medium under various conditions of acidity, temperature and mixing rate were carried out in two different methods, viz. penetration based and surface area based methods, very similar to that for UO₂ pellet dissolution mentioned in the previous chapter. As for as the simulated MOX pellets dissolution modeling is concerned, the

prediction of the concentration profiles of the various species involved in the reaction (like U, Ce and nitric acid) was found to be more accurate using the first method. This was not the case with UO_2 pellets, as discussed in the previous chapter, for which the surface area based method was found to be more accurate. This could be attributed to the lesser accuracy in the measurement of the surface area of the simulated MOX pellets. As the simulated MOX pellets were fabricated by combustion synthesis method wherein the solid powders of MOX was generated straightaway from the solution, their dissolution behaviour was much better than the sintered UO_2 pellets which was prepared by powder metallurgical route. Hence the pellets became porous much earlier during dissolution leading to its crumbling even at around 20-25% of dissolution by mass. Once the pellet crumbles, the uncertainty in measuring the surface area of the dissolving pellet as a function of time also goes up drastically. This leads to higher uncertainty in the surface area measurements and thereby the inaccuracy in the modeling of its dissolution using the surface area data also increased proportionately. But as the dissolution process nears its completion, the number of crumbled pieces also decreased. Hence the accuracy in the measurement of surface area as the process nears completion started getting better. This in turn led to better prediction of the concentration profiles of uranium and cerium towards the end of the dissolution process as seen in Figures 6.21 and 6.23 respectively.

When it comes to the order of the reaction with respect to nitric acid, the results of the models show that predicted concentration profiles are practically the same irrespective of the order being 1 or 2. Similarly, when the catalytic effect of uranyl ions in the solution is neglected, the predicted concentration profiles are closer in agreement with the experimental profiles. This justifies the absence of any catalytic effect due to the uranyl ions.

Another important observation to be made is that as the fabrication route opted for making the simulated MOX pellets aided in their relatively rapid dissolution as against the UO_2 pellets prepared by the conventional powder metallurgical route, the rate of the reaction at 600 RPM (which is the minimum mixing rate required to reduce the diffusion control of the UO_2 dissolution reaction to its bare minimum) was pretty high. This indicated that the diffusion control is not at its lowest point at 600 RPM for the simulated MOX pellets. This was reflected in the value of the apparent activation energy (E_a) calculated for these pellets from the data given in Table 19. The estimated E_a values were less than 20 kJ/mol which by a rule of thumb is the upper limit for a reaction to be predominantly diffusion

controlled¹⁶. This value suggests that the diffusion control on the overall reaction rate could be further reduced by increasing the mixing rate. Thus the estimated rate parameters for the dissolution of simulated urania ceria MOX pellets in nitric acid, under the experimental conditions employed in this research work, would be slightly on the conservative side with respect to that of irradiated pellets which would be more porous in nature due to the presence of more amount of fission gas present in them. Therefore for obtaining a more realistic prediction using this methodology, similar approach should be undertaken with irradiated pellets as well. The facilities currently available in our centre are not sophisticated enough to carry out R&D experiments on irradiated nuclear fuel pellets. Thus the basic research work carried out as a part of this thesis would pave way for further work in future using irradiated fuel samples which would enable development of more accurate dissolution models. In this context, the current work would serve as a launching pad for understanding the dissolution process of irradiated nuclear fuel. This in turn could lead to the development of the continuous dissolution process system which is the need of the hour for designing energy efficient, high throughput and safer FBR fuel reprocessing plants.

6.11 References

-
- ¹ R. D. Shannon and C. T. Prewitt, *Acta Crystallographica Section B*, 1969, 25, 925-946
P. A. Bingham, R. J. Hand, et al., *Mater. Res. Soc. Symp. Pro.*, 2008, 1107, 421
- ² T.L. Markin, R.S. Street, E.C. Crouch, *J. Inorg. Nucl. Chem.* 32 (1970) 59
R. Lorenzelli, B. Touzelin, *J. Nucl. Mater.* 95 (1980) 290
W. Dörr, S. Hellmann, G. Mages, *J. Nucl. Mater.* 140 (1986) 7
Y.W. Lee, H.S. Kim, S.H. Kim, et al., *J. Nucl. Mater.* 274 (1999) 7
D.I.R. Norris, P. Kay, *J. Nucl. Mater.* 116 (1983) 184
E. Zimmer, C. Ganguly, J. Borchardt, H. Langen, *J. Nucl. Mater.* 152 (1988) 169
- ³ Y.S. Park, H.Y. Sohn, D.P. Butt, *J. Nucl. Mater.* 280 (2000) 285
D.G. Kolman, Y.S. Park, et al., Los Alamos National Laboratory Report LA-UR-99-0491
M. Stan, Y.T. Zhu, H. Jiang, *J. Appl. Phys.* 97 (2004) 3358
M. Stan, T.J. Armstrong, et al., *J. Am. Ceram. Soc.* 85 (2002) 2811
- ⁴ Marra, J. C., Cozzi, A. D., Pierce, R. A., Pareizs, J. M., Jurgensen, A. R. and Missimer, D. M. (2006) Cerium as a Surrogate in the Plutonium Immobilized Form, in *Environmental*

Issues and Waste Management Technologies in the Ceramic and Nuclear Industries VII (eds G. L. Smith, S.K. Sundaram and D. R. Spearing), The American Ceramic Society, 735 Ceramic Place, Westerville, Ohio 43081

⁵ Jain A, Ananthasivan K, Anthonysamy S, and Rao PRV, "Synthesis and sintering of (U_{0.72}Ce_{0.28})O₂ solid solution", J Nucl. Mater. 345(2005) 245

⁶ R. Venkata Krishnan, G. Panneerselvam, Brij Mohan Singh, B. Kothandaraman, G. Jogeswararao, M.P. Antony, K. Nagarajan, "Synthesis, characterization and thermal expansion measurements on uranium–cerium mixed oxides", J. Nucl. Mat. 414 (2011) 393–398

⁷ Chandramouli V, Anthonysamy S, Vasudeva Rao PR (1999), "Combustion synthesis of thoria, a feasibility study", J Nucl Mater 265:255–261

⁸ P. Martin, M. Ripert, T. Petit, et al., J. Nucl. Mater. 312 (2003) 103

⁹ ASTM card no. 4-0556 and 4-0593, Powder diffraction file, sets 11-15, Inorganic vol. PDIS-15iRB, Published by Joint Committee on Powder Diffraction Standards, Swarthmore, PA, 1972

¹⁰ D.J. Kim, Y.W. Lee, Y.S. Kim, J. Nucl. Mater. 342 (2005) 192

¹¹ H.P. King, L.E. Alexander, "X-ray Diffraction Procedures for polycrystalline and amorphous materials", Wiley, USA, 1954

¹² Hirotomo Ikeuchi, Atsuhiko Shibata, et al., "Dissolution behavior of irradiated mixed-oxide fuels with different plutonium contents", Procedia Chemistry 7 (2012) 77 – 83

¹³ Hodgson, T. D.: RECOD'87, Vol. 2, 591 (1987)

¹⁴ Taylor, R. F.; Sharratt, E. W., et al., "Dissolution rate of uranium dioxide sintered pellets in nitric acid systems", J. Appl. Chem. 1963, 13, 32–40

¹⁵ Shabbir, M.; Robbins, R. G. "Kinetics of the dissolution of uranium dioxide in nitric acid. I" J. Appl. Chem. 1968, 18, 139–134

¹⁶ Yu J.F., Ji C., Chem. J. Chin. Univ. (1992) "The kinetics of cobalt(II) Extraction with EHEHPA in heptane mixed extraction systems", 13, 224–226

CHAPTER 7. Dissolution kinetics of UO₂-PuO₂ MOX pellets in nitric acid medium

7.1 Introduction

The primary aim of this research work, as mentioned in section 1.10, is to determine the intrinsic dissolution kinetics of typical FBR driver fuel (plutonium rich urania plutonia MOX fuel) under PUREX process conditions. The dissolution kinetics of UO₂ and simulated urania ceria MOX pellets have already been explained in detail in Chapters five and six. Their kinetic parameters have been evaluated under typical PUREX process conditions which were used as the basis for studying the kinetics of FBR plutonium rich MOX fuel. As explained already in section 6.1, we could not afford to carry out many experiments with plutonium fuel system. Hence based on the results of the experiments on UO₂ and urania ceria MOX pellet dissolution in nitric acid and with minimum number of experiments on urania plutonia MOX fuel pellets, the kinetics of dissolution of urania plutonia MOX fuel in nitric acid was studied and modeled. This chapter presents the MOX dissolution studies in detail.

7.2 Nature of fuel pellets

The MOX pellets required for the study were brought from BARC, Mumbai. These represent typical inner core PFBR MOX fuel pellets, whose composition is 21.78 mass percent of PuO₂ and the rest is UO₂ ((U_{0.782}Pu_{0.218})O₂). All the pellets had an annular hole at the centre to decrease the difference between the centre line and surface temperature within each pellet during its irradiation in PFBR (refer Fig. 4.3). All these pellets were dimensionally rejected due to some minor crack/chipping along its surface. The physical features of the pellet used in the experiments are given in Table 7.1.

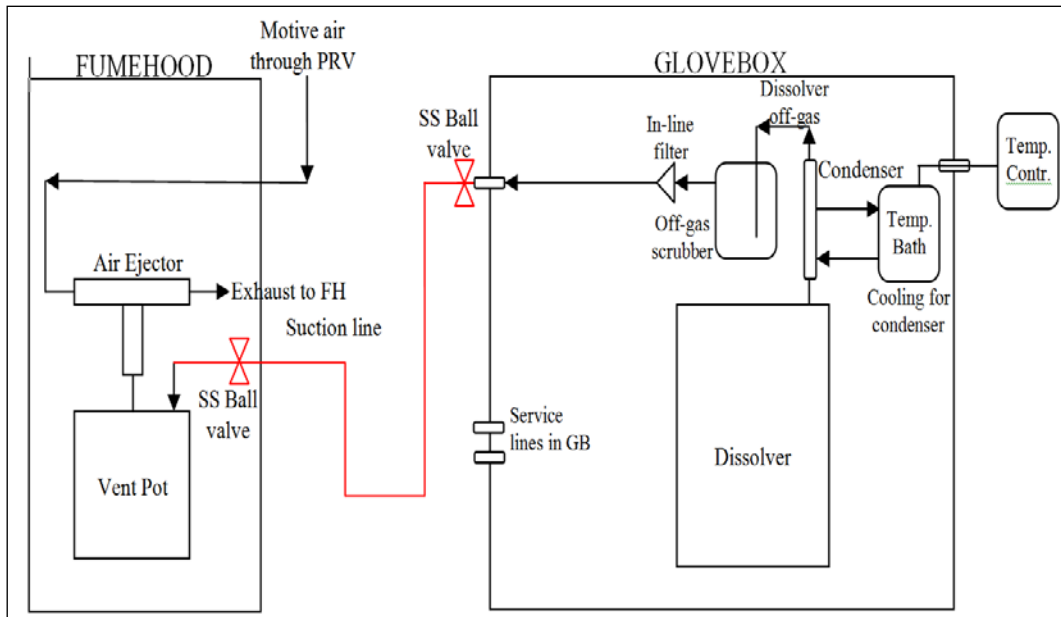
Table 7.1. Details of the inner core PFBR MOX pellets

S.No.	Parameter	Approximate Details
1	Weight (g)	1.5-1.75
2	Diameter (mm)	5-6
3	Length (mm)	10
4	Annular hole diameter (mm)	1-2

7.3 Erection of the experimental set-up

A glass dissolver similar to that used for UO_2 and simulated urania ceria MOX pellets was used for studying the dissolution behaviour of MOX pellets in nitric acid. The design and construction of the dissolution vessel is already explained in section 5.1. The entire dissolution reactor along with the glass impeller for stirring, off-gas condenser, off-gas scrubber, heating mantle with temperature controller etc were installed inside an airtight glove box. The services required for the experimental studies like air-ejector for sucking the off-gas etc. were erected inside a fume hood adjacent to the glove box. Permanent SS lines were laid between the fume hood and glove box for connecting the required services to the experimental set-up. Prior to the experiments, the erected experimental setup was inspected and cleared by the competent safety authority of IGCAR. The schematic sketch of the experimental set-up is shown in Fig. 7.1.

Fig. 7.1. Schematic sketch of the dissolution set-up for dissolving MOX pellets



7.4 Effect of initial concentration of nitric acid on the dissolution kinetics

Similar to the experimental studies on the dissolution behaviour of UO_2 and simulated MOX pellets in nitric acid, initial set of experiments were carried out to study the effect of initial concentration of nitric acid on the dissolution kinetics of MOX pellets at 353 K. Experiments were conducted at initial concentrations of nitric acid of 8, 10, 11.5 and 16 M. The agitation rate and temperature were maintained constantly at 600 RPM and 353 K

as justified in sections 5.2 and 5.5.3 respectively. The graphical representation of the effect of initial concentration of nitric acid on the dissolution of MOX pellets is shown in Fig. 7.2.

Fig. 7.2. Effect of initial acidity on the dissolution kinetics of $(U_{0.782}Pu_{0.218})O_2$ MOX pellet at 353 K and 600 RPM

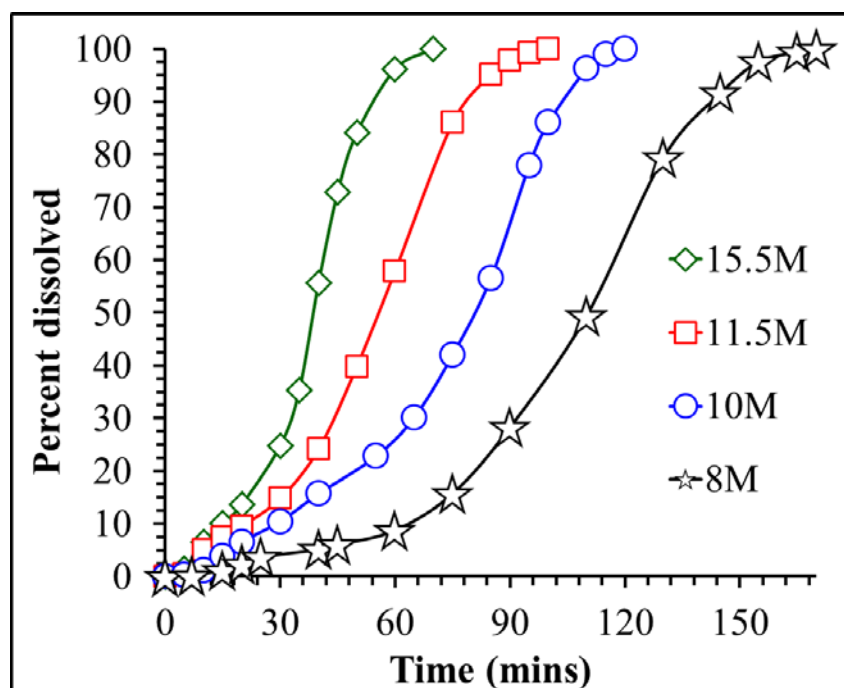


Fig. 7.2 clearly shows that the increase in the initial concentration of nitric acid leads to an increase in the rate of dissolution. Similar to UO_2 and simulated MOX pellets, all these dissolution curves exhibit the sigmoidal shape indicating the presence of an autocatalytic effect. This is due to the autocatalytic dissolution of UO_2 , the major component of the MOX pellets (78.28 wt %). A more interesting and unique behaviour among the fuels used for the present investigations was observed for the urania plutonia MOX pellets. In all the above experiments it was found that uranium always got leached out of the pellet faster than plutonium. This was unlike the case of simulated MOX pellets wherein the uranium and cerium composition in the liquid was always the same and equal to that of the initial pellet. This behaviour of MOX pellet is indicated in Fig. 7.3 which typically shows the percentage dissolution of uranium and plutonium separately and together during the dissolution of urania plutonia MOX pellets in 8 M nitric acid at 353 K.

Fig. 7.3. Typical dissolution curve for $(U_{0.782}Pu_{0.218})O_2$ MOX pellet in 8 M nitric acid at 353 K and 600 RPM

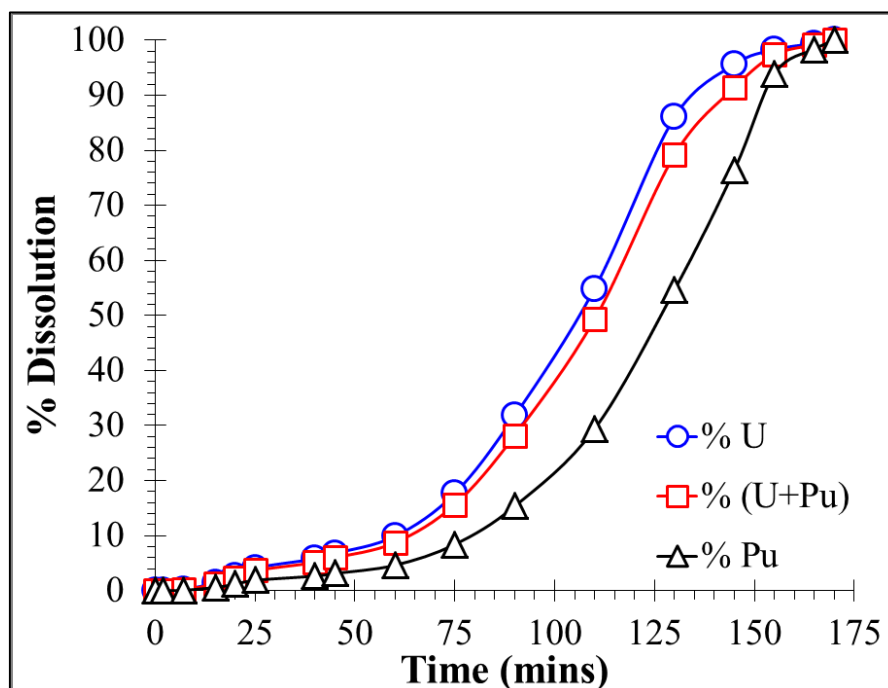


Fig. 7.3 clearly brings out the relative difference in the rate of dissolution of uranium and plutonium from the MOX pellet. Though plutonia dissolves sluggishly when compared to urania as shown here, the very fact that the pellet ultimately dissolves completely re-emphasizes that MOX pellets with plutonium below 35 wt % dissolves completely just by heating in pure nitric acid without the requirement of any other strong oxidizing or reducing agents as mentioned in the literature¹. This behaviour was seen during all the dissolution experiments of urania plutonia MOX pellets in nitric acid carried out as a part of this research work.

The consolidated results of the effect of initial concentration of the acid on the dissolver solution composition are shown in Fig. 7.4. It could be clearly understood from Fig.7.4 that as the concentration of acid increases, the rate of plutonium oxide dissolution increases more than that of uranium oxide. Hence the gap between the percentage uranium and percentage plutonium curve under the given condition narrows gradually with the increase in the initial concentration of nitric acid. All of these data were used for the evaluation of the kinetic parameters of the dissolution of MOX pellets in nitric acid during the modeling of the reaction kinetics.

Fig. 7.4. Effect of acidity on the composition of the dissolver solution during the dissolution of $(U_{0.782}Pu_{0.218})O_2$ MOX pellet at 353 K and 600 RPM

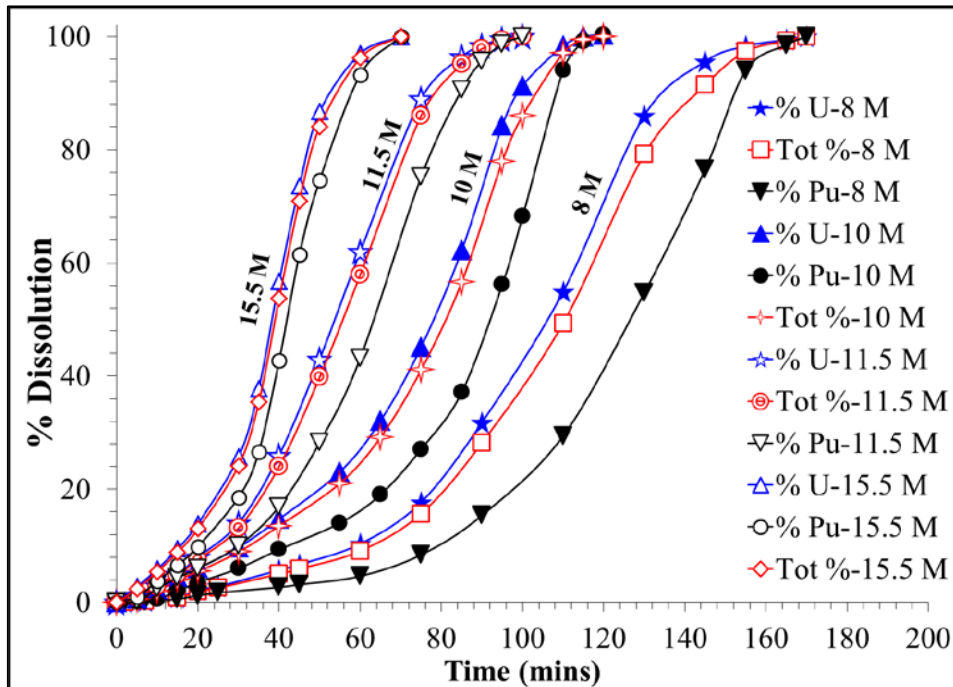
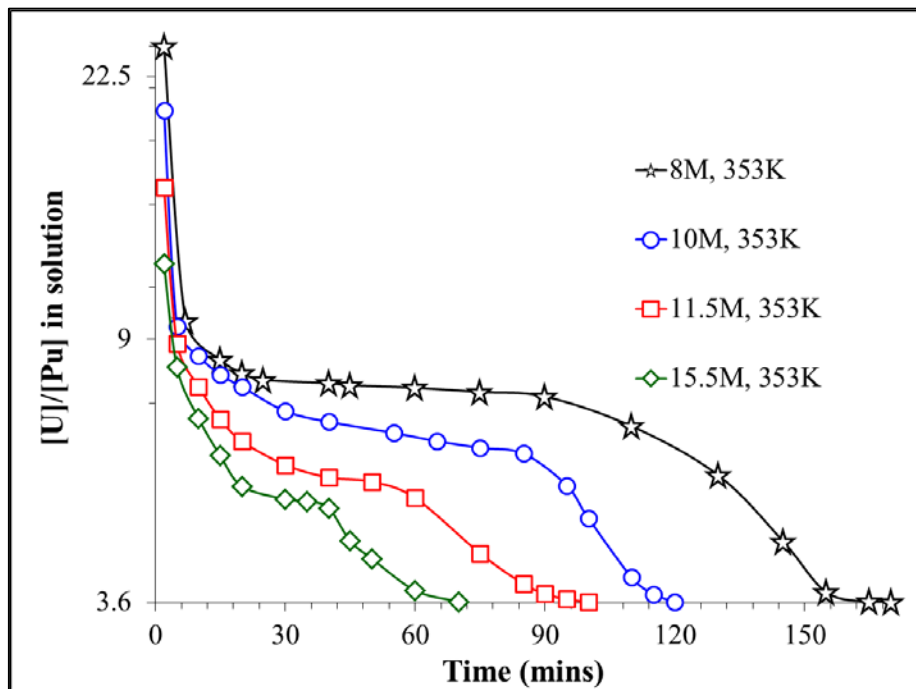


Fig. 7.5. Effect of acidity on the relative dissolution of uranium and plutonium from $(U_{0.782}Pu_{0.218})O_2$ MOX pellet at 353 K and 600 RPM

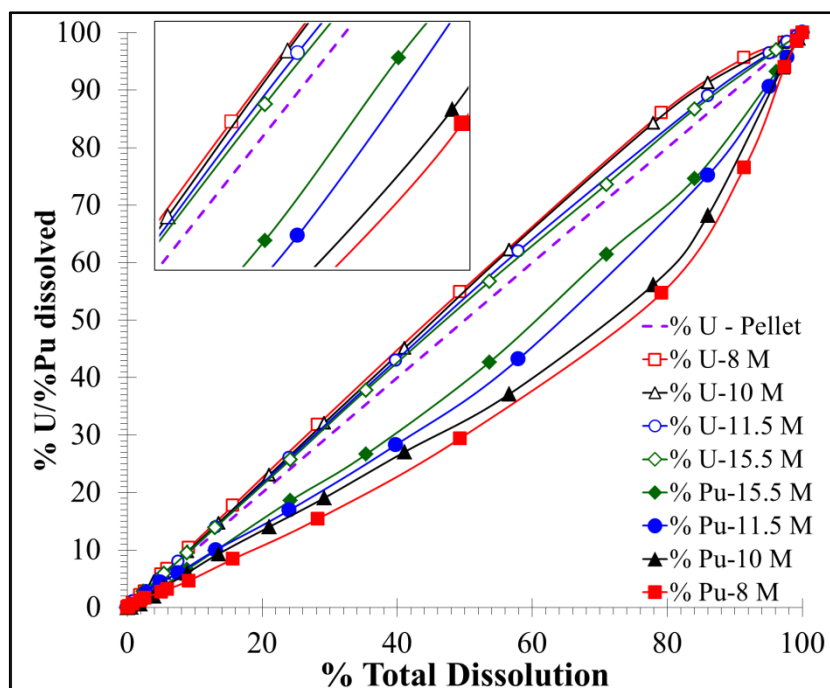


As described already, the composition of the urania plutonia MOX pellets used in the

dissolution studies is 78.22% uranium and 21.78% Pu. Hence the ratio of weight percent of uranium to plutonium in all the pellets is about 3.5872 (78.2/21.8). Therefore for better understanding of the differential dissolution rate of uranium and plutonium from the same MOX pellet, the mole ratio of U to Pu in solution was plotted against time for each of the above experiment and is shown in Fig. 7.5. The lowest value of 3.6 on the y axis in Fig. 102 corresponds to the U/Pu mole ratio of the starting pellet. It could be seen that in all the cases, this value is reached only at the end of the dissolution. Prior to that, this value starts from a much higher number before gradually reaching 3.6 at the end. This translates into the fact that the mole ratio of uranium to plutonium in the solution during the course of dissolution is always higher than that in the starting pellet. That is uranium dissolves more rapidly than plutonium at the start of the dissolution experiment and the rate of plutonium dissolution gradually picks up till their mole ratio reaches a value similar to that in the starting pellet. It should also be noted that this mole ratio at any given time during the course of dissolution is always inversely proportional to the initial concentration of nitric acid. These experimental data were later used in deriving the model equations for the dissolution of MOX pellets in nitric acid which was subsequently employed to determine the kinetic parameters using non-linear regression techniques.

The consolidated results of the effect of initial concentration of nitric acid on the dissolution of MOX pellets is given in Fig. 7.6 by making a parity plot of % uranium and % plutonium against the total % dissolution for each of the condition. The centre most dotted line in Fig. 7.6 corresponds to the composition of uranium and plutonium in the MOX pellet. It could be noted that the percentage uranium dissolution line under the given condition always lies above and the plutonium line always below the centre line. Thus the composition of uranium in the dissolved solution is always higher than that in the starting MOX pellet at any stage of the dissolution reaction. The more the gap between the % uranium and % plutonium line under the given condition, faster would be the dissolution of uranium when compared to plutonium from the pellet. It could be clearly seen that this gap decreases gradually as the initial concentration of nitric acid is increased. This reconfirms two facts; from the same MOX pellet (i) the dissolution of uranium is rapid when compared to plutonium and (ii) with increase in the initial concentration of nitric acid, the rate of dissolution of plutonium increases more when compared to uranium. The relative rate of dissolution of the MOX pellets with respect to the concentration of nitric acid is clearly shown in the inset of Fig. 7.6.

Fig. 7.6. Consolidated effect of acidity on the dissolution of $(U_{0.782}Pu_{0.218})O_2$ MOX pellet at 80°C and 600 RPM with expanded view in the inset



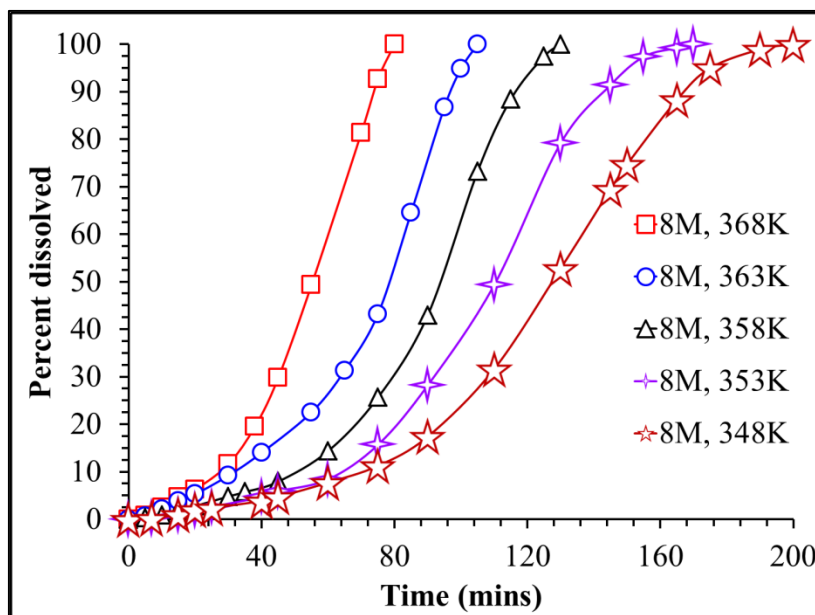
Along the diagonal of the inset from bottom right to the top left, the top four lines are that of urania and the bottom four are that of plutonia. Among the four urania lines, the order of initial concentration of nitric acid increases from top to bottom, whereas in the case of plutonia, the order is reversed. Hence in general, as the initial concentration of nitric acid increases the corresponding lines of % uranium dissolution and % plutonium dissolution comes closer. This indicates that with increase in acidity, the difference in the rates of UO_2 and PuO_2 from the MOX pellet decreases.

7.5 Effect of temperature on the dissolution kinetics of MOX

The next parameter which was chosen to study its effect on the MOX pellet dissolution kinetics was temperature. For this purpose, the acidity and the mixing rate was fixed at 8 M and 600 RPM as described in Chapter 5. The temperature was changed from 348 K to 368 K in steps of 5 K. Thus five different temperatures were chosen. The experiments were carried out in the same set-up as explained in the previous section. The results are presented graphically in Fig. 7.7. The following are some of the salient features of the results presented in Fig. 7.7.

- Like all other previous experiments, these dissolution experiments also exhibit the sigmoidal shape for the conversion curve indicating the presence of autocatalytic effect of nitrous acid on UO_2 dissolution
- As the temperature is increased, the S shape of the curve gradually reduces. This is due to the increased instability of nitrous acid at higher temperature leading to the gradual decrease in its autocatalytic effect

Fig. 7.7. Effect of temperature on the dissolution kinetics of $(\text{U}_{0.782}\text{Pu}_{0.218})\text{O}_2$ MOX pellet in 8 M HNO_3 and 600 RPM



Similar to the results of the experiments to study the effect of initial concentration of nitric acid, in these experiments also it was found that UO_2 preferentially got leached faster than PuO_2 . The difference between the rate of dissolution of UO_2 and PuO_2 was found to reduce as the temperature was increased which is shown in Fig. 7.8.

Though the experiments were carried out at five different temperature, Fig. 7.8 shows the percentage dissolution of urania, plutonia and the total pellet at only three different temperatures as the lines would overlap and make the graph complicated if all were included. The most striking feature of Fig. 7.8 was the reduction in the gap between the % uranium and % plutonium lines as the temperature was increased. The relative dissolution of uranium and plutonium from the MOX pellets as a function of temperature is shown more clearly in Fig. 7.9.

Fig. 7.8. Effect of temperature on the composition of the dissolved solution during the dissolution of $(U_{0.782}Pu_{0.218})O_2$ MOX pellet in 8 M HNO_3 at 600 RPM

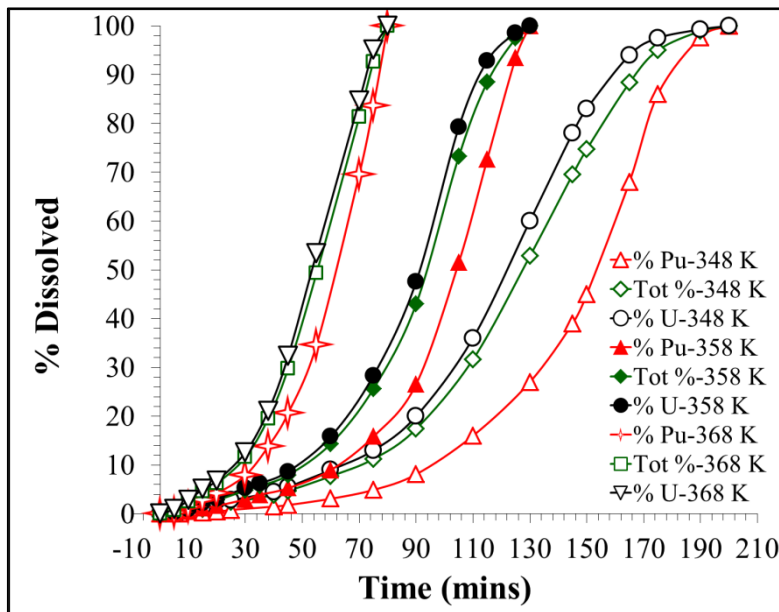
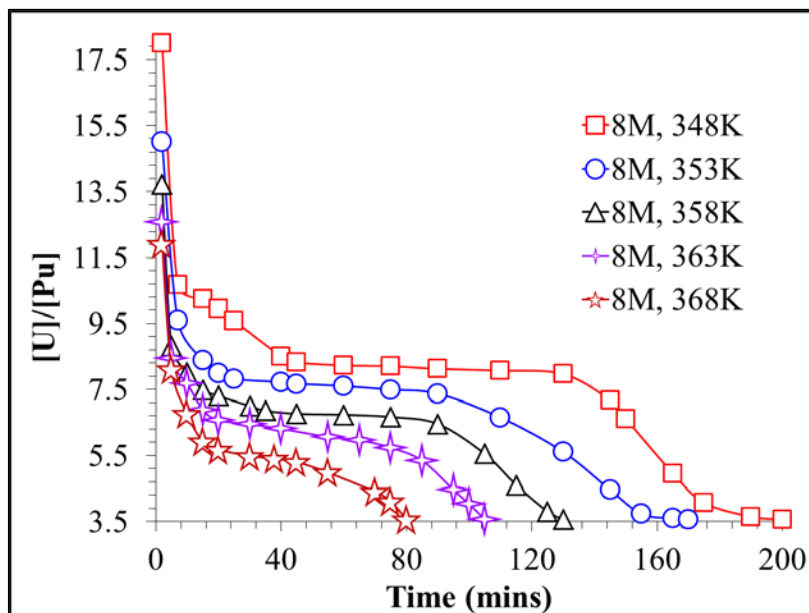


Fig. 7.9. Effect of temperature on the relative dissolution of uranium and plutonium from $(U_{0.782}Pu_{0.218})O_2$ MOX pellet at 8 M nitric acid and 600 RPM

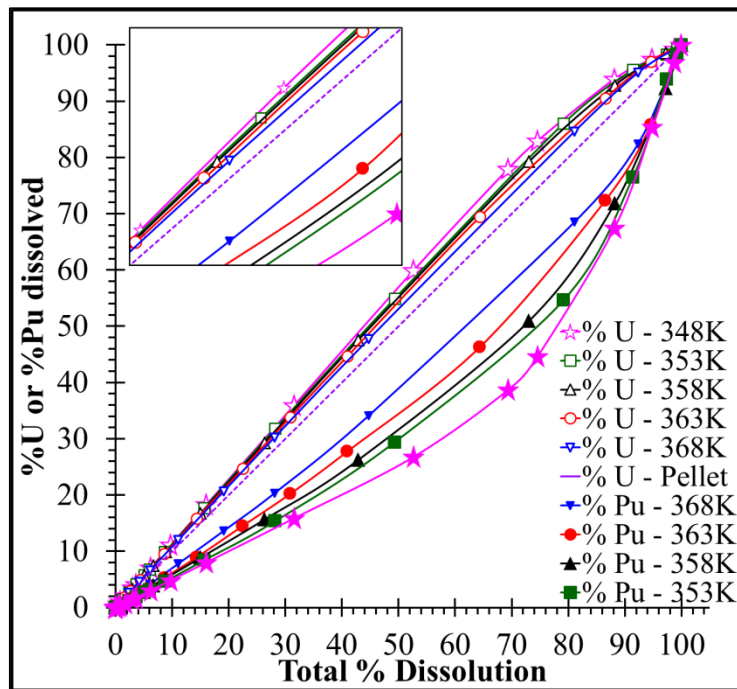


It could be noted from Fig. 7.9 that as the temperature is increased, the difference in the relative dissolution of uranium and plutonia in the MOX pellet decreases. This is indicated by the decrease in the ratio of % U dissolved to % Pu dissolved at any given time as a

function of increasing temperature.

The same information is given in Fig. 7.10 as well, wherein the percentage uranium and plutonium dissolved were plotted against the total percentage dissolved for all the temperatures. As the temperature is increased, the gap between the percentage uranium line and the percentage plutonium line decreases. This is a fair indication that the increase in the rate of plutonia dissolution is higher when compared to urania as the temperature is increased.

Fig. 7.10. Consolidated effect of temperature on the dissolution of $(U_{0.782}Pu_{0.218})O_2$ MOX pellet at 8 M nitric acid and 600 RPM with expanded view in the inset

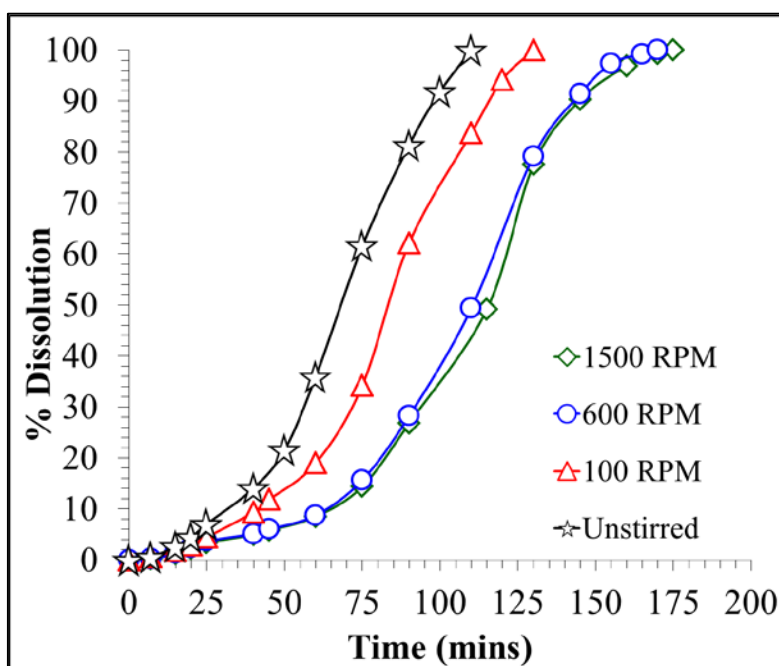


7.6 Effect of mixing on the dissolution kinetics of MOX pellets in nitric acid

Experiments were conducted in a similar fashion to study the effect of mixing intensity on the dissolution kinetics of MOX pellets in nitric acid after understanding the effect of initial acid concentration and temperature. Four different mixing rates were employed for this purpose, namely, 0, 100, 600 and 1500 RPM. The results of the experiments are shown graphically in Fig. 7.11. It could be seen from the Fig. that, as the mixing rate is increased, the rate of dissolution decreases which is similar to the case of UO_2 and simulated urania ceria MOX pellets under the same conditions. It could also be noted that

the difference in the dissolution rate while increasing the mixing rate from 600 and 1500 RPM is negligible. Hence, similar to the case of UO_2 and simulated urania ceria MOX pellets the effect of diffusion from 600 RPM and at further higher mixing rate is at its barest minimum. Therefore the kinetic parameters to be evaluated under these conditions would be intrinsic in nature.

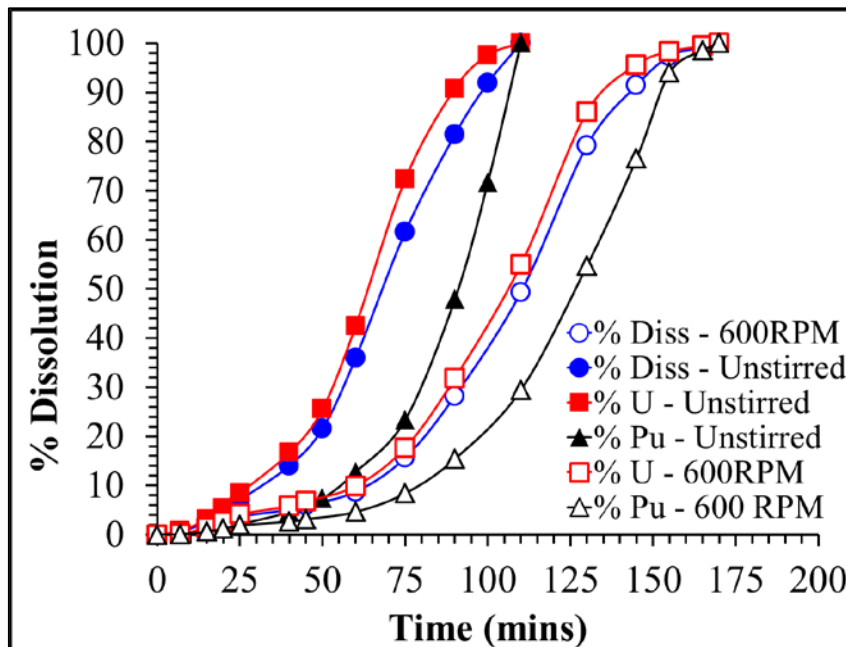
Fig. 7.11. Effect of mixing on the dissolution kinetics of $(\text{U}_{0.782}\text{Pu}_{0.218})\text{O}_2$ MOX pellet in 8 M nitric acid at 80°C



The effect of mixing intensity on the rate of dissolution of urania and plutonia in the MOX pellet is shown in Fig. 7.12. Though four different mixing rates were employed, only two were shown in this Fig. for the sake of simplicity. Otherwise the figure would become more complicated due to overlapping of curves of one mixing rate with the other when the results of all the four mixing rates were included in the same figure. It could be understood from Fig. 108 that, similar to urania, the rate of dissolution of plutonia was also found to be inversely proportional to the rate of mixing. The presence of nitrous acid is not expected to make any difference to the rate of dissolution of plutonia in nitric acid as the oxidation state of plutonium remains the same in both the solid and liquid phases during the dissolution. Hence the mixing intensity is expected to be directly proportional to the rate of dissolution of plutonia similar to any solid dissolving in a liquid medium. This contradicting observation could be explained based on the behaviour of urania. As

explained in Chapter 5, the rate of dissolution of urania is inversely proportional to the rate of mixing due to the catalytic effect of nitrous acid which is present more at the vicinity of the pellet surface at lower mixing rate. Urania being the major component of the MOX pellet, its faster dissolution rate at lower mixing rate renders the pellet more porous. This increases the effective surface area of the pellet leading to better contact between the pellet and acid resulting in the increased rate of dissolution of plutonia. This could be inferred from Fig. 7.12 by the sudden increase in the slope of the plutonia dissolution line when sufficient urania has got dissolved as the mixing intensity is decreased.

Fig. 7.12. Effect of mixing rate on the rate of dissolution of UO_2 and PuO_2 in $(\text{U}_{0.782}\text{Pu}_{0.218})\text{O}_2$ MOX pellet in 8 M HNO_3 at 353 K



For better understanding, the effect of mixing on the relative dissolution of urania and plutonia from the same MOX pellet is given in Fig. 7.13 in terms of ratio of molar concentration of uranium to plutonium in the solution as a function of time for all the mixing rates employed. The lowest point in the y axis of Fig. 7.13 corresponds to 3.556 which is the mole ratio of uranium to plutonium in the starting MOX pellet. It could well be understood from the Fig. that at reduced mixing rate, urania dissolves relatively much faster than plutonia which is reflected by the high molar ratio of uranium to plutonium in the solution. As the mixing rate is increased, this value gradually approaches to that of the initial pellet at the end of dissolution. The curves at 600 and 1500 RPM are almost the

same indicating the negligible presence of diffusion control from 600 RPM and upwards.

Fig. 7.13. Effect of mixing rate on the relative dissolution of uranium and plutonium from $(U_{0.782}Pu_{0.218})O_2$ MOX pellet in 8 M nitric acid at 353 K

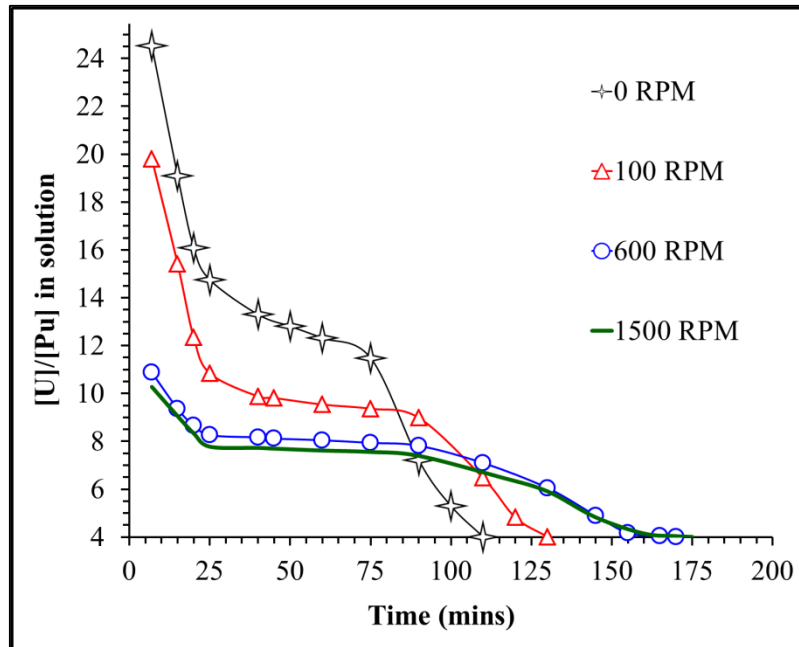
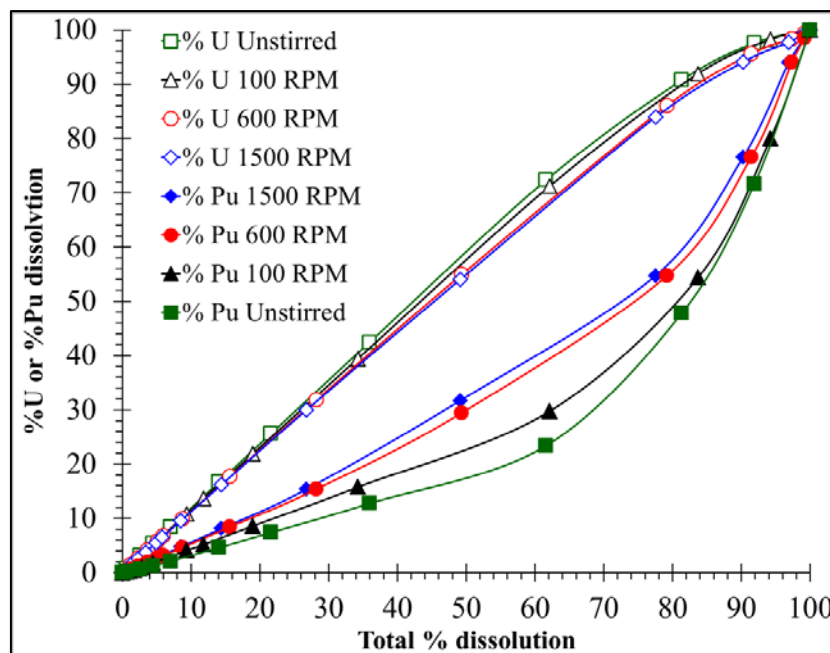


Fig. 7.14. Consolidated effect of mixing rate on the dissolution of $(U_{0.782}Pu_{0.218})O_2$ MOX pellet in 8 M nitric acid at 353 K



The consolidated effect of mixing on the dissolution kinetics of uranium plutonia MOX pellet is given in Fig. 7.14. The construction of Fig. 7.14 is very similar to that of Figures

7.6 and 7.10 except for the fact that the influencing parameter here is the mixing rate. All the above results of dissolution studies of $(U_{0.782}Pu_{0.218})O_2$ MOX pellet in nitric acid has brought out clearly the effect of various parameters on the reaction kinetics. All these experimental data were used for modeling the reaction kinetics. All these results makes an interesting case to study the effect of plutonium composition in the MOX pellet on its dissolution kinetics in nitric acid medium under various conditions. Similar studies on MOX pellets of other compositions would be performed, once they become available.

7.7 Evaluation of dissolution kinetics of UO_2 - PuO_2 fuel pellets

7.7.1 Introduction

The methodology adopted for modeling the dissolution of urania plutonia MOX pellets in nitric acid was similar to the methods which were already developed for understanding the dissolution behavior of simulated urania ceria MOX pellets in nitric acid presented in section 6.9 of this thesis.

7.7.2 Methodologies

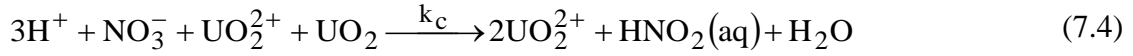
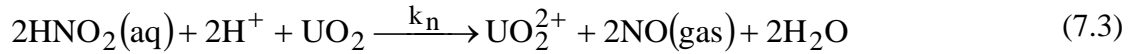
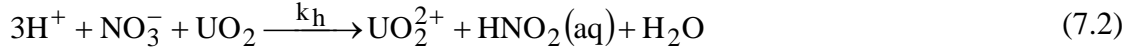
The analytical methods employed for analyzing the dissolution behavior of urania ceria MOX pellets in nitric acid was employed for evaluating the kinetics of dissolution urania plutonia MOX pellets in nitric acid also.

7.7.2.1. Method 1 – Based on surface penetration of nitric acid into solid pellets

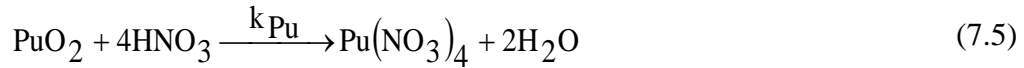
In this method, dissolution reaction is expressed by a two-step scheme as given below².



Where W_{ue} is the unexposed mass of fuel, W_e is the exposed mass and W_d the dissolved mass. The first process in the above equation is the penetration process. The rate of penetration process may be proportional to the concentration of nitric acid in the solution. The latter process in the above equation is considered as the chemical reaction. The reactions between UO_2 and ions in the nitric acid solution under these experimental conditions were assumed as follows^{3, 4}.



The reactions between PuO_2 and ions in the nitric acid solution under these experimental conditions was assumed as



7.7.2.1.1. Case-I: Considering the effect of nitrous acid to be negligible

The dissolution experiments on urania plutonia MOX pellets in nitric acid was conducted at high stirring speed (600 rpm). Hence the concentration of HNO_2 at solid-liquid interface is very much less. So the dissolution of UO_2 due to nitrous acid could be neglected (equation 7.3 is not considered).

The rate equations obtained based on eqn(7.2), eqn(7.4) and eqn(7.5) are given by

$$\frac{dW_{ue}}{dt} = -k_p [\text{HNO}_3] W_{ue} \quad (7.6)$$

$$\frac{dW_e}{dt} = k_p [\text{HNO}_3] W_{ue} - (k_h [\text{HNO}_3]^2 + k_c [\text{HNO}_3]^2 [\text{UO}_2^{2+}] + k_{cc} [\text{HNO}_3]^2) W_e \quad (7.7)$$

$$\frac{d[\text{UO}_2^{2+}]}{dt} = (\text{MV})^{-1} (k_h [\text{HNO}_3]^2 + k_c [\text{HNO}_3]^2 [\text{UO}_2^{2+}]) W_e \quad (7.8)$$

$$\frac{d[\text{Pu}^{4+}]}{dt} = (\text{MV})^{-1} (k_{\text{Pu}} [\text{HNO}_3]^2) W_e \quad (7.9)$$

$$\frac{d[\text{HNO}_3]}{dt} = -(\text{M V})^{-1} (3k_h [\text{HNO}_3]^2 + 3k_c [\text{HNO}_3]^2 [\text{UO}_2^{2+}] + 4k_{\text{Pu}} [\text{HNO}_3]^2) W_e \quad (7.10)$$

Where k_p is the rate constant for the penetration process, M is the molecular weight of mixed oxide and V is the volume of the reacting solution.

The experimental data of concentrations of nitric acid, uranium and plutonium as a function of time were fitted into the above rate equations using a nonlinear regression technique to obtain rate constant that best correlates the experimental data. The best values were obtained by minimizing the following objective function

$$f = \sum_1^n 20 * (C_{U_{exp}} - C_{U_{calc}})^2 + \sum_1^n (C_{HNO_3_{exp}} - C_{HNO_3_{calc}})^2 + \sum_1^n 20 * (C_{Pu_{exp}} - C_{Pu_{calc}})^2 \quad (7.11)$$

The rate constants k_p , k_h , k_c and k_{Pu} were calculated at different conditions of temperature and acidity. The values of rate constants and corresponding standard deviation are given in Table 7.2.

Table 7.2. Rate constants for the dissolution of MOX fuel at different temperatures

T(K)	348	353	358	368
k_p ([L/mol]/min)	4.05E-04	4.97E-04	7.95E-04	7.39E-04
k_h ([L/mol] ² /min)	3.17E-05	2.43E-05	1.81E-05	2.54E-05
k_c ([L/mol] ³ /min)	1.05E-04	2.54E-04	2.98E-04	3.83E-04
k_{Pu} ([L/mol] ³ /min)	1.06E-05	1.46E-05	1.42E-05	1.88E-05
sd(U)	0.0176	0.0083	0.0099	0.0109
sd(HNO ₃)	0.0832	0.0359	0.0449	0.0472
sd(Pu)	0.0085	0.0092	0.0094	0.0088

Table 7.3. Rate constants for the dissolution of MOX fuel at different acidity

[HNO ₃] (M)	8	10	11.5	15.5
k_p ([L/mol]/min)	5.30E-03	4.97E-04	4.11E-04	4.03E-04
k_h ([L/mol] ² /min)	5.13E-06	2.43E-05	1.98E-05	1.48E-05
k_c ([L/mol] ³ /min)	3.57E-04	2.54E-04	2.53E-04	2.77E-04
k_{Pu} ([L/mol] ³ /min)	5.25E-06	1.46E-05	1.24E-05	1.21E-05
sd(U)	0.0108	0.0083	0.008	0.0105
sd(HNO ₃)	0.0298	0.0359	0.0312	0.0385
sd(Pu)	0.0063	0.0092	0.0068	0.0089

The concentration profiles of uranium, nitric acid and cerium during the course of dissolution were determined using the model equations 7.6 to 7.10. The comparison between experimental and calculated values of [U(VI)], [HNO₃] and [Pu] vs time at 348 K were shown as a semi log plot in the Figures 7.15 to 7.17. Similar plots were also generated for each of the conditions mentioned in the two tables given above.

Fig. 7.15. Modelled uranium concentration profile for the dissolution of (U_{0.78}Pu_{0.22})O₂ MOX pellet in 8 M HNO₃ at 348 K and 600 RPM

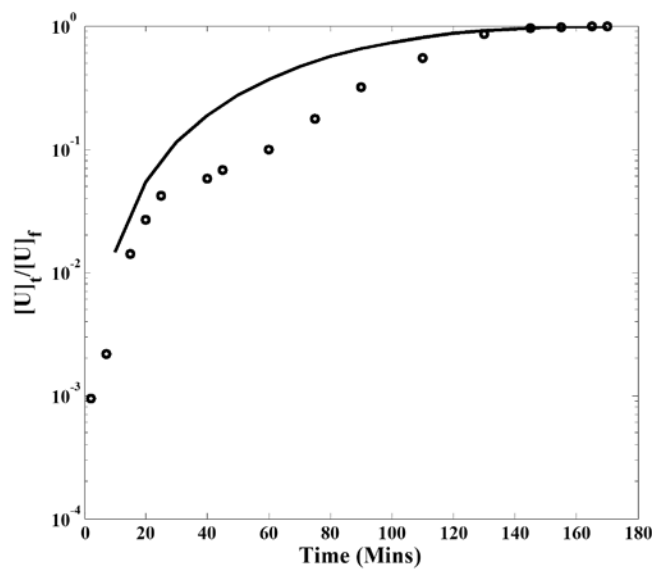


Fig. 7.16. Modeled nitric acid concentration profile for the dissolution of (U_{0.78}Pu_{0.22})O₂ MOX pellet in 8 M HNO₃ at 348 K and 600 RPM

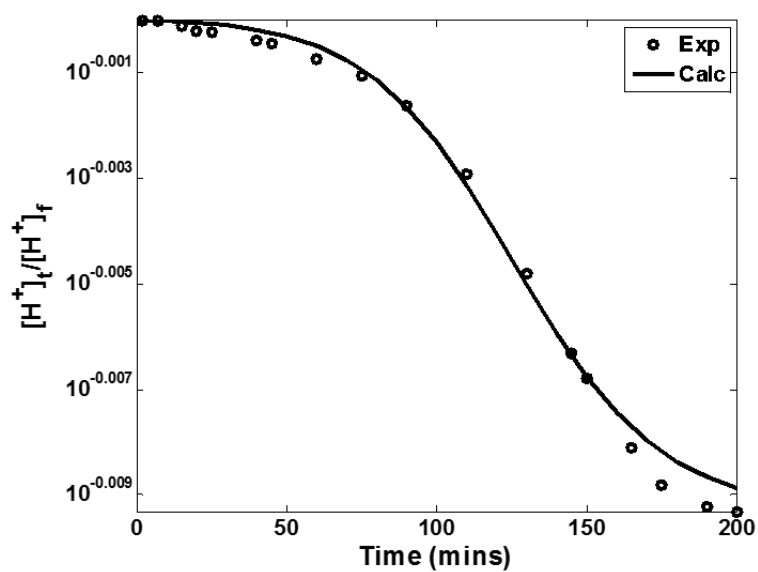
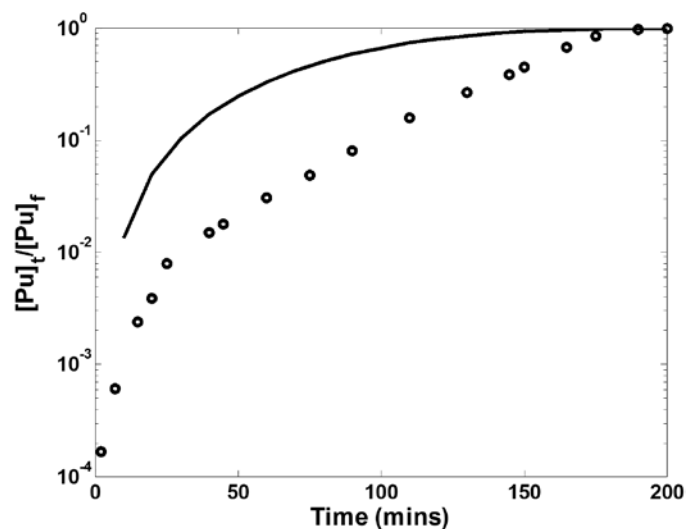


Fig. 7.17. Modelled plutonium concentration profile for the dissolution of $(U_{0.78}Pu_{0.22})O_2$ MOX pellet in 8 M HNO_3 at 348 K and 600 RPM



From the data given in Table 7.2, the activation energy for all the processes was calculated using Arrhenius equation and they were found to be about 31.7, 21.5, 26.6 and 17.5 kJ/mol for the processes with the rate constants k_p , k_h , k_c and k_{Pu} respectively in the temperature range 343-373 K.

7.7.2.1.2. Case II: Neglecting the autocatalytic effect of uranyl ion in solution

If autocatalytic effect of uranyl ion is not considered, then equation (7.4) need not be considered for deriving the rate equations. In that case, the rate equation gets modified as follows.

$$\frac{dW_{ue}}{dt} = -k_p [HNO_3] W_{ue} \quad (7.12)$$

$$\frac{dW_e}{dt} = k_p [HNO_3] W_{ue} - (k_h [HNO_3]^2 + k_{Pu} [HNO_3]^2) W_e \quad (7.13)$$

$$\frac{d[UO_2^{2+}]}{dt} = (MV)^{-1} (k_h [HNO_3]^2) W_e \quad (7.14)$$

$$\frac{d[Pu^{4+}]}{dt} = (MV)^{-1} (k_{Pu} [HNO_3]^2) W_e \quad (7.15)$$

$$\frac{d[HNO_3]}{dt} = -(M V)^{-1} (3k_h [HNO_3]^2 + 4k_{Pu} [HNO_3]^2) W_e \quad (7.16)$$

The experimental data of concentrations of nitric acid, uranium and plutonium as a function of time were fitted into above rate equations using a nonlinear regression technique to obtain the rate constant that best correlates the experimental data. The best values were obtained by minimizing the following objective function

$$f = \sum_{1}^n 20 * (C_{U_{exp}} - C_{U_{calc}})^2 + \sum_{1}^n (C_{HNO_3_{exp}} - C_{HNO_3_{calc}})^2 + \sum_{1}^n 20 * (C_{Pu_{exp}} - C_{Pu_{calc}})^2 \quad (6.17)$$

The rate constants k_p , k_h and k_{Pu} were calculated at different conditions of temperature and acidity. The values of rate constants and corresponding standard deviation are tabulated in tables 7.4 and 7.5.

Table 7.4. Rate constants for the dissolution of MOX fuel at different temperatures

T(K)	70	80	90	100
k_p ([L/mol]/min)	4.12E-04	5.25E-04	6.32E-04	7.02E-04
k_h ([L/mol] ² /min)	4.60E-05	6.21E-05	7.35E-05	8.30E-05
k_{Pu} ([L/mol] ³ /min)	1.11E-05	1.29E-05	1.68E-05	1.88E-05
sd(U)	0.027	0.0278	0.0311	0.0293
sd(HNO ₃)	0.1114	0.1059	0.134	0.1267
sd(Pu)	0.0082	0.0123	0.0108	0.0104

Table 7.5. Rate constants for MOX fuel dissolution at different acidity

[HNO ₃] (M)	6	8	10	11.5
k_p ([L/mol]/min)	5.87E-04	5.17E-04	4.89E-04	5.38E-04
k_h ([L/mol] ² /min)	1.02E-04	6.32E-05	4.23E-05	4.05E-05
k_{Pu} ([L/mol] ³ /min)	1.35E-05	1.32E-05	1.02E-05	1.02E-05
sd(U)	0.0294	0.0277	0.0208	0.0235
sd(HNO ₃)	0.1248	0.1059	0.0997	0.1277
sd(Pu)	0.0037	0.0124	0.0046	0.0053

The concentration profiles of uranium, nitric acid and plutonium during the course of dissolution were determined using the model equations 7.12 to 7.16. The comparison between experimental and calculated values of $[U(VI)]$, $[HNO_3]$ and $[Pu^{4+}]$ vs time at 353 K are shown as semi log plots in Figures 7.18 to 7.20 respectively. Similar plots were also generated for each of the conditions mentioned in the tables 7.4 and 7.5.

Fig. 7.18. Modelled uranium concentration profile for the dissolution of $(U_{0.78}Pu_{0.22})O_2$ MOX pellet in 8 M HNO_3 at 353 K and 600 RPM

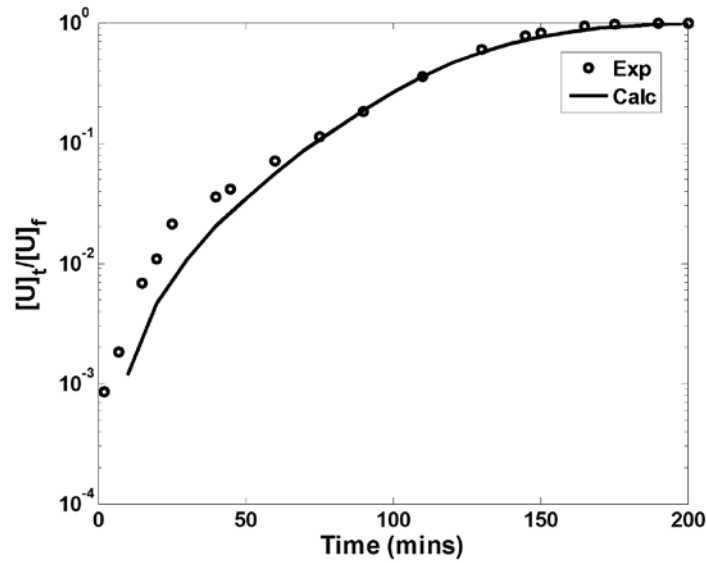


Fig. 7.19. Modelled nitric acid concentration profile for the dissolution of $(U_{0.78}Pu_{0.22})O_2$ MOX pellet in 8 M HNO_3 at 353 K and 600 RPM

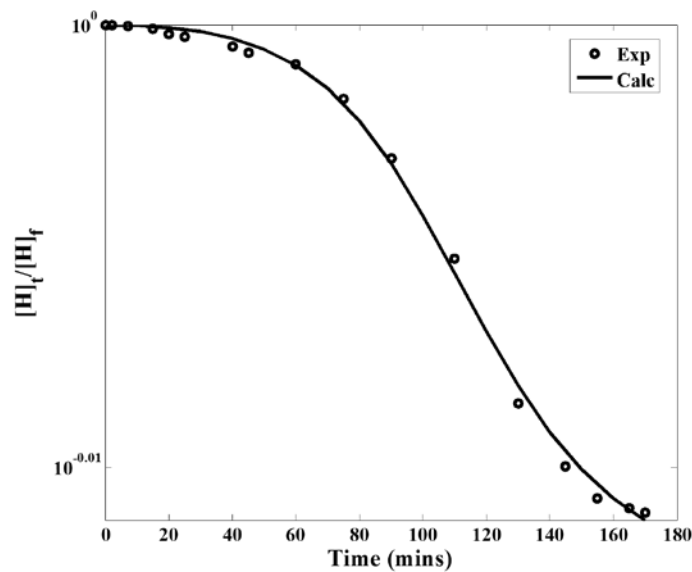
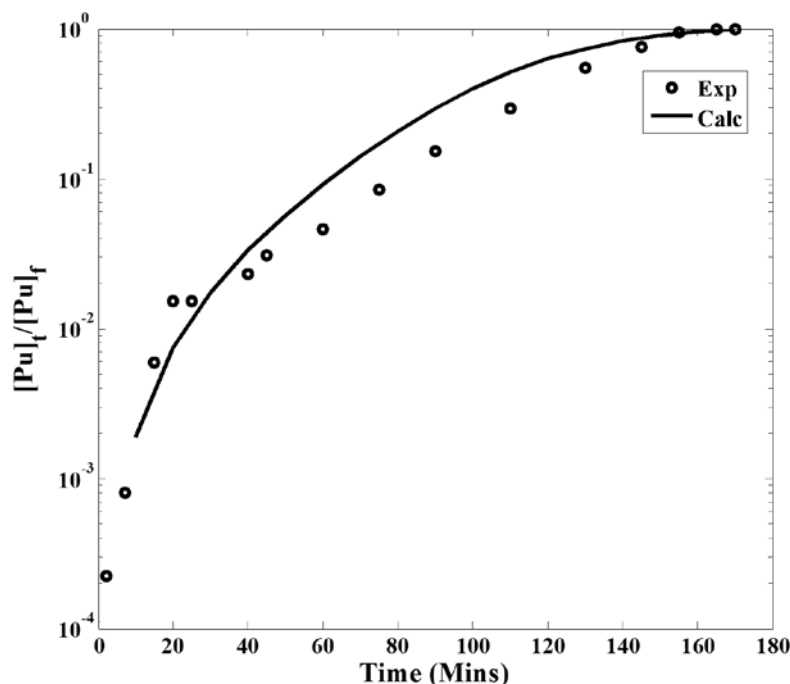


Fig. 7.20. Modelled plutonium concentration profile for the dissolution of $(U_{0.78}Pu_{0.22})O_2$ MOX pellet in 8 M HNO_3 at 353 K and 600 RPM



From the data given in Table 7.4, the activation energy for all the processes was calculated using Arrhenius equation and they were found to be about 19.1, 20.7 and 19.6 kJ/mol for rate constant k_p , k_h and k_{Pu} respectively in the temperature range 343-373 K.

During the dissolution of MOX pellets, it is only uranium which undergoes oxidative dissolution, whereas, plutonium remains in the same oxidation state both in the solid and liquid. Also, as uranium being more than 70% in mass and they have formed a perfect solid solution, the overall dissolution profile is sigmoidal due to the autocatalytic nature of urania dissolution in presence of nitrous acid. Figures 7.15 and 7.18 are the predicted uranium profiles with and without autocatalytic effect. Both the predicted profiles are fairly accurate indicating the insignificance of the catalytic effect of uranyl ion. In fact the predicted uranium profiles match the experimental values more closely in the absence of the catalytic effect of uranyl ion. This further emphasizes the absence of any catalytic action of uranyl ion. Whereas when it comes to predicting the plutonium profiles, shown in figures 7.17 and 7.20, neglecting the catalytic effect of uranyl ion markedly improves the prediction. This clearly shows that uranyl ion doesn't catalyze the dissolution of plutonia.

7.7.2.2. Method 2: Considering non-ideal nature of particle during the reaction

7.7.2.2.1. Introduction

Similar to the data analysis carried out for the dissolution of UO₂ pellets in section 5.10.V, the experimental data of the U, Pu MOX dissolution experiments were also analyzed considering the non-ideal nature of the particle during the reaction for the determinations of its kinetics.

7.7.2.2.2. Model equations

The shrinking particle model was invoked by including the interaction of chemical reaction and diffusion together. Model equations were derived in the same way as that of UO₂ and urania ceria MOX pellet dissolution. As this is a MOX pellet, while deriving the rate equation, the reaction of ceria with nitric acid also needs to be considered. Due to the presence of plutonium as an additional species here, we will be ending up with three rate equations unlike in the case of UO₂ (where it was only 2), i.e. one each for predicting the concentration profile of nitric acid, uranyl ion and ceric ion in the solution as a function of time. In this derivation, the subscript 'A', 'B' and 'E' were used respectively to denote nitric acid, uranyl ion and plutonyl ion respectively. Here also the accessible surface area was taken into account and is denoted by A. It is calculated as per equation 5.88 given in the section 5.10.c.v in the previous chapter. The surface area (A) and the subscript 'A' denoting nitric acid (X_A) are differentiated sufficiently all through the derivation. As the derivations are already explained in detail in section 5.10 of this thesis, the same is not repeated here. The final rate equations for determining the concentration profiles of various species are given in the following equations.

$$\text{for nitric acid, } \frac{dC_A}{dt} = (v_{AB}k_B C_{LA}^s + v_{AE}k_E C_{LA}^s) \cdot A \quad (7.18)$$

$$\text{For uranium, } \frac{dC_B}{dt} = v_B k_B C_{LA}^s \cdot A \quad (7.19)$$

$$\text{For plutonium, } \frac{dC_E}{dt} = v_E k_E C_{LA}^s \cdot A \quad (7.20)$$

The values for the stoichiometric coefficients used are $v_{AB} = 2.75$, $v_{AE} = 4$, $v_B = v_E = 1$.

The rate constants were estimated at different temperatures. Comparison between experimental and calculated values of the concentration profiles of uranyl ion, ceric ion and bulk phase nitric acid were generated graphically as a function of time and are shown in the figures in the following section for various conditions as the cases may be. The temperature dependency of the dissolution rate is governed by the Arrhenius equation. Thus the plot of $\ln(k)$ vs $1/T$ gives a slope equal to $(-E_a/R)$ from which the apparent activation energy of the dissolution reaction under the experimental conditions were estimated. The best values of the rate constants were obtained by minimizing the objective function given in the following equation.

$$f = \sum_1^n 20 * (C_{Bexp} - C_{Bcalc})^2 + \sum_1^n 50 * (C_{Abexp} - C_{Abcalc})^2 + \sum_1^n 50 * (C_{Eexp} - C_{Ecalc})^2 \quad (7.21)$$

The comparison between the experimental and calculated concentration profiles using the model equations were given graphically in the following sections for various cases.

The above model equations are applied for all the experimental data generated to study the effect of initial concentration of nitric acid, mixing rate (RPM) and temperature. For each of the above experiment, model equations were used to determine the rate constants for two different situations namely the order with respect to nitric acid being 1 and 2.

7.7.2.2.2.1. Case 1: Order w.r.t. nitric acid is 1

The comparison between the experimental and the predicted concentration profiles of nitric acid, uranium and plutonium for the dissolution of $U_{0.78}Pu_{0.22}O_2$ MOX pellets in 8 M nitric acid at 353 K, assuming order w.r.t. to nitric acid is unity were shown in Figures 7.21 to 7.23.

Fig. 7.21. Comparison of experimental and calculated profiles of [U(VI)] at 353 K for $U_{0.78}Pu_{0.22}O_2$ MOX pellet dissolution assuming 1st order w.r.t. HNO_3

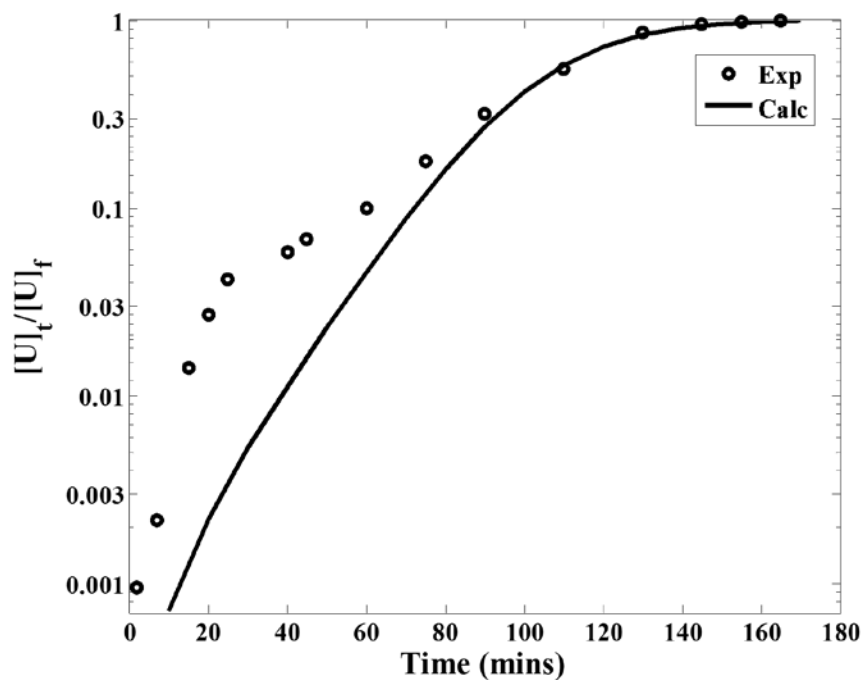


Fig. 7.22. Comparison of experimental and calculated 1st order $[HNO_3]$ profiles at 353 K for $U_{0.78}Pu_{0.22}O_2$ MOX pellet dissolution

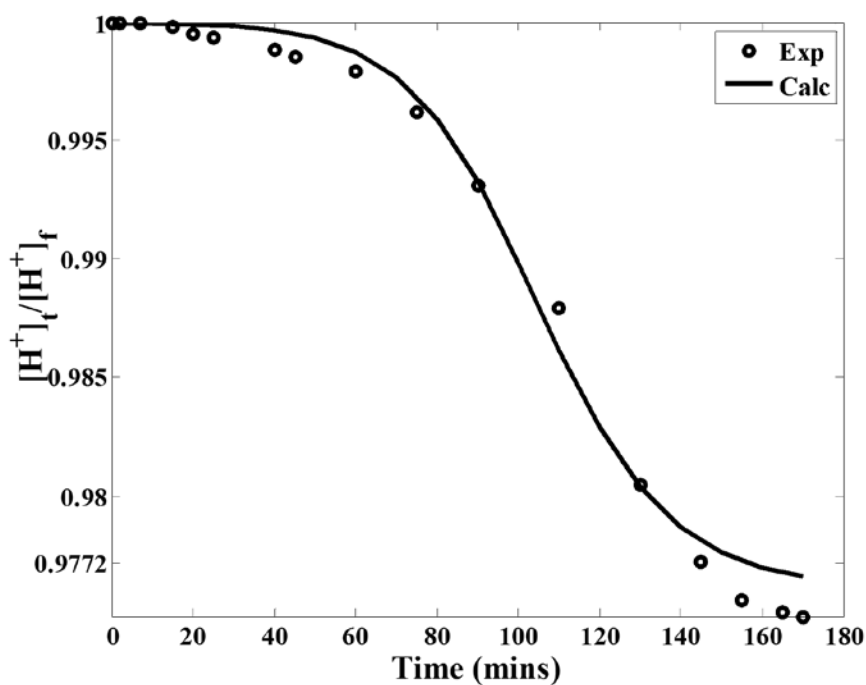
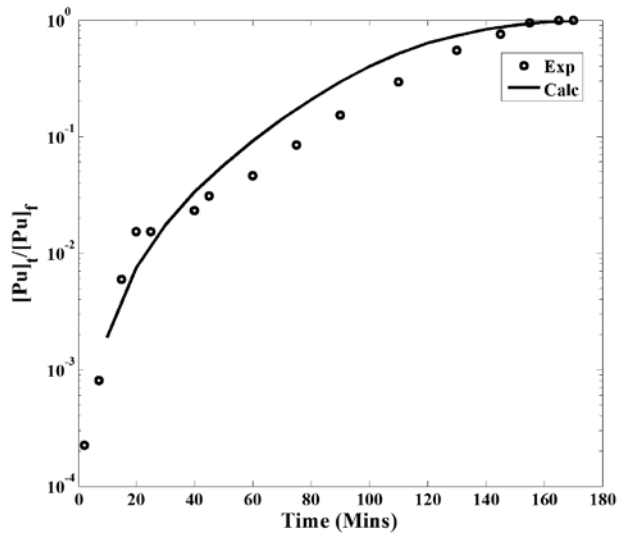


Fig. 7.23. Comparison of experimental and calculated profiles of [Ce(IV)] at 353 K for $U_{0.78}Ce_{0.22}O_2$ MOX pellet dissolution assuming 1st order w.r.t. HNO_3



7.7.2.2.2. Case 2: Order w.r.t. nitric acid is 2

Figures 7.24 to 7.26 shows the comparison between the experimental and the predicted concentration profiles of nitric acid, uranium and cerium for the dissolution of $U_{0.78}Ce_{0.22}O_2$ MOX pellets in 8 M nitric acid at 353 K with the assumption that the order w.r.t. to nitric acid is two. The experimental data only upto 60% of the dissolution was considered for modeling as beyond that the pellets crumbled and the value of the shape factor is no more a constant and changes very drastically.

Fig. 7.24. Comparison of experimental and calculated profiles of [U(VI)] at 353 K for $U_{0.78}Ce_{0.22}O_2$ MOX pellet dissolution assuming 2nd order w.r.t. HNO_3

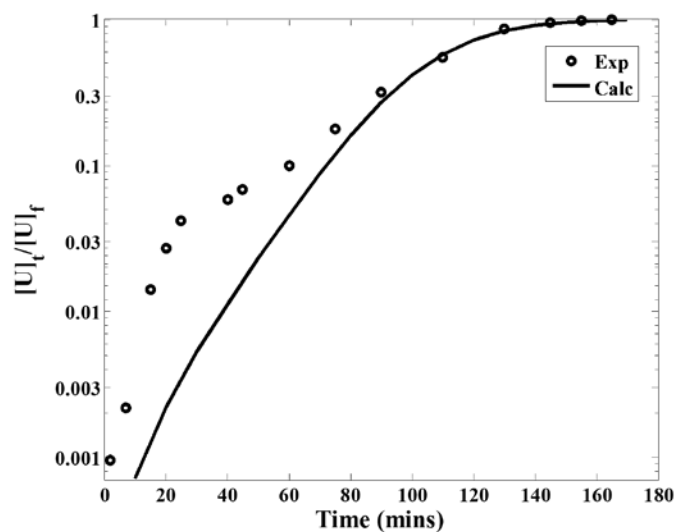


Fig. 7.25. Comparison of experimental and calculated 2nd order [HNO₃] profiles at 353 K for U_{0.78}Ce_{0.22}O₂ MOX pellet dissolution

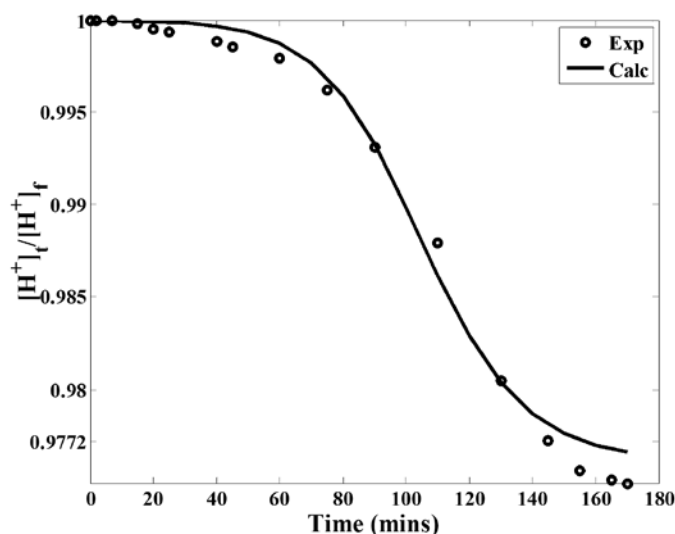
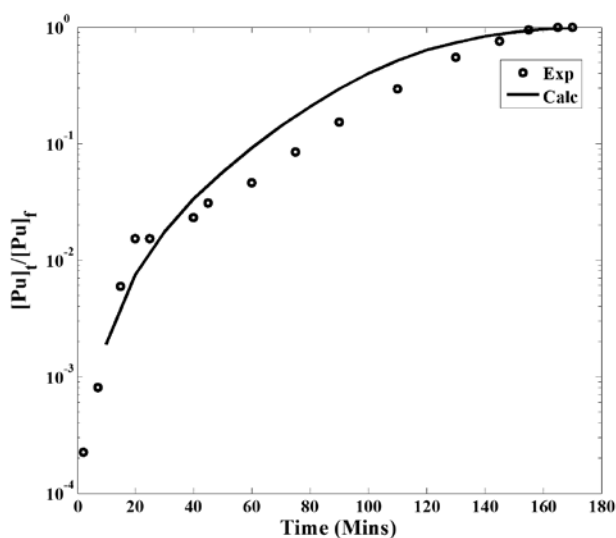


Fig. 7.26. Comparison of experimental and calculated profiles of [Ce(IV)] at 353 K for U_{0.78}Ce_{0.22}O₂ MOX pellet dissolution assuming 2nd order w.r.t. HNO₃



7.7.3 Conclusion on the modeling of simulated U, Pu MOX pellet dissolution

The modeling of the experimental data on the dissolution of urania plutonia MOX pellets in nitric acid under various conditions of acidity, temperature and mixing rate were carried out in two different methods, viz. penetration based and surface area based methods, very similar to that for UO₂ and urania ceria MOX pellets dissolution mentioned in the Chapters 5 and 6 respectively.

The model predictions were presented in section 7.7.2 which shows that the prediction of the concentration profiles to be fairly accurate in both the methods. In the case of plutonium profiles predicted by the penetration method (section 7.7.2.1), the predicted profile was always higher than the actual when the catalytic effect of uranyl ion is considered⁵. But when the catalytic effect of uranyl ion is neglected, the accuracy of the predicted profiles improved substantially, especially in the case of plutonium. This suggests that the uranyl ion does not play any catalytic role during the dissolution process. This is the reason for the reduced accuracy of the model equations in method 1 when the catalytic effect of uranyl ion was considered.

When it comes to the surface area based method, the accuracy of the model equations (equations 7.18 to 7.20) in predicting the concentration profiles of uranium, nitric acid and plutonium was found to be very good similar to the case of UO_2 and urania ceria MOX pellets dissolution studies. This is because, the experimental concentration profiles and the starting area of the pellet before dissolution are the input required for this method and since these parameters are fairly accurate, the method was found to be satisfactory. Ambiguity could arise only in the case of urania plutonia MOX pellet dissolution studies due to the lack of a suitable analytical equipment to measure the pellet surface area resulting in some errors. Since the pellets used for the studies were dimensionally rejected due to surface chippings, the actual area would be higher than that calculated from the pellet dimensions. It could also be noted that the predicted concentration profiles are almost the same irrespective of the order of the reaction with respect to nitric acid being 1 or 2. To sum up on the modeling of the urania-plutonia dissolution behaviour in nitric acid, it could be understood that both the methods used here describes the reaction fairly well. But if one has to employ them for the realistic dissolution of spent fuel pellets, which would be more porous due to the gaseous fission products generated inside the pellet matrix, the former method (penetration based) would be superior. This is due to the difficulty in measuring the starting surface area of these highly radioactive pellets which is the starting data required for the second method (surface area based).

Finally it could be concluded based on the findings of the current work presented in Chapters five to seven that the experiments carried out as a part of this research thesis has generated the fundamental model equations required to predict the dissolution behaviour of a typical plutonium rich MOX nuclear fuel under PUREX process conditions. The

findings reported in this thesis would also pave way for planning and carrying out more work in the future for studying the dissolution behaviour of irradiated fuel samples. This would enable development of more accurate dissolution models and also would serve as a launching pad for understanding the dissolution process of irradiated nuclear fuel.

7.8 Post justification of using cerium as a surrogate of plutonium in its MOX dissolution studies

The experimental results of Chapter six and seven clearly indicate that the behaviour of simulated MOX pellets and the urania plutonia MOX pellets under similar conditions are comparable qualitatively. The faster dissolution rates of these two types of fuel pellets when compared to urania pellets under similar conditions may be attributed to different reasons. In the case of urania ceria MOX pellets, the fast dissolution rate was due to the fabrication procedure wherein the solids were formed directly from the homogenous solution leading to better solid solution formation during sintering. In the case of urania plutonia MOX pellets, though the fabrication method was the same as that of the urania pellets, their densities were slightly lesser and also they had an annular hole in their centre which provided more area of contact between the pellet and acid. Therefore they dissolved rapidly than their urania counterpart under similar conditions. Based on all these experimental observations, it could be inferred and henceforth justify cerium as a good non-radioactive surrogate for plutonium under the conditions that prevailed during the dissolution experiments.

7.9 Overall rate equation for the nuclear fuel dissolution process

The dissolution model equations for the MOX pellets were developed by employing two different methods, namely penetration and surface area based. The calculated concentration profiles are found to be more accurate in the case of penetration method than in the surface area based method. This is because; the penetration method is based on the weight measurements which were done more accurately. But in the case of surface area based method, due to the lack of a suitable facility to measure the surface area of the dissolving pellet containing plutonium, they were arrived based on the initial surface area measurement from the pellet dimensions. It should be recollected at this point that all the fuel pellets employed in this study were dimensionally rejected since they had minor defects in the form of end chipping. This leads to higher surface area of the pellets that are

not accounted for when the surface area of the pellet was calculated from its dimensions assuming ideal geometry. Therefore it could be concluded from the current work that the model equations based on the penetration method given in equations 7.12 to 7.16 correlates to the experimental values better. In the future when equipments were made available for the accurate measurement of surface area for radioactive pellets, the surface area based dissolution model equations give in equations 7.18 to 7.20 would also predict the dissolution behaviour of MOX pellets more accurately.

7.10 References

-
- ¹ Uriarte, A. L.; Rainey, R. H. Dissolution of high-density UO₂, PuO₂, and UO₂-PuO₂ pellets in inorganic acids; 1965
 - ² Hodgson, T. D.: RECOD'87, Vol. 2, 591 (1987)
 - ³ Taylor, R. F.; Sharratt, E. W.; Chazal, L. E.; Logsdail, D. H. Dissolution rate of uranium dioxide sintered pellets in nitric acid systems. J. Appl. Chem. 1963, 13, 32–40
 - ⁴ Shabbir, M.; Robbins, R. G. Kinetics of the dissolution of uranium dioxide in nitric acid. I. J. Appl. Chem. 1968, 18, 139–134
 - ⁵ Shunji Homma, Jiro Koga, Shiro Matsumoto, Tomio Kawata, “Dissolution rate equation of UO₂ pellet”, J. Nucl. Sci. Tech., 30(9), pp.959-961, 1963

CHAPTER 8. Conclusion and scope for future work

8.1. Summary of the findings of the current work

Various experimental studies have been carried out as a part of the present work for evaluating the dissolution kinetics of plutonium rich FBR driver fuel in nitric acid. Due to the complexities and safety requirements involved in handling plutonium based nuclear fuel, a systematic approach was undertaken by first studying the dissolution kinetics of urania followed by urania ceria MOX fuel with cerium acting as a non-radioactive surrogate for plutonium. The results obtained for these two types of fuel pellets paved way for better designing of experimental techniques, equipments and modeling procedures in thorough understanding of the dissolution behaviour of urania plutonia MOX pellets.

8.1.1 Major findings of UO₂ fuel pellet dissolution studies in nitric acid

The following are the major findings with respect to urania fuel dissolution behaviour under typical PUREX process conditions based on the current work.

- 1) The dissolution of UO₂ in nitric acid medium under typical PUREX process condition is chemical reaction controlled with the activation energy typically of the order of 90 kJ/mol
- 2) Sodium hydroxide scrubbers coupled with ion chromatography is a simple and efficient technique to determine the composition of the NO_x gases evolved during the dissolution of UO₂ fuel in nitric acid.
- 3) From the concentration profiles of the NO_x gases in the off-gas stream and nitrous acid in the bulk liquid evolved during dissolution, the mechanism for the dissolution of UO₂ fuel under typical PUREX process condition was determined.
- 4) Nitrous acid plays an autocatalytic role during the dissolution of UO₂ fuel in nitric acid. Thus due to the dispersion of nitrous acid away from the pellet-nitric acid interface under agitated condition, retards the rate of dissolution of UO₂ pellets proportionately.
- 5) Shrinking particle model explains the dissolution behaviour of UO₂ fuel in nitric acid satisfactorily. The model equations developed based on this method with diffusion effects coupled with chemical reaction predicts the concentration profiles of all the important reactant and product species accurately.

- 6) Since agitation of the dissolving mixture is essential to improve the effective surface area of the pellets, addition of NO_2 gas into the reaction mixture is a simple and easy way to improve the dissolution kinetics of UO_2 spent fuel in nitric acid. This would also lead to better production rates in thermal reactor fuel reprocessing plants.
- 7) The order of the reaction with respect to nitric acid, rate constant and the validated model rate equations developed in the present work would be useful tools in designing a continuous dissolution system for processing urania based nuclear fuels.

8.1.2 Major findings of simulated MOX fuel pellet dissolution studies in nitric acid

The following are the major findings with respect to urania ceria MOX fuel dissolution behaviour under typical PUREX process conditions based on the current work.

- 1) Method of fabrication of the MOX pellets influences their dissolution behaviour in nitric acid to a great extent.
- 2) Addition of cerium to urania during the fabrication of urania ceria MOX pellets renders the pellet more difficult to dissolve under typical Purex process conditions.
- 3) The composition of cerium in the pellets is inversely related to the rate of dissolution of the MOX pellets in nitric acid.
- 4) Both the penetration and surface area dissolution model equations based on shrinking particle theory explains the dissolution behaviour of urania ceria MOX pellets satisfactorily.

8.1.3 Major findings of U, Pu MOX fuel pellet dissolution studies in nitric acid

The following are the major findings with respect to urania plutonia MOX fuel dissolution behaviour under typical PUREX process conditions based on the current work.

- 1) The qualitative dissolution behaviour of urania plutonia MOX pellets in nitric acid is comparable to that of its urania ceria counterpart of same composition.
- 2) Thus the choice of cerium as a non-radioactive surrogate of plutonium for studying the dissolution behaviour of MOX pellets in nitric acid is justified.
- 3) Though the presence of nitrous acid does not chemically alter the dissolution rate of plutonia directly, it increases the rate indirectly by catalytically

dissolving urania faster and thereby making the pellet more porous. This leads to better contact between the dissolving pellet and nitric acid enabling faster dissolution of the rest of the pellet.

- 4) The penetration based dissolution model equations coupled with shrinking particle theory predicts the concentration profiles of the various species involved in the reaction more accurately than the surface area based method.
- 5) The lack of a suitable analytical system presently for the surface area measurement equipment of radioactive samples is the reason for the reduced accuracy of the surface area based model equations in predicting the dissolution behaviour of urania plutonia MOX fuel dissolution in nitric acid medium.
- 6) The order of the reaction with respect to nitric acid, rate constant and the validated model rate equations developed for the dissolution of urania plutonia MOX fuel would be useful tools in designing a continuous dissolution system for FBR fuel reprocessing plants.

8.2. Scope for future work

8.2.1 Surface area measurement for radioactive samples

The surface area of the dissolving pellets is an important parameter which influences the rate of its dissolution as explained in this thesis. For the studies on the MOX fuel dissolution, due to lack of a suitable analytical facility to measure the surface area of plutonium based pellets, only its initial surface area calculated from its dimensions were used. Thus there is a plenty of scope in setting up a facility for measuring the surface area of radioactive solids which will facilitate the measurement of surface area of any radioactive solid during the course of its dissolution accurately. This data would improve the accuracy of the model equation which would auger well for designing a continuous dissolver more efficiently.

The results of the MOX pellet dissolution clearly brings out the preferential leaching of UO_2 over PuO_2 in spite of the fact that the MOX pellets are complete solid solutions of urania and plutonia. This is a classic example for the sluggish behaviour of plutonia towards dissolution in nitric acid. Measure of surface area of the dissolving pellet without any ambiguity would go a long way in understanding the influence of lattice collapse mechanism during dissolution of urania and plutonia which could help in fine tuning the

understanding and prediction of the MOX pellet dissolution in nitric acid.

8.2.2 Dissolution experiments on radioactive spent fuel samples

All the experiments carried out as a part of the present work employed only unirradiated pellets. Since the irradiated pellets are expected to dissolve rapidly due to its higher porosity caused by the diffusion of the gaseous fission products produced inside its matrix during irradiation, the prediction based on the current model equations would be more conservative than the actual spent fuel dissolution. Hence for improving the model equations developed through the current work, dissolution experiments are required to be carried out using irradiated fuel samples under typical PUREX process conditions. As this requires dedicated shielded facility with provisions for sampling and remote analysis, this could be an important work to be carried out in the future.

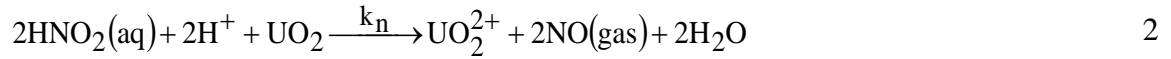
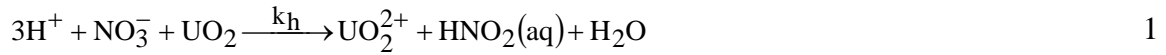
8.2.3 Dissolution of MOX fuel with varying plutonium composition

The effect of plutonium composition on the dissolution behaviour of MOX pellets in nitric acid could only be qualitatively predicted based on the dissolution behaviour of simulated urania ceria MOX pellets. Hence for studying the quantitative effect of plutonium composition on the MOX fuel dissolution kinetics, MOX pellets with varying plutonium compositions are required. Such pellets are currently unavailable as it requires special facilities for their fabrication. Thus it becomes an important and necessary work for the future to determine the existence of any unusual dissolution behaviour of MOX pellets with varied plutonium compositions before and after irradiation. These studies would lead to the development of the continuous dissolution process system which is the need of the hour for designing energy efficient, high throughput and safer FBR fuel reprocessing plants.

CHAPTER 9. Appendix

9.1. Derivation of rate equations for the modelling of UO₂ dissolution reaction by penetration method

The reactions between UO₂ and ions in the nitric acid solution under typical PUREX process conditions are as follows



In this method, dissolution model is expressed by a two-step scheme as given below



Where W_{ue} is the unexposed mass of fuel, W_e is the exposed mass and W_d the dissolved mass.

The first process in the above equation is the penetration process and its rate may be proportional to the concentration of nitric acid in the solution and the exposed mass of fuel (W_e). The second process is considered as the chemical reaction.

Therefore the rate of consumption of W_{ue} is given as follows.

$$\frac{dW_{ue}}{dt} = -k_p [\text{HNO}_3] W_{ue} \quad 5$$

Considering equations 1-3, we get the following mass balance equations

$$\frac{d[\text{UO}_2]}{dt} = -k_p [\text{HNO}_3] W_{ue} - k_h [\text{HNO}_3] [\text{UO}_2] - k_n [\text{HNO}_3] [\text{HNO}_2] [\text{UO}_2] - k_c [\text{HNO}_3] [\text{UO}_2^{2+}] [\text{UO}_2] \quad 6$$

$$\frac{d[\text{HNO}_3]}{dt} = -3k_h [\text{HNO}_3] [\text{UO}_2] - 2k_n [\text{HNO}_3] [\text{HNO}_2] [\text{UO}_2] - 3k_c [\text{HNO}_3] [\text{UO}_2^{2+}] [\text{UO}_2] \quad 7$$

$$\frac{d[\text{HNO}_2]}{dt} = k_h[\text{HNO}_3][\text{UO}_2] - 2k_n[\text{HNO}_3][\text{HNO}_2][\text{UO}_2] + k_c[\text{HNO}_3][\text{UO}_2^{2+}][\text{UO}_2] \quad 8$$

$$\frac{d[\text{UO}_2^{2+}]}{dt} = k_h[\text{HNO}_3][\text{UO}_2] + k_n[\text{HNO}_3][\text{HNO}_2][\text{UO}_2] + k_c[\text{HNO}_3][\text{UO}_2^{2+}][\text{UO}_2] \quad 9$$

At a mixing rate of 600 RPM the concentration of nitrous acid in the bulk of the reaction mixture is high. Hence at the pellet solution interface it can be assumed to be very less. Therefore applying steady state approximation of nitrous acid and taking its concentration to be very minimal, we have

$$\frac{d[\text{HNO}_2]}{dt} = 0 \quad 10$$

Substituting this value in equation 8 and rearranging, we get

$$[\text{HNO}_2] = \left(k_h + k_c[\text{UO}_2^{2+}] \right) / 2k_n \quad 11$$

Substituting equation 11 in equation 6, we get

$$\begin{aligned} \frac{d[\text{UO}_2]}{dt} = & k_p[\text{HNO}_3]W_{ue} - k_h[\text{HNO}_3][\text{UO}_2] - k_c[\text{HNO}_3][\text{UO}_2^{2+}][\text{UO}_2] \\ & - k_n[\text{HNO}_3][\text{UO}_2] \left((k_h + k_c[\text{UO}_2^{2+}]) / 2k_n \right) \end{aligned} \quad 12$$

On rearranging the above equation k_n gets eliminated and we get

$$\frac{d[\text{UO}_2]}{dt} = k_p[\text{HNO}_3]W_{ue} - 1.5 \left(k_h[\text{HNO}_3][\text{UO}_2] + k_c[\text{HNO}_3][\text{UO}_2^{2+}][\text{UO}_2] \right) \quad 13$$

Similarly substituting eqn. 11 in eqns. 7 and 9 and rearranging them, we get

$$\frac{d[\text{HNO}_3]}{dt} = -4 \left(k_h[\text{HNO}_3][\text{UO}_2] + k_c[\text{HNO}_3][\text{UO}_2^{2+}][\text{UO}_2] \right) \quad 14$$

$$\frac{d[\text{UO}_2^{2+}]}{dt} = 1.5 \left(k_h [\text{HNO}_3] [\text{UO}_2] + k_c [\text{HNO}_3] [\text{UO}_2^{2+}] [\text{UO}_2] \right) \quad 15$$

Hence final rate equations that are required to be solved are

$$\frac{dW_{ue}}{dt} = -k_p [\text{HNO}_3] W_{ue} \quad \text{I}$$

$$\frac{dW_e}{dt} = k_p [\text{HNO}_3] W_{ue} - 1.5 \left(k_h [\text{HNO}_3] + k_c [\text{HNO}_3] [\text{UO}_2^{2+}] \right) W_e \quad \text{II}$$

$$\frac{d[\text{UO}_2^{2+}]}{dt} = 1.5 \left(M_{\text{UO}_2} V^{-1} \right) \left(k_h [\text{HNO}_3] + k_c [\text{HNO}_3] [\text{UO}_2^{2+}] \right) W_e \quad \text{III}$$

$$\frac{d[\text{HNO}_3]}{dt} = -4 \left(M_{\text{UO}_2} V^{-1} \right) \left(k_h [\text{HNO}_3] + k_c [\text{HNO}_3] [\text{UO}_2^{2+}] \right) W_e \quad \text{IV}$$

Where $\left(M_{\text{UO}_2} V^{-1} \right)$ is molar concentration of UO_2 .

These are the rate equations given in section 5.10.3.1 of the thesis.

In section 5.10.3.1.2 wherein the effect of nitrous acid is neglected as the reactions were carried out at a sufficiently high mixing rate of 600 RPM during which the concentration of nitrous acid at the pellet solution interface would be negligible to accelerate the reaction. In this case, the stoichiometric reaction given in equation 2 is neglected. Similar derivation is carried out considering only equations 1 and 3 to arrive at the following rate equations.

$$\frac{dW_{ue}}{dt} = -k_p [\text{HNO}_3] W_{ue} \quad \text{V}$$

$$\frac{dW_e}{dt} = k_p [\text{HNO}_3] W_{ue} - \left(k_h [\text{HNO}_3] + k_c [\text{HNO}_3] [\text{UO}_2^{2+}] \right) W_e \quad \text{VI}$$

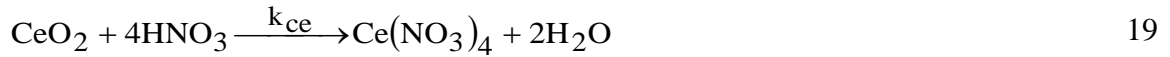
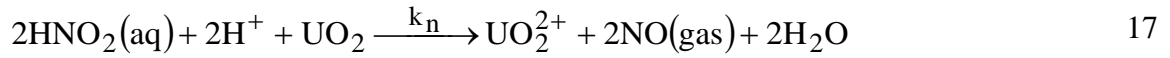
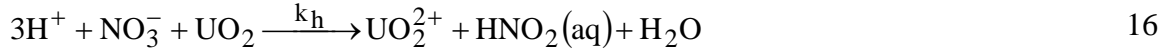
$$\frac{d[\text{UO}_2^{2+}]}{dt} = \left(M_{\text{UO}_2} V^{-1} \right) \left(k_h [\text{HNO}_3] + k_c [\text{HNO}_3] [\text{UO}_2^{2+}] \right) W_e \quad \text{VII}$$

$$\frac{d[\text{HNO}_3]}{dt} = -3 \left(M_{\text{UO}_2} V^{-1} \right) \left(k_h [\text{HNO}_3] + k_c [\text{HNO}_3] [\text{UO}_2^{2+}] \right) W_e \quad \text{VIII}$$

9.2. Derivations of rate equations for simulated MOX fuel dissolution studies by penetration method

Similar to that of UO₂ fuel dissolution, derivations were also carried out for simulated urania ceria MOX dissolution studies. In this case, there would be one additional stoichiometric reaction to be considered for the dissolution of ceria in nitric acid. Hence correspondingly there would be one more rate equation derived additionally for modelling the concentration profile of cerium.

The stoichiometric reactions considered for this derivation are as follows.



Similar to the case of UO₂ fuel dissolution, in this case also, the rate equations are derived by writing down the mass balance equations using the above stoichiometric reactions. The final rate equations after derivation are given as follows which is the same as in section 6.9.2.1.1.

$$\frac{dW_{ue}}{dt} = -k_p [\text{HNO}_3] W_{ue} \quad \text{IX}$$

$$\frac{dW_e}{dt} = k_p [\text{HNO}_3] W_{ue} - (k_h [\text{HNO}_3]^2 + k_c [\text{HNO}_3]^2 [\text{UO}_2^{2+}] + k_{ce} [\text{HNO}_3]^2) W_e \quad \text{X}$$

$$\frac{d[\text{UO}_2^{2+}]}{dt} = (M_{\text{MOX}} V^{-1}) (k_h [\text{HNO}_3]^2 + k_c [\text{HNO}_3]^2 [\text{UO}_2^{2+}]) W_e \quad \text{XI}$$

$$\frac{d[\text{Ce}^{4+}]}{dt} = (M_{\text{MOX}} V^{-1}) (k_{ce} [\text{HNO}_3]^2) W_e \quad \text{XII}$$

$$\frac{d[\text{HNO}_3]}{dt} = -(M_{\text{MOX}} V^{-1}) (3k_h [\text{HNO}_3]^2 + 3k_c [\text{HNO}_3]^2 [\text{UO}_2^{2+}] + 4k_{ce} [\text{HNO}_3]^2) W_e \quad \text{XIII}$$

Here M corresponds to the molecular weight of the simulated MOX fuel with its appropriate chemical composition.

For deriving the rate equations neglecting the catalytic effect of uranyl ion, the reaction given in equation 18 of this appendix is not considered. Similar methodology to that of UO₂ fuel was adopted for deriving the rate equations of simulated MOX fuel dissolution whose final form is given as below. These are same as the equations 6.12 to 6.16 in section 6.9.2.1.2 of this thesis

$$\frac{dW_{ue}}{dt} = -k_p [\text{HNO}_3] W_{ue} \quad \text{XIV}$$

$$\frac{dW_e}{dt} = k_p [\text{HNO}_3] W_{ue} - (k_h [\text{HNO}_3]^2 + k_{ce} [\text{HNO}_3]^2) W_e \quad \text{XV}$$

$$\frac{d[\text{UO}_2^{2+}]}{dt} = (M_{\text{MOX}} V^{-1}) (k_h [\text{HNO}_3]^2) W_e \quad \text{XVI}$$

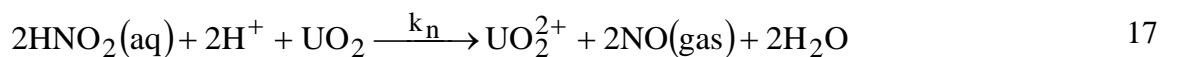
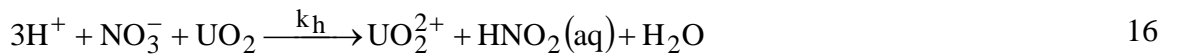
$$\frac{d[\text{Ce}^{4+}]}{dt} = (M_{\text{MOX}} V^{-1}) (k_{ce} [\text{HNO}_3]^2) W_e \quad \text{XVII}$$

$$\frac{d[\text{HNO}_3]}{dt} = - (M_{\text{MOX}} V^{-1}) (3k_h [\text{HNO}_3]^2 + 4k_{ce} [\text{HNO}_3]^2) W_e \quad \text{XVIII}$$

In the case of urania plutonia MOX fuel dissolution studies, the rate equations are derived in the same way with Pu/Pu⁴⁺ in place of Ce/Ce⁴⁺ respectively.

9.3. Derivations of rate equations for urania-plutonia MOX fuel dissolution studies by penetration method

The derivation of the rate equations for (U, Pu) MOX fuel by penetration based method is very similar to that of simulated MOX fuel. Instead of Ce, it should be replaced by Pu and for k_{Ce} by k_{Pu}. Thus the chemical reactions to be considered for this derivation would be as follows.



These are the equations 7.2 to 7.5 given in chapter seven of the thesis.

The rate equations derived by writing down the mass balance equations from the above set of balanced stoichiometric equations are as follows when a steady state approach was considered for nitrous acid.

$$\frac{dW_{ue}}{dt} = -k_p [\text{HNO}_3] W_{ue} \quad \text{XIX}$$

$$\frac{dW_e}{dt} = k_p [\text{HNO}_3] W_{ue} - (k_h [\text{HNO}_3]^2 + k_c [\text{HNO}_3]^2 [\text{UO}_2^{2+}] + k_{ce} [\text{HNO}_3]^2) W_e \quad \text{XX}$$

$$\frac{d[\text{UO}_2^{2+}]}{dt} = (M_{\text{MOX}} V^{-1}) (k_h [\text{HNO}_3]^2 + k_c [\text{HNO}_3]^2 [\text{UO}_2^{2+}]) W_e \quad \text{XXI}$$

$$\frac{d[\text{Pu}^{4+}]}{dt} = (M_{\text{MOX}} V^{-1}) (k_{\text{Pu}} [\text{HNO}_3]^2) W_e \quad \text{XXII}$$

$$\frac{d[\text{HNO}_3]}{dt} = -(M_{\text{MOX}} V^{-1}) (3k_h [\text{HNO}_3]^2 + 3k_c [\text{HNO}_3]^2 [\text{UO}_2^{2+}] + 4k_{\text{Pu}} [\text{HNO}_3]^2) W_e \quad \text{XXIII}$$

During the experiments on the dissolution kinetics of (U, Pu) MOX fuels in nitric acid, it was found that uranyl ion was not found to accelerate the dissolution process. Hence the rate equations derived from equations 16-19 neglected equations 18 (catalytic effect of uranyl ion) would be as follows.

$$\frac{dW_{ue}}{dt} = -k_p [\text{HNO}_3] W_{ue} \quad \text{XXIV}$$

$$\frac{dW_e}{dt} = k_p [\text{HNO}_3] W_{ue} - (k_h [\text{HNO}_3]^2 + k_{\text{Pu}} [\text{HNO}_3]^2) W_e \quad \text{XXV}$$

$$\frac{d[\text{UO}_2^{2+}]}{dt} = (M_{\text{MOX}} V^{-1}) (k_h [\text{HNO}_3]^2) W_e \quad \text{XXVI}$$

$$\frac{d[\text{Pu}^{4+}]}{dt} = (M_{\text{MOX}} V^{-1}) (k_{\text{Pu}} [\text{HNO}_3]^2) W_e \quad \text{XXVII}$$

$$\frac{d[\text{HNO}_3]}{dt} = -(M_{\text{MOX}} V^{-1}) (3k_h [\text{HNO}_3]^2 + 4k_{\text{Pu}} [\text{HNO}_3]^2) W_e \quad \text{XXVIII}$$